Adaptation Mechanisms in the Salmonid Visual System

by

Luc Beaudet
B.Sc. Université de Montréal, 1990

A Dissertation Submitted in Partial Fulfillment of the
Requirements for the Degree of

DOCTOR OF PHILOSOPHY

in the Department of Biology

We accept this dissertation as conforming
to the required standards

Dr. C.W. Hawryshyn, Supervisor (Department of Biology)

Dr. D.H. Paul, Departmental Member (Department of Biology)

Dr. N. Sherwood, Departmental Member (Department of Biology)

Dr. M.E. Corcoran, Outside Member (Department of Psychology)

Dr. D.P.M. Northmore, External Examiner, (Neuroscience Program, University of Delaware)

Supervisor: Dr. Craig W. Hawryshyn

ABSTRACT

Animals in general, but fish in particular, inhabit environments characterized by dynamic photic conditions that are influenced by cyclical events such as the night-day cycle, or by spatial heterogeneity in the distribution of light. Effects of these dynamic properties on the visual system are compounded in salmonid fishes by migrations that expose individuals to various types of habitats, at various stages of their ontogeny. This dissertation examines some of the adaptations that enable the retina of salmonid fishes to cope with their changes of "visual environment" caused by migration and by the night-day cycle.

In the first part of this dissertation, I used a combination of optic nerve response (ONR) recordings and conventional histology of the retina to investigate the ontogeny of sensitivity to ultraviolet (UV) light in salmonid fishes. I found that the UV cone mechanism contributed mostly to the ON response of retinal ganglion cells in rainbow trout (*Oncorhynchus mykiss*). Furthermore, the presence of UV sensitivity in rainbow trout was associated with the presence of accessory corner cones in the retinal cone mosaic, as both UV sensitivity and these cones were absent in larger (59.5-835g) juveniles. These results suggest that corner cones in the salmonid retina are sensitive to UV light, and that their ontogenetic disappearance leads to the loss of UV sensitivity.

The changes in the photic environment that occur when mature salmonid fishes return to their natal stream to reproduce mirror those undergone during the first migration. To determine if the accessory corner cones, lost during this first migration, reappear at the time of the return migration, I studied the structure of the photoreceptor layer in sexually mature Pacific salmonids from four species: chinook (*O. tschawytscha*), chum (*O. keta*) and coho (*O. kisutch*) salmon, and rainbow trout. I found accessory corner cones over a large area of the dorso-temporal retina in all four species examined, which provides support for the contention that these cones are the product of late cellular addition.

I investigated possible pathways for visual information to various brain centers in rainbow trout by labelling retinal projections and torus semicircularis connections in the same individuals. Double-labelling of neuronal tracts revealed two possible indirect pathways between the retina and the torus semicircularis, through the accessory optic center of the diencephalon and the optic tectum respectively.

In the second part of this dissertation, I qualitatively and quantitatively examined the effects of various levels and spectral types of ambient lighting conditions on the sensitivity and time course of multi-unit responses recorded from the optic nerve of juvenile rainbow trout. Change in threshold from the dark-adapted state to progressively brighter ambient light conditions was examined at four wavelengths (380, 430, 540 and 620 nm) and found to be linear over most of the scotopic range, with a slope around 0.8. The results also suggested that, under mesopic conditions, rods and the long-wavelength cone mechanism were active simultaneously, in their respective parts of the spectrum.

Implicit time, or time-to-peak of the scotopic responses decreased with stimulus intensity following a logarithmic relationship with a slope of -0.10, suggesting that the scotopic system of trout acts as an 11-stage low-pass filter, a number similar to that inferred in cat and rat, but different from other non-mammalian vertebrates. Similarly, implicit time at threshold decreased logarithmically with background intensity for the scotopic system, with a slope of -0.09.

Varying the spectral content of ambient light led to differences in sensitivity and time course of ONRs across the spectrum, suggesting physiological differences between cone mechanisms. Possible implications for the coding of visual information are briefly discussed. In conclusion I provide a qualitative model of light adaptation in the trout visual system.

Examiners:

Dr. C.W. Hawryshyn, Supervisor (Department of Biology)

Dr. D.H. Paul, Departmental Member (Department of Biology)

Dr. N. Sherwood, Departmental Member (Department of Biology)

Dr. M.E. Corcoran, Outside Member (Department of Psychology)

Dr. D.P.M. Northmore, External Examiner, (Neuroscience Program, University of Delaware)

TABLE OF CONTENTS

LIST OF TABLES

LIST OF FIGURES

Acknowledgments

I would first like to take this opportunity to thank Craig Hawryshyn, who supervised my graduate work at the University of Victoria. Thank you for your consistent support throughout the past several years. I also very much enjoyed our long conversations about fish eyes, work and life in general. It is my hope that the relationship we developed during my studies will outlast my stay in Victoria.

I would also like to thank the members of my supervisory committee, Drs. Michael Corcoran, Dorothy Paul and Nancy Sherwood, for their support and encouragement throughout my studies. I would particularly like to thank Dorothy Paul, with whom I had several discussions about various aspects of my work, and who kindly reviewed a draft of a manuscript.

Thanks to all of you who have read various versions of this dissertation and helped turn it into something that resembles the English language (with a French accent). For the abuse, the anti-Québec jokes, the daily surprises (that I almost came to fear after a while), the heated but so ephemeral arguments about so many different subjects and above all, for his friendship, I thank Iñigo Novales Flamarique (yes, I put the little thingy on the n of Iñigo). Thanks to Daryl Parkyn, who taught me many things about the English language (including things I would probably have been better off not knowing!), and for being a good friend. Thanks to Craig McDonald for the many discussions and for his friendship. Thanks to the students who passed through the lab during my stay, they contributed to a friendly atmosphere and I greatly enjoyed their friendship: Kathy Veldhoen, Karen Barry, Josée Desbarats, Qi Tian and Brad Ryan. I would also like to thank Howard Browman,

David Coughlin and Victor Rush, who contributed professionally and personally to my endeavors, during their stay as postdoctoral fellows.

I thank Gordon Davies, Patrick Kerfoot and Heather Down for their valuable technical support. Thanks also to Tom Gore who was always a great source of information and surprises.

This work would have been made considerably more difficult without the help of several work-study students: Adrian Decker, Joy McKnight, Dave Vadnais and Jeff Whitset, all of whom I thank very much.

As this work depended on the availability of healthy fish, I thank the Fraser Valley Provincial Trout Hatchery, the Big Qualicum Fish Hatchery, and Kevin Nicholichuk for providing the study animals.

I would like to acknowledge the financial support of NSERC, the Fonds FCAR of the Province of Quebec, and the University of Victoria.

Finally, and most importantly, I would like to express my most sincere thanks to Lisa Hartman, my life companion, for her never-ending and unconditional support, her enormous help with critiquing and editing this dissertation, and for her invaluable friendship.

To my parents,

Gilles and Marguerite Beaudet

Chapter 1: Introduction and literature review.

Animals in general, but fish in particular, inhabit environments characterized by dynamic photic properties. Effects of these dynamic properties on the visual system are compounded by the fact that some species undergo short- and/or long-term migrations that expose them to various types of habitats, at various stages of their ontogeny. This dissertation examines some of the adaptations that enable the retina of salmonid fishes to cope with their changes of "visual environment" caused by migration and by the night-day cycle.

Most salmonid fishes undertake a long range migration at some point during their life history, the timing of which varies among species. In some species, this migration leads to the ocean, and in others to lakes. This migration is followed, in adults, by one in the opposite direction, back to the spawning grounds. As I will show in the first part of this dissertation, there are physiological and anatomical changes at the retinal level associated with these migratory events. These pertain mostly to the ability of the animals to see ultraviolet (UV) light. In addition, light intensity and spectral quality also vary on a more short-term basis, coincident with the diel night/day cycle. This requires the visual system to adjust its sensitivity, in a reversible fashion, through the process of light adaptation. Thus, the second part of this dissertation investigates some aspects of light adaptation in the rainbow trout retina.

In this introduction, I will review the types of retinal adaptations that have evolved in response to constraints associated with these larger scale movements by animals and to

the need to maintain an effective visual system during the diel night/day cycle. To do this, I will provide an overview of :

I. The various types of ontogenetic transformations that the visual system of some fish and amphibian species undergoes in response to movements from one environment to another that differ in their light characteristics[1]. This will be done through the examination of several "case studies" that illustrate the various processes involved in these transformations. In addition, this discussion will also include a section on the visual adaptations associated with seasonal changes in the light environment but not necessarily related to animal movements.

II. The distribution of UV sensitivity in vertebrates, with a brief discussion of the roles it may play in visually guided behaviors.

III. The mechanisms that underlie the processes of light and dark adaptation in the fish retina.

Although many of the processes reviewed in this chapter probably also apply to invertebrates, vertebrates will represent the main focus of my discussion.

I. Effects of migration and seasonal changes on the visual system

The life history of many species is comprised of several stages, each characterized by distinct anatomical, physiological, behavioral and ecological adaptations. Through evolution, some species have come to select different habitats for each of the stages of their life history. This is because some environments provide conditions favorable to early

[1] Part of this review will appear in a modified form as Beaudet and Hawryshyn (accepted).

growth and development, but may be limiting for the juvenile and adult stages. To take advantage of conditions more favorable to the later stages of their life history, animals often move to other environments, at some point in their ontogeny. Movement from one habitat to another, while providing benefits to an organism, also subjects it to new environmental conditions, some of which may affect the visual system's performance. Through ontogenetic adaptation processes, the visual system of such species is modified, presumably to increase its efficiency in each of the new environments it encounters.

In some species, several of the changes that the visual system undergoes in association with these shifts in environment occur abruptly relative to the entire life span of the animal, and generally entail substantial morphological and physiological modifications. The most spectacular of such changes are those undergone by some fish and amphibian species at metamorphosis.

The changes that affect the visual system during metamorphosis or comparable events occur at different levels of organization and thus vary in their magnitude. They may affect large structures, such as the eye and associated musculature, alter the cellular composition of the retina, modify the morphology of existing retinal cells, or simply change some chemical properties of retinal or other cells. Changes may be accomplished through one or more of the following processes: cell addition, cell deletion, morphological transformations of existing cells, and changes in the expression of specific genes, resulting in new physiological properties of photoreceptors (e.g. expression of a new visual pigment protein). Subtle changes can also affect the chemical composition of the visual pigment's chromophore and result in significant shifts in the spectral absorption properties of the

visual pigment. In the following sections, I discuss examples of responses to two sources of changes of visual environment: migration and seasonal changes These examples will illustrate some of the above transformation processes, and relate them to the visual ecology of animals.

Migration and changes in the visual system

Migration from one habitat to another often exposes organisms to light regimes which differ in spectral quality and intensity. Changes in the visual system associated with migratory events are presumed to improve foraging abilities, and provide increased predator avoidance capabilities, but this has never been directly and convincingly tested.

Although complex and varied in nature, migratory events can, for the purpose of our discussion, be classified in general as either vertical or horizontal. Vertical migrations are experienced by fish that spend part of their life as pelagic larvae or juveniles and eventually settle to deeper layers of the water column or to the benthos, as exemplified by flatfishes and some reef fishes. In this case, movement to greater depth is the major source of environmental change impacting the visual system.

Horizontal migrations can be classified as anadromous or catadromous. Anadromy is characteristic of salmon and lamprey and involves a larval or early juvenile stage in freshwater, followed by a movement to the marine environment, where most of the adult life is spent. Catadromy, conversely, involves a larval stage in the marine environment followed by juvenile and adult phases in freshwater, and is characteristic of the eel life

history. Migration in fishes is normally preceded by metamorphosis or, in salmonid fishes, by a similar process called smoltification (Hoar, 1988).

Vertical migration[2]

1. Flatfishes

Flatfishes (flounder, plaice, sole etc.) provide a good example of the visual adaptations that can be associated with vertical migrations. The life history of all species of flatfishes is characterized by two discrete phases: the larval, pelagic phase, and the juvenile/adult, benthic phase (Fig. 1, right hand side). In some species, the intervening metamorphosis may also be considered a phase as it can last several months (Markle et al., 1992).

The larval, pelagic phase is believed to favor dispersal and foraging opportunities. Effective foraging in these animals is crucial not only to ensure proper development, but also because the larva often has to store energy for metamorphosis, during which it ceases to feed. The distribution of flatfish larvae is heavily influenced by that of their zooplanktonic prey, which are most abundant in the top layers of the water column, the euphotic zone. Thus, the pelagic, predatory larva forages in a bright light environment, and is characterized by positive phototaxis and negative geotaxis (Champalbert et al., 1991).

[2] In this first section, the discussion will only pertain to migration of the "ontogenetic" type, as opposed to the type of daily vertical migrations that some species experience, for example.

Figure 1: Summary of the main ontogenetic visual adaptations discussed in this chapter and their associations with the different types of changes of environment. Changes caused by seasonal variation have been omitted but would likely have an additive effect to those illustrated. Although, for reasons of clarity, exceptions to the processes illustrated here have been omitted, the reader should be mindful of the complexity that exists amongst ontogenetic trajectories.

Horizontal migrations

Vertical migrations

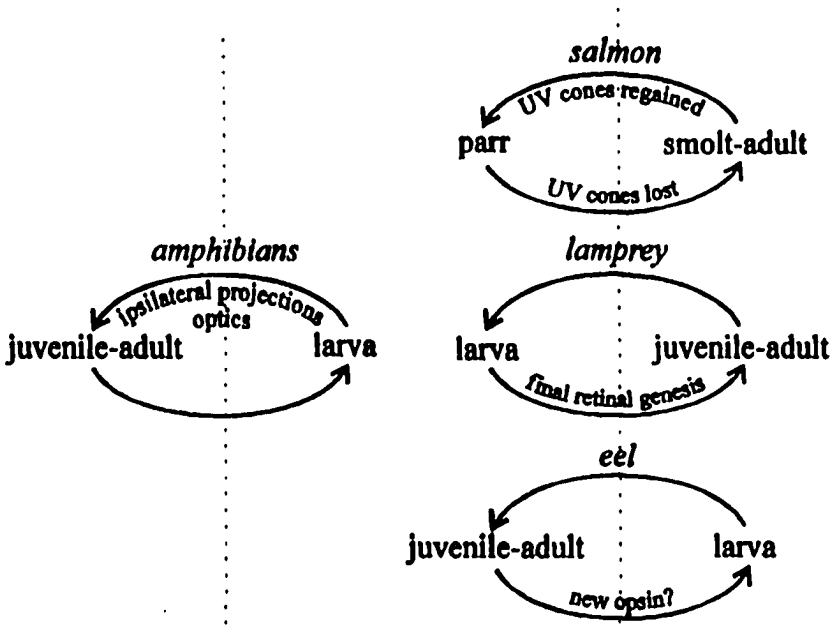

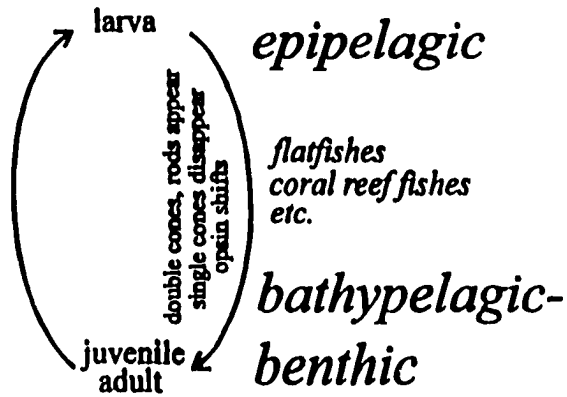

terrestrial
rhodopsin-dominant
(vitamin A1)

freshwater
porphyropsin-dominant
(vitamin A2)

marine
rhodopsin-dominant
(vitamin A1)

The larvae of flatfish are bilaterally symmetrical with eyes located on either side of the head. Consistent with the pelagic lifestyle described above, the retina is typically adapted to vision in bright light environments, as its photoreceptor layer contains exclusively single cones found in highest density in the dorso-temporal retina, and shows no evidence of retinomotor movements (Blaxter, 1968; Evans and Fernald, 1993; Evans et al., 1993). In larvae of the winter flounder, Evans et al. (1993) found a single visual pigment, indicating that these larvae are not capable of color vision and thus probably rely solely on brightness contrast to locate prey items. According to these authors, the peak absorbance (λ_{max} 519 nm) of this cone photopigment is offset from the spectral distribution of the ambient light in which the larvae live, thus providing increased contrast for the prey. Finally, the visual system of flatfish larvae in general is characterized by a gradual increase in visual acuity which, coupled with an increase in swimming speed, probably improves foraging ability (Neave, 1984).

Metamorphosis in flatfishes begins when the larva reaches a certain size or age, which differs from species to species. Metamorphosis brings about adaptations for the benthic life style of the juveniles and adults which affects the general body plan, physiology and behavior of the animals. Whereas the larva was a swimming and active zooplanktivore, the juvenile and adult forms are more sedentary, spending most of their time on or near the ocean floor, feeding on benthic invertebrates. In addition, juvenile and adult flatfish lie flat on their side, an adaptation accompanied by a loss of bilateral body symmetry that is reflected in jaw shape and dentition, body coloration and eye position. The most obvious effect on the visual system is the migration of one eye to the

contralateral side of the head, adjacent to the other eye, such that in postmetamorphic animals both eyes are on the exposed side of the body and scan the environment located above the plane in which the animal lies (Evans and Fernald, 1993).

This transition from a pelagic to a benthic habitat is associated with a corresponding decrease in the intensity of ambient light, and a spectral shift towards shorter wavelengths. At the retinal level, the best described transformations occur in the photoreceptor layer, and involve the addition of new cell types, and changes in opsin gene expression. Whereas the larval retina contains only single cones, at metamorphosis rod photoreceptors are added, mostly to the ventral retina, in keeping with the lower light intensities found at greater depths (Blaxter, 1968, Neave, 1984, Evans and Fernald, 1993). Double cones (λ_{max} 531 and 547 nm) are added, mostly to the dorsal retina (Evans and Fernald, 1993). Thus, the juvenile flatfish retina contains mostly cones in the dorsal and rods in the ventral half. Evans and Fernald (1993) suggest that the rod-dominated ventral retina might serve as "an effective visual detector for viewing objects silhouetted against the reduced [downwelling] incident light" at twilight. So far, there is no evidence that this would be the case. On the contrary, it would seem that the scotopic system of fish is most sensitive to increments of light, and thus designed to respond to bright targets that appear over a darker background (see Wheeler, 1979b and chapter 5 of this dissertation). The exact manner in which the rod-dominated retina is used by the organism therefore remains to be determined. The cone-dominated dorsal retina, conversely, is probably used to scan the surface of the substrate in search of prey during daytime.

With metamorphosis, the peak absorbance of the photopigment contained in the single cones also shifts, towards shorter wavelengths (from 519 nm to 457 nm in winter flounder, Evans et al., 1993). This represents an adaptation to the blue-shifted light environment that prevails at the depths at which adults live. In winter flounder, this shift in the spectral sensitivity of the single cones probably reflects the expression of a different gene, resulting in an opsin with new spectral properties (Evans et al., 1993). Therefore, whereas in the larval winter flounder the visual pigment contained in the single cones was offset with respect to the ambient light spectral composition, in the juvenile/adult, these cones contain a pigment that is matched to this ambient light.

The above changes in retinal structure and pigment content are accompanied by several other changes in the flatfish visual system, including the appearance of retinomotor movements, development of photonegative behavior, and increased visual acuity, although the latter appears to be the continuation of a process initiated early in the larval stage (Blaxter, 1968, Neave, 1984). In addition, an increase in absolute sensitivity occurs; in plaice, for example, the threshold for dark adaptation falls by two orders of magnitude during metamorphosis (Neave, 1984). The appearance of rods and double cones adapts the visual system of flatfish to a dimmer environment. Furthermore, the appearance of additional spectral classes of cones indicates the potential for color vision, which could greatly improve visual ability, allowing discrimination not only on the basis of brightness but also of hue.

2. Vertical migration in other species

Transformations associated with vertical migration are also encountered in other species of fish, albeit not as spectacular as those found in flatfishes. In some species, such as *Sebastes diploproa* (Boehlert, 1979) and *Gempylus serpens* (Munk, 1990), single cones disappear from the retina during migration to greater depths and only double cones and rods remain. In yellow perch, single cones sensitive to violet light are lost during vertical migration (Loew and Wahl, 1991) whereas in pollack, single cones are not lost, but rather become sensitive to longer wavelengths through a change in visual pigment content (Shand et al., 1988).

Changes in photoreceptor density and spectral sensitivity have also been related to settlement into the reef environment in coral reef fishes (Shand, 1994, 1997). This transition from the pelagic to the reef environment is marked by a change in feeding behavior, decrease in ambient light levels and shift toward shorter wavelengths (McFarland, 1991). The timing of settlement differs between species, and the timing of changes in the visual system differs accordingly. Shand (1994, 1997) found that an increase in rod density and a decrease in cone density occurred at a smaller size in early-settling species than in species with a prolonged pelagic phase. The final photoreceptor densities depended on the lifestyle of the adults. Fish active exclusively during daytime had lower rod densities than those whose activity extended into the crepuscular periods. Using microspectrophotometry, Shand (1993) also found a loss of red cones in goatfish which she related to the movement towards deep zones of the coral reef after settlement. Whereas larvae possessed double cones with two visual pigments (λ_{max} 487 and 580 nm),

settled goatfish lacked the long-wavelength photopigment (λ_{max} 580 nm) which had been replaced with a combination of 515 and 530 nm λ_{max} photopigments.

Horizontal migration

1. Eels

American and European eels reproduce in the Atlantic ocean. After a larval stage that lasts up to three years, metamorphosis occurs, the juvenile swims upstream and remains in freshwater until sexual maturation. Following maturation, a second metamorphosis occurs and the eel migrates back to the ocean to reproduce. This catadromous pattern of migration is the reverse of that observed in lamprey and in salmon, hence the changes observed in the eel visual system are the reverse of some of those of salmon and lamprey (see below).

While in the marine environment, the retina of the larval eel contains only "rod-like" photoreceptors (Pankhurst, 1984). Nothing is known of the type of visual pigments present in these photoreceptors. This implies that in eel, rods appear before cones, which is not usually the case in vertebrates. However, since the photoreceptors of the larval eel have been identified as rods only on morphological grounds, it is too early to draw definitive conclusions regarding their identity. Following metamorphosis and migration to freshwater, the eel retina contains both rods and cones (Pankhurst, 1984). Furthermore, it is dominated by a vitamin A_2-based photopigment (λ_{max} 523 nm) (Beatty, 1975) in agreement with the view that this is an adaptation to environments richer in longer wavelengths (see Beatty, 1984).

The migration back to the marine environment is associated with a change in both retinal structure and visual pigment content. There is an increase in the size of the eye and the number of rods, whose density thus remains constant (Pankhurst, 1984). Cone density decreases as a result of eye growth and possibly also due in part to cellular degeneration (Pankhurst, 1984). The change in visual pigment content is two-fold. First, there is a shift from a dominance of vitamin A_2-based photopigments to that of A_1-based photopigments. Second, while the 523 nm A_2-based photopigment disappears and is replaced by the 501 nm A_1-based photopigments, a new opsin, a 482 nm A_1-based photopigment emerges and eventually becomes the main visual pigment of the sexually mature animal (Beatty, 1975; Archer et al., 1996). This shift towards a preponderance of A_1-based photopigments and the eventual appearance of a new opsin with its λ_{max} at shorter wavelengths, is probably an adaptation to the deep marine environment in which eels reproduce.

2. Lamprey

In contrast to most species that undergo metamorphosis, lamprey are characterized by an unusually long larval phase, spent in streams (Potter, 1980). The lamprey larva, called the ammocoete, hatches from eggs that were buried in the substrate at the time of spawning (Potter, 1980). Emergence occurs a few weeks later and gives rise to larval dispersal, normally over relatively short distances, mostly at night. After dispersing, the ammocoetes bury themselves in the substrate in areas where current and mechanical disturbances are minimal (Just et al., 1981). They remain buried in the substrate or exhibit very limited movements for the remainder of their larval life, which can last up to 8 years

depending on the environmental conditions and the species (average of 6 years for most anadromous species). During this time, lamprey are filter feeders (Just et al., 1981).

The behavior of the ammocoete, which remains mostly inactive, points to a reduced role for vision during this phase of the lamprey's life cycle. It is commonly held that the ammocoete eye, which remains subdermal until metamorphosis, is non-functional. Thus, ammocoetes are normally referred to as blind. Although there is no electrophysiological evidence that the ammocoete eye is sensitive to light, some anatomical and behavioral observations suggest that it may be. Studnicka (1912) found that the ammocoete eye contains a patch of differentiated retina that contains all the retinal layers, including fully differentiated photoreceptors. Kennedy and Rubinson (1977) and De Miguel et al. (1990) report the presence of retinofugal projections to the diencephalon, and retinopetal projections from the mid-brain tegmentum, in young larvae. Finally, the nocturnal dispersal and movement patterns of the ammocoete have been regarded as displays of photonegative behaviors (Potter, 1980). Although it has been proposed that extra-retinal photoreceptors may be responsible for the response to light in the ammocoete, the possibility of a retinal involvement warrants closer consideration.

Lamprey metamorphosis is associated with increased activity levels and movement from areas of low to higher water flow (Potter, 1980). This movement is followed by downstream migration and the adoption of a parasitic lifestyle (Potter, 1980; Just et al., 1981). Downstream migration primarily occurs at night and, depending on the species, may lead to the ocean for marine species, or to a lake environment in freshwater species (Just et al., 1981). Although changes in water current and temperature appear to trigger

the lamprey's postmetamorphic migration, light cues play a role in restricting migration to nighttime, which may represent an adaptation to reduce predation (Potter, 1980).

In most fishes, the eye of the premetamorphic larva is fully differentiated, and only a few populations of cells are modified at metamorphosis. In lamprey, the changes that occur at metamorphosis affect the eye as a whole, including the retinal projections to the brain. During metamorphosis the eyes emerge from under the skin, the extraocular muscles increase in size, the retina differentiates and adopts an appearance in many respects similar to that of teleosts. Metamorphosis also results in the final maturation of the retinal projections into a pattern similar to that of teleost fishes (De Miguel et al., 1990).

The metamorphosed lamprey retina contains two morphological classes of photoreceptors, one with a short tapered and the other a longer and slender outer segment (Ohman, 1976). Based on their ultrastructure, Ohman (1976) concluded that both classes of photoreceptors of the metamorphosed lamprey were "rod-like" although they also possessed some characteristics of cones. Govardovskii and Lychakov (1984), however, based on electrophysiological recordings, claim the retina of *Lampetra fluvialis* is duplex, containing both rods and cones. Based on microspectrophotometric measurements, Harosi and Kleinschmidt (1993) drew similar conclusions, detecting both "rod-like" and "cone-like" photopigments in the retina of adult *Petromizon marinus*. Although the data seem to point to the presence of both rods and cones in lamprey, they also highlight some of the ambiguity in defining these structures.

Sea lamprey, in addition to shifting from a sedentary to a more active lifestyle following metamorphosis, also move from an environment dominated by longer wavelengths (freshwater) to one richer in mid- to short-wavelengths (marine environment). The ability of the lamprey visual system to adapt to this change may lie in the spectral properties that visual pigments can exhibit depending on the type of chromophore they are attached to. The visual system of sea lamprey contains both vitamin A_1- (rhodopsin) and vitamin A_2-based (porphyropsin) photopigments (Cresticelli, 1972). It is not clear whether these two types of photopigment are associated with different stages of the life history of lamprey. One theory, put forth by Wald (1945) attributes vitamin A_2-based photopigments to the freshwater part of the life cycle in sea lamprey and vitamin A_1-based photopigments to the marine phase (Fig. 1). Conversely, Cresticelli (1958), found only vitamin A_1-based photopigments in both downstream- and upstream-migrating sea lamprey and concludes that this theory may not apply to all cases. Depending on the timing of the measurements and the stage of the migration, however, the A_2-based photopigments may not have had time to become expressed in the upstream migrating animals studied by Cresticelli (1958). A recent study by Harosi and Kleinschmidt (1993) found only vitamin A_2-based photopigments in the upstream migrants, providing further support to Wald's (1945) contention that it is the photopigment associated with freshwater.

3. Amphibians

The movement from the larval, aquatic environment to the juvenile or adult, terrestrial environment in some amphibian species is akin to the migratory events described

in the previous sections. These two environments differ in their optical properties and are likely to require specific morphological, physiological and behavioral adaptations. The different visual requirements of the aquatic and terrestrial environments are illustrated by the transformation that the visual system of amphibians undergoes at metamorphosis. Larval amphibians are generally aquatic animals. They possess a fish-like body form, and features such as external gills, a lateral line and an escape motor system involving Mauthner cells. In addition, larval amphibians are mostly herbivorous, feeding on algae and detritus. At metamorphosis, there is a transition to the terrestrial environment, and amphibians take on a carnivorous, predatory lifestyle. Metamorphosis leads to the loss of larval characters, and the appearance of adaptations to the new physical characteristics of the terrestrial environment and to the changes in behavior of the animals. This process also includes changes to the eyes and the central visual pathways.

The aquatic and terrestrial environments differ in many aspects, all of which have an impact on the visual system. First, the desiccant effect of air in the terrestrial environment requires the presence of protective integuments on the eye such as nictitating membranes (Kaltenbach, 1953). Second, because of the differing density indices of water and air, in water the cornea is more or less optically inactive and most of the refractive properties of the eye lie in the lens; the reverse is true in the terrestrial environment (Sivak and Warburg, 1983). Third, the spectral distribution of light is much narrower in the aquatic environment and, in freshwater where amphibians are found, contains longer wavelength radiation, i.e. yellow to red colors (Reuter, 1969). Fourth, the predatory lifestyle of the terrestrial juvenile and adult requires good stereoscopic vision and the

necessary ipsilateral visual projections associated with it. All of the changes in the visual environment and behavior that occur at the time of metamorphosis produce changes in the optics, spectral sensitivity and pattern of central retinal connections.

The larval eye of amphibians is slightly myopic or emmetropic in water and strongly myopic in air (Sivak and Warburg, 1980, 1983; Mathis et al., 1988). The adult eye, on the other hand, is strongly hyperopic in water and emmetropic or slightly myopic in air. This indicates that changes in the refractive state of the eye occur at metamorphosis. Using infrared refractometry to measure the refractive state of the eye in air, Sivak and Warburg (1980, 1983) and Mathis et al. (1988) showed a progressive shift from strong myopia to emmetropia or slight hyperopia after metamorphosis. The transformations were dramatic not only because of their amplitude, but also because of the speed at which they occurred; in *Bufo sp*, Mathis et al., (1988) found an hourly increase of approximately 10 dioptres during metamorphosis. As a result, the transformations were completed within a few days. The change in refractive state of the eye is likely to result from an increase in the refractive power of the cornea and a decrease in that of the lens. The increase in the cornea's refractive effect is achieved through a change in curvature and probably protein composition (Sivak and Warburg, 1980, 1983; Mathis et al., 1988). The decrease in the refractive power of the lens is accomplished by a relative flattening and a change in protein composition (Polansky and Bennett, 1973).

Metamorphosis in anurans is associated with distinct patterns of expression of rhodopsin and porphyropsin. Generally speaking, tadpole photoreceptors contain a larger proportion of porphyropsin (Wald, 1945; Cresticelli; 1958; Wilt, 1959; Reuter, 1969).

Reuter (1969) found a "red rod" porphyropsin with maximal absorbance at 523 nm in *Rana temporaria* tadpoles. At metamorphosis, the relative abundance of porphyropsin decreased, concomitant with a shift in spectral absorbance of the photopigment extracts towards shorter wavelengths (Fig. 2, modified from Reuter, 1969). The shift was abrupt at first and eventually continued until the photoreceptors contained mostly the rhodopsin, which corresponded to a peak absorbance of 502 nm, characteristic of the adult. Interestingly, one exception to this rule appears to exist: rods in the retina of *Bufo bufo* contain rhodopsin at the larval stage and retain it in the adult stage (Muntz and Reuter, 1966).

With metamorphosis, some changes occur in the physiology and morphology of the retinal ganglion cell (RGC) layer of tadpoles. Using single unit recordings, Reuter (1969) discovered the emergence of new RGC receptive field properties at metamorphosis. A physiological type of RGC, responding to the presence of convex edges within its receptive field, was absent from the tadpole retina but was prominent in the adult. Reuter (1969) presumed this type of RGC would be most sensitive to small objects, such as insects, and believed it could "transmit the information which elicits the feeding behavior of the adult frog [...]."

Reuter (1969) further suggested that the appearance of this new receptive field type could be the result of the maturation of RGC already present in the tadpole. Findings by Pomeranz (1972), using Golgi silver impregnation, appeared to contradict this, suggesting the appearance of a new morphological class of RGC at metamorphosis. Using a more sensitive technique (HRP labelling), however, Frank and Hollyfield (1987) later

Figure 2: Wavelength of peak absorption of photopigment extracts and percent of vitamin A_2-based photopigment as a function of age in *Rana temporaria* tadpoles. As the relative amount of vitamin A_2-based photopigment decreases during metamorphosis, the peak absorbance gradually shifts towards shorter wavelengths. Open squares = percent of vitamin A_2 photopigment and filled circles = peak spectral absorption of photopigment extracts. Adapted from Reuter (1969).

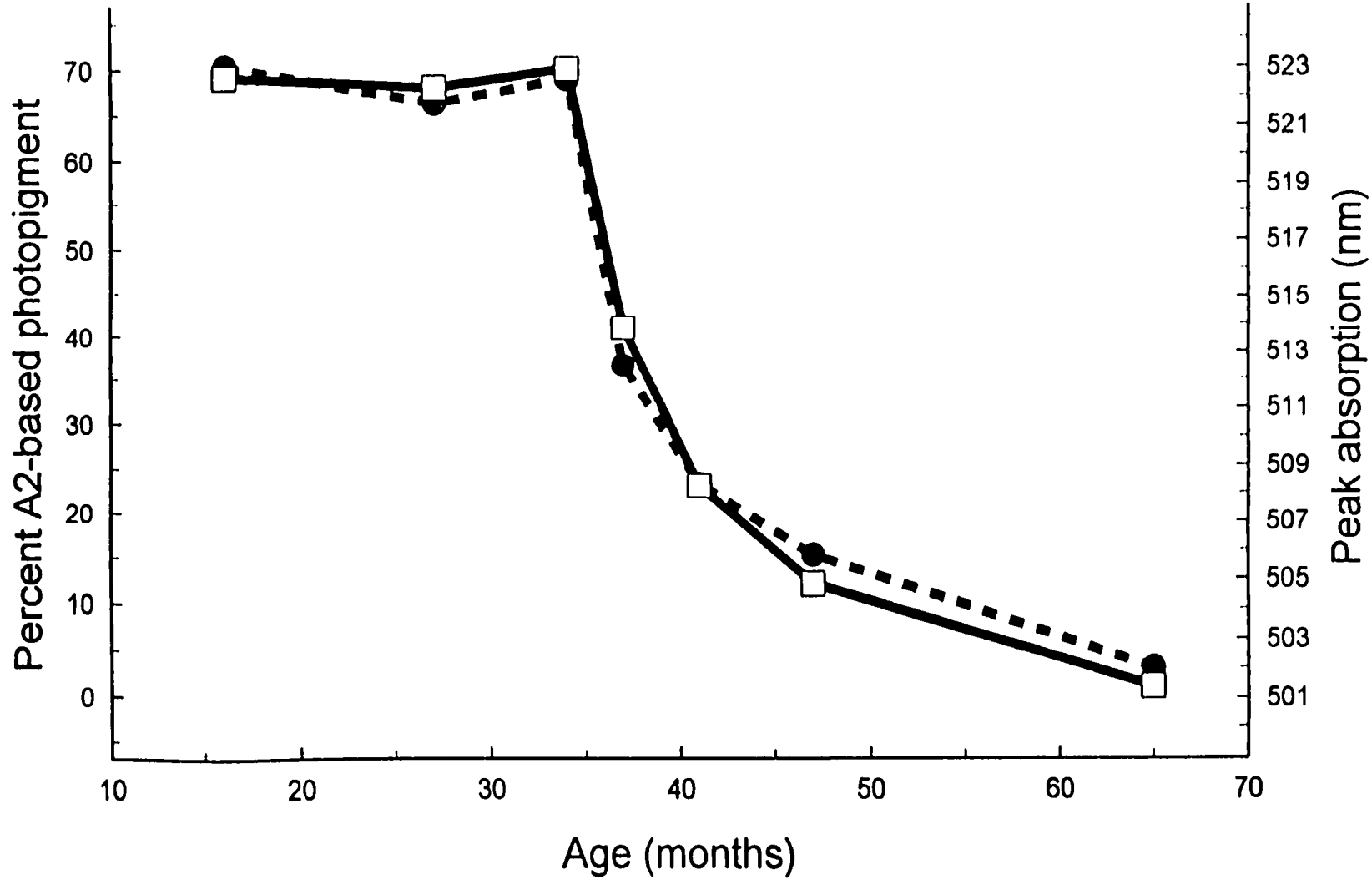
Percent A2-based photopigment
0
10
20
30
40
50
60
70
Peak absorption (nm)
501
503
505
507
509
511
513
515
517
519
521
523
10
20
30
40
50
60
70
Age (months)

confirmed that all the morphological RGC classes present in adult *Rana sp.* (7 classes in total) are also present in tadpoles. What is the anatomical basis, if any, for the difference in RGC receptive field properties? Frank and Hollyfield found a delayed dendritic development of certain classes of RGC, coinciding with metamorphosis, which they associated with the emergence of the new type of receptive field. This development was characterized by an increase in the complexity of the dendritic arbor. In *Xenopus laevis* (the African clawed toad) which retains an aquatic lifestyle throughout it life, there is no such maturation of the RGC dendritic arbors at metamorphosis (Dunlop and Beazley, 1984).

In anurans the transition from aquatic to terrestrial life is accompanied by a displacement of the eyes from a lateral to a more frontal location, permitting stereoscopic vision. Stereoscopic vision requires comparison of the signals that originate from those parts of both retinae that sample the same region of the visual field. This comparison depends on the presence of optic fibers that project to both sides of the brain: contralaterally, to the opposite side of the brain and ipsilaterally, to the same side as the eye. In tadpoles, all retinal fibers project contralaterally. Hoskins (1990) reports that a new class of ipsilaterally projecting RGCs are produced at the time of metamorphosis in anurans. These cells appear late in larval development, from the temporal retina, corresponding to the binocular visual field. The development of these fibers follows the increase in overlap between the visual field of the two eyes.

4. Salmonids

As in lamprey and eel, the general life history of salmonids is generally

characterized by two migrations. The first one occurs after smoltification, a process analogous to metamorphosis in other fishes. This process involves major physiological and morphological transformations that take place, in many cases to adapt the freshwater juvenile to the marine environment (Hoar, 1988). During this first migration, the juvenile leaves the stream where it has hatched and swims to the ocean (salmons and some trout), or to deeper strata in lakes (several trout and kokanee salmon), where it spends most of its life. The adult salmonid later returns to its natal stream to reproduce, and, in the case of Pacific salmon, to die. The visual characteristics of the parr and smolt[3] environments differ substantially. Parr live in the broad-spectrum light environment that characterizes shallow freshwater. The light environment experienced by smolts and adults is narrower in its spectrum, and is shifted to shorter wavelengths for animals that migrate to the marine environment, or longer wavelengths for animals that migrate to greater depths in lakes (Novales Flamarique et al., 1992). Feeding habits of juvenile salmonids also differ from those of adults, with young salmonids feeding mostly on small zooplankton and larger animals foraging on large zooplankton and fish. As a result, the visual system of the freshwater juvenile differs appreciably from that of the saltwater, smolted fish.

The parr retina is characterized by a relatively high cone to rod ratio. It contains both double and single cones, organized in a square pattern: four double cones form the side of a square and surround a central single cone. The pattern is completed by the presence of single cones at each of the four corners of this square arrangement. The parr

[3] Parr refers to the developmental stage at which vertical markings (parr marks) are visible on the fish's skin. This stage is associated with the freshwater environment in sea-going species, and with a zooplanktivorous lifestyle. The smolt stage follows smoltification. At this stage, the animal has lost the parr marks and, in sea-going species, has undergone the physiological adaptations to the marine environment.

retina possesses four cone and one rod visual pigments (brown trout: Bowmaker and Kunz, 1987; rainbow trout: Hawryshyn and Hárosi, 1994). The cone photopigments are sensitive to UV, short, middle, and long wavelengths, respectively, and the rod pigment to middle wavelengths.

At smoltification, the physiology and structure of the retina are transformed noticeably. Evidence suggests that sensitivity to ultraviolet light is affected at the time of smoltification (Bowmaker and Kunz, 1987; Hawryshyn et al., 1989). These studies have indicated that sensitivity to ultraviolet light disappears at the time when salmonid fishes undergo their first migration, and that this change in spectral sensitivity is accompanied by the loss of a morphological class of retinal cone photoreceptors. Histological studies have shown that a class of cones, the accessory corner cones, present in the parr stage is absent in larger juveniles or adults (brown trout: Lyall, 1957a; rainbow trout: Bathelt, 1970; brown trout and Atlantic salmon: Ahlbert, 1976). In addition, the number of rods per unit mosaic almost doubles during this period, possible reflecting an increase in visual sensitivity associated with migration to darker environments.

Several questions regarding the changes that the salmonid visual system undergoes at smoltification remain to be answered. First, although the disappearance of corner cones was presumed to be linked to that of UV sensitivity, the direct relationship between retinal structure and sensitivity to UV light had not been established at the onset of my study. More specifically, no study had related the presence of sensitivity to UV light to that of corner cones, within the same individuals. This, however, represented an important, but

missing, step towards the determination of the relation between UV sensitivity and retinal structure in salmonid fishes.

In addition, although changes that may affect the retina of salmonid fishes in the early stages of their life history have received some attention (Lyall, 1957a; Ahlbert, 1976; Bowmaker and Kunz, 1987), none has been directed at those that may occur when the animals return to their spawning grounds as adults. Since this migration is in the opposite direction to that undergone by the juveniles, one might suspect that some of the changes observed earlier in the life history are reversed at the time of the second migration. Although some experimental results have indicated the potential of the fish retina to regenerate (Braisted et al., 1994), and for salmonids to reintegrate UV cones previously lost (Browman and Hawryshyn, 1994), there is no evidence that the potential for neuronal plasticity suggested by these studies is used under natural conditions. The presence of corner cones in areas of the retina from which they are known to have disappeared would provide strong support for the argument that they are indeed produced *de novo* later in the life of salmonid fishes. This would also have far-reaching implications regarding the question of neuronal plasticity in the visual system and its adaptation to a changing environment.

Seasonal changes in photopigment characteristics

In addition to the major ontogenetic changes accompanying migration, organisms may be exposed to significant seasonal variations in their light environment. Seasons are associated with changes in a number of environmental factors, including light intensity, photoperiod, spectral characteristics and temperature. Some environments are highly

seasonal, some less so. Organisms have developed visual adaptations to cope with changing seasonal conditions, such as alterations in the spectral characteristics of their visual pigments.

As we have seen, the retina of certain groups of vertebrates possesses both vitamin A_1- and vitamin A_2-based photopigments (rhodopsin and porphyropsin, respectively) i.e. a paired-pigment visual system. In 1961, Dartnall et al. reported that in the rudd (*Scardinius erythrophthalmus*) relative proportions of rhodopsin and porphyropsin vary depending on the light regime under which the animals are kept. Under conditions of constant lighting, rhodopsin becomes dominant in the retina, whereas under constant darkness, porphyropsin becomes dominant. Rhodopsin was thus associated with the summer months and porphyropsin with winter. This lability of the paired-pigment visual system of fish in response to photoperiod has since been observed in several other species and the reader is referred to Beatty (1984) for a detailed review.

The interplay of factors contributing to a change in the proportion of the two types of pigment is complex, and the response to similar light regimes is not consistent from one species to the next. Some species respond to constant light or darkness in a manner opposite to that observed for the rudd. Hence, McFarland and Allen (1977) coined the expressions "rudd" and "anti-rudd" to refer to the two types of response.

Even within a species, seasonal variations in the behavior of the paired-pigment visual system may be manifested differently in different habitats. For example, Muntz and Mouat (1984) measured annual changes in the light characteristics of three bodies of water and the visual pigment content in brown trout that inhabit them. In all sites, they found

the retina to be dominated by porphyropsin for most of the year, with rhodopsin appearing for a few months in the summer. The increase in rhodopsin content during summer was best correlated with an increase in temperature and light intensity. In trout inhabiting the most dystrophic, reddish body of water, however, they only found a reduced amount of rhodopsin. They concluded that in such an environment dominated by longer wavelengths, porphyropsin probably increases the sensitivity of the visual system.

As we have just seen, light alone is not the only determinant of the relative proportions of rhodopsin and porphyropsin (Muntz and Mouat, 1984; Beatty, 1984). Moreover, when artificial lighting conditions were used to simulate the change of seasons, the response of cutthroat trout was opposite to that observed based on normal seasonal changes (Allen et al., 1973). This further indicates that factors other than the spectral characteristics of the environment must be considered to account for the variation in visual pigment. Temperature is one factor that has been singled out as determining behavior of the rhodopsin-porphyropsin system, even overriding the effect of light (McFarland and Allen, 1977).

II. Vision in the ultraviolet

Taxonomic distribution

The presence of vision in the ultraviolet part of the spectrum (from approximately 300 to 400 nm) in vertebrates[4] has been known for a little over 20 years, and a great deal of research has focused on this area in recent years. Ultraviolet sensitivity related to a

[4] UV vision also occurs in many invertebrate species, but this goes beyond the scope of this introduction.

specific UV-sensitive photoreceptor is common: it has been found in several species, from six of the seven vertebrate classes (Table 1). All groups, however, have not received equal attention. In the summary of the distribution of UV sensitivity in vertebrates presented in Table 1, bony fishes and birds are well represented. This undoubtedly reflects the relative effort that has been placed on examining their sensitivity to UV light and should not be misconstrued as representing the true distribution of UV sensitivity in vertebrates.

In bony fishes, UV sensitivity has been found in the relatively more recently evolved orders, of Cypriniformes, Salmoniformes, Cyprinodontiformes, Scorpaeniformes and Perciformes (asterisks on Fig. 3). UV vision has not been reported in cartilaginous fishes yet. Since several species of cartilaginous fishes inhabit environments that are rich in the UV part of the spectrum, however, it is not unreasonable to suspect the presence of UV photoreceptors in some of them as well (McFarland, 1991). At present, the lack of studies that have addressed specifically sensitivity to UV light in those other, less recently evolved bony fish orders and in cartilaginous fishes precludes any speculation on the evolution of UV vision and UV cones in fishes.

Among salmonid fishes, UV sensitivity has been found in the three genera that have been investigated (Fig. 4, Table 1). Although UV sensitivity has not been assessed in representatives of the whitefishes, the presence of corner cones in the retinal mosaic of the *Coregonus sp.* fry (Eigenmann and Shafer, 1900, cited in Ahlbert, 1969) suggests these animals may be UV sensitive.

Table 1: Distribution of ultraviolet sensitivity in vertebrates.

Animals	Technique	λ_{max}	Reference
AGNATHA			
river lamprey pineal (*L. japonica*)	EP	380	Uchida and Morita (1990)
OSTEICHTYES			
Salmoniformes			
brown trout (*Salmo trutta*)	MSP	~355	Bowmaker and Kunz (1987)
cutthroat trout (*S. clarki*)	ONR	390-400	this study, see Appendix A
rainbow trout	HRA	~360	Hawryshyn et al. (1989)
(*Oncorhynchus mykiss*)	HRA	360	Browman and Hawryshyn (1992)
	ONR	390	Beaudet et al. (1993)
	MSP	400	Kusmic et al. (1994)
	MSP	365	Hawryshyn and Hárosi (1994)
sockeye salmon (*O. nerka*)	ONR	380	Novales Flamarique and Hawryshyn (1996)
Cypriniformes			
giant danio	EP	358	Palacios et al. (1996)
(*Danio aequipinnatus*)	MSP	358	Levine and MacNichol (1979)
	MSP	360	Hárosi (1994)
Danio sp.	MSP	360	Hárosi and Fukurotani (1986)
zebrafish (*D. rerio*)	MSP	360	Nawrocki et al. (1985)
	MSP	362	Robinson et al. (1993)
roach	MSP	355-360	Avery et al. (1982)
(*Rutilus rutilus*)	OC	361-398	Douglas (1986)
	MSP	360	Downing et al. (1986)
goldfish	HRA	~380	Hawryshyn and Beauchamp (1985)
(*Carassius auratus*)	OC	--	Neumeyer (1985)
	MSP	355-360	Bowmaker et al. (1991)
	ERG	350-370	Chen and Stark (1993)
carp	MSP	377	Hawryshyn and Hárosi (1991)
(*Cyprinus carpio*)	HRA	380-400	Hawryshyn and Hárosi (1991)
Rudd	MSP	355-360	Whitmore and Bowmaker (1989)
(*Scardinius erythrophthalmus*)			
Dace	MSP	350-370	Hárosi and Hashimoto (1983)
(*Tribolodon hakonensis*)			
Notemigonus sp.	MSP	360	Hárosi and Fukurotani (1986)
Ctenopharyngodon sp.	MSP	375	Hárosi and Fukurotani (1986)

Table 1: (continued)

Animals	Technique	λ_{max}	Reference
Barbus sp.	MSP	375-380	Hárosi and Fukurotani (1986)
Scorpaeniformes			
Misgurnus sp.	MSP	360	Hárosi and Fukurotani (1986)
Cyprinodontiformes			
Fundulus sp.	MSP	360	Hárosi and Fukurotani (1986)
guppy (*Poecilia reticulata*)	MSP	--	Archer and Lythgoe (1990)
Perciformes			
Dascyllus sp.	MSP	~360	McFarland and Loew (1994)
Pomacentratus sp.	MSP	~360	McFarland and Loew (1994)
Chromis sp.	MSP	~360	McFarland and Loew (1994)
yellow perch[2] (*Perca flavescens*)	MSP	403	Loew and Wahl (1991)
AMPHIBIA			
Tiger salamander	EP	<400	Perry and McNaughton (1991)
(*Ambystoma tigrinum*)	EP		Craig and Perry (1988).
Axolotl (*A. mexicanum*)	ERG	~360	Deutschlander and Phillips (1995)
REPTILIA			
turtle (*Pseudomys scripta elegans*)	PP	--	Arnold and Neumeyer (1987)
Gecko	MSP	362	Loew (1994)
(*Gekko gekko*)	MSP	363-366	Loew et al. (1996)
lizard (*Anolis sp.*)	MSP	365	Fleishman et al. (1993)
AVES			
hummingbird	Behavior	--	Goldsmith (1980)
pigeon	ERG	370	Vos Hzn et al. (1994)
	PP	--	Palacios and Varela (1992)
	Behav	--	Emmerton and Delius (1980)
Peking robin	MSP	355	Maier and Bowmaker (1993)
(*Leiothrix lutea*)	MSP	355	Maier (1994)
	Behav	370	Maier (1994)
Zebra finch[1] (*Taeniopygia guttata*)	Behav	--	Bennett et al. (1996)
European starling[1] (*Sturnus vulgaris*)	OC	--	Parrish et al. (1984)
common grackle[1] (*Quiscalus quiscula*)	OC	--	Parrish et al. (1984)
brown-headed cowbird[1] (*Molothrus ater*)	OC	--	Parrish et al. (1984)

Table 1: (continued)

Animals	Technique	λ_{max}	Reference
dark-eyed junco[1] (*Junco hyemalis hyemalis*)	OC	--	Parrish et al. (1984)
American tree sparrow[1] (*Spizella arborea*)	OC	--	Parrish et al. (1984)
Harris' sparrow[1] (*Zonotrichia querula*)	OC	--	Parrish et al. (1984)
white-crowned sparrow[1] (*Zonotrichia leucophrys*)	OC	--	Parrish et al. (1984)
rock dove (*Columba livia*)	ERG	370	Chen and Goldsmith (1986)
ruby-throated hummingbird (*Archilocus colubris*)	ERG	370	Chen and Goldsmith (1986)
blue jay (*Cyanocitta cristate*)	ERG	370	Chen and Goldsmith (1986)
barn swallow (*Hirundo rustica*)	ERG	370	Chen and Goldsmith (1986)
black-capped chickadee (*Parus atricapillus*)	ERG	370	Chen and Goldsmith (1986)
gray catbird (*Dumetella carolinensis*)	ERG	370	Chen and Goldsmith (1986)
brown thrasher (*Toxostoma rufum*)	ERG	370	Chen and Goldsmith (1986)
wood thrush (*Hylocichla mustelina*)	ERG	370	Chen and Goldsmith (1986)
American robin (*Turdus migratorius*)	ERG	370	Chen and Goldsmith (1986)
house sparrow (*Passer domestica*)	ERG	370	Chen and Goldsmith (1986)
house finch (*Carpodacus mexicanus*)	ERG	370	Chen and Goldsmith (1986)
northern cardinal (*Cardinalis cardinalis*)	ERG	370	Chen and Goldsmith (1986)
red-winged blackbird (*Agelaius phoeniceus*)	ERG	370	Chen and Goldsmith (1986)
song sparrow (*Melospiza melodia*)	ERG	370	Chen and Goldsmith (1986)
white-throated sparrow (*Zonotrichia albicollis*)	ERG	370	Chen and Goldsmith (1986)

Table 1. (continued)

Animals	Technique	λ_{max}	Reference
MAMMALIA			
gerbil (*Meriones unguiculatus*)	ERG	360	Jacobs and Deegan (1994)
house mouse (*Mus musculus*)	ERG	359	Jacobs et al. (1991)
rat (*Rattus norvegicus*)	ERG	360	Jacobs et al. (1991)
	melatonin synth. inhib.	--	Brainard et al. (1994)
gopher (*Thomomys bottae*)	ERG	360	Jacobs et al. (1991)
golden hamster[1] (*Mesocricetus auratus*)	melatonin synth. inhib.	--	Brainard et al. (1994)

[1] Animals that exhibit UV sensitivity but for which a distinct UV cone mechanism has not been identified.
[2] The yellow perch λ_{max} 403 nm photopigment has been included in this Table because of the proximity of its λ_{max} to the near-UV wavelengths, and because it apparently resides in the accessory corner cone of the square retinal cone mosaic, a position typical of the UV cones of other fish species.
Legend for techniques used: ERG, electroretinogram; MSP, microspectrophotometry; ONR, optic nerve response recordings; HRA, heart rate conditioning; PP, other psychophysical technique; EP, electrophysiology from photoreceptors; OP, operant conditioning; behav, other behavioral techniques; melatonin synth. Inhib. light-induced inhibition of melatonin synthesis. Dashes indicate that a λ_{max} was not provided.

Figure 3: Distribution of UV sensitivity among the main orders of bony fishes. Note that at present, UV sensitivity has been recognized only in the more recently evolved orders. The reader should be aware, however, that this distribution may have been influenced by the paucity of data from those relatively less recently evolved orders. UV indicates that an independent UV mechanism has been found in at least one species that belongs to the order. The distances between the various branches of the cladogram are arbitrary.

Acipenseriformes
Osteoglossiformes
Anguilliformes
Clupeiformes
Cypriniformes UV
Salmoniformes UV
Cyprinodontiformes UV
Scorpaeniformes UV
Perciformes UV

Figure 4: Distribution of UV sensitivity in the order Salmoniformes.

UV indicates that an independent UV mechanism has been found in at least one species that belongs to the genus. The distances between the various branches of the cladogram are arbitrary.

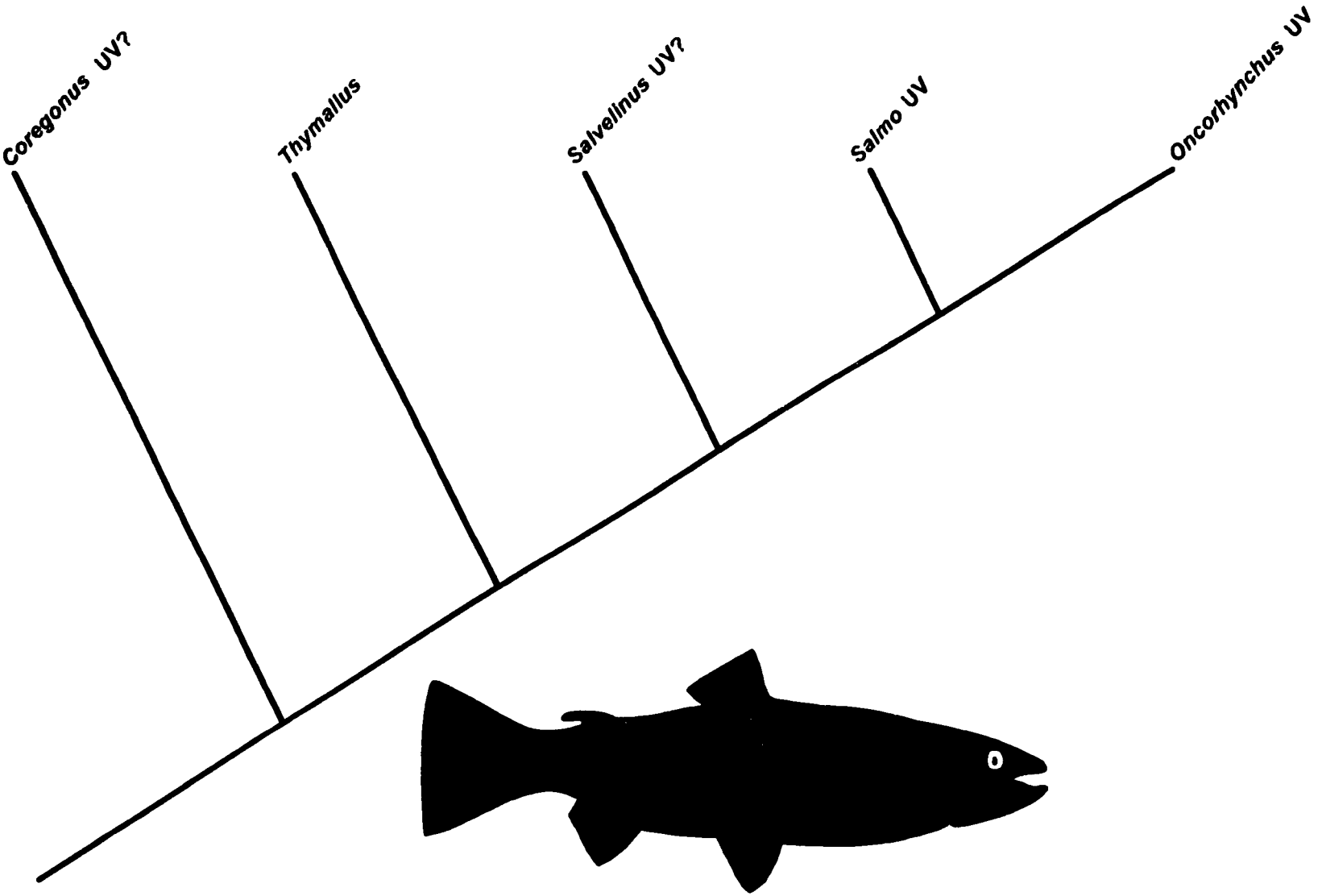
Coregonus UV?
Thymallus
Salvelinus UV?
Salmo UV
Oncorhynchus UV

Despite the lack of spectral sensitivity information, histological data suggests a widespread distribution of UV sensitivity in bony fishes. This is because, in fish, the presence of the accessory single cone, positioned at the corner of the square cone mosaic, has been associated with sensitivity to UV or violet light (Bowmaker and Kunz, 1987; Loew and Wahl, 1991; Beaudet et al., 1993; Novales Flamarique and Hawryshyn, 1996). This suggests that several species, known to possess accessory corner cones (Table 2), may prove to be UV sensitive. I argue that study of the distribution of UV sensitivity in bony fishes should initially focus on these species, as they represent some of the most likely candidates. Such an investigation would certainly contribute to our understanding of the relationships between retinal structure and function.

It can be seen from this brief discussion that our understanding of the taxonomic distribution and evolution of UV vision in vertebrates is limited by the paucity of data available. It is not known, for example, whether UV sensitivity is an ancestral character or whether its presence in the various vertebrate classes indicates UV sensitivity has appeared independently at various times during evolution. The sequence comparisons of the UV opsin genes from representatives of the various classes of vertebrates should shed some light on the origins and evolution of the UV photopigment, and UV vision. It is likely, however, that a purely phylogenetic approach will not permit a complete understanding of the processes responsible for the distribution of UV vision across the various taxonomic groups; rather, phylogenetic data will need to be interpreted within a relevant ecological context.

Table 2. Bony fish genera known to possess accessory corner cones but for which UV sensitivity has not been determined.

Order Family Genus	Reference
Perciformes	
Labridae	
Labrus sp.	Engström (1963)
Centrolabrus sp.	Engström (1963)
Crenilabrus sp.	Engström (1963)
Ctenolabrus sp.	Engström (1963)
Anarhichadidae	
Anarhichas sp.	Engström (1963)
Mugilidae	
Rhinomugil sp.	Narayanan and Khan (1995)
Scombridae	
Scomber sp.	Engström (1963)
Agonidae	
Agonus sp.	Engström (1963)
Pleuronectidae	
Platessa sp.	Engström (1963)
Pleuronectes sp.	Engström (1963)
Scorpaenidae	
Scorpaena sp.	Bathelt (1970)
Blenniidae	
Blennius sp.	Bathelt (1970)
Cyprinodontiformes	
Cyprinodontidae	
Panchax sp.	Engström (1963)
Poecillidae	
Xiphophorus sp.	Bathelt (1970)
Lebistes sp.	Bathelt (1970)
Gasterosteiformes	
Gasterosteidae	
Gasterosteus sp.	Bathelt (1970)
Spinachia sp.	Engström (1963)

Ontogeny of UV sensitivity

In the genera *Salmo* and *Oncorhynchus*, sensitivity to UV light is greatly reduced at the later development stages, after the parr-smolt transition (Bowmaker and Kunz, 1987; Hawryshyn et al., 1989; Novales Flamarique and Hawryshyn, 1996). Ahlbert (1969) suggests that the corner cones of *Coregonus sp.* may be lost during ontogeny, which would suggest that ontogenetic disappearance of UV sensitivity may also occur in this genus. Although several gaps exist in our knowledge of the distribution of UV sensitivity and its ontogenetic fate in salmonid fishes, findings to date suggest that UV vision and its ontogenetic loss is a common characteristic of the salmonid visual system.

The ontogenetic disappearance of UV sensitivity is not restricted to the order Salmoniformes, but has also been reported Cypriniformes and Perciformes (Fig. 3) (Chen and Stark, 1993; Bowmaker and Kunz, 1987; Hawryshyn et al., 1989; Loew and Wahl, 1991). Interestingly, McFarland and Loew (1994) report the late appearance of cones sensitive to UV light in the adult *Chromis sp.*, a relatively recently evolved teleost (from the Family Pomacentridae, Order Perciformes). This contrasts with the general trend observed in all the other species in which there is an ontogenetic change in the sensitivity to UV light. This late appearance of UV sensitivity suggests the evolution of UV vision and its ontogeny has followed a complex course in fishes.

The ontogenetic disappearance of UV sensitivity may be restricted to teleost fishes, as the loss of UV sensitivity in other vertebrate classes has not been documented. This could reflect the lack of data on the spectral sensitivity of animals in those other groups, particularly with respect to the ontogeny of UV sensitivity. The absence of an

ontogenetic disappearance of UV sensitivity is conspicuous in birds, however, even though they have been studied as intensely as fish (see Bennett and Cuthill, 1994 for a discussion of UV sensitivity in birds).

Functions of UV sensitivity

Undoubtedly, one of the most important and interesting questions facing visual ecologists is that of the function of UV sensitivity. What appears evident is that there probably is not a single dominant function of UV sensitivity, no more than there may a single function of red or green sensitivity (Bennett and Cuthill, 1994). Sensitivity to UV light certainly expands the range of wavelengths over which the visual system is functional. Therefore, the use of signals from the UV part of the spectrum probably contribute to increasing the richness of an animal's visually-guided behavioral repertoire. Functions that in the past have been attributed to signals originating from the "visible" part of the spectrum can now probably also be attributed to those from the UV. One such use could be communication. For example, animal coloration in the "visible" part of the spectrum has been shown to play a role in sexually driven behaviors such as mate selection or courtship (e.g. courtship behavior in stickleback, McDonald et al., 1995). Likewise, such uses have been discovered for signals that contained wavelengths from the UV part of the spectrum. For example, mate choice in female zebra finches was recently shown to be influenced by the presence of UV light reflection from the plumage of males (Bennett et al., 1996). Such use of UV signals for communication has also been suggested in anoline lizards (Fleishman et al., 1993).

Ultraviolet sensitivity may also enhance foraging ability (Tovée, 1995). UV sensitivity has been shown to influence the foraging behavior of fish. Foraging success of juvenile trout and pumpkinseed sunfish was suggested to improve slightly, but significantly, in the presence of UV light (Browman et al., 1994). Similar results were also found in yellow perch (Loew et al., 1993). Recently, a role for UV light has been postulated in foraging by a bird, the Eurasian kestrel (*Falco tinnunculus*), although it is not clear that this species possesses a specific UV cone (Vlitala et al., 1995).

A wider visible spectrum for an animal may also provide a means of overcoming camouflage mechanisms to improve predator detection. This is important as several properties of the interaction of light and matter are wavelength-dependent. Refraction, for example, is one of them and is the major cause of chromatic aberration in the optical system of animals (Fernald, 1990). The result of the wavelength-dependence of some interactions between light and matter is that optical mechanisms that are effective in one part of the spectrum are likely to be less so in other parts. One example of the exploitation of this phenomenon has been suggested recently for mantis shrimp by Cronin et al. (1994). Some fish use quarter-wave plates as mirrors on the surface of their body to reflect the ambient light and thus camouflage themselves. Cronin et al. (1994) suggest that UV sensitivity enables the mantis shrimp to "see through" this camouflage and thus detect the presence of these fish. The explanation lies in the wavelength-dependent reflectance of these structures; they cannot be effective in the middle and the UV parts of the spectrum simultaneously. For some reason, the fish have "decided" to maximize the effectiveness of their reflective surfaces for the middle wavelength part of the spectrum,

and to neglect the UV wavelengths. As a result, their ineffectiveness at reflecting UV wavelengths makes them appear dark on a bright UV background, which renders them conspicuous to the UV sensitive mantis shrimp (Cronin et al., 1994).

Another use of UV vision has been proposed recently in vertebrates. Hawryshyn et al. (1990) showed behaviorally that UV light may be necessary for rainbow trout to orient to the field of polarized light. These authors argue that the UV cone, which presents a polarization sensitivity that is orthogonal to that of the M and L cone mechanisms (Hawryshyn and McFarland, 1987), participates in a multi-mechanism detection system (Hawryshyn et al., 1990). This has been supported by the findings of UV-polarized light-sensitive RGCs in the retina of various salmonid species (Parkyn and Hawryshyn, 1994; Coughlin and Hawryshyn, 1994a, b; Novales Flamarique and Hawryshyn, 1996). Thus, a recently proposed biophysical model has postulated a role for UV sensitivity and the UV cones in polarized light detection by the salmonid retina (Novales Flamarique, 1997). According to this model, the UV cones would be stimulated by polarized light selectively reflected by the ellipsoid of adjacent double cones.

To achieve an understanding of the functions of UV vision in vertebrates will require knowledge of how UV signals are processed by the visual system. This means that knowledge of the electrophysiology and neuroanatomy of UV-carrying visual pathways is needed. When the work described in this dissertation was initiated, recordings from UV sensitive RGCs had not been reported. Thus, there was no information concerning the types of responses UV stimuli generate in the visual system. In addition, central pathways carrying UV information are still poorly understood. Despite reports of UV-sensitive

single units in the torus semicircularis of rainbow trout (Coughlin and Hawryshyn, 1994a,b), little is known of the central pathways that may carry UV information to this and other parts of the brain.

III. Retinal light and dark adaptation

Above, I described some of the changes that affect the visual system of animals in association with shifts to different light environments. Organisms, however, are also subjected to the cyclical changes in intensity and spectral quality of their environment caused by the night/day cycle. Compared to the changes that affect migrating animals, or those brought about by the passing of seasons, those associated with the diel cycle are highly dynamic, repetitive and reversible. Animals adapt to these changes partly through the processes of light and dark adaptation, which are the object of my attention in the second part of this dissertation.

Everyone has experienced the process of light or dark adaptation on moving from a dark room to the bright sunlight. During this process, sensitivity of the visual system is adjusted to conform to a different level of ambient illumination. For example, during dark adaptation, sensitivity of the visual system to light stimuli is increased so that a smaller number of photons is required to elicit a response of a given amplitude. Conversely, during light adaptation, sensitivity is decreased in such a way that more light is required to produce a response of a given amplitude. Koch (1992) defines adaptation in photoreceptors as the "mechanisms that cause a change in sensitivity and the kinetics of the photoresponse". Thus, "the relationship between a cell's response and the stimulus

changes according to the prevailing level of stimulation" (Laughlin, 1989). Its function, according to Laughlin (1989) is to "increase the amount of sensory information an organism uses". The process of adaptation is not restricted to the visual system, but is also encountered in other sensory systems (Laughlin, 1989). In this dissertation, the discussion of adaptation will be confined to the processes of light and dark adaptation as they occur in the vertebrate retina.

Light and dark adaptation are processes that occur over a relatively small time scale, in the order of milliseconds to minutes. These processes are reversible and reflect the ecological constraints that are placed on animals. Animals live in a dynamic light environment, affected by the diel light cycles of night and day, and the presence of heterogeneous brightness distributions. In fish, in addition, because of the absorptive properties of water bodies, light intensity also varies with depth, and so does its spectral distribution or color (see Novales Flamarique et al., 1992: Loew and McFarland, 1990). Light and dark adaptation expands the foraging opportunities of animals in both the spatial and temporal domains by allowing the visual system to adjust its sensitivity according to the prevailing conditions; without this ability, foraging in a given fish species, for example, would be limited to a particular depth/time of day range beyond which visually guided behaviors would lose their effectiveness. Therefore, light and dark adaptation permit movement by animals between various parts of their environment that differ in their ambient level of illumination, or allow them to continue their activities during crepuscular periods.

Adaptation is reflected in a number of the properties of responses from various cellular elements within the retina. Changes in sensitivity and time course of responses have long been recognized as representing signs of light and dark adaptation in retinal neurons, including the photoreceptors (Koutalos and Yau, 1996; Fain et al., 1996). In addition, adaptation influences the extent of physical connections between horizontal cells, between horizontal and bipolar cells, and between horizontal cells and photoreceptors (Djamgoz and Yamada, 1990). This results in changes in the geometry of retinal neuron receptive fields, and thus affects the spatial discrimination abilities of animals.

Werblin and collaborators (Normann and Werblin, 1974; Werblin, 1974; Werblin and Copenhagen, 1974) were the first to systematically and extensively study the effects of light and dark adaptation on the sensitivity of retinal neurons. Studying the mudpuppy (*Necturus sp.*) retina, they found that the decrease in sensitivity of RGCs during light adaptation resulted from successive transformations that occured at various "stages of sensitivity control" at: i) the photoreceptor, ii) the outer plexiform and iii) the inner plexiform levels. Although they found quantitative differences in the effects of light adaptation at these three levels, a constant was always present: light adaptation caused a displacement of the stimulus-response (S-R) curve along the intensity axis, and a compression of this curve along the response axis (Fig. 5A). The curve displacement results in a criterion voltage being reached at higher and higher stimulus intensities with increasing levels of light adaptation (Fig. 5A). Response compression, on the other hand, causes a decrease in the maximum response voltage that a given neuron can reach (R_{max} on Fig. 5A). Response compression and the displacement of the S-R curve are properties of

Figure 5: Summary of the effects of adaptation in the vertebrate retina.

A. Light adaptation causes a compression and a displacement of the S-R curve. **B** Adaptation also causes changes in the center-surround and color opponency in RGC receptive fields. The surround effect present in the light adapted state (outer ring on right hand side), is greatly reduced or nonexistant in dark (outer dashed ring on left hand side). Color opponency, mediated by cones, also disappears during dark adaptation, and the size of the receptive field center (inner disk on both sides) increases slightly. In addition, the cone-dominated, light adapted receptive field becomes dominated by rod inputs in the dark. **C** The interplexiform dopaminergic system feedback loop is responsible for the changes in receptive field organization. On the right hand side are the names of the main retinal layers. In the dark, neuronal connections responsible for the generation of the receptive field surround are removed (arrow heads), under the influence of dopamine (DA) released by the disinhibited interplexiform cell. AC, amacrine cell; BC, bipolar cell; HC, horizontal cell; IPC, interplexiform cell; P, photoreceptor; RGC, retinal ganglion cell. Asterisk indicates location of bipolar cell inhibitory synapse onto amacrine cell (diagrams based on various sources).

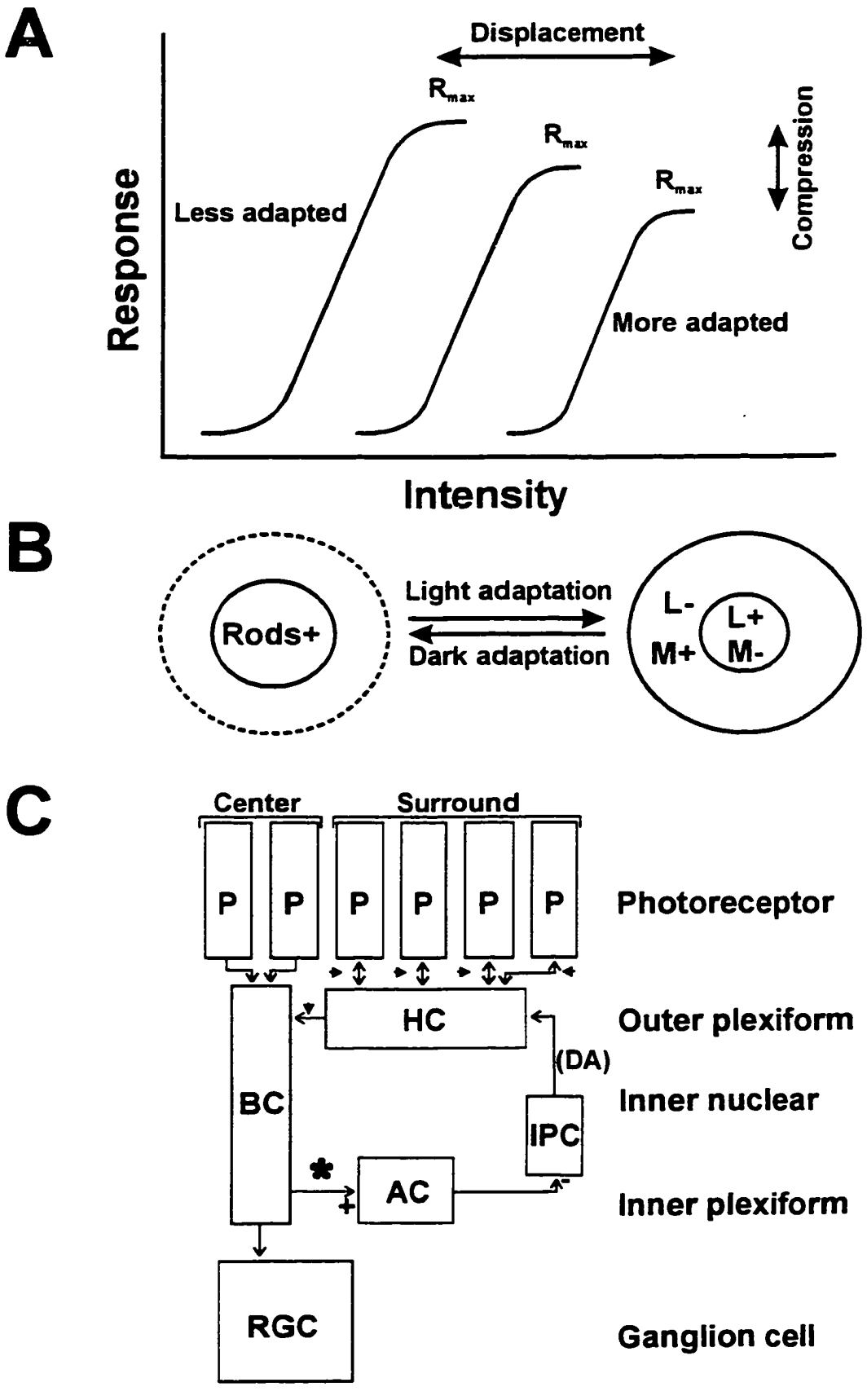
A
Displacement
R_{max}
R_{max}
R_{max}
Compression
Response
Less adapted
More adapted
Intensity
B
Rods+
Light adaptation
Dark adaptation
L-
L+
M+
M-
C
Center
Surround
P
P
P
P
P
P
Photoreceptor
HC
Outer plexiform
(DA)
BC
Inner nuclear
IPC
AC
Inner plexiform
RGC
Ganglion cell

adaptation that first emerge at the photoreceptor level. At the subsequent levels of processing in the retina, these properties are refined and modified, but nevertheless reflect the behavior of the photoreceptor responses. Therefore, understanding the effects of light and dark adaptation on the physiology of the visual system begins at the photoreceptor level, with the process of phototransduction.

The phototransduction cycle: a brief overview

In the dark, the steady state of photoreceptors is characterized by a resting potential from about -60 to -70 mV, by a steady influx of sodium (Na^+) and calcium (Ca^{2+}) ions at the outer segment level through ionic channels, and by a steady outward flow of Na^+ ions at the inner segment level. In addition, there is an exchange of intracellular potassium (K^+) and Ca^{2+} ions for extracellular Na^+ ions at the outer segment level (4 Na^+ for 1 K^+ and 1 Ca^{2+}) through an ATP-driven ion exchanger (Pugh and Lamb, 1990). The result is a positive current that flows into the outer segment and exits the photoreceptor at the inner segment level, resulting in no net current in or out of the photoreceptor in the dark.

Phototransduction refers to those biochemical events that occur between the moment light strikes the photoreceptor outer segment and the generation of an electrical signal. Phototransduction in vertebrate and invertebrate photoreceptors has long been known to require the action of a second messenger system (Cone, 1973), which was shown to involve cGMP by Fesenko et al. (1985). Figure 6 shows that phototransduction is initiated by the light activation of rhodopsin, the visual pigment molecule (Fein and

Figure 6: Phototransduction in vertebrate photoreceptors.

The solid lines indicate the processes that lead to the reduction of free cGMP in response to light stimulation. The dashed lines indicate the feedback mechanisms that tend to counteract the effects of the light stimulation. On the right hand side, the gain of the phototransduction process is dissected into the various steps of the cascade. Sites of action of calcium ions are indicated by the + and - signs, which refer to excitatory and inhibitory effects respectively. From various sources.

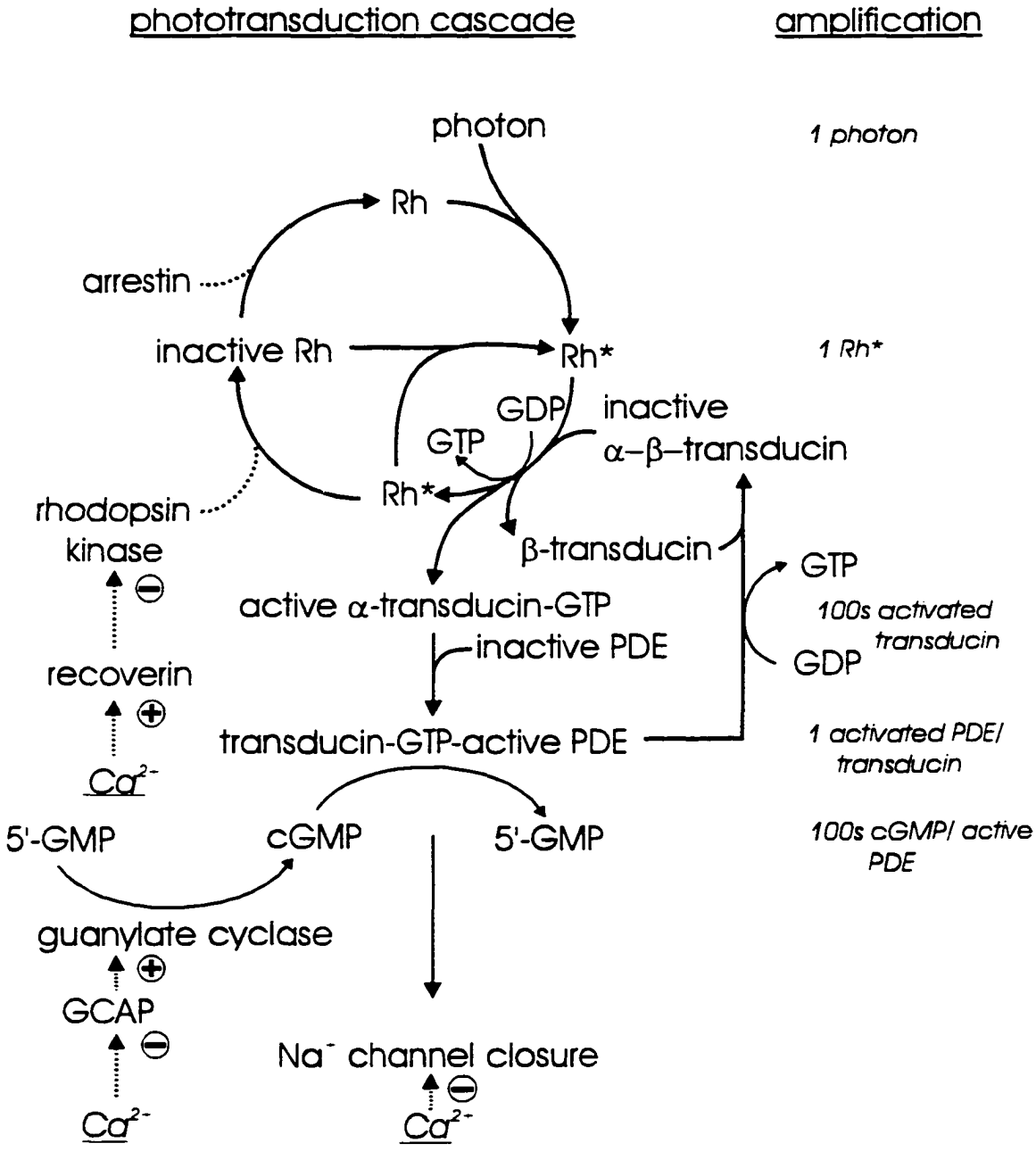
phototransduction cascade
amplification
photon
1 photon
Rh
arrestin
inactive Rh
Rh*
1 Rh*
GDP
inactive
α–β–transducin
GTP
Rh*
rhodopsin
kinase
β-transducin
GTP
active α-transducin-GTP
100s activated
transducin
inactive PDE
GDP
recoverin
transducin-GTP-active PDE
1 activated PDE/
transducin
Ca2-
5'-GMP
cGMP
5'-GMP
100s cGMP/ active
PDE
guanylate cyclase
GCAP
Na- channel closure
Ca2-
Ca2-

Szuts, 1982). The activated rhodopsin molecule (Rh*) in turn activates the protein transducin, a G-protein, which triggers the series of biochemical reactions described on Figure 6. The ultimate result of the phototransduction cascade is the reduction in the amount of cytosolic cGMP and the closure of ionic channels permeable to Na^+ and Ca^{2+} which leads to a hyperpolarization of the photoreceptor membrane.

Each step of the phototransduction cascade is coupled to a feedback mechanism that counteracts the effects generated by light stimulation of the photoreceptors (dashed lines on Fig 6). The first feedback mechanism deactivates the Rh* molecule. Rhodopsin kinase catalyzes this reaction, producing of an "inactive" Rh (Koutalos and Yau, 1996). Rhodopsin kinase is under the inhibitory control of recoverin, an enzyme whose activity is increased in the presence of calcium. Thus, in the dark, activity of recoverin is maximal. As the "inactive" Rh can activate transducin and thus to participate in the phototransduction cascade, Rh becomes truly inactive only after it is bound by arrestin, a 48kDa protein (Koutalos and Yau, 1996).

The second feedback mechanism targets the enzyme guanylate cyclase, which is responsible for the production of cGMP from 5'-GMP (Fig. 6). This enzyme is under the excitatory influence of the guanylate cyclase activating protein (GCAP). GCAP's activity is inhibited by high intracellular calcium concentration. Therefore, during light stimulation, when intracellular Ca^{2+} concentration is low, GCAP activity is increased, and cGMP production is maximal.

A third feedback mechanism involves the active transducin molecule and targets the PDE activity (Fig. 6). Intrinsic GTPase activity of the transducin molecule is

responsible for the spontaneous hydrolysis of GTP into GDP, and thus permits the re-binding of the b-subunits to the transducin molecule. This results in the inhibition of the PDE activity and a decrease in the rate of cGMP hydrolysis (Koutalos and Yau, 1996). Finally, in the light, the affinity of the cationic channel for cGMP is increased due to the decrease in intracellular calcium concentration.

Role of calcium in photoreceptor light adaptation

The photoreceptor response to a sustained light stimulus has several components. Following the onset of the stimulus, the cell's potential changes from its resting state and reaches a minimum (or a maximal hyperpolarization level) the magnitude of which depends on the stimulus intensity. The potential does not remain at this level of hyperpolarization, but settles at a lower level of hyperpolarization, at which it remains for the duration of the stimulus. The shift in potential from the maximum hyperpolarization level to the sustained level is the hallmark of photoreceptoral light adaptation. The key player in the process of light adaptation is the calcium ion (Pugh and Lamb, 1990). The importance of this ion in the process of light adaptation has been recognized in "lower" vertebrate rods since the early 1980s (Lamb and Matthews, 1988; Koutalos and Yau, 1996). Recently, Matthews (1990) convincingly demonstrated the dependence of light adaptation on intracellular calcium concentration in mammalian rod photoreceptors as well.

Calcium causes light adaptation through the multilevel system of feedback mechanisms described above. Thus, the decrease in calcium stimulates rhodopsin kinase and guanosine cyclase activities, and increases the ion channels' affinity for cGMP. The

most convincing evidence for the role of calcium in light adaptation came from experiments that used calcium buffers injected intra- or extracellularly into salamander rods (Lamb and Matthews, 1988) and guinea-pig rods (Matthews, 1991). These experiments showed that when intracellular (or extracellular) calcium concentration is prevented from decreasing following light stimulation of rods, the photoreceptor potential remains at the maximal hyperpolarization level that is reached in the early stages of the photoresponse. Hence, as the level of ambient light increases, changes in calcium concentration that result from the activation of the phototransduction cascade trigger the feedback mechanisms, which leads to a decrease in the overall sensitivity of the photoreceptor. Thus, following adaptation, more Rh* is needed to cause a response of a given amplitude, as its rate of inactivation by rhodopsin kinase is increased. In addition, more PDE is required because the rate of cGMP synthesis is increased, and so is the ion channels' affinity for it.

Light adaptation in the inner retina

Changes in ambient light levels lead to other changes, in addition to those observed at the photoreceptor level. These changes are generally referred to as neuronal (light or dark) adaptation because they take place in the synaptic or plexiform layers of the retina, and involve changes not directly related to the phototransduction cascade (Frumkes, 1990). The most obvious changes associated with neuronal adaptation in the retina are those that affect the receptive field properties of RGCs (Barlow et al., 1957). Namely, there is a reduction of center surround antagonism and color opponency during dark adaptation (Fig. 5B). For example, Donner (1981a) found that in dark-adapted frog

RGCs, area-threshold curves showed no surround effect, contrary to the situation in light adapted RGC's. Similarly, Mangel and Dowling (1987) found reduced antagonism from receptive field surrounds following dark adaptation in the carp retina. These effects of dark adaptation are probably related to the decoupling of horizontal cells from each other and from various neuronal elements within the outer plexiform layer (Fig. 5C). As center-surround antagonism in retinal ganglion and bipolar cells depends in part on extensive electrical coupling between horizontal cells, and on their connectivity to photoreceptors, changes that influence these patterns of connectivity necessarily result in the modification of receptive field properties (Mangel and Dowling, 1987).

The dopaminergic interplexiform system has been implicated in these changes (Mangel and Dowling, 1987; Lasater, 1990; Djamgoz and Yamada, 1990). Dopamine, released at the interplexiform cell terminals in the outer plexiform layer, is suspected of being responsible for initiating dark adaptation in fish horizontal cells (Mangel and Dowling, 1987; Lasater, 1990). In daylight conditions, the dopaminergic interplexiform cell is under the continuous inhibitory effects of amacrine cells (Fig. 5C, asterisk). When ambient light levels decrease, inhibition is halted and dopamine released in the outer plexiform layer, where horizontal cells are located (Fig. 5C, **DA**). Through a second messenger system that involves cAMP, dopamine binding by horizontal cells triggers a decrease in electrical coupling between horizontal cells, and a reduction in their contacts with photoreceptor synapses (Fig. 5C, arrow heads) (Mangel and Dowling., 1987). Hence the elimination of center-surround antagonism and of color opponency.

In addition to the effects described above, adaptation also causes changes in the time course of visual responses. It has been shown on numerous occasions that light adaptation causes a shortening of time-to-peak and latency of responses in vertebrate photoreceptors (Baylor and Hodgkin, 1974; McNaughton, 1990; Miller and Korenbrot, 1993). These changes in time course occur at various levels in the retina, but principally at the photoreceptor level, such that, as pointed out by Donner et al. (1995), changes observed at the RGC level, for example, can be taken as reflecting the behavior of the photoreceptors themselves. The temporal aspect of responses is important when considering the effects of light or dark adaptation on the visual system. Because much of the effectiveness of the visual system depends on the production of integrated responses by retinal neurons, inputs to these neurons from various sources not only need to be sufficiently strong to interact adequately, but they must also coincide temporally (Donner, 1981a, b). It has become clear, also, that the temporal aspect of the visual system's response to light stimuli also plays an important role in structuring the neuronal interactions that lead to visual perception in animals (Donner, 1981a, b; Gouras and Zrenner, 1979). Therefore, as adaptation influences the time course of photoreceptor responses, important consequences for neuronal coding within the retina, and possibly visual perception, may result from variations in the quantity and spectral quality of ambient illumination.

Few studies have attempted to describe the change in threshold associated with light adaptation in fish. Northmore (1977) and Hawryshyn (1991) have used psychophysical techniques to investigate the adaptational properties of the goldfish visual

system, but the technique they used did not allow them to investigate possible changes in response time course. Other studies have also addressed various aspects of light adaptation in the teleost retina (Miller and Korenbrot, 1993; Douglas, 1982a, b; Mangel and Dowling, 1987), but have not focused attention on the RGCs, nor investigated the temporal aspects of responses, despite the fact that this retinal layer represents the last level of integration before visual information is transmitted to the brain. In addition, despite the fact that the kinetic properties of photoresponses have been described in a few species, this has rarely been done quantitatively, which precludes a discussion of the comparative effects of adaptation on the vertebrate visual system.

Finally, because they differ in their spectral absorption, the various cone types are light adapted differently when ambient light contains wavelengths predominantly from one part of the spectrum (Enoch, 1972). This is likely to generate discrepancies in the threshold and time course of responses among the various cones. As neuronal interactions within the visual system often involve inputs from different spectral classes of cones, changes in their relative state of adaptation may have important repercussions on an organism's vision. The temporal aspect of this differential adaptation, however, has not been investigated to date.

Summary and objectives

The first section of this chapter described several strategies that are used by animals to presumably maximize the efficiency of their visual system when migrating to a different environment, or when subjected to seasonal environmental changes. The changes

associated with the various types of migrations have been summarized in Figure 1. Changes associated with these migratory events vary dramatically in their extent and are represented at one extreme by the major morphological and histological transformations undergone by flatfishes, and by more subtle ones affecting the visual pigments of returning sea lamprey at the other extreme. At the center of this spectrum of visual system changes are found the salmonid fishes, which have been shown to undergo both changes in their spectral sensitivity and the structure of their retina during smoltification. Questions regarding the relationship between retinal structure and spectral sensitivity in salmonids, regarding the distribution of central UV inputs and the possible return of UV vision and UV cones later in life still remain to be answered.

In chapter 2 of this dissertation, I investigate the ontogenetic loss of UV sensitivity in rainbow trout by correlating the spectral sensitivity of responses recorded from optic nerve fibers with the structure of the retina in the same individuals. To do this I used a multi-unit recording technique that provides basic information on the coding of UV information in the RGC layer. In chapter 3, I continue the investigation of the ontogeny of UV sensitivity in the salmonid retina by studying the topography of cone photoreceptors in large, sexually mature salmonids, returning to their natal stream to reproduce. The aim of this particular study is to test the hypothesis that the loss of corner cones that occurs at smoltification is reversed when the organisms undertake their return migration.

In section II, I indicated that UV vision is quite common among vertebrates. However, not enough information is available to permit a clear understanding of the evolution and biology of UV vision in vertebrates. The physiological and anatomical

aspects of UV vision are also poorly understood. Little is known, for example, of the anatomy of the visual pathways involved in the transmission of UV information to various visual centers of the brain. Although it is known that the torus semicircularis of the mid-brain in rainbow trout is a center for the integration of UV information (Coughlin and Hawryshyn, 1994a, b), pathways from the retina to this structure have not been identified. Thus, in chapter 4, I investigate the connections of the retina and torus semicircularis using double labelling techniques. The goal of this study is to label areas of the brain where retinal projections and torus semicircularis connections converge, and thus identify the possible pathways between the retina and torus semicircularis. This work should facilitate future electrophysiological investigations by indicating the structures most likely to carry visual information, particularly from the retina to the torus semicircularis.

Finally, in section III, I discussed the processes of light and dark adaptation, as they occur in photoreceptors, and also in the deeper layers of the retina. Changes in sensitivity and receptive field organization were some of the important effects of adaptation on the vertebrate retina. This discussion highlighted some gaps in our knowledge, particularly those pertaining to the effects of adaptation on fish RGCs. The need to examine changes in sensitivity and time course of responses during adaptation was also underlined. In chapters 5 and 6, I investigate the effects of various intensities and spectral characteristics of ambient light on multi-unit responses recorded from optic nerve fibers. In chapter 5, I examine how increases in the level of ambient light affects response threshold and time course. Chapter 6 investigates how varying the relative state of adaptation of the various spectral types of cones influences their relative sensitivity and

response time course. The information contained in these two chapters, I believe, will further our understanding of the effects of adaptation on retinal physiology in rainbow trout, and possibly in bony fishes in general.

The preceding discussion indicates that a substantial amount of knowledge has been garnered regarding the structure and function of the vertebrate visual system in the recent decades. Nonetheless, there are numerous questions that remain unanswered within the general fields of visual ontogeny, UV vision and visual adaptation. This dissertation addresses several of these questions, and attempts to improve our understanding of the ecology of visual systems in general, and the visual system of salmonids in particular.

Chapter 2: Optic nerve response and retinal structure in rainbow trout of different sizes[5].

Introduction

Several studies have characterized the UV sensitivity in fish, using psychophysical techniques (Hawryshyn and Beauchamp, 1985; Neumeyer, 1985; Douglas, 1986; Hawryshyn et al., 1989; Hawryshyn and Harosi,1991; Hawryshyn, 1991) and microspectrophotometry (Avery et al., 1983; Harosi and Hashimoto, 1983; Bowmaker and Kunz, 1987; Hawryshyn and Harosi, 1991; Bowmaker et al., 1991; Kusmic et al., 1992). These studies describe a UV cone mechanism, and a photopigment maximally sensitive to 355-380 nm light. In addition, in some cyprinids, recordings have been made from tetraphasic horizontal cells, bipolar and amacrine cells, which are sensitive to UV light (Harosi and Fukurotani, 1986; Hashimoto et al.,1988). To date, no study has examined the physiological response of RGCs to UV light.

Retinal ganglion cells convey visual information to the brain. This information leaves the retina by two different functional pathways: ON- or OFF-type ganglion cells (Wheeler, 1979; DeMarco and Powers, 1991). The ON-type carries information relative to increments in light intensity, whereas the OFF ganglion cells carry information about decrements in light intensity. Multiunit responses (ONR) recorded from the optic nerve provide information on the spectral characteristics of these two information channels (Wheeler, 1979).

---

[5] Published in a modified version as Beaudet et al. (1993).

Juvenile rainbow trout (*Oncorhynchus mykiss*) experience a normal developmental loss of UV photosensitivity (Hawryshyn et al., 1989). In this study, I used a combination of electrophysiology and light microscopy to investigate this developmental event. I characterized the spectral sensitivity of ON and OFF responses recorded from the ONR of small (18-28.5 g) rainbow trout, paying particular attention to UV sensitivity, and compared it to that of larger individuals (59.5-835.0 g). Examination of the retinal cone mosaic in small and large fish allowed correlation between the observed loss of UV sensitivity and the disappearance of a class of cone photoreceptors.

Material and methods

Rainbow trout (Fraser Valley Trout Hatchery, Abbotsford, B.C.) were maintained at 15^{o} C under a 12:12 hr light:dark photoperiod for at least 8 weeks prior to the experiments. Fish were fed daily with a constant ration of BioDiet Grower pellets (BioProducts Inc., Warrenton, Ore.). The experiments were performed between 10:00 and 18:00 hr. Illumination in the holding facility was provided by fluorescent bulbs at an intensity of 33.54 +/- 14.39 mW cm^{2} (integrated irradiance, 200-1100 nm, measured with a Photodyne Inc. radiometer). The small fish used in these experiments weighed between 18.0 and 28.5 g and the large ones between 59.5 and 914 g (Table 3).

Surgical procedures

Fish were anesthetized by immersion in MS-222 (tricaine methanesulfonate, 0.1 g/l), paralyzed by intramuscular injection of Pavulon (pancuronium bromide, 0.038 mg/g body weight) and respired with water flow (400 ml/min., 15° C) over the gills. A local

Table 3. Weight and total length for the rainbow trout used in the experiments.

Fish #	Weight (g)	total length (mm)
HC1	21.0	125
HC2	18.0	125
HC3	20.5	135
HC9	24.0	140
HC11	28.5	140
T1	59.5	185
L2	835.0	410
L4	756.0	370
L7	713.0	385
L9*	914.0	405
L10	85.0	210

* not used in the electrophysiology experiments

anesthetic was applied to the surgical area (tetracaine, 0.5%). The recording area was accessed by removing the tissues over the rostral optic tecta. During the surgery and the recording session, the physical condition of the fish could be monitored by direct observation of the regularity and strength of the tectal surface blood flow.

Recording technique

Optic nerve responses (ONR) were obtained by inserting a tapered Teflon-coated silver wire (0.45 mm diameter; A-M Electronics, WA) through the rostral optic tectum and into the lumen of the optic nerve, at the level of the optic chiasm. A reference electrode was inserted into the olfactory epithelium. The large size of the electrode allowed a direct visual evaluation of its position during preliminary studies. Subsequently, the electrode was positioned using stereotaxic reference points based on these initial assessments. The accuracy of electrode position was also evaluated by monitoring the configuration of the components of the response (see below). Signals were differentially amplified 50,000 times by a Grass preamplifier (P50 Series) with bandpass 0.3 Hz-0.1 kHz and displayed on an oscilloscope (see Fig. 7 for experimental set up).

The optic nerve response

The recording technique I used in this study monitors the activity of the major populations of fibers active within the optic nerve (Vanegas, 1974). The ONR is characterized by a sharp negative deflection of the baseline usually followed by a positive deflection, at the onset (ON) and at the termination (OFF) of the stimulus (Fig. 8a). Its amplitude depends on the intensity of the stimulation. In addition, at certain wavelengths,

Figure 7: Diagrammatic depiction of the optical and recording setup.
A/D, analog to digital converter; Amp, amplifier; F, Faraday cage; IF, interference filters; M, monochromator; ND neutral density filters; Oscil, oscilloscope; Ref, reference electrode; Rec, recording electrode; S1, stimulus light source; S2 background light source; Sh, shutter; W neutral density wedge.

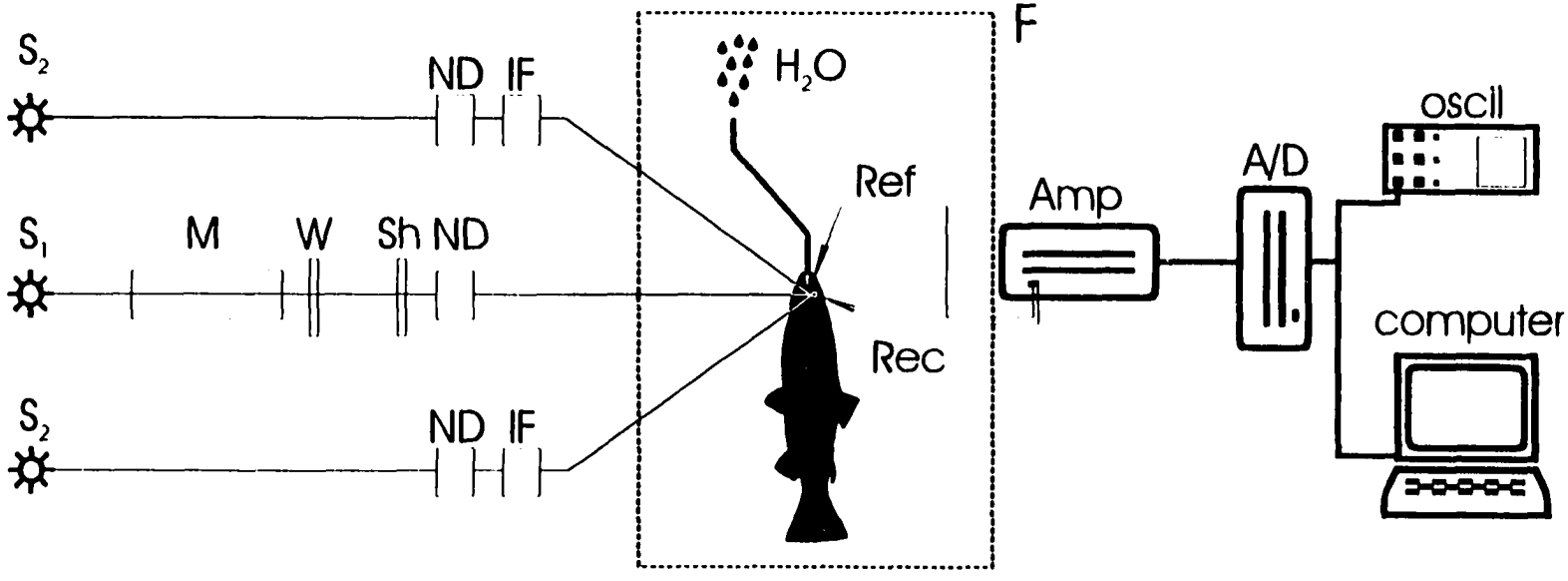
S2
ND IF
S1
M W Sh ND
S2
ND IF
H2O
Ref
Rec
F
Amp
A/D
oscil
computer

Figure 8: Optic nerve response traces and sensitivity determination

(a) Optic nerve responses to a 580 nm stimulus of increasing intensity (two responses averaged per trace). The intensity of the stimulation was increased by 0.1 log unit starting from the bottom. The amplitude measured was that of the first deflection (negative) for both ON and OFF responses. Negative upward. (b) Amplitude of the responses in (a) plotted against the intensity of the stimulations. A third order polynomial function fitted to the data points was used to determine the criterion intensities.

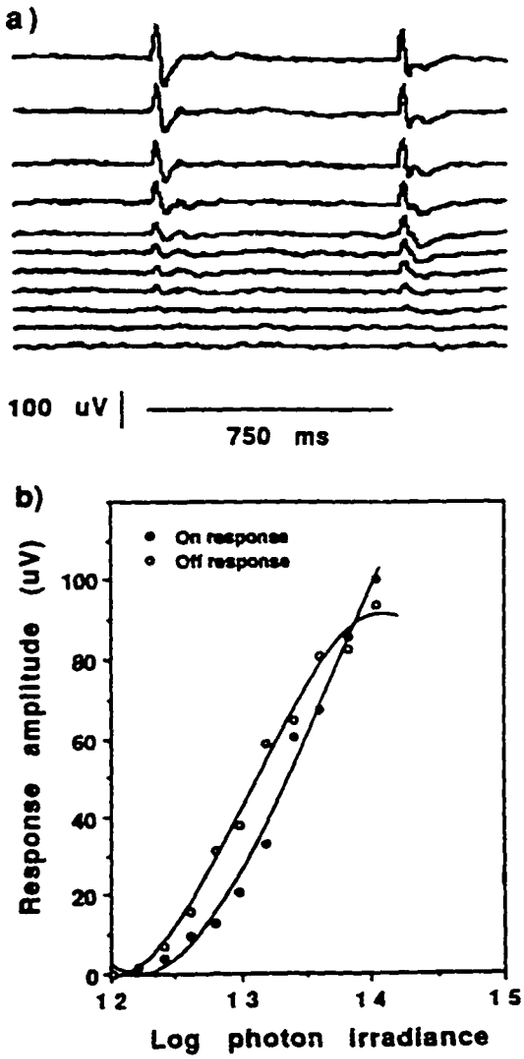
a)
100 uV
750 ms
b)
On response
Off response
Response amplitude (uV)
0
20
40
60
80
100
1 2
1 3
1 4
1 5
Log photon irradiance

I observed the presence of secondary negative peaks with longer latencies; either at the ON or at the OFF. This has also been observed by DeMarco and Powers (1991).

Stimulus and background conditions

A 150 W Xenon lamp was used as a light source for the stimulus. An Inconel coated neutral density wedge (nominal 4.0 neutral density) was used to control the stimulus intensity and a monochromator (ISA) to control its spectral characteristics. The stimulus consisted of a 750 ms square wave pulse of given intensity and wavelength, generated by a shutter controlled by computer. Combinations of interference (500 nm long pass and 650 nm long pass, Oriel Corp.) and neutral density filters were used to produce an adapting background from two tungsten-halogen light sources. The colored background was used to selectively adapt the middle (M)- and long-wavelength (L) cone mechanisms, favoring expression of the short-wavelength (S) and, if present, the UV cone mechanisms. The stimulus and the background illumination were projected onto the fish's eye via UV-transmitting liquid light guides (Oriel Corp.), positioned to produce overlap of the illumination from all three optical channels onto the ventro-temporal quadrant of the retina. For each wavelength-intensity combination, the energy measured in W/cm^2 was converted to quantal irradiance.

Experimental procedures

Prior to each experiment, the fish were subjected to the adapting background for a minimum of 1 hr. Each test wavelength was presented in a series of increasing intensities (0.1 log unit steps), superimposed over the adapting background. In this way, a series of responses (ON and OFF) of increasing amplitude were recorded and used to produce

stimulus-response (S-R) curves (Fig. 8a). For each intensity, two or three responses were averaged, depending on the clarity of the signal, and the amplitude of ON and OFF first negative deflections measured. Usually, thirteen test wavelengths, covering the spectrum from 360 to 660 nm, were presented in an order preventing selective adaptation of any one cone mechanism. In some cases the amount of energy generated by the stimulus source was insufficient to allow testing wavelengths >580 nm.

I recorded from more individuals than those for which I report the results in the present paper. This means that I eliminated experiments from the data set. The data were discarded for some or all of the following reasons: i) the animal died before the experiment could be completed. In this case, the death of the animal indicated that its state of health was not optimal and suggested that some or all the results obtained in the course of the experiment may have been affected. ii) Points repeated at the end of the experiment would not coincide with those recorded earlier, indicating that an overall shift in sensitivity had occurred, in which case, again, the data were deemed uncertain. iii) Unexpected animal movement resulted in shift in animal position. Therefore, the results reported herein were collected during experiments not plagued by the problems just mentioned.

Analysis of the ONR responses and threshold determination

The amplified signal was digitized through an A/D board and analyzed by computer during the experiment. For each wavelength-intensity combination, the amplitude of the ON and OFF negative deflection was measured and the averaged prestimulus noise band (200 ms prestimulation) subtracted from it. At each wavelength, the amplitude of the ON and OFF responses was plotted against log photon irradiance

(Fig. 8b). A third order polynomial function was fitted to the ON and OFF amplitude-intensity data points (Fig. 8b). Thresholds were calculated from the irradiance required to produce a criterion response of 30 μV. The criterion response was selected at a relatively low level to ensure that the sensitivity of the RGCs receptive field center was measured (see Discussion).

The photopigment absorption curves fitted to our spectral sensitivity data were generated by an eighth order polynomial template for vertebrate cone visual pigments (Bernard, 1987; Gary D. Bernard, personal communication). These absorption curves were corrected for the differential absorption of small and large fish ocular media, as determined by Hawryshyn et al. (1989).

Retinal histology

At the end of each experiment, fish were light adapted for 30 min, euthanized by decerebration and the retinae removed for histological study. Fixation, postfixation and embedding of retinae were performed following the protocol used by Ali and Anctil (1976). Tangential sections (1 μm) at the level of the cone inner segments were made and stained with Richardson's stain. The stimulated area was examined to determine whether accessory corner cones were present. All of the procedures described in this paper were in accordance with the regulations of the Canadian Council for Animal Care.

Results

Spectral sensitivity of the ON response

Small fish. In small fish subjected to an M+L adapting background, the ON response revealed the presence of a UV sensitivity peak (Fig. 9a). This peak matched a photopigment absorption curve of λ_{max} 390 nm. However, the sensitivity of the short wavelength limb of its action spectrum was slightly lower than predicted by the photopigment absorption curve. In addition to the UV peak, a short-wavelength sensitivity peak was present and matched best the absorption spectrum of a photopigment with a λ_{max} at 420 nm (Fig. 9a). Under these background conditions, the relative sensitivity of the ON response to mid and long wavelengths was approx. 1 log unit lower than those of the UV and short (Fig. 9a).

Large fish. The spectral sensitivity of the ON response in large fish was characterized by a single peak with a λ_{max} in the short-wavelength part of the spectrum (Fig. 9b). The action spectrum of this cone mechanism matched the absorption curve of a photopigment with a λ_{max} at 420 nm. The UV sensitivity peak was not present in these fish. Although the same background conditions were used for both small and large fish, the relative sensitivity of the response to longer wavelengths (above 540 nm) differed (Fig. 9a,b). In small fish, sensitivity to these wavelengths decreased steadily to a relative sensitivity 2 log units lower than for the UV and S peaks (compare sensitivity at 390nm with that at 580 nm, for example). In large fish, however, sensitivity in this range remained more or less constant at about 1 log unit below that of the S peak. In addition, sensitivity could be recorded up to 660 nm in large fish; this was not possible in small fish.

Figure 9: Spectral sensitivity of the optic nerve ON response in (a) small (<30g) and (b) large (59.5-835g) rainbow trout, under a mid+long-wavelength adapting background.

390 and 420 nm λ_{max} photopigment absorption curves (solid lines), corrected for ocular media absorption, were compared to the sensitivity points in the small fish. A 420 nm λ_{max} photopigment absorption curve, corrected for ocular media absorption, was compared to the sensitivity points in large fish. Means ± SD.

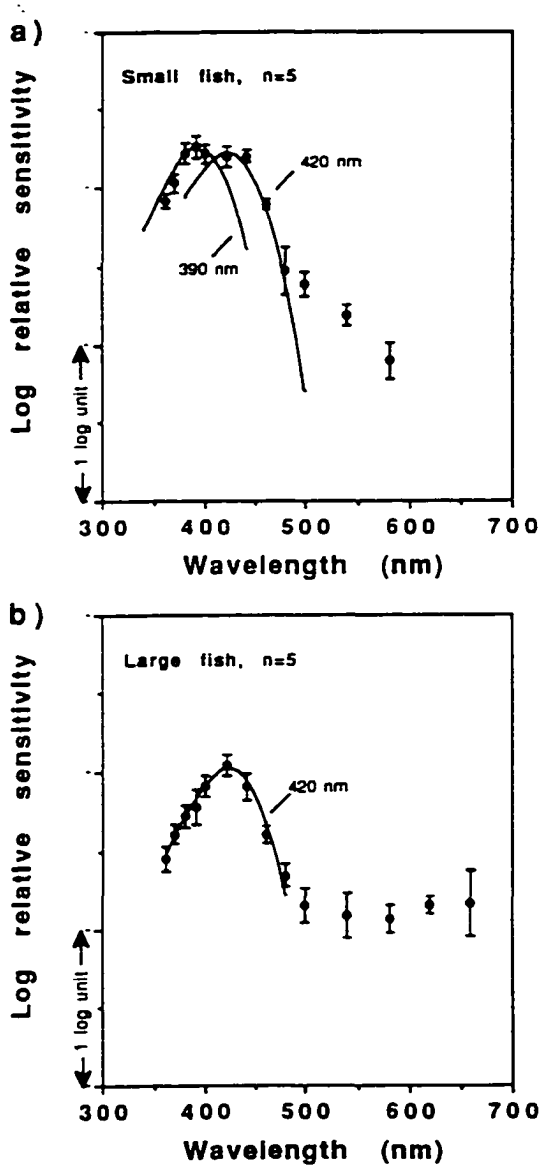
a)
Small fish, n=5
420 nm
390 nm
1 log unit
Log relative sensitivity
300
400
500
600
700
Wavelength (nm)
b)
Large fish, n=5
420 nm
1 log unit
Log relative sensitivity
300
400
500
600
700
Wavelength (nm)

Spectral sensitivity of the OFF response

In both small and large fish, the spectral sensitivity of the OFF response was characterized by a single peak in the mid-wavelength part of the spectrum. In small fish, this peak matched closely the absorption curve of a photopigment with a λ_{max} at 510 nm (Fig. 10a). In large specimens, it matched the spectral absorption of a photopigment with a 520 nm λ_{max}. Furthermore, there was a discrepancy between the pigment absorption curve and the sensitivity points on the long-wavelength limb of the sensitivity peak. These points were more sensitive than predicted by the absorption curve (Fig. 10b).

Retinal histology

The ventro-temporal retina of the small fish from which the spectral sensitivity curves were obtained showed a square cone mosaic which included accessory single corner cones (Fig. 11a). The square mosaic was composed of four double cones whose axes were directed toward a central single cone. The accessory single cones occupied the corners of a square having its sides running perpendicular to the double cones middle axes (Fig. 11a).

The retina of large fish exhibited a square cone mosaic lacking accessory corner cones in the ventro-temporal part of the retina (Fig. 11c). However, the arrangement pattern of the cones showed heterogeneity, ranging from a square mosaic in the central retina to a row mosaic at the periphery. Furthermore, I found that the absence of a UV peak in the large fish is not correlated with a complete absence of the corner cones from the retinal mosaic: in two large fish (L10, 85 g and L9, 934 g), I found a restricted area of the central retina, located near the optic nerve head and the embryonic fissure, where

Figure 10: Spectral sensitivity of the optic nerve OFF response in (a) small (<30g) and (b) large (59.5-835g) rainbow trout under a mid+long-wavelength adapting background.

510 nm λ_{max} and 520 nm λ_{max} photopigment absorption curves (solid lines), corrected for ocular media absorption, were compared to the sensitivity points in small and large fish respectively. Means ± SD.

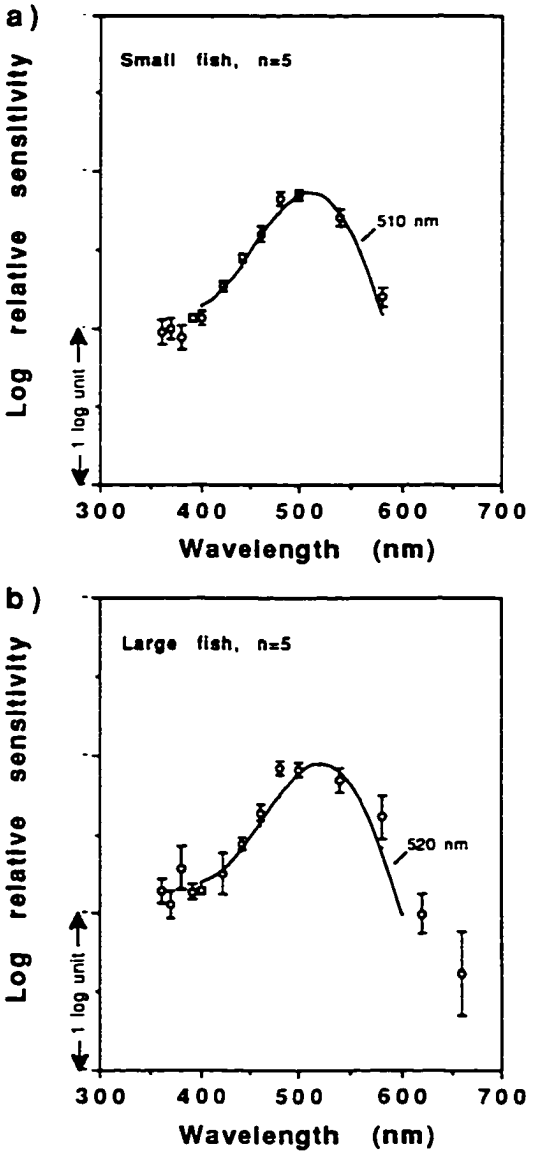
a)
Small fish, n=5
510 nm
Log relative sensitivity
1 log unit
300
400
500
600
700
Wavelength (nm)
b)
Large fish, n=5
520 nm
Log relative sensitivity
1 log unit
300
400
500
600
700
Wavelength (nm)

Figure 11: Spectral sensitivity and cone mosaic in individual rainbow trout.
(a) Tangential section (1 μm thick) through the inner segments of photoreceptor cells in the temporo-ventral retina of a small rainbow trout (18 g) whose spectral sensitivity is illustrated in (b). (c) Tangential section (1 μm thick) through the inner segments of photoreceptor cells in the temporo-ventral retina of a large rainbow trout (85 g) whose spectral sensitivity is illustrated in (d). Spectral sensitivity curves were obtained under a UV-S wavelength isolating background. Solid circles, ON response; open circles, OFF response; **d**, double cone; **c**, central single cone; **a**, accessory corner cone; scale bar=10μm.

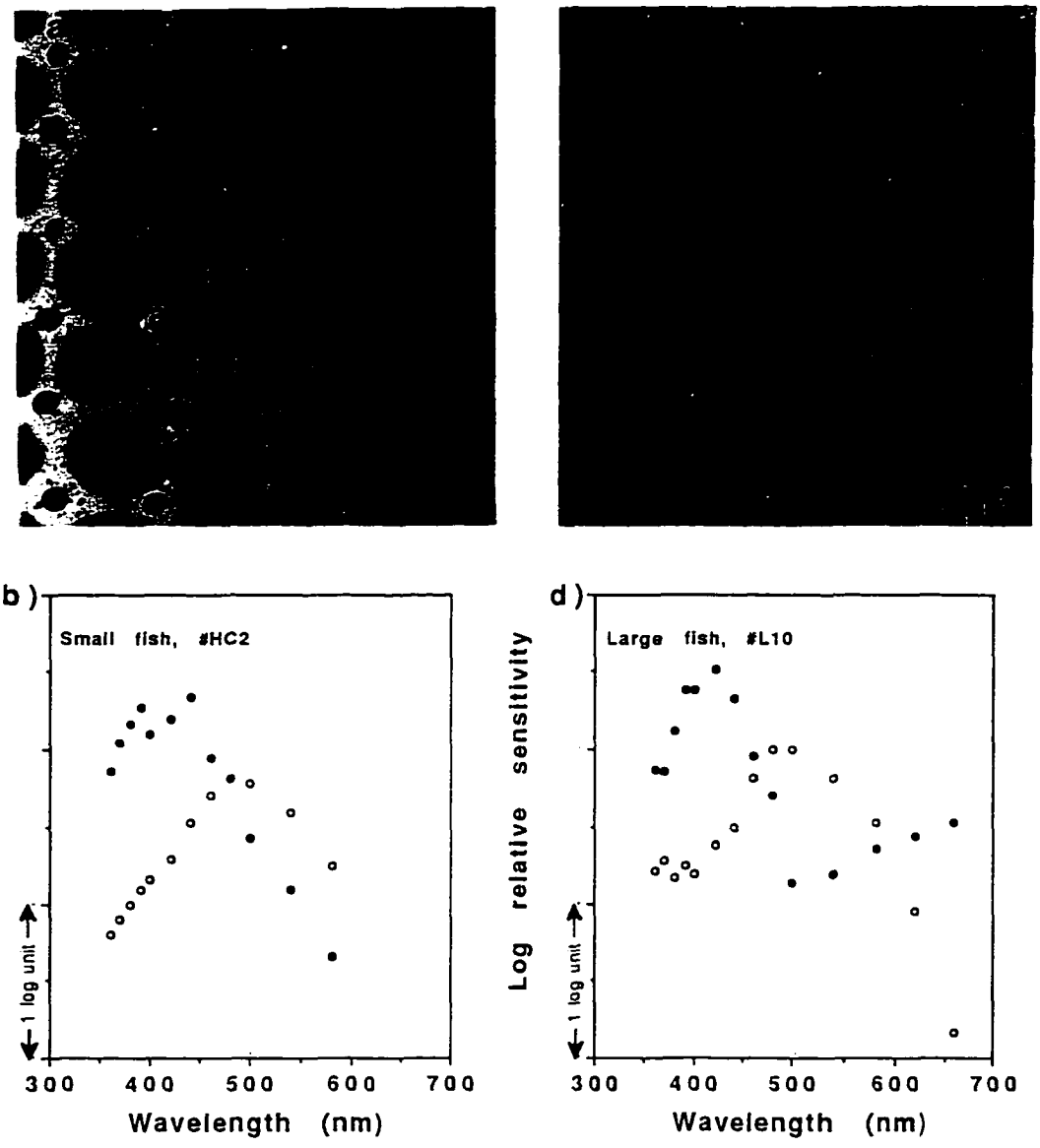
b)
Small fish, #HC2
Log relative sensitivity
1 log unit
300
400
500
600
700
Wavelength (nm)
d)
Large fish, #L10
Log relative sensitivity
1 log unit
300
400
500
600
700
Wavelength (nm)

Figure 12: Resident population of corner cones in the large rainbow trout retina.

Figure 12. Tangential sections (1 μm thick) through the inner segments of photoreceptor cells in the vicinity of the optic nerve head of (a) rainbow trout L9 (914 g) and (b) rainbow trout L10 (85 g). On this Figure, only the accessory corner cones, **a** have been indicated. Scale bar=10μm.

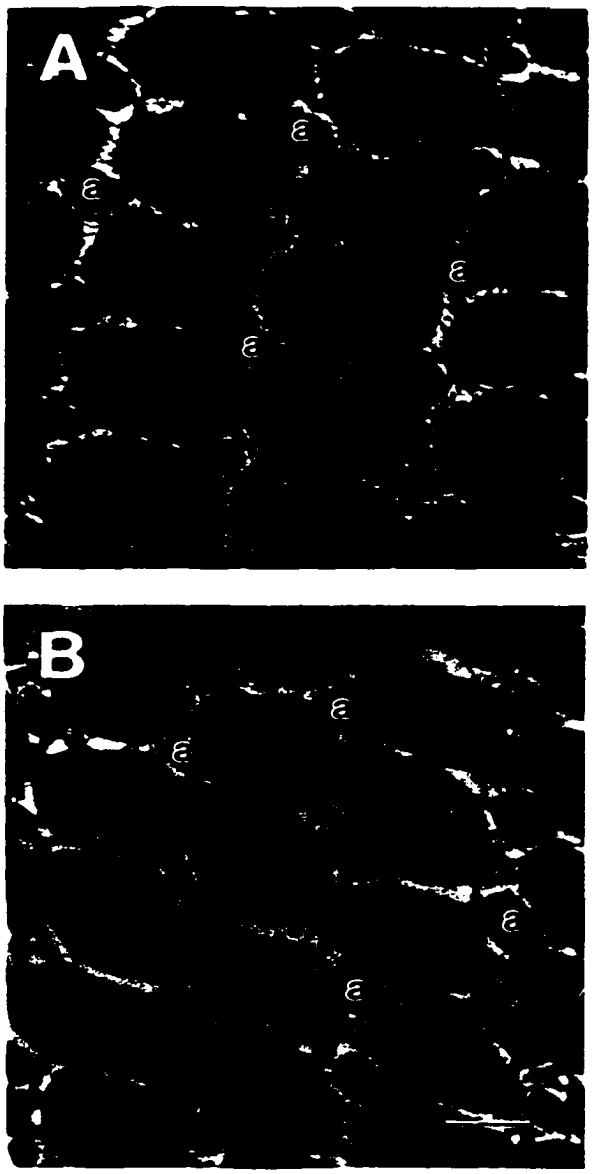
A
B

accessory corner cones were present (Fig. 12a, b). These corner cones appeared to be few in number, however.

Discussion

The ONR

Both the center and periphery of a large number of RGCs receptive fields are stimulated under broad field illumination. As a result, ONR recordings reflect the simultaneous activity of several classes of fibers which might differ in their spectral characteristics, absolute sensitivity, latencies etc. For example, a 400 nm light stimulus might trigger a response from the center and/or the periphery of UV- and/or S-wavelength-sensitive ganglion cells. Hence, care must be taken when interpreting this type of response and, especially, when trying to relate its characteristics to the activity of specific cells as is done with single unit recordings. However, if we operate under the following assumptions, information extracted from ONR recordings reveals characteristics of specific classes of RGCs.

The first assumption is that at threshold, or slightly above it, the sensitivity of the RGCs center is higher than that of its periphery. In goldfish, the sensitivity of the receptive field center can be 10-20 times that of the periphery (Daw, 1968; Spekreisje et al., 1972). The first assumption is that rainbow trout RGCs share more or less the same properties as the goldfish's, and that under stimulation of moderate intensity (up to about 1 log unit suprathreshold), the response recorded reflects the activity of receptive fields center. At higher intensities, the periphery may begin to inhibit response of the ON center as has been observed in single unit recording experiments (Spekreisje et al., 1972).

The second assumption is that at low intensity, the contribution of the isolated cone mechanism to the response is predominant. Under this assumption, peaks of sensitivity represent the activity of discrete cone mechanisms. At higher intensities, more than one cone mechanism might be stimulated, especially at wavelengths located between the sensitivity peaks of two cone mechanisms. In such cases, the ONR would represent the activity of a more or less heterogeneous population of optic fibers.

Optic nerve fibers sensitive to ultraviolet light

Our results show that under a UV isolating background, the UV cone mechanism mostly contributes to the ON response. I interpret the UV sensitivity peak as reflecting the activity of UV-sensitive, ON center ganglion cells within the retina of small rainbow trout. It is not possible to determine whether the UV input to the center of these cells is the only one or one amongst several. The lack of an OFF response sensitivity peak in the UV and S wavelength part of the spectrum suggests an absent or reduced contribution of the UV cone mechanism to the OFF response. This also indicates an absence, or a greatly reduced number, of UV sensitive, OFF center RGCs (see chapter 6 for a more detailed discussion of the spectral sensitivity of the OFF response).

When a sensitivity peak is obtained in the UV part of the spectrum, there is the possibility that it results from β-band absorption by M or L photopigments. Under the background conditions used in this study, the relative sensitivity of the M and L cone mechanisms' ON response was 1.0-1.5 log unit lower than that of the UV and S cone mechanisms. Hence, β-band absorption cannot account for the presence of the UV peak

since the relative sensitivity of the β-band of a photopigment is usually 0.5-0.8 log unit lower than that of the α-band (Beauchamp and Lovasik, 1973).

Comparison of ON response spectral sensitivity with psychophysical data.

The ON response action spectrum approximates the UV and S cone mechanisms action spectra as determined in small rainbow trout using a heart-rate conditioning protocol (Hawryshyn et al., 1989; Browman and Hawryshyn, 1992). The ON spectral sensitivity curve in the UV-short wavelength part of the spectrum is characterized by two maxima, indicating the presence of at least two cone mechanisms. However, the λ_{max} of the UV cone mechanism characterized here (390 nm) differs from that reported (360 nm) by Hawryshyn et al.(1989) and Browman and Hawryshyn (1992). These results indicate that the two techniques, although they yield similar results, are not directly comparable. That different techniques lead to somewhat different results has already been discussed (Neumeyer, 1984; Neumeyer and Arnold, 1989). In some cases, different techniques may yield differing action spectra, and even differing numbers of cone mechanisms for a species (Northmore, 1973; Goldsmith, 1994). Similarly, different techniques have also been shown to yield spectral sensitivity functions that differed in their λ_{max}, as was the case in the study by Hawryshyn and Hárosi (1991), who compared UV photoreception in carp using microspectrophotometry and heart-rate conditioning. It is interesting to note, however, that heart-rate conditioning, the technique used by Hawryshyn et al. (1989) and Browman and Hawryshyn (1992) yields the same number of cone mechanisms in the UV-short wavelength part of the spectrum as the technique I used in this study in rainbow trout.

Loss of UV sensitivity and change in cone photoreceptor mosaic

The recordings showed the loss of a chromatic class of optic fibers: the UV-sensitive, ON centers. Furthermore, the disappearance of the UV peak was correlated with the loss of the accessory corner cones from most of the retina. These findings support the contention that these cones contain a UV-sensitive photopigment (Bowmaker and Kunz, 1987; Hawryshyn et al., 1989; Browman and Hawryshyn, 1992). This study was the first to attempt a direct correlation of the change sensitivity to UV light and the transformation of the photoreceptor layer. Recently, the ontogeny of UV sensitivity was studied in goldfish using electroretinographic recordings (Chen and Stark, 1993). Unfortunately, the absence of histological examination of the retina in their study animals makes the link between UV sensitivity and retinal structure in these animals speculative at best.

The results presented here suggest a developmental reorganization of the ganglion cell, as well as the photoreceptor cell layers. The reorganization resulting from the loss of UV sensitivity could follow at least two patterns. First, the disappearance of the corner cone from the photoreceptor mosaic could result solely in the removal of one class of inputs to the center-surround organization of the RGCs. Hence, the neuronal elements responsible for carrying the information relative to UV stimuli would remain in place and continue to fill their functions with the remaining elements.

Alternately, the loss of UV-sensitive fibers could be accompanied by the degeneration of a class of RGCs. Developmental degeneration of RGCs has been reported in other species (Oppenheim, 1991; Wong and Hughes, 1987; Dunlop and Beazley, 1987;

Young, 1984). Although Lyall (1957a) did not find any indication of accessory corner cone degeneration, this possibility cannot be discarded.

Since the first publication of the present paper, support for both patterns has been reported (Kunz et al., 1994; Coughlin and Hawryshyn, 1994b). Coughlin and Hawryshyn (1994b), in a study comparing the distribution of inputs to single units in the torus semicircularis of small and large rainbow trout, found a predominance of single units with inputs from the four cone mechanisms in small rainbow trout. In larger fish, this type appeared to have been replaced with a similar type of unit but that lacked the UV input. Presumably, the disappearance of the UV cones in these animals does not involve a major reorganization of RGC receptive fields. Conversely, Kunz et al. (1994) have reported the presence of pyknotic bodies, indicative of cellular death, in the photoreceptor and horizontal cell layers of the Atlantic salmon retina, and suggest that apoptosis may be involved in the removal of UV cones and other cell types from the retina.

The disappearance of the accessory corner cones from the retina of growing trout is not an all or nothing event. In large fish, accessory corner cones are still present near the optic nerve head and embryonic fissure, albeit in a much reduced number (see Discussion, chapter 3). These cones have also been found in small numbers in two year-old brown trout and Atlantic salmon (Kunz, 1987). Since the disappearance of the accessory corner cones is believed to proceed from the center toward the periphery of the retina (Lyall, 1957a, b), I suggest that they represent a population of "resident" corner cones i.e. a population of corner cones which remain in the retina for the entire life of the animal. This proposal is supported by the observation that corner cones were found in

individuals of very different size (85 and 914 g). As recently suggested by Coughlin and Hawryshyn (1994b), the small number of "resident" accessory cones present in the retina of large specimens may be UV sensitive.

The OFF response: a shadow detecting mechanism

The spectral sensitivity of the OFF response in small and large fish differed in two ways: the λ_{max} of the OFF response appeared to be displaced toward longer wavelengths in larger fish, and the sensitivity function also appeared broader. The most plausible explanation for this shift in λ_{max} may be a change in the chromophoric content of the photopigments contained in the cone outer segments. In this case, the difference in sensitivity would be due to a shift from a vitamin A_1- to a vitamin A_2-based photopigment content. As for the broadening of the spectral sensitivity curve, it may also be explained by small contributions of the L mechanism in the larger fish. This change in the shape and λ_{max} of the OFF response with animals size will require further investigation.

The spectral sensitivity of the OFF response in both small and large rainbow trout differed from that reported for the goldfish (Wheeler, 1979; DeMarco and Powers, 1991). These studies interpret the optic nerve OFF response as being dominated by a L-wavelength-sensitive cone mechanism. Under our experimental conditions, the spectral sensitivity of the OFF response in rainbow trout appears to be dominated by input from an M-wavelength cone mechanism.

Wheeler (1979) suggests that the role of the L-wavelength-dominated OFF response of goldfish is to act as a predator- (or prey) detecting mechanism. I postulate that this system should be tuned to the prevailing wavelength, or the mid-spectrum of

ambient light. The presence of a predator (or a prey) in the path of the downwelling light would produce a shadow, perceived at the optic nerve level as an OFF response. Similarly, in deeper waters, where the ambient spectrum tends to lose its directional heterogeneity, targets are likely to appear darker than their surroundings, and thus also to be perceived through the OFF response system. This shadow, or darker target will generally be interrupting the illumination of the retina by the background light, making an OFF system optimally functional if tuned to this background. That is to say that the visual pigment contained in the photoreceptors that subserve the shadow-detecting function should be of the matched type (see Lythgoe, 1979). This leads to the prediction that the shadow-detecting mechanism (OFF response) should be dominated by one photopigment, matched to the spectral distribution of ambient light, and more precisely to the narrowest spectral distribution encountered by the animal, i.e. that for which a match requires the finest tuning. In the case of rainbow trout, the determining factor would be the spectral distribution of the sidewelling light: any pigment matched to the narrower spectral distribution of the sidewelling light will necessarily be matched to the more encompassing spectral distribution of the downwelling light.

This supposition is supported by the fact that rainbow trout, and the cichlid *H. burtoni*, whose natural photic environments are richer in wavelengths from the S-M part of the spectrum (*H. burtoni*: Fernald and Hirata, 1977; trout: Novales Flamarique et al., 1992) have an OFF response dominated by input from the M cone mechanism (*H. Burtoni*: Hawryshyn et al., 1991 and see Appendix B; trout: this study). Furthermore, juvenile rainbow trout eventually leave their native stream to enter a lake environment

where they will spend their adult life until returning to spawn in the stream (Northcote, 1969). This migration is accompanied by a movement to greater depths where the mid-spectrum wavelengths of downwelling light field are shifted towards longer wavelengths (Loew and McFarland, 1990; Novales Flamarique et al., 1992). Our results show that the OFF response in large fish is relatively more sensitive to longer wavelengths than that of small fish.

Note: Since the publication of this manuscript, in 1993, more reports of RGCs sensitive to ultraviolet light have been published (Novales Flamarique and Hawryshyn, 1996; Coughlin and Hawryshyn, 1994b). These studies further support our findings of a correlation between the presence of corner cones in the salmonid retina and that of sensitivity to ultraviolet light. Still missing, however, are *in situ* microspectrophotometric measurements of the absorption of cone photoreceptors in the salmonid retina. In addition, a study by McDonald and Hawryshyn (1995) recently provided support for the hypothesis that the OFF response in fish may be dominated by inputs from a cone mechanism whose visual pigment is matched to the spectral distribution of the ambient light. In a comparison of the spectral sensitivity of ON and OFF responses from the optic nerve of stickleback with the spectral distribution of the light environment, these authors found a close correlation between the λ_{max} of the OFF response and the dominant side-welling wavelengths.

Chapter 3: Cone photoreceptor topography in the retina of sexually mature Pacific salmonid fishes[6]

Introduction

The photoreceptor layer, the last layer of the neuro-retina to be reached by light stimuli, plays an important role in determining the visual abilities of animals. Not only does the nature of the photoreceptors underlie the visual abilities of the animal but their topographical distribution also determines how different parts of the visual field are sampled. For instance, spectral sensitivity of an animal is a function of the spectral tuning of visual pigments contained in the photoreceptors' outer segment (Stell and Hárosi, 1976; Cresticelli, 1990; Tovée et al., 1992). Likewise, distribution of the different spectral types of cones across the retina affects how the spectral sensitivity of the animal changes across the visual field (McFarland and Muntz, 1975; Wortel et al., 1987; Szél and Röhlich, 1992). Quantitative variations in the topographical distribution of photoreceptors, giving rise to areas of higher density and probably underlying higher visual acuity, also define functional regionalization within the retina (Browman et al., 1990; Zaunreiter et al., 1991; Logiudice and Laird, 1994).

Cone photoreceptors are often organized into mosaics (Lyall, 1957a,b; Engström, 1960, 1963a,b; Bathelt, 1970; Marc and Sperling, 1976). In fish, mosaics are defined by the geometrical arrangement of single- and double-cone photoreceptors into repeated patterns that form a lattice-like organization. The morphology of these mosaics varies

[6] Published as Beaudet et al. (in press).

greatly among different species (Lyall, 1957b; Engström, 1960, 1963a,b; Zaunreiter et al., 1991), among animals of different sizes (Lyall, 1957a; Ahlbert, 1976; Bowmaker and Kunz, 1987; Beaudet et al., 1993), and even among different locations within the retina (Lyall, 1957a; Ahlbert, 1969, 1976). Presumably, the morphological variations in cone mosaics reflect an underlying functional diversity as well (van der Meer, 1992; van der Meer and Bowmaker, 1995). Although it has been postulated that the regular arrangement of cones into mosaics influences spatial resolution or contrast (Bathelt, 1970; Ahlbert, 1976; Marc and Sperling, 1976; van der Meer and Anker, 1984), or provides a more uniform spectral sampling (Bowmaker, 1990), the function of mosaics remains unclear.

Several studies have reported ontogenetic changes in the organization of the retinal cone mosaic in salmonid fishes (Lyall, 1957a; Ahlbert, 1976, Bowmaker and Kunz, 1987; Beaudet et al., 1993). Notably, these changes involve the almost complete elimination of a type of cone associated with sensitivity to ultraviolet (UV) light (Bowmaker and Kunz, 1987; Hawryshyn et al., 1989; Browman and Hawryshyn, 1992; Beaudet et al., 1993). These cones, the accessory corner cones, identifiable by their position within the retinal square mosaic, are lost at the time of smoltification, when the animals migrate to the ocean or towards greater depths. Hence, the disappearance of these cones, and the associated sensitivity to UV light, have been related to a possible decrease in the intensity of UV light in the new environment (Bowmaker and Kunz, 1987).

At the time of reproduction, salmonid fishes return to their environment of origin to spawn. Although this migration is accompanied by changes in the visual environment

that are converse to those associated with the first migration, there are no studies reporting the retinal structure of animals in this final stage of their life history. This study provides the first data on the retinal structure of sexually mature salmonid fishes, at the time of reproduction or shortly after the completion of their return migration.

I examined photoreceptor topography in sexually mature chinook, chum and coho salmons and rainbow trout. My primary objective was to determine whether accessory corner cones were present in these animals. A secondary goal was to gather information on the qualitative and quantitative characteristics of retinal cone topography and cone arrangements in the retina of large salmonids. I found large areas of the retina containing accessory corner cones in the four species studied. Given their distribution, I inferred that they are probably not involved in visual tasks that are associated with higher photoreceptor densities. Furthermore, their presence over extensive areas of the retina provides an initial support to the contention that they may be the product of late cell addition, at least in rainbow trout.

Material and methods

Four species of Pacific salmonid fishes were chosen for this study, to provide an overview of the generality of the retinal characteristics under study: chum salmon (*Oncorhynchus keta*), chinook salmon (*O. tschawytscha*), coho salmon (*O. kisutch*), and rainbow trout (*O. mykiss*). I obtained *O. keta (n=3)*, *O. tschawytscha* (n=3) and *O. kisutch (n=3)* from the Big Qualicum River Provincial Hatchery, on Vancouver Island, B.C. These animals were caught wild, during their upstream migration, and were in

sexually mature condition at the time of sampling: females contained large quantities of ripe eggs and males contained milt that could be easily extracted. *Oncorhynchus mykiss* (n=2) in sexually mature condition were obtained from a local fish farm where they had been raised in a small lake, under natural light conditions. Table 4 lists the specimens used and their size. All procedures described herein are in accordance with the guidelines established by the Canadian Council on Animal Care. Protocols were approved by the University of Victoria Animal Care Committee.

Sampling of the retinae and histological procedures

I collected both retinae from adult salmonids freshly killed by a blow to the head or by MS-222 (tricaine methanesulphonate) overdose. All specimens were collected at midday, in a light-adapted state. After removing the cornea and lens and hemisecting the eyes along the horizontal meridian, I immersed the two halves in a buffered solution of fixative (2.5% glutaraldehyde, 1% paraformaldehyde in 0.06M phosphate buffer, pH 7.2, 4° C). I kept the eyes in fixative for at least 2 days and up to 2 weeks before further processing.

Because of the large number of rods, the presence of the pigment epithelium and the small size of some of the cones, retinae could not be examined as wholemounts but had to be sectioned histologically. Since my aim was to study the topographic organization of the retina, I adopted procedures that would allow me to assign histological sections to specific locations in the retina. To achieve this goal, I kept records of the position and orientation of the retinal tissue throughout the histological procedures, from fixation to embedding, as follows.

Table 4. Length of the animals used in the retinal cone topography study.

Animal ID	Total length (cm)
RT3*	36.25
RT4	33.75
OT1	84.00
OT2	84.00
OT9	85.00
CO3	46.25
CO4	56.25
CO5	61.25
CH6	70.00
CH7	67.50
CH10	62.50

*RT = rainbow trout, OT = chinook salmon, CO = coho salmon and CH = chum salmon.

Prior to embedding, I cut each retina into 4 quarters using radial incisions, two quarters originating from the dorsal and two from the ventral hemiretinae. Using an overhead projector, the 4 quarters were projected onto a sheet of paper and traced. Distortion of the image, along the X and Y axes, was minimal. I further cut each quarter of retina in half, with radial incisions, and again projected and traced them. The eight pieces of retina were then dehydrated through a graded series of ethanol, infiltrated with Epon resin and placed into embedding molds. All eight pieces were positioned topographically in the mold and further divided into smaller pieces that could then be sectioned. The result was a block of plastic containing approximately 100 pieces of retina, all of them organized topographically, and matched to specific positions on our drawings of the entire retina. This approach allowed me to reconstruct the original flattened retina. Shrinkage after embedding was estimated at approximately 25%.

Retinae from *O. mykiss* were processed differently. Retinae were flat-mounted by making 4 or 5 incomplete radial incision. I excised 1-mm^2 samples from locations evenly distributed over the retina using broken pieces of razor blade mounted on small wooden sticks. Using the overhead projector, I then traced the contours of the retina and marked the location of each sampling site. I post-fixed the pieces of retina in osmium tetroxide, dehydrated and embedded them in Epon resin. The two processing techniques yielded similar results. The latter, however, was less labor-intensive and required less manipulation of the tissue.

I selected samples evenly distributed across the surface of the retinae to provide a uniform and consistent survey. A minimum of 17 areas were sampled for each retina, and

for one individual per species (2 for rainbow trout), 28-30 sites were examined. I sectioned each sample tangentially through the photoreceptor layer, at 1-2 μm and stained the sections with Richardson's stain. Since single and double-cones lie in different planes in the light-adapted retina, I sectioned through the entire thickness of the photoreceptor layer.

Analysis of the histological sections

To achieve my primary objective, the determination of putative UV/accessory corner cones (referred to as corner cones in the reminder of the paper) distribution, I identified the types of cones and cone mosaics present at each location. Two morphologically distinct types of cones are present in the salmonid retina: single cones appear circular in cross section, whereas double cones are larger and have an elliptical cross section. Based on their morphology and position within the mosaic, single cones were categorized as either corner cones or central single cones in square mosaics (Fig. 13). When a mosaic pattern other than square was present, they were categorized only as single cones. Double cones were also identified based on their morphology. Cone densities were determined for each location sampled. Densities of each type of cone were determined by counting the number of cones present in a 30,000 μm^2 grid, using a 25X objective, and converting the values into numbers of cones per mm^2. As the relative proportion of the different morphological types of cones may be used to quantitatively characterize retinal mosaics, I calculated the ratio of the number of double to that of single cones at each location. Finally, I determined double cone packing, the percentage of total area occupied by double cones at each sampled site, to provide information on

Figure 13: Tangential sections (1 μm thick) through the ellipsoid region of cone photoreceptors in four species of sexually mature salmonids.
A rainbow trout, **B** coho salmon, **C** chinook salmon and **D** chum salmon. Micrographs taken from a representative individual from each species. All exhibit the complete square mosaic. Arrows indicate the location of accessory corner cones. dc = double cone and c = central single cone. Bar = 20μm.

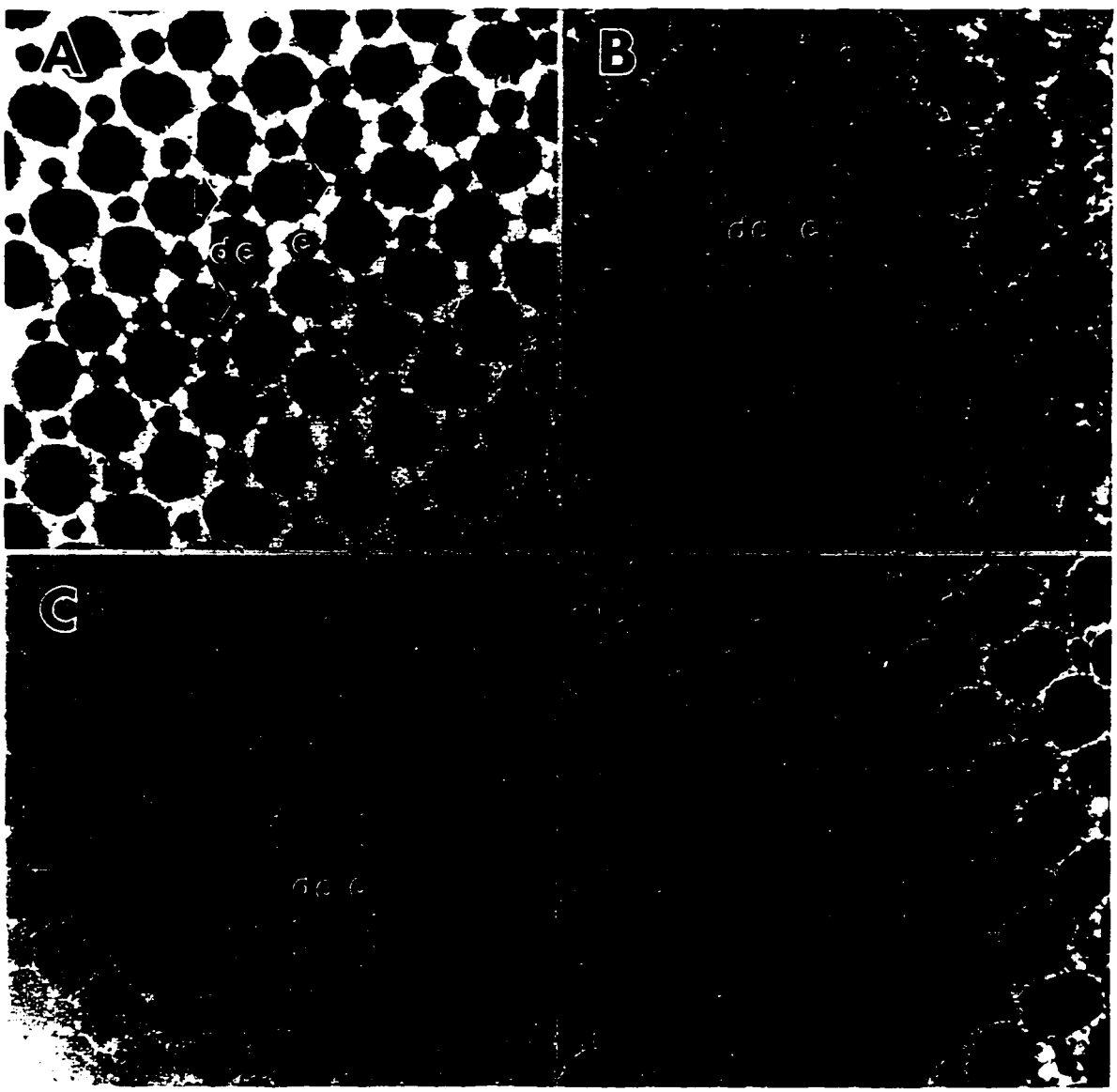
A
B
C

how the ability to capture light may vary across the retina. I determined double cone packing by multiplying the double cone density by the average cross-sectional area of the ellipsoid (region adjacent to the outer segment) of 20 double cones, at each location. Ellipsoid cross-sectional areas were measured from digitized video images of the histological sections (40X objective) with a computerized image analysis system (Optimas Corp.). I took the micrographs with a Zeiss microscope, equipped with a 40X objective. Cone density and area measurements were not corrected for shrinkage.

Results

Corner cones in the retina of sexually mature salmonids

The complete square mosaic is composed of four double cones whose long axes align with and lie along the sides of a square, surrounding a central single cone. Corner cones are located at the corners of the square (Fig. 13). This complete square mosaic was present in each species I studied, and was always found in an area extending from the center of the retina towards the dorso-temporal quadrant (Figs. 13-14). The area containing corner cones was estimated at 15-20% of the total retinal surface. Because of the low sample size and the relatively small number of locations examined within each retina, I cannot conclusively determine whether or not the size of the areas that contained corner cones differed among the 4 species studied.

In some cases, square mosaics could not be identified consistently over the entire 30 000 μm^2 analysis area, and in those cases it was difficult to assign some of the single cones to a particular position (central or corner). However, since these areas contained

Figure 14: Distribution of putative UV cones and cone mosaic types in the retina of four sexually mature salmonids: rainbow trout, coho, chinook and chum salmon. Letter symbols represent the mosaic types: SCC = complete square mosaic, containing accessory corner cones, SQ = square mosaic without accessory corner cones, R = row, and AR = alternating row. Polygons represent the minimum area over which corner cones were found. The maps also contain the values of the double to single cone ratio for the different locations sampled. Retinae are oriented with dorsal (D) side up and nasal (N) side to the left. The embryonic fissure runs from the center to the naso-ventral margin of the retina. Bars = 5 mm.

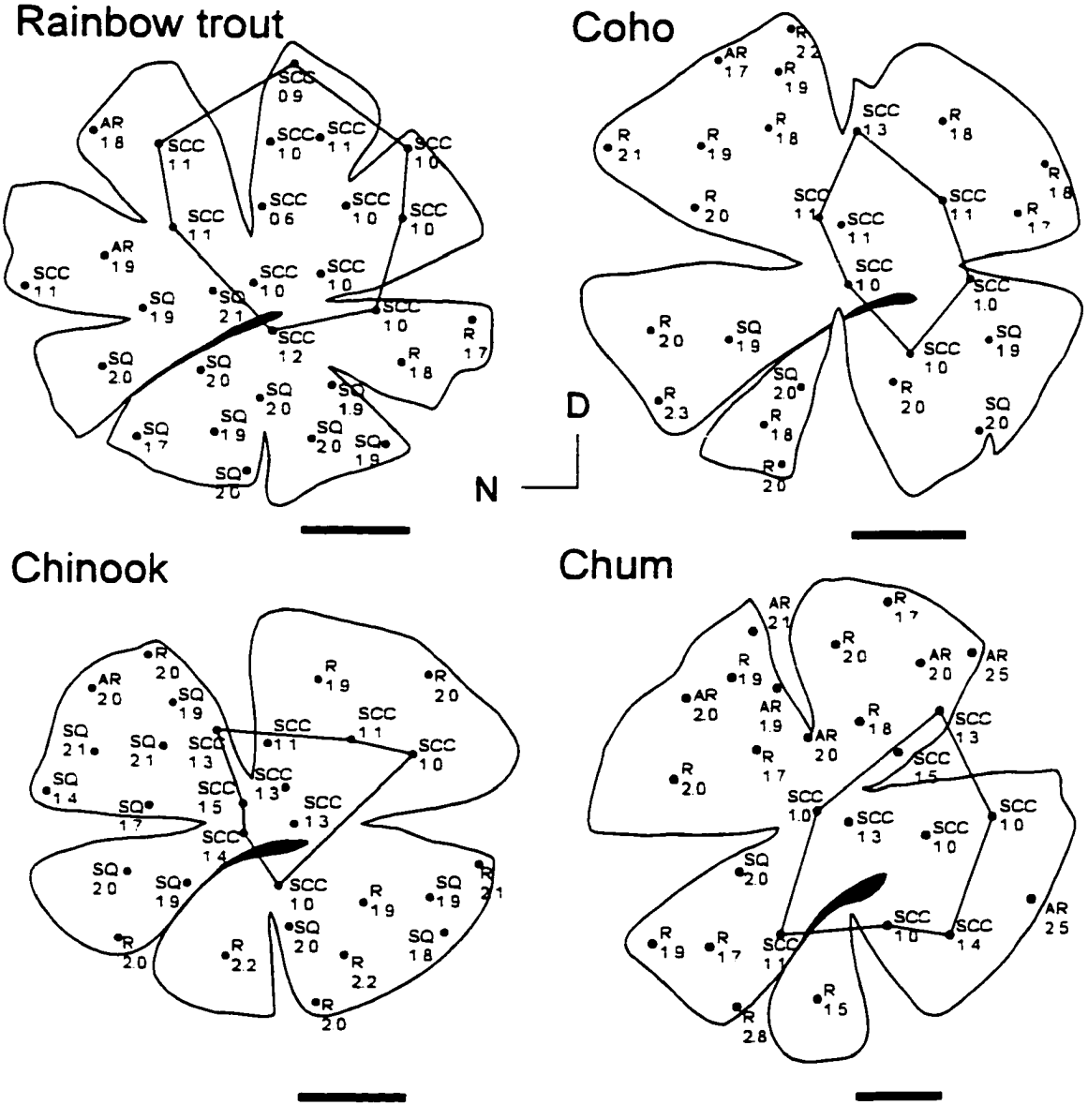
Rainbow trout
Coho
Chinook
Chum
N
D

some identifiable corner cones, were mostly interspersed among or adjacent to those areas containing complete square mosaics, and also contained similar proportions of double and single cones, I included them in the distribution maps of the corner cones (Fig. 14). The mean ratio of double to single cones in the areas containing corner cones was 1.08±0.13 SD (n=241, for the pooled data from all animals studied).

Variations in the retinal mosaics

In addition to the complete square mosaic, I found three other distinct cone arrangements in all individuals (Fig. 15): (i) square mosaics which lacked corner cones (Fig. 15A); (ii) row mosaics similar to those described by Lyall (1957a) and Ahlbert (1976) in brown trout and Atlantic salmon (Fig. 15B); (iii) a novel mosaic which I named "alternating row mosaic" (Fig.15C). It consisted of double cone rows alternating with rows composed of both double and single cones. In the double cone rows, double cones were organized side-by-side in a straight line, with their long axis perpendicular to the orientation of the row. The other type of row consisted of double-single cone pairs organized perpendicular to the orientation of the row. In this type of row, the double cones had their long axis perpendicular to the orientation of the row, and they alternated position within the pair, from one pair to the next (Fig. 15C). In all species, some mosaics, presumably located at the transition between areas containing different cone mosaics, often exhibited characteristics of both the row and square mosaics, indicating they are part of a continuum as reported by other authors (Lyall, 1957a; Ahlbert, 1976).

Figure 15: Tangential sections (1 μm thick) through the ellipsoid region of cone photoreceptors showing the different types of retinal cone mosaic encountered. Histological sections are accompanied by diagrams: **A** square mosaic lacking corner cones, **B** row mosaic, and **C** alternating row mosaic. DC = double cone. S = single cone. Bar = 20μm.

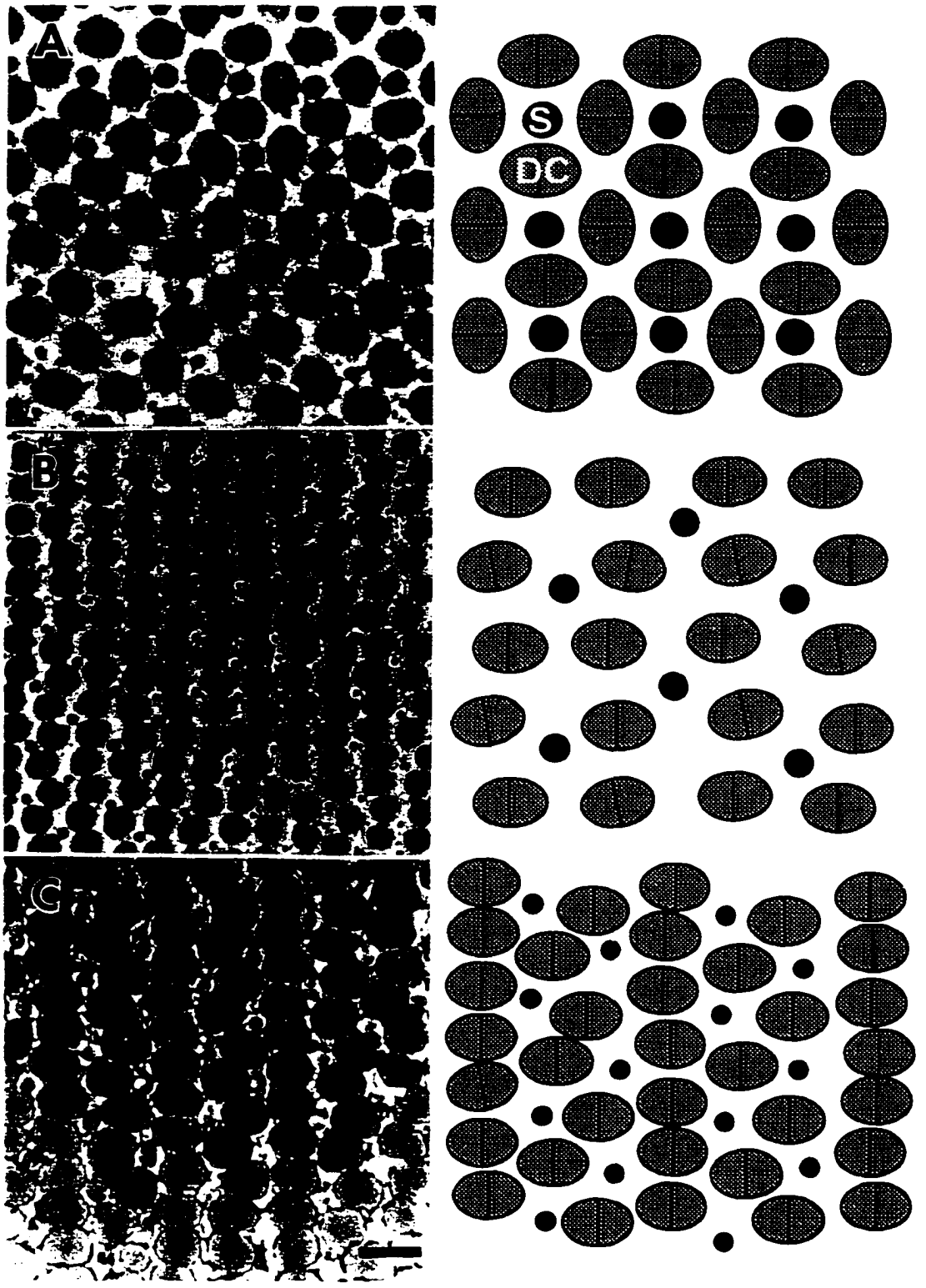
A
B
C
S
DC

Retinal cone topography.

I found regionalization of the different retinal mosaic types and cone densities. As a general rule, square mosaics occurred centrally and row mosaics more peripherally (Fig. 14). Some exceptions were noticed, however (Fig. 14). Cone density was highest peripherally (Fig. 16, shaded areas), and lowest dorso-centrally (Fig. 16, smaller empty circles). Cone densities typically remained high throughout the ventro-temporal retina, albeit lower than at the most peripheral locations (Fig. 16, larger filled circles). Highest cone densities in the dorsal hemiretina were generally found near the retinal margin, in the dorso-nasal quadrant (7 out of 11 fish). There was little overlap between the areas containing corner cones and the areas with higher cone density (Fig. 16).

Whereas location of the areas of higher cone densities was consistent between species, the type of mosaic found in these areas varied (compare Figs. 14 and 16); In rainbow trout, only square mosaics occurred in the ventral area of higher cone density (Figs. 14 and 16); In the three salmon species, both row and square mosaics were found to varying degrees in these areas. The size of the animals was correlated with the type of mosaic found in these areas: the smaller animals (rainbow trout) had mostly square mosaics whereas larger animals had mostly row mosaics. Coho salmon, with an intermediate size between that of rainbow trout and the other species of salmon, exhibited an intermediate condition (Figs. 14 and 16).

Figure 16: Maps showing the distribution of cone densities and double cone packing (in parentheses) in the retina of representative individuals from four species of sexually mature salmonids.

Cone densities are expressed in thousands per mm^2 and cone packing expresses the percentage of retinal area occupied by double cones. Areas with cone densities higher than one standard deviation above the mean are identified with stippling. Cone densities higher than 6000 cones per mm^2 (high density) are represented by the largest filled circles, and those smaller than 5000 cones per mm^2 (low density) by the smallest empty circles. Intermediate values are represented by the small full circles. The area containing corner cones (complete square mosaic) is represented by the polygons (compare to Fig. 14). Orientation as in Figure 14. Bars = 5mm.

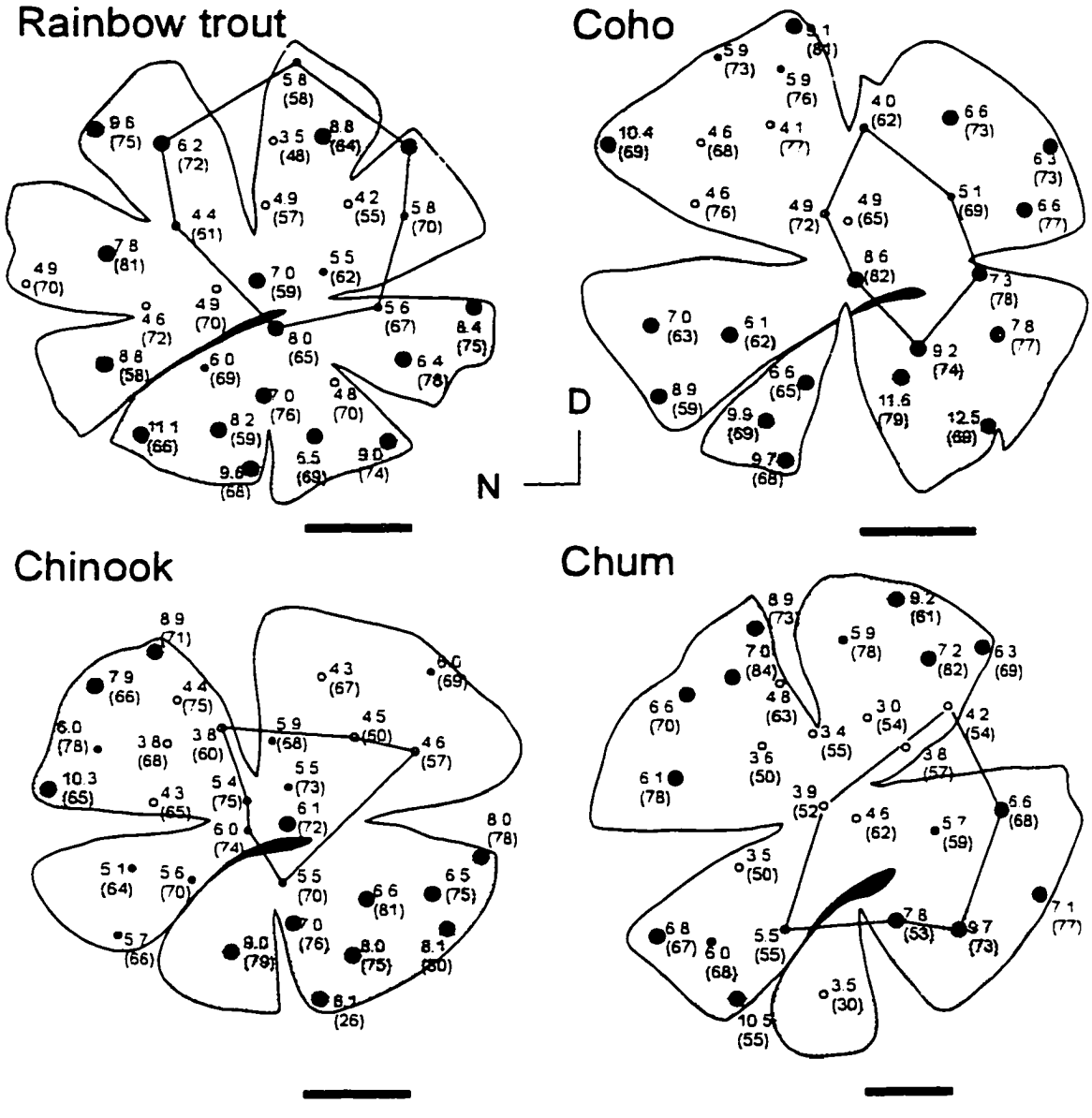
Rainbow trout
Coho
Chinook
Chum
D
N

Quantitative analysis of retinal cones

Double cone cross-sectional area and cone density showed a strong negative relationship (correlation coefficient -0.83, $P < 0.001$). As cone density increased, double cone area decreased, following the relation shown on Fig. 17A. Although the relative proportion of double and single cones varied, the frequency distribution revealed two modes, centered on 1.0 and 2.0 respectively, indicating the predominance of two types of cone arrangements (Fig. 17B).

Cone packing in the salmonid retina

The average double cone packing, or the proportion of total available area occupied by double cones, was estimated at 66% ± 11 SD (data pooled from all animals). Although the regions exhibiting higher double cone packing were often in the vicinity of the zones of higher cone density (Fig. 16), no consistent trend could be identified: higher cone packing occurred in both higher and lower cone density areas. Furthermore, higher and lower cone packing values were found in all areas of the retina (Fig. 16). Inter-individual variation in double cone packing was not different from interspecific variation. Since the measure of cone packing involved double cones only, I examined whether the relative number of double and single cones could have had an influence on double cone packing. I did not find any significant relationship between double cone packing and the proportion of the two morphological cone types (average correlation coefficient for all animals 0.049, n=241). Because of the negative relationship between double cone cross-

Figure 17: Quantitative relationships between cone size, density and ratios

A Relationship between double cone density and double cone cross sectional area.

B Frequency distribution of double to single cone ratios for all samples (n=241). Ratios of around 1 were characteristic of areas containing corner cones.

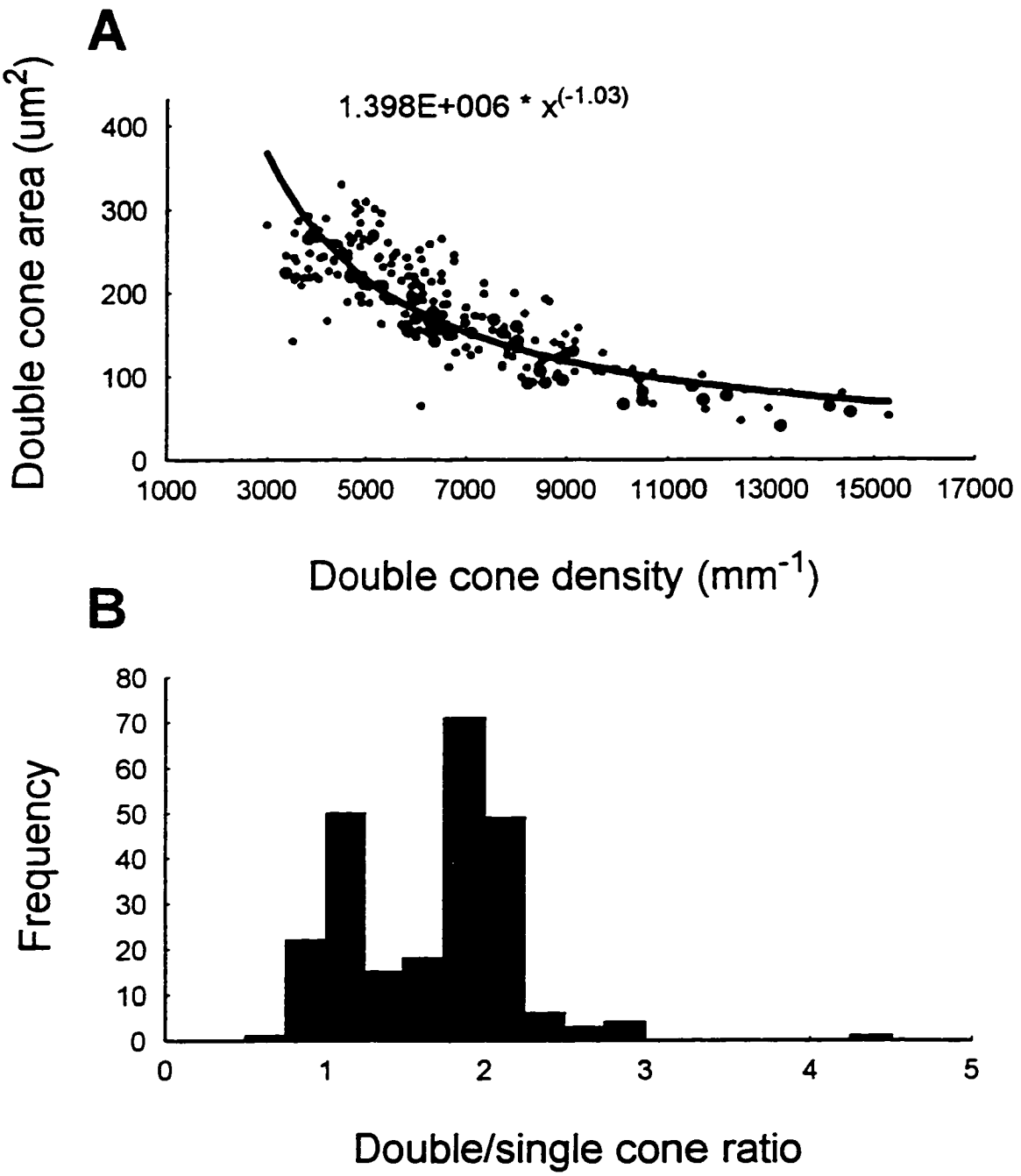
A
1.398E+006 * x(-1.03)
Double cone area (um2)
400
300
200
100
0
1000
3000
5000
7000
9000
11000
13000
15000
17000
Double cone density (mm-1)
B
Frequency
80
70
60
50
40
30
20
10
0
0
1
2
3
4
5
Double/single cone ratio

sectional area and double cone density, a lower cone density did not necessarily result in lower double cone packing.

Discussion

Putative UV cones in the retina of sexually mature Pacific salmonids

These results show that, similar to the situation in small juvenile salmonids (Lyall, 1957a; Bowmaker and Kunz, 1987; Browman and Hawryshyn, 1992; Beaudet et al., 1993), corner cones occur over large areas of the retina in large, sexually mature salmonid fishes. Direct identification of the corner cone's phenotype using antibody labelling or *in situ* hybridization has not been made yet in salmonids, but it has in goldfish (Hisatomi et al., 1996; Stenkamp et al., 1996). Furthermore, indirect evidence strongly suggests that the corner cones contain a photopigment sensitive to UV light in salmonids, as well. In salmonids (Bowmaker and Kunz, 1987; Browman and Hawryshyn, 1992; Beaudet et al., 1993; Kusmic et al., 1993; Novales Flamarique and Hawryshyn, 1996) behavioral and physiological sensitivity to UV light have been associated with the presence of the corner cones. Using microspectrophotometry, Bowmaker and Kunz (1987) and Kusmic et al. (1993) found that the presence of UV light-absorbing single cones in the retina of trout was tightly correlated with the presence of corner cones in the retinal mosaic. Similarly, Browman and Hawryshyn (1992), using a psychophysical technique, and Beaudet et al. (1993), using electrophysiological recordings, found that sensitivity to UV light in rainbow trout was associated with the presence of the corner cones. Recently, similar conclusions were reached by Novales Flamarique and Hawryshyn (1996) in sockeye salmon. Based on

the evidence presented in the literature, I conclude that putative UV cones are spread over an extensive area (15-20%) of the retina in adult, sexually mature Pacific salmonid fishes.

Could UV cones be reincorporated in the retina?

Changes in the structure and physiology of the retina associated with changes in visual environment have been reported in numerous articles (Blaxter, 1968; Neave, 1984; Evans and Fernald, 1990, 1993; Evans et al., 1993; Pankhurst et al., 1993; Shand, 1993, 1994). Among these changes, developmental loss of a class of cones has been reported in several species of fish. For example, single cones in some fish are lost from the retina when the animals migrate to greater depths (Boehlert, 1979; Munk, 1990). In salmonid fishes, similar changes in retinal structure have been noted around the time when animals would undertake their seaward migration (shortly after the metamorphose-like process called smoltification). Specifically, several studies have indicated that corner cones, or putative UV cones, are lost around the time of smoltification and migration (Lyall, 1957a; Bathelt, 1970; Ahlbert, 1976; Bowmaker and Kunz, 1987; Beaudet et al., 1993; Kusmic et al., 1993; Novales Flamarique and Hawryshyn, 1996). Although corner cones have been reported previously in larger, sexually immature fish, they were confined to growth zones, near the embryonic fissure and the retinal margin in brown trout and Atlantic salmon (Kunz, 1987), or close to the optic nerve head and embryonic fissure in rainbow trout (Beaudet et al., 1993). Kunz (1987) and Kunz et al. (1994) presumed them to be non-functional and short-lived, whereas Beaudet et al. (1993) proposed they constituted a small residual population whose response could not be discerned in mass potentials recorded from the optic nerve. The populations of putative UV cones identified in these

studies occupied no more than a 200μm-wide band along the embryonic fissure and retinal marginal growth zone, representing at most less than 2% of the retinal surface, an area one order of magnitude smaller than what I found in this study. Furthermore, in these studies corner cones were absent from the remaining retina, that is away from the embryonic fissure and marginal growth zone, where most of the corner cones were found in our study. Thus, I conclude that the populations of corner cones described in this study are distinct from those reported previously in larger salmonid fishes. Recently it was reported that larger, sexually immature fish do show some sensitivity to UV light, but significantly less than in small animals (Coughlin and Hawryshyn, 1994b; Novales Flamarique and Hawryshyn, 1996).

I do not know if the corner cones disappear during normal maturation from the retina of coho, chum and chinook salmon at the time of smoltification. These animals, however, experience similar changes in photic environment, and exhibit migratory behaviors similar to those of Atlantic and sockeye salmons, brown trout and rainbow trout (also called steelhead trout). Furthermore, the fact that this phenomenon has been encountered in closely related species within the genera *Salmo* (Brown trout and Atlantic salmon) and *Oncorhynchus* (rainbow trout and sockeye salmon) as well as between these two genera suggests it may be a characteristic of salmonid fishes in general. However, until the earlier stages in the life history of coho, chum and chinook salmon are examined, the fate of UV cones in their retinae cannot be certain.

For many fish species, a migration early in life is followed by one in the opposite direction, at the time of reproduction. During these "return" migrations, fish experience

changes in their visual environment that are mirror images of those experienced earlier in their life. As a result, retinal structure and physiology sometimes undergo transformations that are the mirror images of those undergone earlier in their life (see chapter 1; also reviewed in Beaudet and Hawryshyn, accepted). One of the transformations that one could expect to see reversed in salmonids is the disappearance of the putative UV cones. The presence of corner cones in large, sexually mature Pacific salmonids, and especially in rainbow trout, provides some support for the contention that the disappearance of these cones, early in life, could be followed by their reincorporation in the retina at the time of reproduction. Final conclusions regarding the possible reappearance of the UV cones in salmonid fishes, however, will require detailed histological studies in those species and life history stages that have not yet received attention. To demonstrate that the putative UV cones found in the retina of adult salmonids are the product of late cellular proliferation and differentiation will require experiments involving the use of cellular mitotic indicators (e.g. BrdU, Cameron, 1995). Furthermore, the mechanisms that would underlie the late addition of these cones to the retina need to be demonstrated. Such a mechanism could involve thyroxine acting as the hormonal trigger of both the disappearance and reappearance of these cones in the salmonid retina, as recently proposed by Browman and Hawryshyn (1994). Indeed, both the seaward and the return migrations are associated with elevated levels of thyroxine in salmonid fishes (see discussion in Browman and Hawryshyn, 1994). Although these authors concluded that thyroxine treatment leads to the disappearance and subsequent reappearance of corner cones in rainbow trout, the lack of an extensive histological investigation of representative areas of the entire retina in their

study animals suggests further work is needed. A detailed topographic study of the retina in thyroxine-treated and control animals would have been necessary to eliminate the possibility of sampling errors. Thus, confirmation of thyroxine's involvement in the determination of the putative UV cones' fate is still needed.

Cone photoreceptor topography and retinal function

The finding of a ventral zone of higher cone density is consistent with Ahlbert 's (1976) findings in other salmonids. Areas of higher cellular densities (photoreceptors and/or RGCs) in the vertebrate retina have been associated with the principal visual axes of the eye, or directions of main visual interest (Williamson and Keast, 1988; Collin and Pettigrew, 1988a,b; Zaunreiter et al., 1991). Thus, I believe the ventro-temporal retina in the animals I studied may be associated with a principal visual axis extending rostro-dorsally. This would be consistent with the feeding behavior of salmonid fishes, which tend to strike at prey items located above and in front of them (Ahlbert, 1976). In addition, visual acuity, which depends on several factors, has been related to photoreceptor density (Browman et al., 1990; Zaunreiter et al., 1991; Collin and Ali, 1994; Logiudice and Laird, 1994). For example, Wikler et al. (1990) write that "variations in the number, size and distribution of photoreceptors across the retina are among the most important determinants of visual acuity under different levels of illumination and in different parts of the visual field". The presence of areas of higher photoreceptor density in the salmonid retina raises the possibility that visual acuity varies across the visual field. Behavioral assessment of visual acuity for the different parts of the visual field, however, is needed to confirm predictions based on anatomical observations.

Distribution of the putative UV cones, mostly outside the areas of higher cone densities, suggests that these cones may not participate in the visual tasks involving the main visual axis, as defined by the location of higher cone photoreceptor densities. My data, however, suggest the presence of a different type of specialized retinal area in adult salmonid fishes, one based on the topographical distribution of the putative UV cone, and directed at the part of the visual field located forward and down. Again, behavioral experiments are needed to determine the functional and ecological significance of this apparent retinal specialization.

Functional significance of retinal cone mosaics

The significance of regular cone mosaics in the teleost retina is not fully understood (Zaunreiter et al., 1991). Variation in the type of mosaic has been attributed to differences in photic environments and visual behavior. For instance, the square mosaic with corner cones has been associated with an active lifestyle, characterized by predatory behavior in a bright environment (Lyall, 1957b; Boehlert, 1979; van der Meer, 1992), and Engström (1963a, b) suggests that regular mosaics in general may represent a cone arrangement that optimizes visual acuity in fish (presumably within the constraints established by other factors such as cone density, degree of convergence onto higher-order retinal neurons etc.). However, studies that compare visual acuity among species that differ in the level of organization of their retinal cone mosaic are needed to test these hypotheses. Recently, a role in the detection of polarized light has been postulated for the square mosaic, although no underlying biophysical mechanism has been demonstrated

conclusively (Cameron and Pugh, 1991; Cameron and Easter, 1993; Rowe et al., 1994; Novales Flamarique et al., 1995).

As in other salmonids (see Lyall, 1957a; Ahlbert, 1976), row mosaics in Pacific salmonids occur in the peripheral retina, regardless of cone density. As the peripheral retina is generated later than the central retina, and larger specimens exhibited relatively more row mosaics than smaller ones, it is possible that row mosaics are generated mostly when the retina reaches a certain size in salmonids. Whether specific cone organizations are related to specific functions, however, still remains to be determined.

Cone packing in the salmonid retina

The finding that the cross-sectional area of double cones is tightly related to double cone density suggests that cones tend to optimize their areal coverage, within the constraints established by varying cell densities. Furthermore, as single and double cones lie on different planes within the photoreceptor layer, variations in the proportion of the two types of cones did not have an influence on double cone packing. This suggests that whenever the ratio of single to double cones increases, so should the amount of retinal surface occupied by cone photoreceptors, as the increased areal coverage offered by single cones is not accommodated by a corresponding decrease in double cone packing. Assuming that the size of cone ellipsoids, and therefore the area they occupy, is related to probability of light striking them (van der Meer and Anker, 1984 and van der Meer and Bowmaker, 1995), higher single-to-double cone ratios should result in higher probabilities of light striking cone photoreceptors in general. Whether absolute photopic sensitivity varies over the retina, however, requires a knowledge of the degree of cone convergence

onto higher order neurons, and also of the topographic distribution of the different spectral types of cones.

A novel retinal cone mosaic

Although extensive work has been published on the vertebrate retinal structure, there are no reports of the alternating row mosaic in the literature. The frequency with which this type of mosaic was encountered varied greatly from one individual to another and although it was mostly encountered in the dorsal retina, it was also found elsewhere. I do not know the functional significance, if any, of this new type of mosaic.

Conclusions

The results of this study show the presence of putative UV cones in central areas of the retina in sexually mature chinook, chum and coho salmons, and in rainbow trout. These data, together with earlier reports, are consistent with the proposal that the putative UV cones are the product of late cellular addition to the retina, at least in rainbow trout. Similar conclusions regarding the salmon species must await further investigation. Thyroxine has been proposed as the hormonal trigger for the loss and recovery of putative UV cones in the trout retina, but sufficient evidence of its direct involvement is still missing. Appropriate molecular techniques, combined with detailed topographical analyses of the retina throughout the different life stages, are needed to ascertain the fate of the putative UV cones in salmonid fishes and to determine the underlying cellular mechanisms.

Chapter 4: Double labelling of retinal projections and torus semicircularis connections in juvenile rainbow trout[7]

Introduction

Recently, Coughlin and Hawryshyn (1994a, b) found a large proportion of single units with UV inputs in the optic nerve and torus semicircularis of juvenile rainbow trout, but none in the optic tectum. This was surprising as the main known pathway from the retina to the torus semicircularis in fish is via the optic tectum (Schellart, 1990). These results suggest that UV inputs may be reaching the torus semicircularis via an alternate pathway, one that does not involve the optic tectum. This chapter describes my attempts to identify the potential pathways from the retina to the torus semicircularis in small, UV-sensitive rainbow trout.

The torus semicircularis is a multimodal nucleus that lines the floor of the tectal (mesencephalic) ventricle in several species, including rainbow trout (Schellart, 1990). In several species, it constitutes the largest nucleus of the dorsal tegmentum, a major component of the midbrain. Like the torus semicircularis in amphibians, reptiles and birds, and the inferior colliculus, its mammalian homologue (Schellart, 1990), it is a center where auditory, balance, visual and somatosensory information is processed and integrated (Nederstigt and Schellart, 1986; Manteuffel and Naujoks-Manteuffel, 1990; Echteler, 1985a,b; Lu and Fay, 1993; Wild, 1995). Also, in some fish and amphibians, electroreceptive information is integrated with visual and auditory inputs to provide a

[7] Published in abstract form as Beaudet (1995).

representation of the space surrounding the animal (Hopkins, 1983). As such, the torus semicircularis receives extensive ascending projections from the octavolateralis system (and from the superior olive and lateral lemniscus nuclei) and descending projections from the optic tectum and the thalamus (Fig. 18, dashed lines), among other structures (Schellart, 1990).

Although the patterns of retinal projections and torus semicircularis connections have been investigated separately in salmonid fishes (Mansour-Robaey and Pinganaud, 1991; Pinganaud and Clairambault, 1979; Ebbesson et al., 1988; de Wolf et al., 1983), these connections have never been examined within the same individual. The absence of simultaneous labelling of retinal projections and torus semicircularis connections precludes a clear identification of possible pathways between the retina and the torus semicircularis. Nonetheless, based on the information available, it is unlikely that the alternate visual pathway from the retina to the torus semicircularis is a direct one. A direct retinal projection to the torus semicircularis in vertebrates has been noted only on one occasion, in sockeye salmon (Ebbesson et al., 1988). Retinal projections in rainbow trout (Mansour-Robaey and Pinganaud, 1991; Pinganaud and Clairambault, 1979) and other teleosts (Butler and Saidel, 1993) (Fig. 18, solid lines), however, do not reach the torus semicircularis directly. It is therefore likely that the alternate pathway to the torus semicircularis in trout involves at least one intermediary structure.

Anatomical identification of an indirect pathway between two structures has to show that axons of the putative presynaptic component of the pathway make contact with the putative postsynaptic elements (cell body or dendritic tree). By its nature, such

Figure 18: Diagram of the main retinofugal pathways (solid lines) and retinal targets in the trout brain, and connections (dashed lines) of the torus semicircularis (TS).
The inset shows the approximate layout of the various structures described on the main diagram.

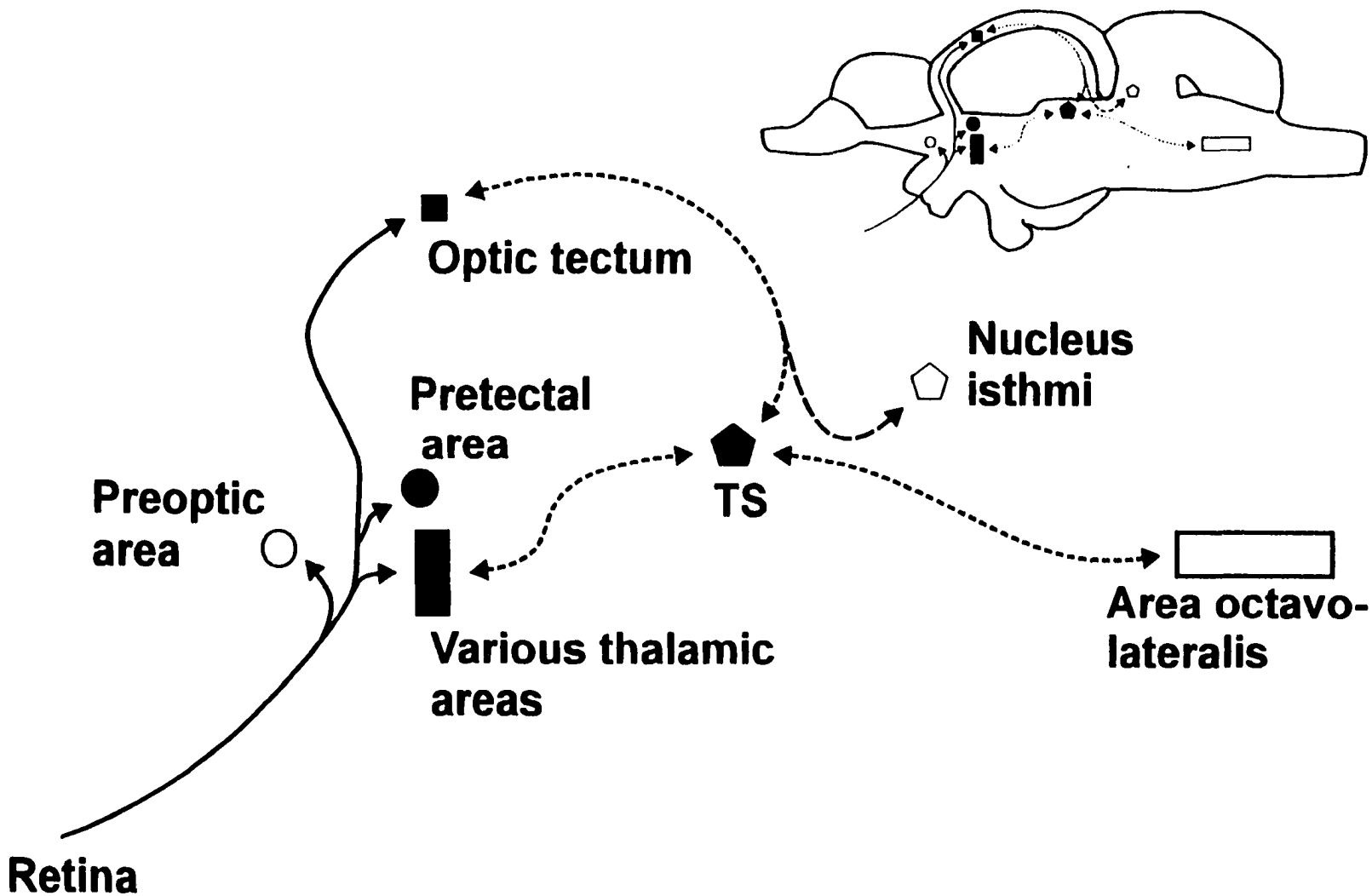
Optic tectum
Nucleus isthmi
Pretectal area
Preoptic area
TS
Various thalamic areas
Area octavo-lateralis
Retina

identification requires ultrastructural information, which may be difficult to obtain without the knowledge of possible sites where such contacts between pre- and postsynaptic elements may occur. This means that prior knowledge of the location of convergence between retinal projections and torus semicircularis-projecting neurons would be required.

The aim of this study was therefore to identify those areas of the rainbow trout brain that contain both RGC projections and cell bodies which project to the torus semicircularis. Based on work by de Wolf et al. (1983) and Pinganaud and Clairambault (1979), one potential area of convergence between retinal projections and torus semicircularis-projecting neurons is located near the latero-ventral thalamic area of the diencephalon (Fig. 18, solid rectangle). In this study, I simultaneously labelled the retinal projections and torus semicircularis connections in juvenile rainbow trout, using carbocyanine and dextran amine-conjugated fluorescent dyes.

Materials and methods

I obtained juvenile rainbow trout (*Oncorhynchus mykiss*) from the Fraser Valley trout hatchery (Abbotsford, B.C.). The fish were housed under a 12L:12D photoperiod, at 15° C. All the procedures described in this study have been approved by the University of Victoria Animal Care Committee.

Neuronal labelling

I used either DiI (1,1'-dioctadecyl-3,3,3',3'-tetramethylindocarbocyanine perchlorate, Molecular Probes, Eugene OR) and DiO (3,3'-dioctadecyloxacarbocyanine perchlorate, Molecular Probes, Eugene OR) or tetramethylrhodamine- (RD, 3 000 MW)

and rhodamine green-conjugated (GD, 10 000 MW) dextran amines (Molecular Probes, Eugene, OR) to simultaneously label the connections of the torus semicircularis and the retinal projections. Double labelling was possible with these dye combinations as the peak wavelengths of re-emission differed between each pair (DiI and RD, peak around 580 nm, DiO and GD, peak around 530 nm). In both cases, I used one of the labels to trace the connections of the torus semicircularis and the other to trace the retinal projections. I applied the label directly to the surgically exposed torus semicircularis and optic nerve stump as follows.

Labelling with DiI and DiO. I fixed the brains by transcardial perfusion with freshwater teleost Ringer (pH 7.2; Oakley and Schafer, 1985), followed by fixative (4% paraformaldehyde in phosphate buffer, 0.1M, pH 7.2). I then cut a window in the fixed optic tectum to expose the torus semicircularis which lies on the surface of the mesencephalic ventricle (Fig. 19) (Schellart, 1990). Once exposed, the torus semicircularis was blotted with lint-free tissue paper to remove excess fluids and the ventricle filled with a warm solution of agar (3% in fixative). Agar ensured the protection of non-target tissue from unintentional labelling. After agar had solidified, I made a well in it to expose the torus semicircularis. Crystals of DiI were then applied to the torus semicircularis using the tip of a glass microelectrode or a fine needle and the site was covered with melted agar. Similarly, DiO was applied to the contralateral optic nerve stump, previously blotted dry with tissue paper. Once the dye crystals were in place, agar was poured over the area to secure the dye and prevent non-target labelling. Brains

Figure 19: Diagram showing the general external organization of the trout brain. Dorsal view is on the right, side view on the left. Diagram on the right hand side shows the position of the left torus semicircularis, as seen after removal of the overlying optic tectum.

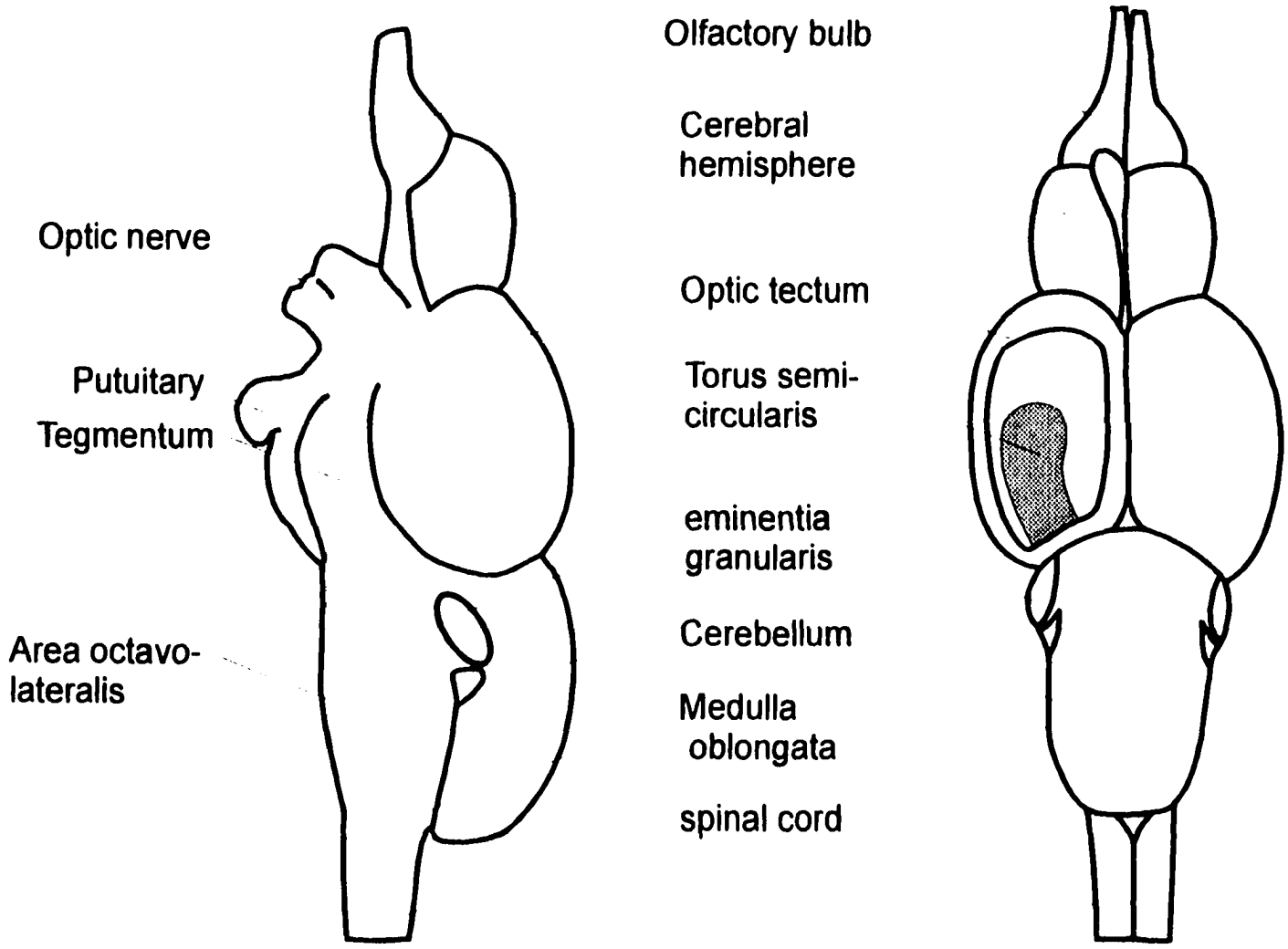
Optic nerve
Putuitary
Tegmentum
Area octavo-
lateralis
Olfactory bulb
Cerebral
hemisphere
Optic tectum
Torus semi-
circularis
eminentia
granularis
Cerebellum
Medulla
oblongata
spinal cord

(whole heads) then incubated in fixative at 4°C, at room temperature or at 40°C for various periods of time.

Labelling with dextran amines. Labelling with RD and GD was carried out on live animals. After general anesthesia with MS-222 (1:10 000; tricaine methanesulphonate, Crescent Research Chemicals, Phoenix AZ), the animal was placed in a holder and respired with water and anesthetic. To expose the torus semicircularis, skin, bone, fatty tissue and part of the optic tectum were first removed, and some cerebrospinal fluid was sucked out with a modified Pasteur pipette connected to a vacuum. Hemorrhage was reduced by heat cauterization of damaged blood vessels. Dye was applied to the torus semicircularis under micromanipulator control using the tip of a tungsten microelectrode dipped in an aqueous solution of the dye (Collin and Northcutt, 1995). Since the torus semicircularis is clearly visible on the floor of the mesencephalic ventricle, dye could be applied to the structure under direct visual guidance (Fig. 19). Generally, the microelectrode penetrated the surface of the mesencephalic floor by no more than 50-100 μm. The dye-laden microelectrode remained in position for 5-10s to allow diffusion of the dye in the surrounding tissue. Once the dye was applied, the area was washed several times with teleost ringer to prevent contamination of non-target tissue by leaked dye. The cavity was then filled with a mixture of mineral oil and Vaseline to provide mechanical support to the brain, and the skin folded back over the opening and glued with a tissue adhesive (Vetbond, Animal Care Products-3M).

Following application of RD to the torus semicircularis, the fish was placed on its side to expose the eye contralateral to the labelled torus semicircularis. Connective tissues

surrounding the eye were incised, some of the extraocular muscles severed and the eye rotated to expose the optic nerve. The optic nerve was then cut with iris scissors, taking care not to sever the ophthalmic artery and vein. This was not always possible, however. When the blood vessels were damaged, rolled up pieces of lint-free tissue paper were used to blot out some of the blood and allow a relatively clear surgical site. Label was applied to the cut optic nerve with an insect pin (# 000) dipped into and aqueous solution of dextran dye. The connective tissues surrounding the eye were finally glued back together, the fish revived, and allowed to survive for 24 h. At the end of the incubation period, the animal was killed with an overdose of anesthetic, perfused transcardially first with teleost Ringer then with fixative (paraformaldehyde 4% in phosphate buffer, 0.1M, pH 7.2), and the heads with partially dissected brain stored overnight in cold fixative. The following day, the brains were dissected free of connective tissue.

Both carbocyanine- and dextran-labelled brain were cryopreserved in a sucrose solution (30% in phosphate buffer) before being embedded in Tissue Tek (1:2 solution in 30% sucrose phosphate buffer; Barthel and Raymond, 1990) and sectioned frozen at 30-50 μm on a cryostat (Microm HM500, Microm Laborgerate GmbH, Germany). Sections were mounted in glycerol and observed under epifluorescence with the appropriate combinations of excitatory and blocking filters (rhodamine filter combination for DiI and rhodamine-conjugated dextran, FITC for DiO and rhodamine-green conjugated dextran). Pictures were taken either as single or double exposures (Leitz Aristoplan microscope). In addition, a camera lucida device (Leitz) was used to produce outlines of the histological sections brain nuclei presented in Figure 20. Identification of the various nuclei mentioned

in this chapter was performed using a comparison of Nissl stained, paraffin-embedded material (prepared by Dr. D.J. Coughlin) and direct visualization of uncleared, non mounted frozen sections under FITC epifluorescence conditions with labelled sections. These observations were then compared with Pinganaud and Clairambault (1979). The results reported herein represent the summary of observations made from 30 labelled rainbow trout brains.

Results

General considerations

I observed differences between the labelling properties of DiI and RD, and those of DiO and GD. Generally, DiI and RD were more visible, especially in non mounted, uncleared tissue. Consequently, clearing of the tissue resulted in substantial improvements to the visibility of DiO- and GD-labelled structures, while providing relatively lower improvement of structures labelled with DiI and RD. However, even in cleared tissue, DiI and RD remained most visible. In addition, as reported by Holmqvist et al. (1992), I found that details of labelled structures were lost in carbocyanine-dyed material, possibly due to damage incurred during the freezing process and subsequent leakage of the dye. Thus, the general labelling pattern of the two types of dye (carbocyanines and dextrans) was similar, but better resolution was achieved with the dextran conjugates. Therefore, in the following sections, emphasis will be placed on the results obtained with the dextran conjugates.

Specificity of labelling

When applying label in a given part of the brain, chances are that structures not targeted by the dye will nevertheless be "contaminated". Unless the dye is applied intracellularly, or to an homogeneous structure (such as the optic nerve), non-targeted labelling may be difficult to avoid (Hechteler, 1984). To determine the likelihood of labelling en passant fibers by dye applied to the torus semicircularis, I examined fiber tracts known to pass through or near the torus semicircularis, but also known to not contact it. Two such structures were the anterior and posterior mesencephalocerebellar tracts (Nieuwenhuys and Pouwels, 1983). Although the area surrounding these neuronal tracts was heavily labelled at times, no evidence of labelled fibers was found in them, in any of the animals I studied. This suggested that label was not taken up by *en passant* fibers, at least those that were part of bundles or tracts. However, some labelling of *nucleus isthmi* neurons was found on occasion, coinciding with the presence of labelled tectal neurons. Since the *nucleus isthmi* is known to have reciprocal connections with the optic tectum through fibers that pass near the torus semicircularis (Ito et al., 1982; Gruberg et al., 1994; see also diagram on Fig. 18), it is possible that labelling in the optic tectum originated from these fibers. In light of this, conclusions regarding the origin of the labelled tectal neurons will have to be made with caution (see discussion). Next, I will describe the retinal projections and the connection patterns of the torus semicircularis separately, and then focus on areas of convergence.

Retinal projections

The pattern of retinal projections in rainbow trout has been described in detail elsewhere (Pinganaud and Clairambault, 1979; Mansour-Robaey and Pinganaud, 1991: see solid lines on Fig. 18), and I will thus concentrate on the differences I found with these earlier reports. The main difference between my results and those from earlier reports was a small contingent of ipsilateral projections. Contrary to what was reported by Ebbesson et al. (1988) in sockeye salmon smolts, I did not find any non-decussating fibers at the optic chiasm. The ipsilaterally projecting fibers that I found reached their target by re-crossing the midline of the brain at the level of the posterior commissure (Figs. 20 and 21A). Again, contrary to what was found in sockeye salmon smolt (Ebbesson, et al., 1988), none of these fibers could be followed to the optic tectum. Instead, these ipsilateral projections seemed to terminate in the pretectal area (Figs. 20 and 21A).

Connections of the torus semicircularis

Following labelling of the TS, an extensive pattern of connections was revealed. The general pattern of toral connections did not differ from that reported by de Wolf et al. (1983) in rainbow trout. By far the most substantial number of labelled cell bodies was found bilaterally in the octavolateral area of the myelencephalon. Fibers were also consistently found in the transverse commissure of the mesencephalon, a structure known to reciprocally link the tori semicircularis on both sides of the brain.

A major portion of the descending projections to the torus semicircularis originated in the ipsilateral optic tectum. Neurons labelled retrogradely from the torus

Figure 20: Diagram of cross section of the brain at the level of **A** the torus semicircularis and **B** the posterior commissure and various diencephalic nuclei.
The level at which these sections were taken is indicated in the inset. Diagram in **B** describes the location from which the micrographs presented in figures 4 and 5 originate. **A.th.l.** = *area thalamica lateralis*; **C.o.l.th.** and **C.o.b.th.** = *centrum opticum laterale* and *basale thalami*, respectively; **OT** = optic tectum; **PC** = posterior commissure; **TS** = torus semicircularis **V** = ventricle. Nomenclature after Pinganaud and Clairambault (1979).

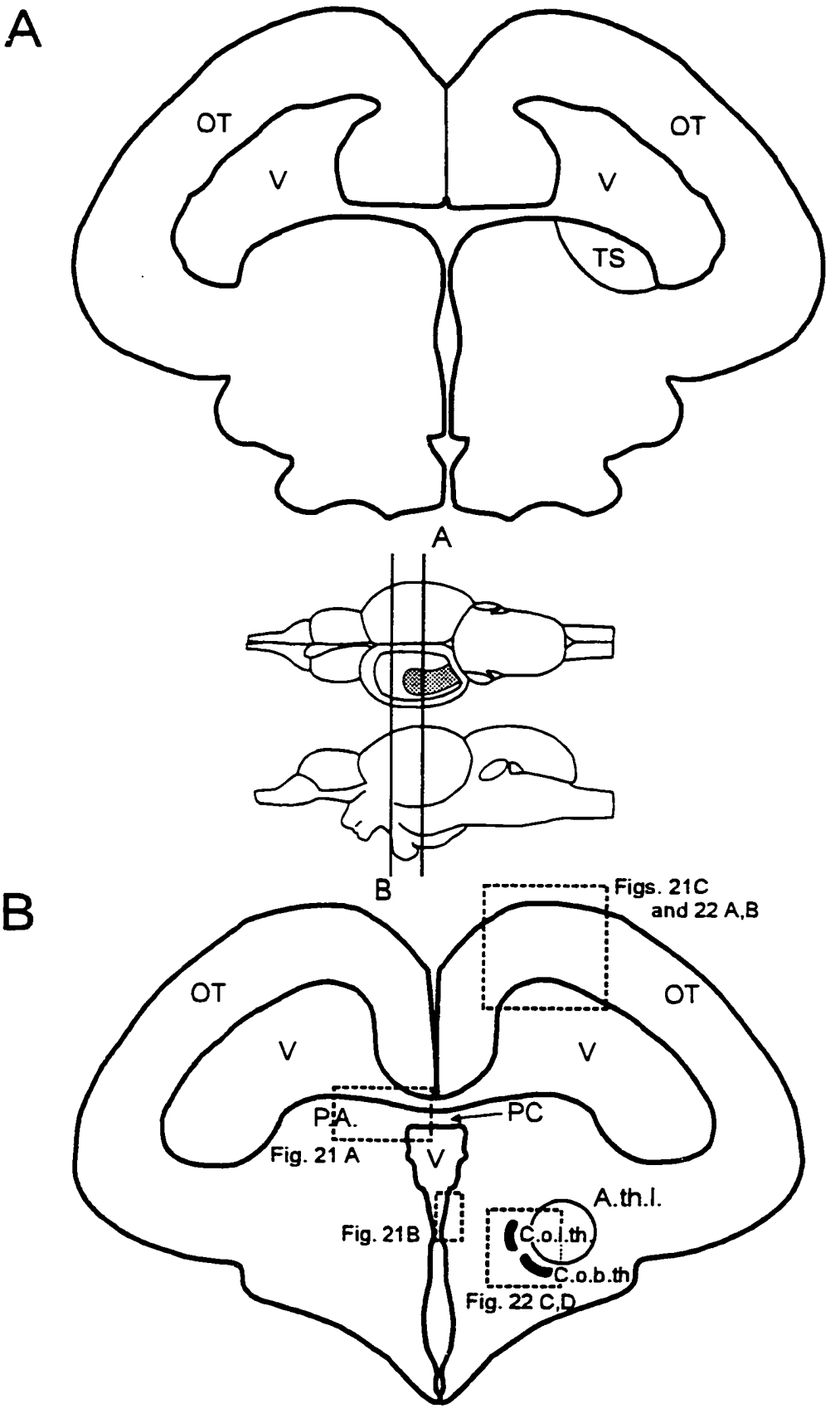
A
OT
V
OT
V
TS
A
B
B
Figs. 21C
and 22 A,B
OT
V
OT
V
P.A.
PC
Fig. 21 A
V
A.th.l.
Fig. 21B
C.o.l.th.
C.o.b.th
Fig. 22 C,D

Figure 21: Retinal projections and neurons labelled retrogradely from the torus semicircularis.

A Anterogradely labelled ipsilateral retinal fibers in the posterior commissure of the trout brain, and their terminal field in the ipsilateral pretectal area. Arrows point to fibers as they exit the posterior commissure, on the side of the brain ipsilateral to the labelled optic nerve stump. Arrow heads point to labelled fibers in the ipsilateral pretectal area. **B** Periventricular thalamic neurons labelled retrogradely from the torus semicircularis. **C** Tectal neuron labelled retrogradely from the torus semicircularis. Cell body of this neuron is located in the **sgc** (see Fig. 22A, B) of the optic tectum, and dendrites (arrow heads) extend to and bifurcate in the **sfgs**. **sfgs** = *stratum fibrosum* and *griseum superficiale*; **sgc** = *stratum griseum centrale*. Nomenclature of tectal layers from Meek (1990). Calibration bar 10 μm.

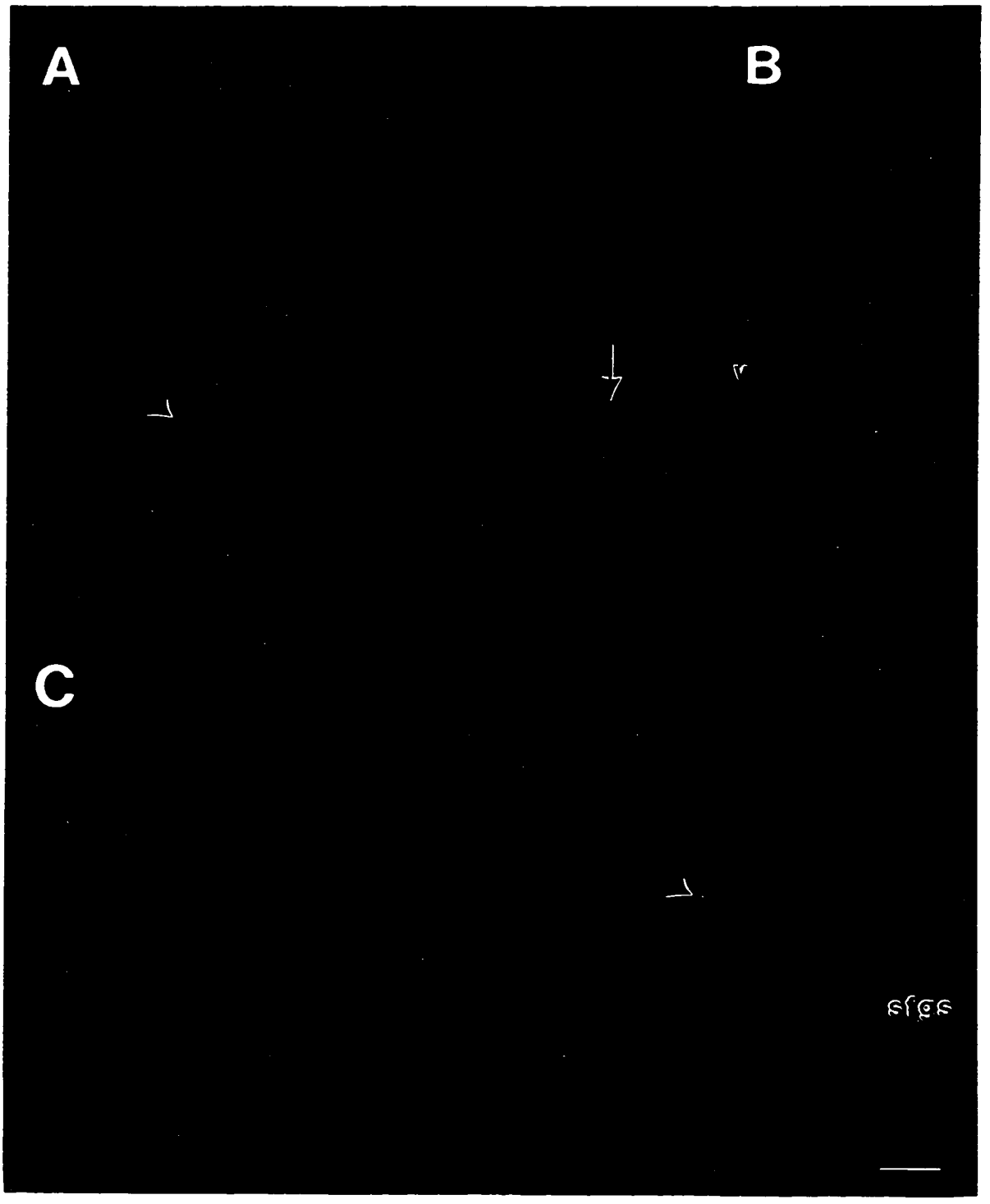
A
B
C

semicircularis were piriform in shape, had their cell body located in the **sac** and **sgc** of the optic tectum, and extended dendrites to more superficial layers such as the **sfgs** (Figs. 21C and 22B; nomenclature according to Meek, 1990. See Figure captions for explanation of these abbreviations). This projection to the torus semicircularis, however, appeared to be present only when label reached the deeper layers of the torus semicircularis and also coincided with the presence of labelling in the *nucleus isthmi*. A second group of neurons retrogradely labelled from the torus semicircularis was also present, albeit more inconsistently. These neurons were also piriform, and were located in the periventricular area, at the level of the posterior commissure (Figs. 20 and 21B). The third group of neurons projecting to the torus semicircularis was consistently found in the diencephalic area, ventro-medial to the *area thalamica lateralis* of Pinganaud and Clairambault (1979). These labelled neurons were always in very small numbers, although many labelled fibers lead to the area where these neurons were found (Figs. 20 and 22C,D).

Convergence of retinal projections and torus semicircularis connections

Since information in the trout visual system is presumed to follow from the axon of a presynaptic neuron to the dendrites or the cell body of postsynaptic neuron(s), the putative retino-toral pathway should have been composed of RGC axons, and cell bodies which sent their axon to the torus semicircularis. Two of the areas mentioned above met these requirements: the optic tectum from the side ipsilateral to the labelled torus semicircularis and the accessory optic center.

The most prominent area of convergence was the optic tectum located ipsilateral to the labelled TS (Figs. 20 and 22A). Retinal projections to the contralateral optic

Figure 22: Convergence of retinal projections and torus semicircularis connections. **A** Pattern of retinal projections onto the various layers of the optic tectum of rainbow trout. Abbreviations on the right hand side represent various tectal layers, as defined by Meek (1990). Retinal projections are present in three tectal layers: **so**, **sfgs** and **sac**. **B** Tectal neurons (yellow) retrogradely labelled from the torus semicircularis extend dendrites (arrow head) into retino-recipient layers (green labelling) of the optic tectum. **C** and **D** Area of convergence between retinal projections (green) and thalamic neurons (gold) retrogradely labelled from the torus semicircularis. **sac** = *stratum album centrale*; **sfgs** = *stratum fibrosum* and *griseum superficiale*; **sgc** = *stratum griseum centrale*; **so** = *stratum opticum*. Calibrations bar 25 μm for **A**, and 10 μm for **B**, **C** and **D**.

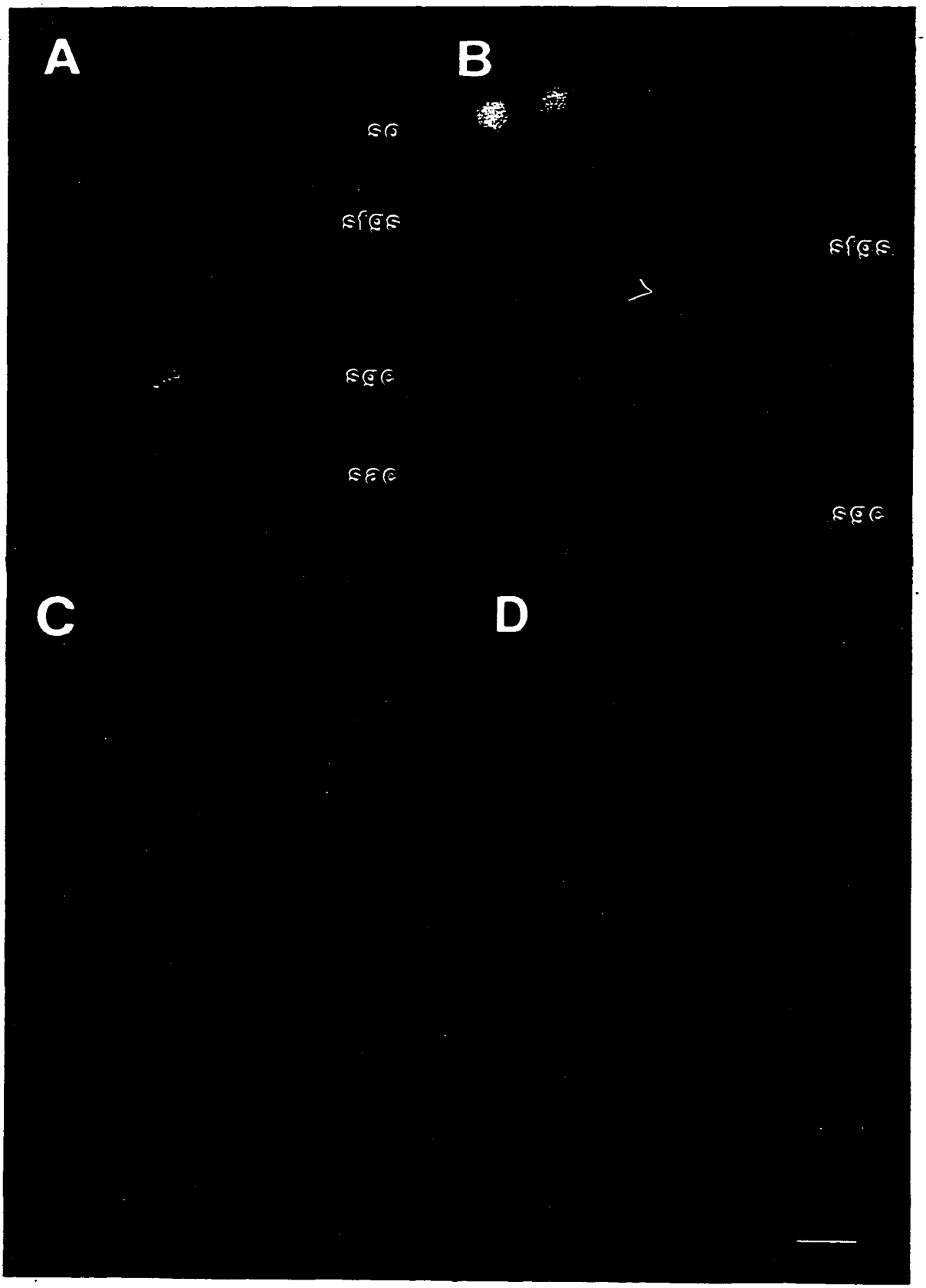
A
B
C
D

tectum were directed at the **sac**, **sfgs** and **sgc** (Fig. 22A). Labelled cells bodies were also found in the optic tectum following labelling of the torus semicircularis. The cell body of these neurons was located in the **sac** and **sgc** (Fig. 22B). Generally, these tectal neurons extended processes into the retino-recipient layers of the optic tectum, as shown by the double labelling presented on Figure 22B. On this Figure, retinal projections appear in green, and the tectal neurons appear in yellow. Tectal neurons labelled retrogradely from the torus semicircularis were of the piriform type described by Pinganaud and Clairambault (1979).

The second area of convergence was located in the areas described as *centrum opticum basale thalami* and *centrum opticum laterale thalami* by Pinganaud and Clairambault (1979), which these authors believe are homologous to the accessory optic center in other teleosts. These areas were located medial to the *nucleus anterior thalami* (Nieuwenhuys and Pouwels, 1983), also referred to as the *area thalamica lateralis* by Pinganaud and Clairambault (1979) (Fig. 20). In this area, neurons retrogradely labelled from the torus semicircularis (Fig. 22C,D) extended dendrites in or around the area where direct retinal projections were apparently terminating (Fig. 22C, D).

Discussion

Although some precautions were taken to ensure that the structures identified as connected to the torus semicircularis were not contaminated by non-target labelling, this possibility remains. As mentioned above, only intracellular dye injections practically eliminate the chance of non-targeted labelling. In this study, the use of control structures

as safeguards against non-target labelling indicated that dye uptake was acceptably specific to the structures connected to the torus semicircularis, with the exception of retrogradely labelled tectal neurons (see below).

Ipsilateral retinal projections in rainbow trout

Ipsilateral retinal projections in trout have not been demonstrated previously. Three other studies examined the pattern of retinal projections in rainbow trout, and did not find evidence of direct ipsilateral projections (Pinganaud and Clairambault, 1975, 1979; Mansour-Robaey and Pinganaud, 1991). Using HRP, Mansour-Robaey and Pinganaud (1991) examined the ontogeny of retinal projections in rainbow trout, from hatching to 3 months of age. Two explanations may account for their failure to find ipsilateral retinal projections in their animals. First, it is possible that the ipsilateral projections appear at a later stage than those examined by Mansour-Robaey and Pinganaud (1991). Second, according to Fritzsch and Wilm (1990), the dyes used in the present study, conjugated dextran amines, are more sensitive neurotracers than HRP, the substance used by Mansour-Robaey and Pinganaud (1991). The failure of HRP to label structure that are nevertheless present was underlined by Prasada Rao and Sharma (1982) in catfish. In their study on the catfish, Prasada Rao and Sharma (1982) showed that ipsilaterally projecting fibers labelled by autoradiography failed to be revealed by HRP injections. Given the paucity of the ipsilateral projections in juvenile rainbow trout, it is plausible that a less sensitive tracing technique, such as HRP, may fail to reveal them.

Using a combination of degeneration and autoradiography, which are considered very sensitive techniques (Collin and Northcutt, 1995), Pinganaud and Clairambault

(1975, 1979) did not find any ipsilateral projections in rainbow trout either. In this case, the most likely explanation for the discrepancy between my results and theirs may relate to the size of the animals that were used in the two studies. Pinganaud and Clairambault (1975, 1979) used rainbow trout that were larger than those used in the present study. This would thus suggest an ontogenetic disappearance of the ipsilateral projections, around the time when UV sensitivity is lost. Whether or not the two events are related is still a matter of speculation.

Ontogenetic disappearance of ipsilateral projections have been reported in another teleost species, the yellow-finned bream, *Acanthopagrus australis* (Collin, 1987). In addition, Collin and Northcutt (1995) recently found ipsilaterally projecting RGCs in the retina of juvenile garfish, and speculate as to the possibility of their disappearance later in life in this species as well.

Convergence of retinal projections and toral connections

A single report of direct retinal projections to the torus semicircularis has been made (Ebbesson et al., 1988). According to Ebbesson et al. (1988), these projections are transient, appearing only around the time of smoltification in sockeye salmon. As the animals I studied were presumably at an earlier developmental stage than those studied by Ebbesson et al. (1988), it is possible that my failure to find them in rainbow trout is due to the transient character of these projections. As the animals studied by Coughlin and Hawryshyn (1994a, b) were of a developmental stage similar to the ones I studied, however, it is unlikely that the UV inputs to the torus semicircularis these authors identified resulted from direct retinal projections. This therefore suggests that visual

information to the torus semicircularis travels through at least one intermediate structure. The results from this study point to two candidates: the accessory optic center of the thalamus and the optic tectum.

Neurons retrogradely labelled from the torus semicircularis have been found in rainbow trout, using HRP (de Wolf et al., 1983). It was not clear, however, whether or not these neurons served any visual function. As shown in the present study, the presence of retinal projections to the accessory optic center, where neurons labelled retrogradely from the torus semicircularis are also present, suggests a visual role for these neurons. This further suggests their possible involvement in the transmission of visual information to the torus semicircularis. My results, however, do not show that retinal projections establish a direct contact with these thalamic neurons. As mentioned earlier, an ultrastructural analysis would be required to ascertain the presence of such physical contacts. The results from this study, however, indicate that retinal projections do appear to terminate in the accessory optic center of trout, where neurons labelled retrogradely from the torus semicircularis are also present. These findings are supported by results of radioactive proline autoradiography experiments (Pinganaud and Clairambault, 1979) which specifically labels projection terminal fields. Furthermore, the close proximity of these retinal projections to dendritic arborizations of retrogradely labelled neurons suggests this may constitute a visual pathway to the torus semicircularis. Nevertheless, at this time, there is no indication that these retinal projections to the accessory optic center of trout carry any UV information.

My results indicate that the optic tectum may also be a substantial contributor of inputs to the torus semicircularis and, as such, still remains a possible candidate for the origin of the UV inputs to the toral single units described by Coughlin and Hawryshyn (1994a, b). It is not possible at this stage, however, to be certain that the retrogradely labelled tectal neurons are truly projecting to the torus semicircularis. This possibility, however, may be supported by results from de Wolf et al.(1983), who also found tectal neurons labelled retrogradely from the torus semicircularis. Similar to what I found, tectal neurons were labelled only when the deeper layers of the torus semicircularis were reached by the label injection (de Wolf et al., 1983).

Some of my results generally agree with those of Hechteler (1984) in carp, who also found thalamic neurons retrogradely labelled after HRP injection in the torus semicircularis. The neurons this author found in the periventricular central posterior thalamic nucleus may correspond to those I found in the periventricular thalamus of rainbow trout. However, because of the complexity and high degree of variation that exists in the brains structure among various species of fish, homologies between cell groups are difficult to establish. In carp, the central posterior thalamic nucleus is involved in the processing of auditory information and reciprocally connected to the torus semicircularis (Hechteler, 1985b). It would be of interest to determine whether in trout, the neurons labelled retrogradely from the torus semicircularis are also involved in processing of auditory information.

More work is needed to understand the organization of the visual inputs to the torus semicircularis. Based on the results presented here, future electrophysiological

investigations should focus on the accessory optic center, and the pathway that connects this thalamic area to the torus semicircularis. Much remains to be learned about the physiology of visual centers in the fish brain, particularly with respect to UV sensitivity and spectral coding.

Chapter 5: Adaptation in the photopic and scotopic systems of rainbow trout

Introduction

Vision in many vertebrates is subserved by two systems that operate under different levels of ambient illumination. Rod photoreceptors mediate the response of the scotopic[8] system which operates at low light levels, whereas cone photoreceptors mediate that of the photopic system, active mostly at higher ambient light levels (see Frumkes, 1990). The scotopic and photopic systems complement each other and allow animals to perform visually-guided behaviors over a wide range of ambient light intensities, which spans over 12 decades for the human eye (Fein and Szuts, 1982). During light and dark adaptation, there is a transition between the activity of these two systems, which in fish involves physiological and morphological changes at the retinal level (Douglas, 1982a, b; Ali and Klyne, 1985). In addition, light and dark adaptation also involve physiological changes within the photopic and scotopic systems themselves, which result in changes in the sensitivity and time course (speed) of responses.

The physiological constraints imposed by the conditions under which these two systems operate have created differences in the sensitivity and temporal characteristics of the two classes of photoreceptors that subserve vision in dim and bright environments. Generally, rods are designed to maximize photon capture and thus sensitivity, at the cost

---

[8] For the purpose of this paper, I define scotopic state as that dominated by rod responses and photopic state as that under which mostly cone photoreceptors are active. I reserve the term mesopic to situations in which there are reasons to believe that inputs from both rods and cones are present, in similar proportions. Accordingly, I also use the terms scotopic, photopic and mesopic to refer to the underlying mechanisms: scotopic mechanism (rods), photopic mechanism (cones) and mesopic mechanism (both rods and cones).

of lower temporal and spatial resolution. By contrast, cones have evolved to provide maximal temporal and spatial resolution, at the expense of sensitivity (Fein and Szuts, 1982). The first thorough evaluation of the physiological properties of rods and cones was by Baylor and Hodgkin (1973), who found that the saturating response of individual turtle photoreceptors to weak flashes of light was reached approximately three times later in rods than in cones. Conversely, absolute sensitivity of the rod photoreceptors was close to one order of magnitude higher than in cones. These characteristics of rods and cones have been described in other species since then, and have been attributed mainly to the different morphological organization of their outer segments (see Miller and Korenbrot, 1993). Rods and cones, however, share several physiological characteristics that probably reflect a similarity in the biochemical processes that underlie their response to light. Among these, their response to background lights of increasing intensities, i.e., their light adaptation properties, is of primary importance.

With increasing stimulation, response amplitude increases, and response time course decreases for both rods and cones (Baylor and Hodgkin, 1973, 1974; McNaughton, 1990; Miller and Korenbrot, 1993). In addition, there is a general loss of sensitivity and a decrease in response time course associated with increases in steady background intensity: these are the hallmarks of light adaptation (Daly and Norman, 1985; Donner et al., 1995; Koutalos and Yau, 1996). The change in sensitivity associated with light adaptation is expressed by a shift and compression of the stimulus-response (S-R) curve along the intensity axis with increasing ambient light levels (Normann and Werblin, 1974; see also chapter 1). The change in time course associated with light

adaptation is expressed by a gradual decrease in the latency of responses at threshold with increasing ambient light levels, among other parameters.

Certain types of interactions within the visual system depend not only upon the relative strengths of various inputs, but also on the relative timing of these inputs (see Gouras and Zrenner, 1979). To understand the effects of ambient light levels on the physiology of the visual system, it is therefore important to provide accurate descriptions of the changes that occur in both the sensitivity and temporal properties of visual responses during light adaptation.

To date, changes associated with light adaptation have been mostly examined psychophysically, electrophysiologically (at the level of single photoreceptors and horizontal cells) or with electroretinogram (ERG) recordings (Peachey et al., 1989; Robson and Frishman, 1995). Recently, Donner et al. (1995) described the effects of light adaptation on the temporal properties of responses recorded extracellularly from RGCs, intracellularly from rods, and from rod ERG in *Rana temporaria*. Similar information on the responses of fish RGCs is still missing.

In this study, I examined the change in threshold and time course of ONRs with adaptation in juvenile rainbow trout. As mentioned in chapter 2, this level of recording represents an intermediate stage in the processing of visual information, between the photoreceptor response and the whole animal response. My specific aim was to quantify the relationship between changes in relative ambient light levels and changes in the sensitivity and time course of the trout ONR. I examined how response threshold and time course varied with backgrounds of increasing intensity. The protocol was designed

to allow the study of adaptation in the middle wavelength part of the spectrum, where rods and M cone mechanism are active, with minimum intrusion by cone mechanisms from other parts of the spectrum. I found that response time course in rainbow trout RGCs varied as a logarithmic function of both stimulus and ambient light intensities. Comparison with previous literature suggests that this may be a general rule for vertebrate photoreceptors.

Material and methods

Study animals

The animals used in this study (rainbow trout, *Oncorhynchus mykiss*, n=5) were obtained from the Fraser Valley Trout Hatchery (Abbotsford, B.C.). They were kept at 15°C, under a constant 12L:12D photoperiod, and ambient illumination was provided by white fluorescent tubes (33.54±14.39 mW at the surface of the holding tanks). The animals (8.5±2.3g body weight) were presumed to possess ultraviolet light sensitivity, based on previous studies (Browman and Hawryshyn, 1992; Beaudet et al., 1993; Chapters 2 and 6 of this dissertation). Experiments were carried out at 15°C, and all protocols were approved by the University of Victoria Animal Care Committee.

Electrophysiological recordings

The surgical and recording procedures used to obtain optic nerve responses have been described previously (Beaudet et al., 1993; chapter 2 of this dissertation) and will only be summarized briefly here. I recorded multiunit responses from the optic nerve of anesthetized animals (MS222, 1:10 000, Crescent Research Chemicals, Phoenix AZ) using

a Teflon-coated silver wire (0.45 mm, A-M Systems) inserted through the surgically exposed optic tectum. Signals were differentially amplified 20 000 to 50 000 times with a pre-amplifier (Grass, P-50 Series), digitized and analyzed with a personal computer. Stimulus duration was 500 ms, and the interstimulus interval was 1 min, but was reduced to 15 s for subthreshold stimulus intensities.

Responses were typically multiphasic, composed of an initial negative potential followed by a positive deflection, and sometimes by another negative deflection (Fig. 23). These were generated at the onset and offset of the stimulus (ON and OFF responses respectively), and analyzed separately. Two parameters were measured from the ONRs: its amplitude and implicit time, for the ON and OFF components. Response amplitude was measured from the baseline to the maximum of the ONR's first negative deflection. Response implicit time at a given intensity-wavelength combination was given by the time between the onset (or the offset) of the light stimulus and the absolute maximum of the first negative deflection (ON and OFF) (Fig. 23). This measure should not be confounded with the latency of a response, which I did not measure, and which refers to the time delay between the stimulus onset and the initiation of the response. Implicit time was chosen mainly because it is more easily determined objectively, but nonetheless covaries with response latencies over a broad range of response intensities.

At each test wavelength, two types of curve were generated using results from the measurements of response amplitude and implicit time. First, stimulus-intensity (S-R) curves were generated for the ON and OFF responses by plotting the amplitude of the response against stimulus irradiance, and were fitted with a third order polynomial

Figure 23: Rainbow trout optic nerve response to the onset of a 380 nm light stimulus. Response amplitude *A* was measured from the average baseline to the peak of the first negative deflection, and implicit time *IT* from the onset of the stimulus to the absolute maximum of the first deflection. The vertical deflection of the stimulus trace was represents at 80 μV on the vertical axis.

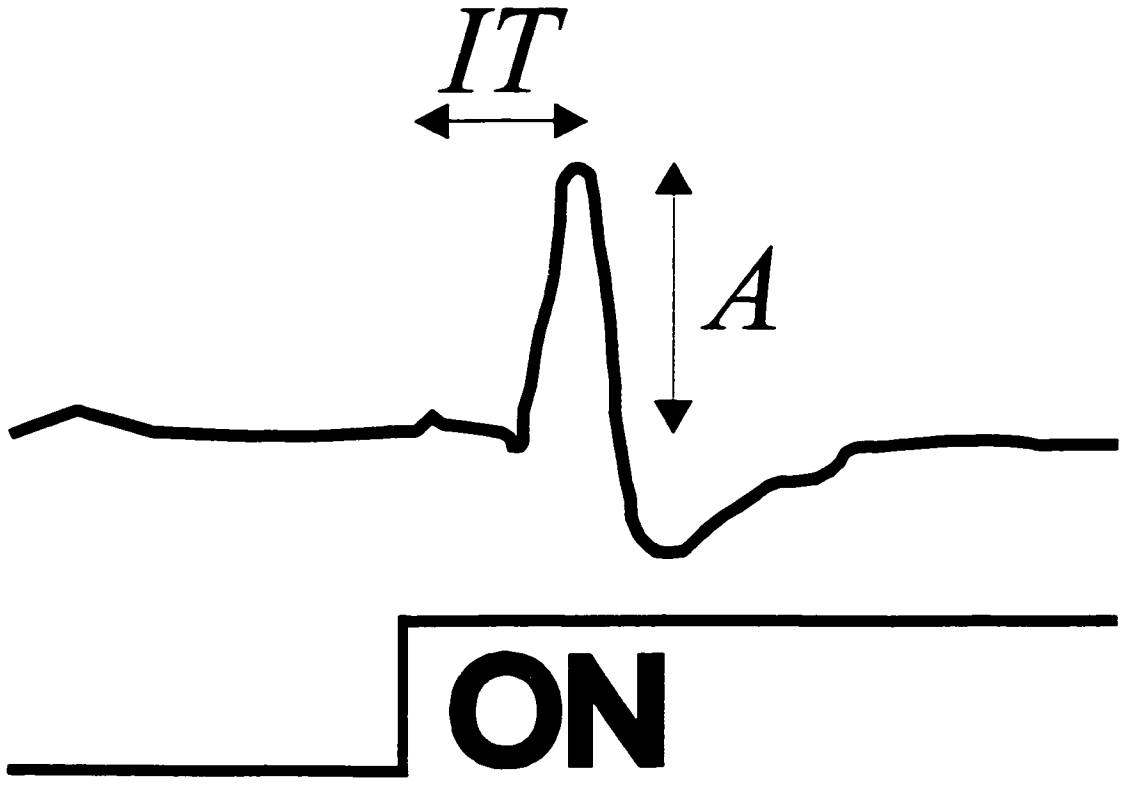
IT
A
ON

function from which a threshold irradiance was determined. Sensitivity was determined as the reciprocal of this threshold irradiance. A third order polynomial function was preferred to the Naka-Rushton function (Naka and Rushton, 1967) because it provided a better fit overall, especially at higher stimulus intensities. The threshold irradiance was that which elicited a criterion response of 30μV, which lay in the linear part of the S-R curve. Second, stimulus-implicit time (S-IT) curves were obtained by plotting implicit time values against stimulus intensity, on a log-log graph. These curves were fitted with the logarithmic function described in the Results section.

Optical system

The light stimulus was superimposed over a constant background that was used to simulate various levels of ambient illumination. The optical system consisted of a stimulus channel powered by a 400 W Xenon light source, and two background channels, each powered by a 250 W tungsten halogen source. The three channels converged, via liquid light guides, onto a diffusing screen made of 0.8 mm thick sanded plastic placed directly in front of the fish's eye. This acted as a diffusing screen and was used to provide even retinal illumination by the three optical channels. Chromatic properties of the stimulus channel were adjusted by a monochromator (Instruments SA), and those of the background by interference filters (550LP filter, Corion, Holliston, MA, allowing through wavelengths above 550 nm mostly, see Fig. 24). Stimulus intensity was controlled by a combination of neutral density filters and an Inconel coated neutral density wedge (nominal 4.0 neutral densities [ND]), whereas that of the background channels was controlled by combinations of neutral density filters (Corion, Holliston, MA). Stimulus

Figure 24: Background irradiance curve (550 LP interference filter) superimposed on the absorption spectra of the visual pigments present in the parr rainbow trout retina. Left axis pertains to the photopigment absorption curves, the right axis to the irradiance spectrum of the background. Letters UV, S, M and L refer to the ultraviolet, short, middle and long wavelength cone mechanisms subserved by the various cone types, and R to the rod mechanism.

Relative absorbance
1
0
UV
S
R
M
L
550 LP
-2
-3
-4
-5
Log irradiance
300
400
500
600
700
Wavelength (nm)

duration was controlled by a computer-driven shutter (Uniblitz). During the recording session and for the duration of dark adaptation, I kept the study animal in a Faraday cage light-proofed with thick black plastic, in a dark room.

Recording protocol

Prior to each recording session, fish were dark-adapted for a minimum of 1.5 h. In the dark-adapted state, S-R and S-IT curves were obtained at the test wavelengths. After thresholds were determined in the dark-adapted state, the two backgrounds, with 8 ND in each optical path, were turned on and the animal left to adapt for 15 min. Stimulus-response and S-IT curves were obtained at the end of the new adaptation period. Background intensity was then increased by removing 1 ND from each background channel and the procedure was repeated until no neutral density filter remained in the background channels. The typical experiment lasted about 12 h from the beginning of dark adaptation. Thus, thresholds were determined in the dark-adapted state, and over an 8 log unit range of background intensities. Eight neutral density units was chosen as the dimmest background intensity because it corresponded to an intensity imperceptible to the dark-adapted human eye, and 1 log unit below the sensitivity threshold of our radiometer (see Appendix C for a list of the background radiances and the corresponding neutral density values used). It was therefore deemed sufficiently dim to adequately represent the early stage of the light adaptation process. For the purpose of this study, I will refer to the relative background intensity in relation to the dimmest background that was not complete darkness (8.0 ND in both background channels). Under this scheme, dark corresponds to an arbitrary -1, 8 ND to 1, 7 ND to 2 and so on. Thus, according to this scale, the

background ranged in relative intensity from an arbitrary -1 value, to a maximum of 9, with each background intensity representing and increase of 1 log unit over the preceding one, with the exception of -1 and 1.

This procedure led to the generation of curves depicting the change in response threshold as a function of relative background intensity (TVI curves). These curves were fitted with a linear function over their linear part by a least sum of square procedure (Cricket Graph for Windows, Computer Associates, San Diego, CA). Non-linear portions of the curves were fitted by eye. A more detailed description of the TVI curves is provided in the Results section.

The four test wavelengths chosen were: 380, 430, 540 and 620 nm. The choice of these four wavelengths and the chromatic background resulted from a compromise between maximizing stimulus efficiency for the rods and M mechanism and minimizing the likelihood of intrusions from the other cone mechanisms. This meant that the wavelength chosen for the rods and M cone mechanism was displaced toward longer wavelengths with respect to their λ_{max} (Fig. 24), to maximize the distance from the λ_{max} of the UV and S cone mechanisms. A 550LP interference filter background was preferred to a "white" background because it provided a relatively good overlap with the absorbance spectrum of both the rod system and the M mechanism while providing maximal adaptation of the L cone mechanism (Fig. 24). This allowed us to study the effects of light adaptation on rods and a cone mechanism with a similar λ_{max} (the M mechanism), under conditions where interference from the L mechanism was minimal due to the long-wavelength bias of the chromatic background. I expected that the absence of significant overlap between the

adapting background and the UV and S cone mechanisms' action spectra would lead to little adaptation of these cone mechanisms. This was expected to generate differences between the shape of TVI curves at 540 nm and at shorter wavelengths under conditions where the photopic systems were active. The presence of these differences was expected to help ascertain the identity of the active mechanism, scotopic or photopic, for the various parts of the TVI curves.

Results

In this section, I will examine the effects of light adaptation on various aspects of the ONR, namely: (i) the ONR waveform, (ii) thresholds obtained at various wavelengths, over a wide range of background intensities and (iii) various aspects of the temporal properties of responses in relation to the various background intensities. Note that under conditions of full field stimulation such as those used in this study, the optic nerve responses were presumed to originate from the center of RGCs' receptive field (Daw, 1968; Spekreijse et al., 1972; Werblin, 1974).

Light adaptation and the ONR waveform

The state of adaptation of the retina was partially reflected in some properties of the ONR waveform. First, maximum amplitude of the optic nerve responses of the dark-adapted retina (presumably dominated by rod inputs) were about half (43±5%, n=3) of that at higher background intensities (presumably dominated by cone inputs). This is exemplified in Figure 25 which represents the S-R curve of a dark-adapted fish for stimulations spanning 7 log units. This S-R curve contains two peaks of response amplitude: the first, smaller peak, which presumably represents scotopic system

Figure 25: Stimulus-response curve of a dark-adapted fish over 7 log units, at 540 nm. The two maxima likely represent the activity of the scotopic and photopic systems, respectively. Note the difference in maximum amplitude of the response between the scotopic and photopic conditions. Also note the "dip" in amplitude that occurs between the maxima. Units for the horizontal axis are in photons cm^{-2} s^{-1}.

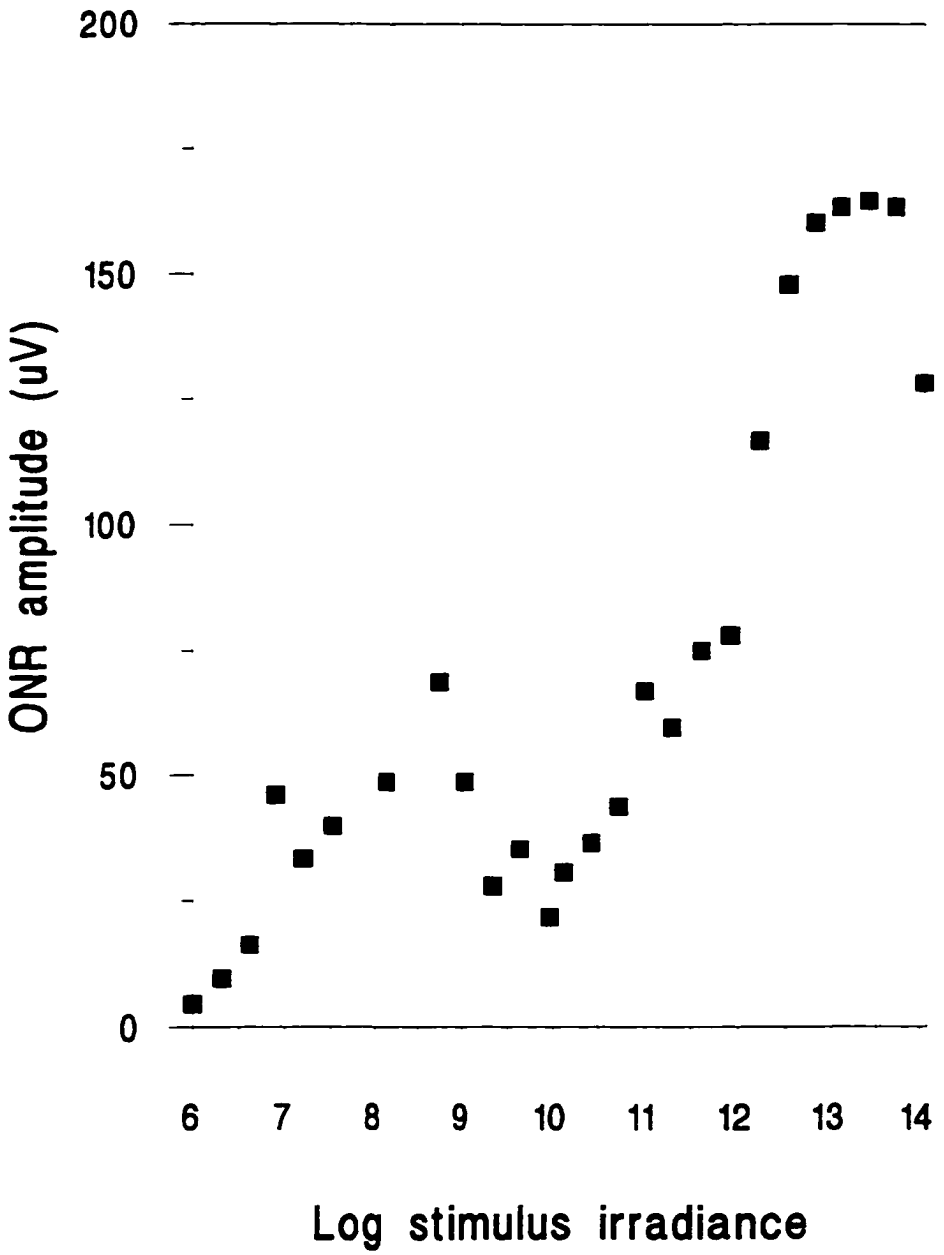
200
150
100
50
0
ONR amplitude (uV)
6
7
8
9
10
11
12
13
14
Log stimulus irradiance

responses, and the second, larger peak, corresponding to those of the photopic system (see Schneider et al., 1986). The two peaks in this S-R were separated by a "dip" similar to that reported by Schneider et al. (1986) in the cat ERG b-wave.

Second, the half-bandwidth of the ONR's first negative deflection tended to be greater under completely dark conditions than when the background light was turned on. Half-bandwidth refers to the width of the waveform at half of its maximal amplitude. I did not attempt to quantify the differences observed.

Third, in the dark-adapted retina, the electrophysiological waveform consisted of an ON response exclusively. The OFF response was visible only when relative background intensity was increased to 6 - 7 log units. This, however, may have been due to the much lower sensitivity of the OFF response in the dark-adapted state, as opposed to the genuine absence of an OFF response (as noted by Wheeler, 1979b, in the dark-adapted goldfish ONR). In the following sections, the OFF response is discussed only on a few occasions. Because the OFF response's sensitivity was always much lower than that of the ON response over a wide range of relative background intensities, data for the former were normally not collected over a range of intensities sufficient to permit the establishment of precise trends. This was due to the fact that I did not want to stimulate at intensities that would be too much above the point of saturation of the ON response, to avoid undue adaptation of the retina by the stimulus.

Threshold versus background intensity

As reported in amphibian RGCs (Werblin and Copenhagen, 1974), light adaptation

in trout resulted in the lateral shift of the S-R curve, along the log intensity axis, as shown in Figure 26. In this Figure, the S-R curve for a single individual at 3 increasingly brighter backgrounds is shown to shift toward progressively higher stimulus intensity ranges. The magnitude of this lateral shift depended on the overall level of adaptation, and likely corresponded to the changes in threshold that are described below. This lateral shift was observed to a varying degree under low and high relative background intensities, indicating that it is a property of both the scotopic and photopic systems.

Threshold versus intensity curves, for a given mechanism, can often be dissected into a minimum of 4 basic segments, each representing a physiological state of adaptation (Enoch, 1972). When several mechanisms are successively active over a given range of background intensities, a corresponding number of TVI curves are normally recognized. Confusion may thus arise when attempting to describe such composite curves as the terminology used is the same for the individual and the overall curves; both are TVI curves. Therefore, in this section, I will consider the overall curve generated at a given wavelength as the TVI curve, and refer to regions where different mechanisms are active as the various parts of this curve, each composed of the basic segments.

Threshold increased with relative background intensity conforming, for the most part, to typical TVI curves (see Granda and Sisson, 1989; Hawryshyn, 1991). Generally, the TVI curves I obtained over the whole range of background intensities were composed of 2 major parts, corresponding to the activity of the scotopic and photopic systems, respectively. These curves could be dissected into 4 or 6 segments, depending on the test wavelength, such that the first 3 segments represented the activity of the scotopic system,

Figure 26: Effect of light adaptation on the stimulus-response curve at 540 nm. Increases in relative background intensity cause a shift of the S-R curve toward a higher stimulus intensities range (to the right). In this example, relative background intensity was increased in 1 log unit steps from left to right. Data points were fitted by eye to a Naka-Rushton-type function. Units for the horizontal axis are in photons cm^{-2} s^{-1}.

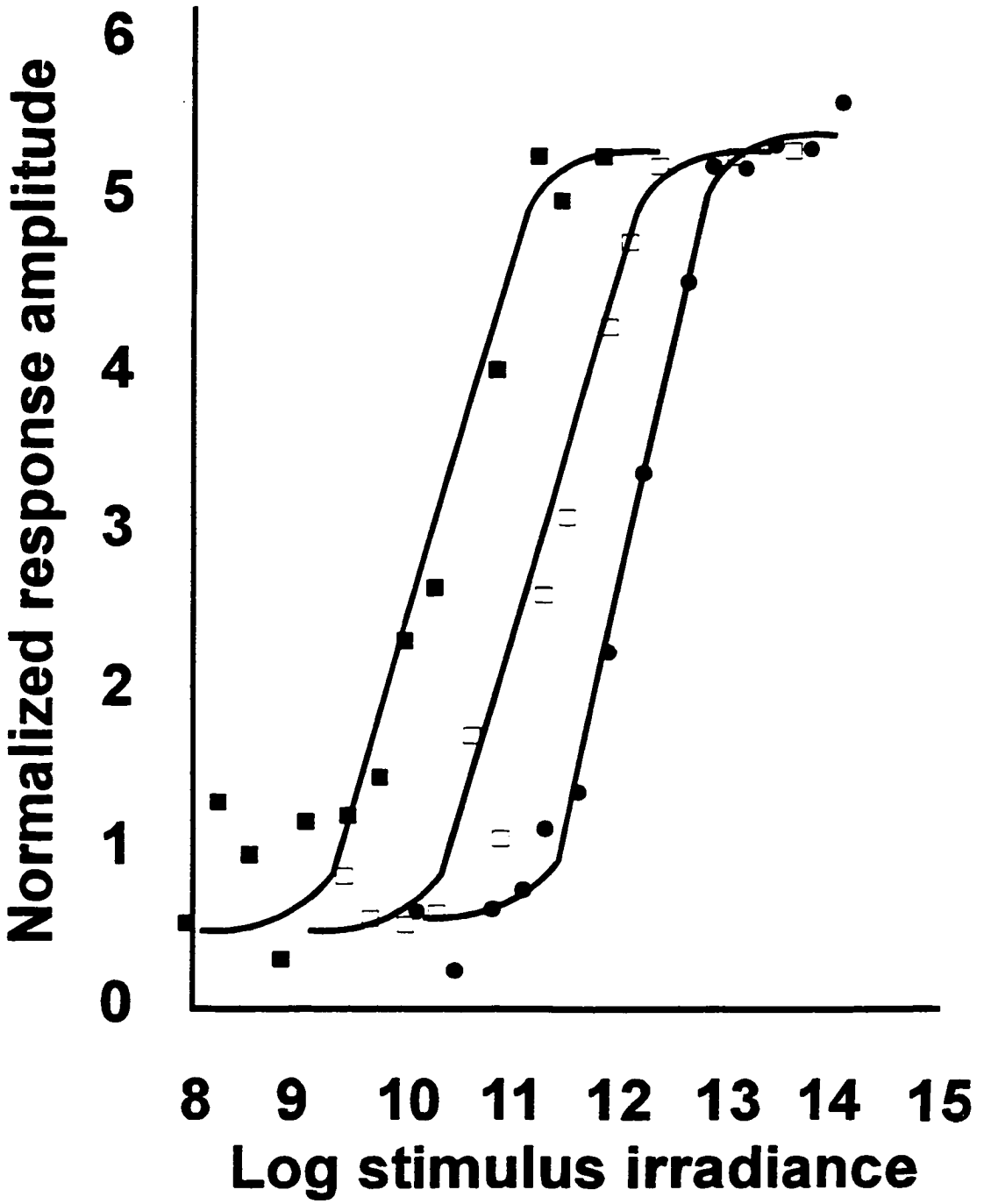
Normalized response amplitude
0
1
2
3
4
5
6
8
9
10
11
12
13
14
15
Log stimulus irradiance

the 4th segment values near the absolute threshold of the active photopic mechanism, and the 5th and 6th segments the activity of the photopic system. From this, it should be gathered that the second part of the TVI curve was incomplete in every cases, lacking the last 2 or 3 segments.

At 380 nm, the TVI curve included the first 4 of the segments described above (Fig. 27A, 380 nm). As similar results were obtained for 430, only the results at 380 nm will be examined here. The first 2 segments of the TVI curve at 380 nm were confounded and extended from the fully dark-adapted condition (referred to as the absolute threshold) to the next lowest background intensity (1 log relative background intensity). Typically, the relationship between background intensity and threshold in this second segment of the TVI curve is non-linear (Enoch, 1972). This non-linearity was not apparent in my results and, consequently, separation between these 2 initial segments was not noticeable, probably because of the large increments in relative background intensity that I used. From 1 to 5 log units relative background intensity, threshold increased linearly (3rd segment), with a slope of about 0.74 ($R^2 = 0.99$). At 5 log units relative background intensity, the rate of threshold change decreased to practically zero (Fig. 27A). This was to be expected as the background used probably adapted the UV mechanism minimally, such that it remained at its absolute threshold (4th segment), despite increases in background intensity. Therefore, above 5 log units relative background intensity, the ONR was probably dominated by inputs from the UV cone mechanism.

A salient feature of the results was the difference in the shape of the second part of

Figure 27: Threshold versus background intensity curves for various wavelengths. Data points represent the mean ± SD after individual curves were adjusted vertically to minimize inter-individual variability. In addition, position of the fully dark-adapted threshold along the relative background intensity axis is arbitrary, as it should theoretically be placed at $-\infty$. **A** Comparison of TVI data between 380 and 540 nm. **B** Comparison between 540 and 620 nm. The curves have been displaced on the vertical axis to emphasize their correspondence at lower relative background intensities. Arrow head points to part of the 620 nm TVI curve more sensitive than predicted theoretically.

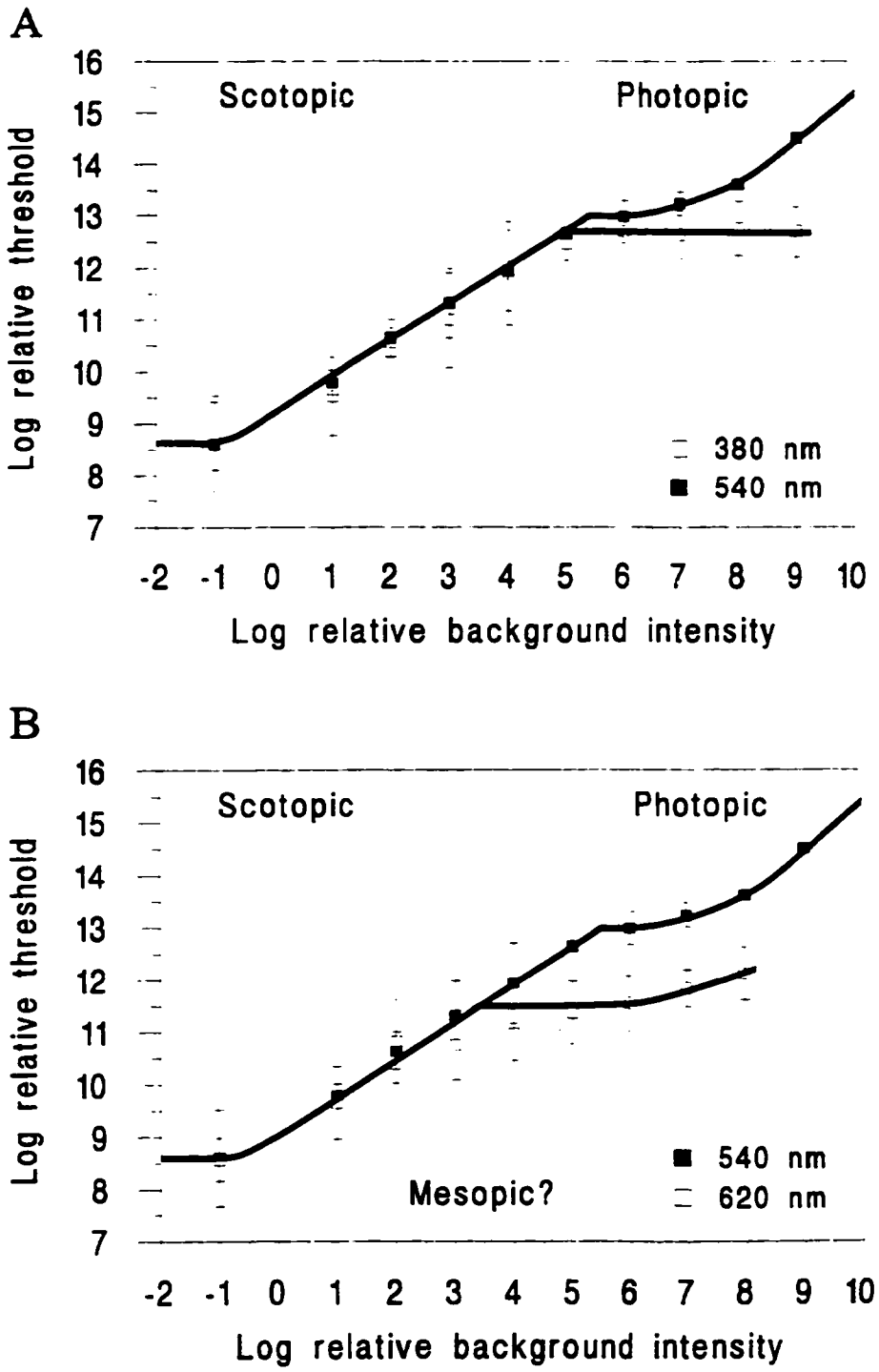
A
Scotopic
Photopic
380 nm
540 nm
Log relative threshold
Log relative background intensity
16
15
14
13
12
11
10
9
8
7
-2 -1 0 1 2 3 4 5 6 7 8 9 10
B
Scotopic
Photopic
Mesopic?
540 nm
620 nm
Log relative threshold
Log relative background intensity

the TVI curves among the various test wavelengths. Because of the spectral heterogeneity of the adapting background, TVI curves from the various parts of the spectrum differed at higher relative background intensities, as the various cone mechanisms probably differed in their adaptation state. This difference of adaptation state was best exemplified by comparing TVI curves for 380 nm and 540 nm (Fig. 27A). In the initial stages of light adaptation (from 1 to 5 log relative background intensity), the TVI curve at 540 nm generally paralleled that at 380 nm at a slope of 0.82 ($R^2 = 0.98$), presumably because a single system, the scotopic system, dominated the ONR at these relative background intensities. At higher relative background intensities (5 log units and above), TVI curve at 540 nm comported 3 identifiable segments: a short plateau representing the absolute threshold of the active mechanism, followed first by a non-linear increase in threshold and then by a linear increase. Because of the insufficient amount of energy generated by our optical system, I was not able to obtain any points above 9.0 log units relative background intensity. Therefore, the slope of the linear segment for the second part of the TVI curve at 540 nm could only be approximated at between 0.8 and 1.0.

There were also differences between the TVI curves for 540 and 620 nm. Threshold versus intensity curves paralleled one another only for the first three background intensities, i.e. under dark adaptation, 1 and 2 log units relative background intensity (Fig. 27B). At 2 log units relative background intensity, there was an inflection in the TVI curve at 620 nm, which resulted in a shorter 3rd segment, when compared to 540 nm. Over the range of background intensities expanding from 2 to about 5 log units,

threshold at 620 nm appeared to be somewhat lower than the predicted curves would indicate (see arrowhead on Fig. 27B). This suggested that over this range of intensities, summation of inputs from different mechanisms may have occured, as also suggested by measurements of implicit times at threshold at 620 nm (see below).

Light adaptation and ONR implicit time

In the following sections, I examine the effects of light adaptation on the implicit time of the ONR. First, I describe quantitatively the relationship between stimulus intensity and ONR implicit time, and then the effects of light adaptation on this relationship. This will be followed by a description of the effects of light adaptation on the ONR implicit time at threshold. I end this section by describing the differences that I observed in the implicit time at threshold under the brightest background, and by comparing the implicit time of the ON and OFF responses.

Implicit time and stimulus irradiance: rod and cone curves

Longest implicit time, obtained under complete dark adaptation (at absolute threshold), was around 400ms. With increasing stimulus intensity, implicit time decreased as shown in Figure 28. When pooled S-IT data from a given experiment were plotted for all relative background intensities, two distinct patterns were apparent (Fig. 28), corresponding to low and high stimulus/background intensities respectively.

Figure 28: : Pooled S-IT data for a single individual for four test wavelengths and various relative background intensities (n=1).
Outliers have not been removed from the data set. Units for the horizontal axis are in photons cm^{-2} s^{-1}.

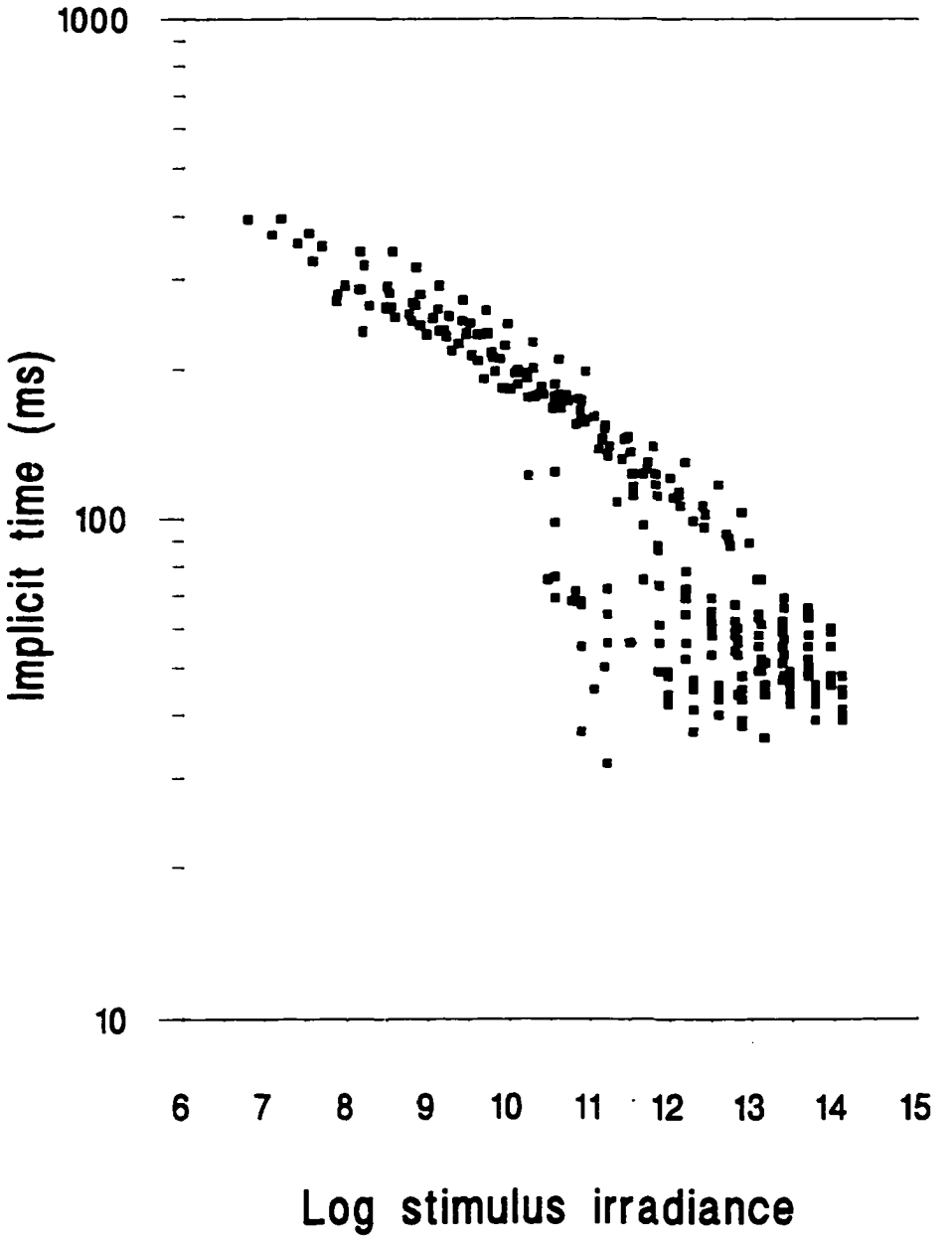
1000
100
10
Implicit time (ms)
6
7
8
9
10
11
12
13
14
15
Log stimulus irradiance

The first pattern was described empirically by the logarithmic equation

$$\log \mathbf{T} = \log \mathbf{a} + \mathbf{b} \log \mathbf{I_S} \qquad (1)$$

where **T** is the implicit time, **a** is a constant, **b** is the slope of the function and $\mathbf{I_S}$ is the stimulus irradiance (Fig. 29). The value of **b**, averaged from all fish, for the lower relative background intensities, was -0.10±0.01 (mean±SD, n=3). This function was likely characteristic of the scotopic system. As relative background intensity increased, the S-IT data were displaced towards shorter implicit time values along the vertical axis, and toward higher stimulus irradiance values along the horizontal axis, but remained on the same function, without a change in **a** or **b**. This is shown on Figure 29, which depicts the implicit time data as a function of stimulus irradiance for four relative background intensities, at 540 nm. This pattern of response was consistent for all the animals studied.

The logarithmic relationship between stimulus irradiance and implicit time held for higher background intensities. At a relative background intensity of about 4 log units, the relationship, however, presented a discontinuity from the scotopic function, represented by a distinct drop in implicit time values. Figure 30 illustrates the shift from the first (scotopic) function to the second (photopic) one. As relative background intensity increased from 3 to 4 log units, in this example, implicit time values for stimuli of similar irradiances decreased substantially, and were obviously part of a different function, characterized by a lower slope and a smaller **a** value. I interpret this shift in the behavior of S-IT as representing a shift from a response dominated by the scotopic visual

Figure 29: Implicit time versus stimulus irradiance for four scotopic backgrounds of increasing relative intensity.

Empty squares=1, full squares=2, empty diamonds=3 and full diamonds=4 log units relative background intensity. Note the displacement of implicit time values along the logarithmic function with increasing relative background intensity. Units for the horizontal axis are in photons cm^{-2} s^{-1}.

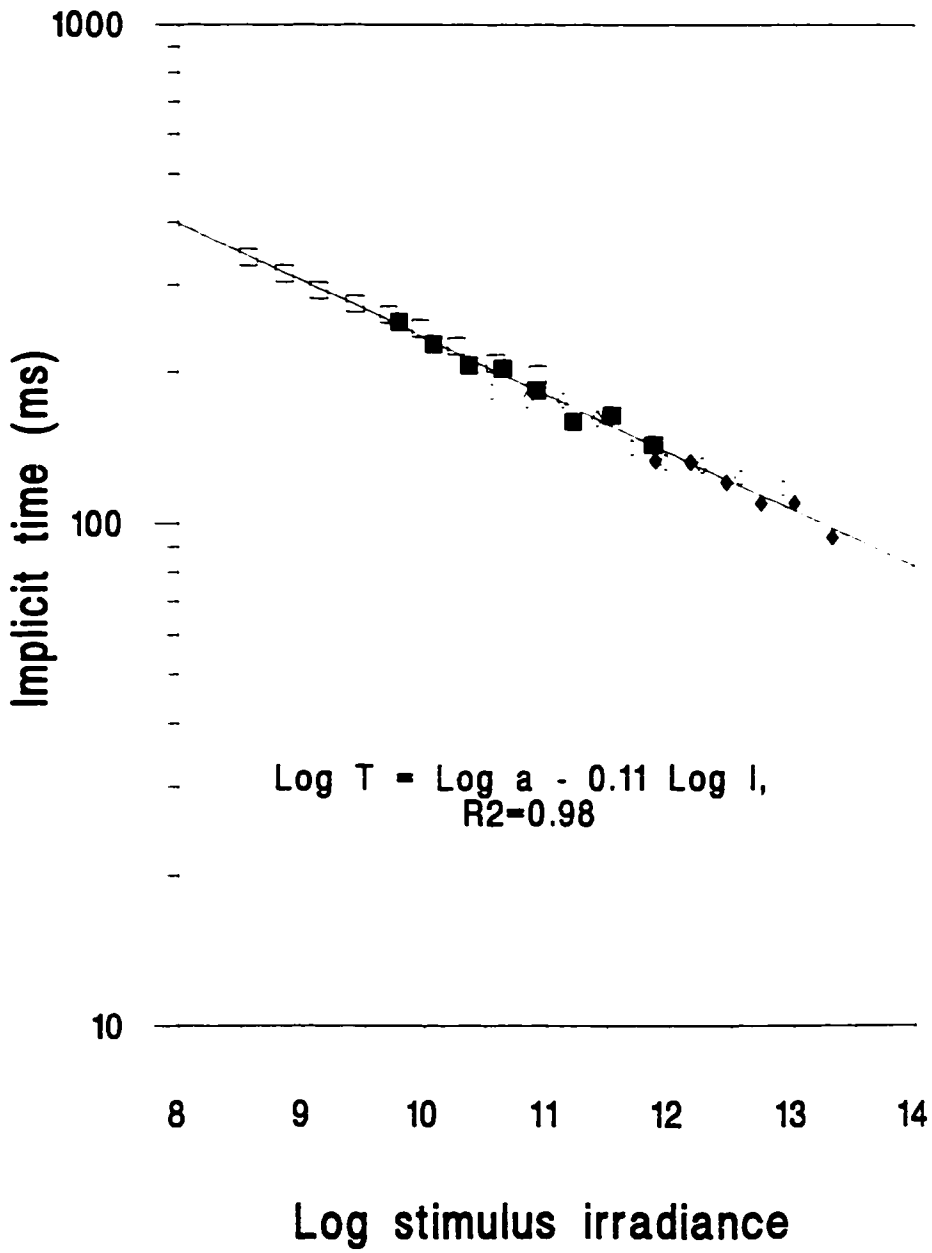
1000
100
10
Implicit time (ms)
Log T = Log a - 0.11 Log I,
R2=0.98
8
9
10
11
12
13
14
Log stimulus irradiance

Figure 30: Implicit time versus stimulus intensity for two relative background intensities around the scotopic (full squares) to photopic (empty squares) ONR transition. Both sets of data points were fitted with equation (1). Units for the horizontal axis are in photons cm^{-2} s^{-1}.

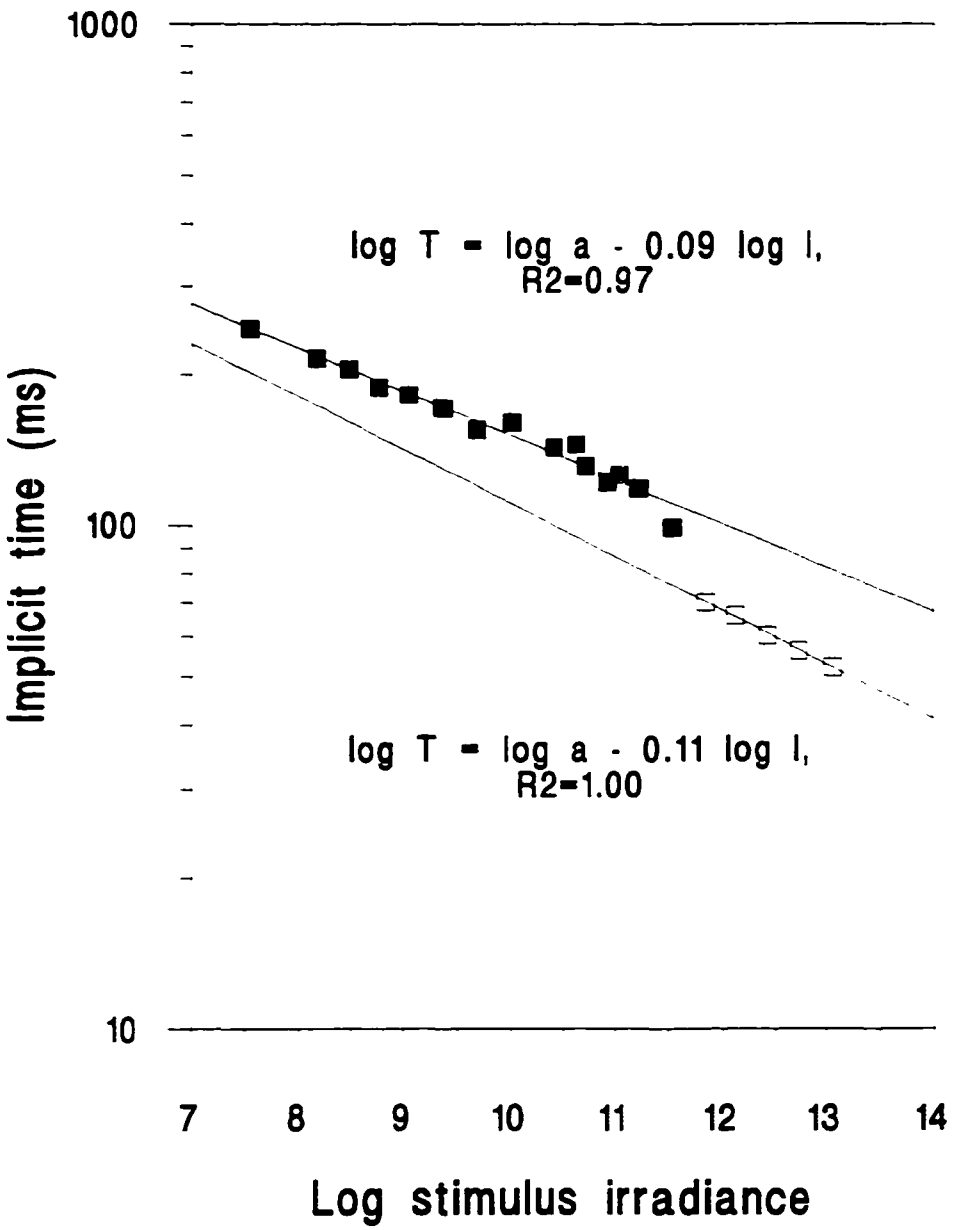
1000
100
10
Implicit time (ms)
log T = log a - 0.09 log I,
R2=0.97
log T = log a - 0.11 log I,
R2=1.00
7
8
9
10
11
12
13
14
Log stimulus irradiance

system to one dominated by the photopic visual system. The shift from the scotopic to the photopic system was also illustrated by stimulating a fish previously dark-adapted over the entire range of stimulus irradiances that was available to us (Fig. 31). The break in the S-IT function was clear under these circumstances as well. Interestingly, the data in this case hint to the presence of a third component in addition to the scotopic and the photopic ones. This third component was composed of intermediate values and characterized by a steeper slope than either the scotopic or the photopic functions. This part of the curve possibly corresponded to background intensities that could be characterized as mesopic. It also corresponded to the part of the S-R curve (Fig. 25) located between the scotopic- and photopic-dominated responses, and characterized by a decrease in the amplitude of the responses with increasing stimulus intensity (the "dip", between 9 and 11 log units stimulus irradiance).

Unlike the scotopic implicit times, the photopic ones could not be described by a single linear function: generally, slopes varied both with background intensity and wavelength, suffered a vertical displacement toward shorter implicit times and higher stimulus intensities, as background intensity was increased. The slope of the S-IT curves in the example illustrated in Figure 32 decreased in absolute values from 0.11 to 0.07 over three ND increase in the intensity of the background. Although I observed this trend on several occasions, there were also situations in which S-IT data did not follow any particular linear function for a given wavelength and background intensity, with values appearing to fall on more than one function, especially at higher stimulus intensities. This made the identification of a clear trend more difficult in these cases but suggested that, at

Figure 31: Implicit time versus stimulus irradiance of a dark-adapted individual. In this case, stimulations spanned a 7 log unit range and shows the transition between a rod- to the cone-dominated responses. The rod- and cone-dominated portions of the curve have been fitted with equation (1). Units for the horizontal axis are in photons cm^{-2} s^{-1}.

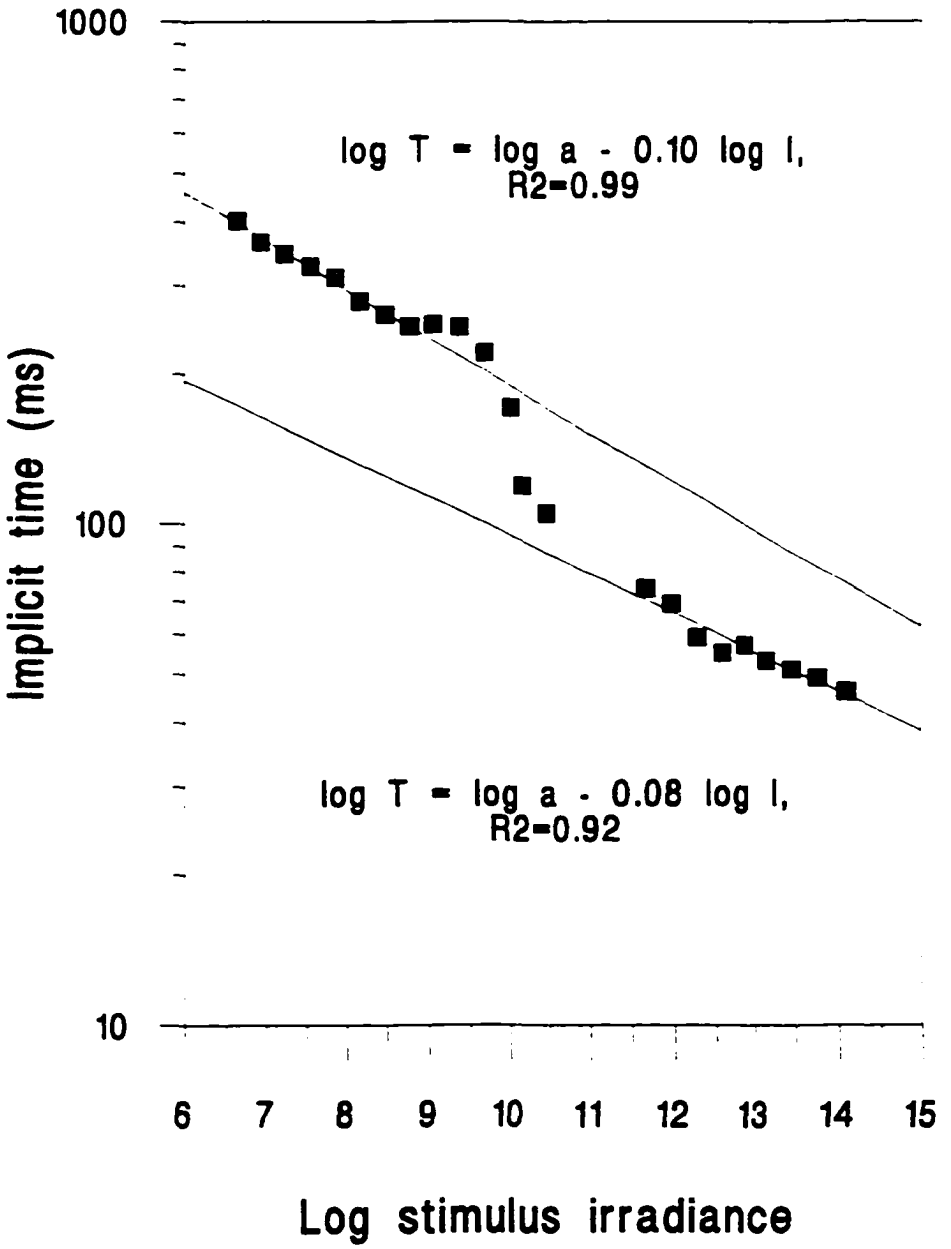
1000
100
10
Implicit time (ms)
log T = log a - 0.10 log I,
R2=0.99
log T = log a - 0.08 log I,
R2=0.92
6
7
8
9
10
11
12
13
14
15
Log stimulus irradiance

Figure 32: Effects of adaptation on the slope of the photopic S-IT curve, at 540 nm. Relative background intensity was increased in 1 log unit steps from top to bottom curves. Values for the slope **b** were as follows: full squares, - 0.11, empty squares, - 0.09 and full diamonds, - 0.07. Units for the horizontal axis are in photons cm^{-2} s^{-1}.

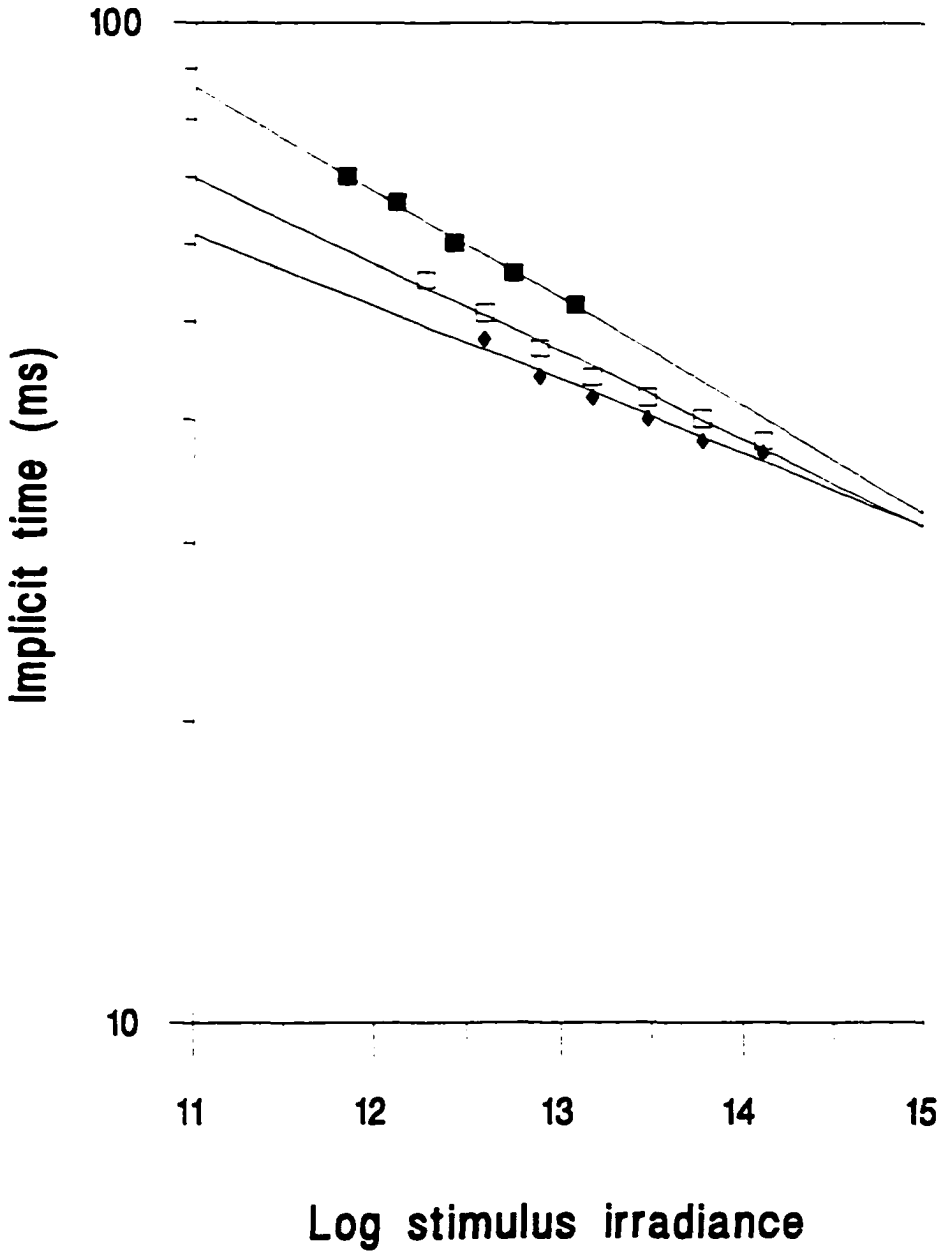
100
10
Implicit time (ms)
11
12
13
14
15
Log stimulus irradiance

higher intensities, mixing of inputs from various cone mechanisms probably occurred, especially when chromatic adaptation was not complete. This is why I did not proceed to a detailed analysis of the slopes in this paper (see Chapter 6 for a more in-depth analysis of the effects of adaptation on the ON response slopes).

Implicit time at threshold and background intensity

Implicit time at threshold was consistently longer at lower relative background intensities than at higher intensities. At low background intensities, implicit time at threshold varied as a function of relative background intensity according to the empirically determined function

$$\log \mathbf{T_T} = \log \mathbf{a} + \mathbf{b} \log \mathbf{I_B} \qquad (2)$$

where $\mathbf{T_T}$ is the implicit time at threshold, **a** is a constant, **b** is the slope of the function and $\mathbf{I_B}$ is the relative background intensity. At lower background intensities, which probably corresponded to the scotopic values, slope **b** was -0.09 (Fig. 33). When the whole range of relative background intensities was considered, for 380 and 540 nm, the function comprised two parts which generally corresponded to the two parts of the TVI curves (Fig. 34A, B). At higher relative background intensities, which probably corresponded to photopic values, slope b was markedly lower. At 620 nm, there was more variability in the relationship between implicit time at threshold and relative background intensity (Fig. 34C). Four components could be discerned in this relationship (numbered 1-4 in Fig. 34C). First, a decrease in implicit time at threshold was found, corresponding to the initial rise in threshold as demonstrated by the TVI curve superimposed on the same graph (Fig.

Figure 33: Implicit time at threshold as a function of relative background intensity for the lower background intensity range.

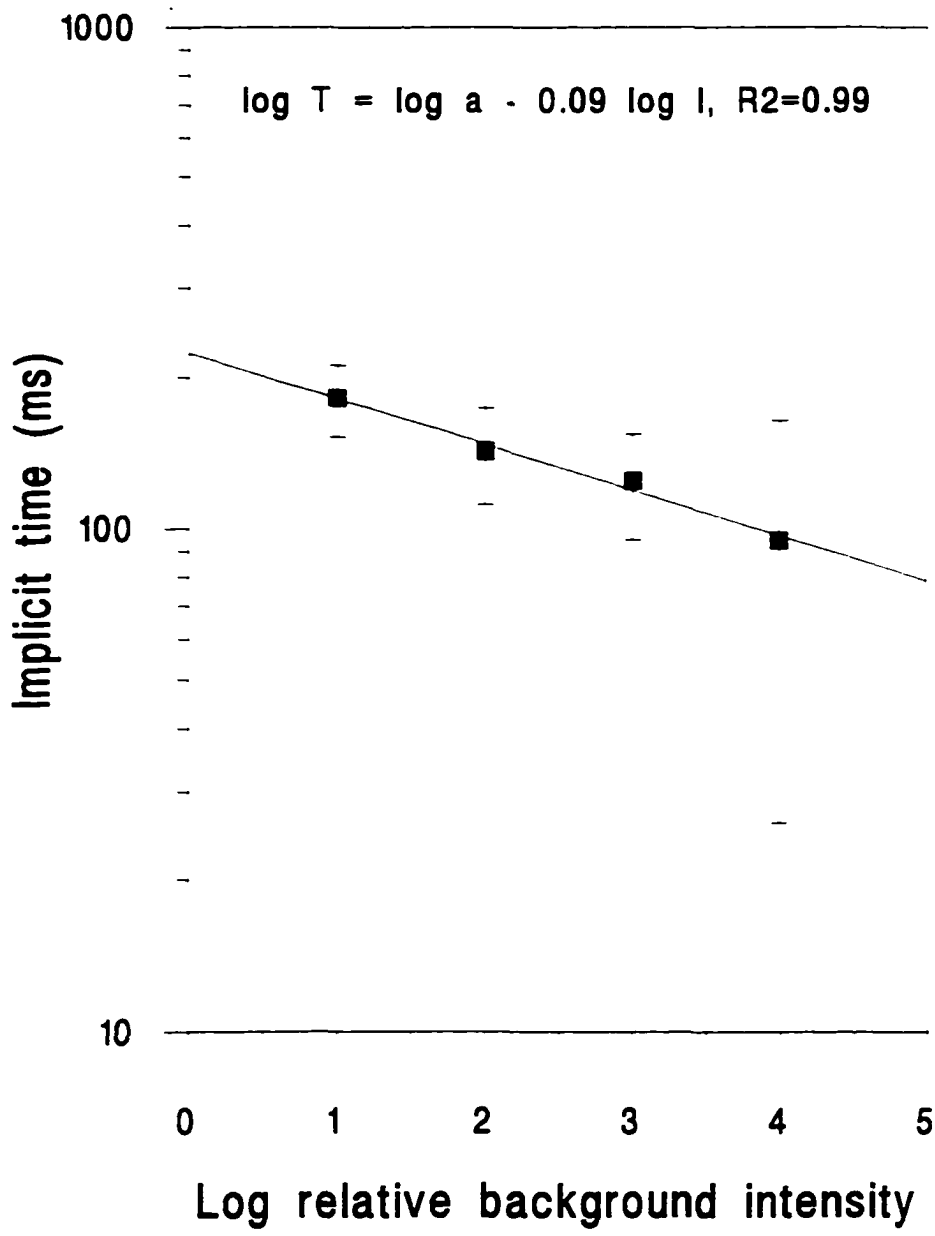
1000
log T = log a - 0.09 log I, R2=0.99
Implicit time (ms)
100
10
0
1
2
3
4
5
Log relative background intensity

Figure 34: Comparison of response thresholds and implicit times at threshold as a function of relative background intensity, at various wavelengths. **A** 540 nm, **B** 380 nm and **C** 620 nm. Full squares represent the threshold values, and the empty squares implicit time values.

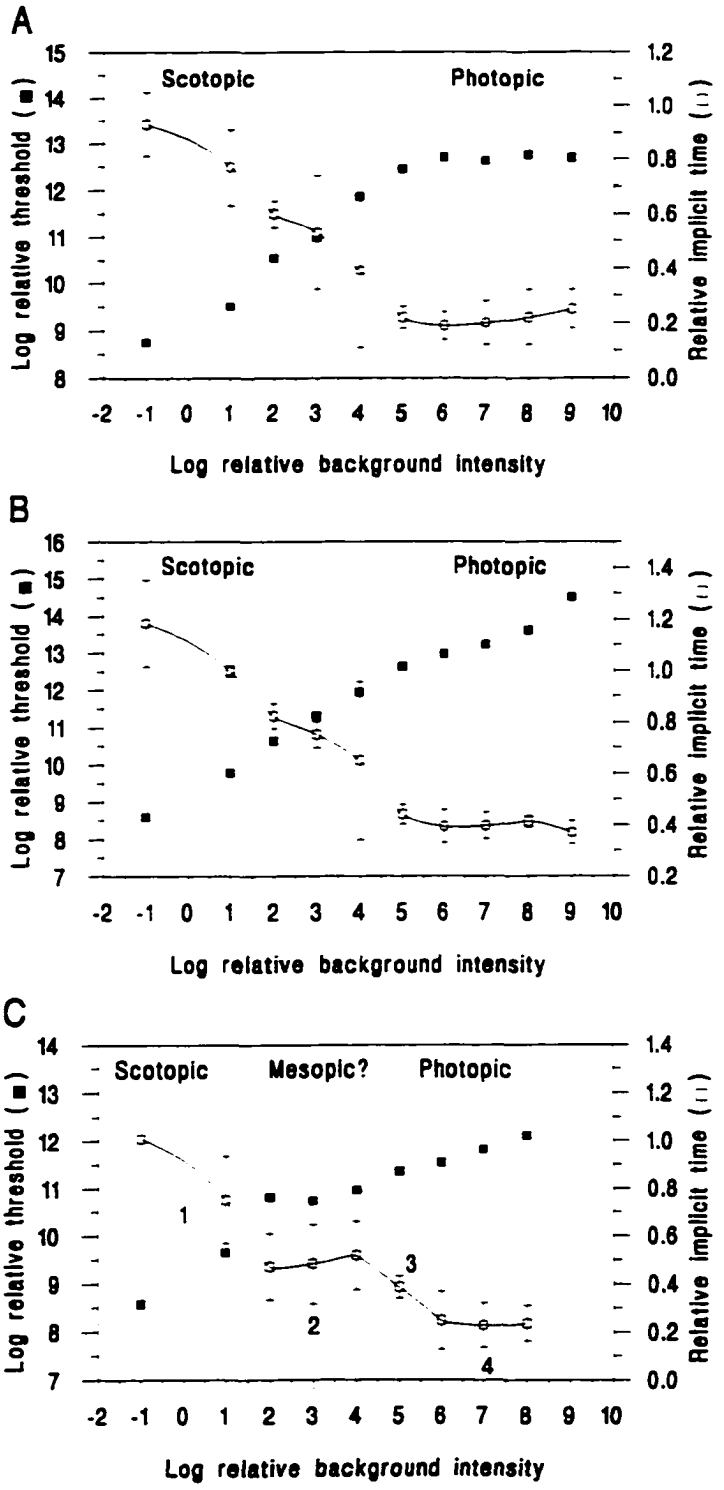
A
Scotopic
Photopic
Log relative threshold (■)
Relative implicit time (□)
Log relative background intensity
B
Scotopic
Photopic
Log relative threshold (■)
Relative implicit time (□)
Log relative background intensity
C
Scotopic
Mesopic?
Photopic
1
2
3
4
Log relative threshold (■)
Relative implicit time (□)
Log relative background intensity

34C). Next, implicit time reached a first plateau, located between 2-4 log relative background intensities, the beginning of which corresponded to the inflection point observed on the TVI curve (arrow, Fig. 34C). The decrease in implicit time resumed from 4 log units relative background intensity and reached a second plateau, around 6 log units. The presence of the first plateau, at implicit times intermediate between those of scotopic and photopic values, may suggest that these represented a mixing of inputs from the scotopic and photopic systems.

Implicit time at threshold and chromatic adaptation

At 8 log unit relative background intensity, under which threshold at 380 nm was close to one log unit lower than that at 540 nm, and 2 log units lower than at 620 nm, implicit time of the response at threshold varied across the spectrum (Fig. 35). Implicit time was longest at 380 and 430 nm (67±4 ms and 71±4 ms respectively, mean±SD, n=3), the isolated part of the spectrum, and was significantly longer than at 540 nm (49±5 ms, n=3), the most adapted part of the spectrum (ANOVA, $P<0.01$). The average difference in implicit time between 380 nm and 540 nm was 18 ms, and that between 430 nm and 540 nm was 22 ms. Mean implicit time at threshold for 620 nm was 62±22 ms (n=3), and was not significantly different from that at any of the other three test wavelengths. This was due to the high variance associated with the values at 620 nm, which suggested a higher level of heterogeneity of implicit times in that part of the spectrum (see also chapter 6).

Figure 35: Implicit time at threshold as a function of wavelength under an 8 log units relative background intensity (n=3).

Data points represent means ± SD. Note the high variability associated with the value at 620 nm.

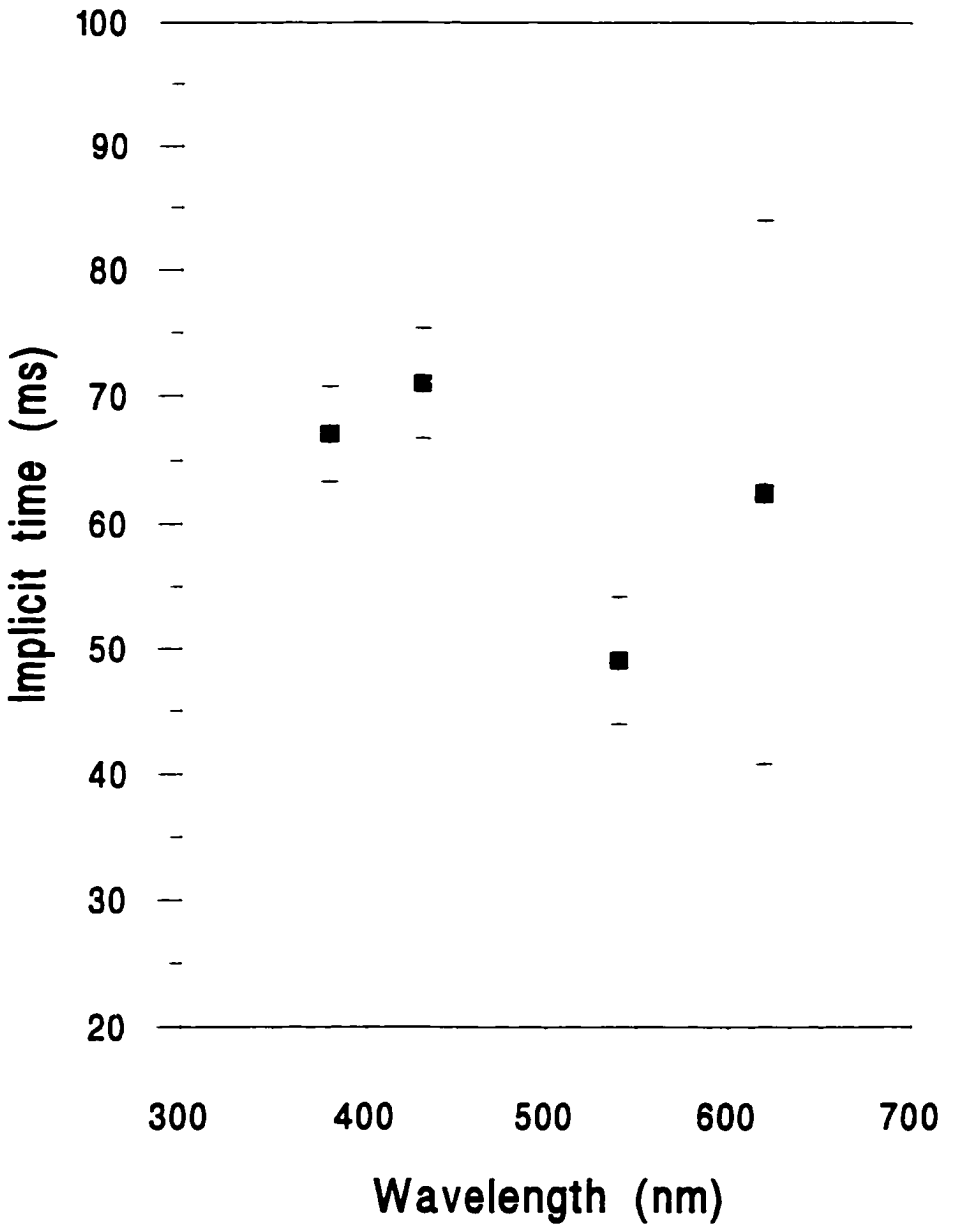
100
90
80
70
60
50
40
30
20
Implicit time (ms)
300
400
500
600
700
Wavelength (nm)

ON-OFF implicit time comparison at 540 nm, the M cone mechanism

The ONR at 540 nm is dominated by inputs from the M mechanism for both the ON and OFF responses at near-threshold stimulus intensities (see Chapter 6). This allowed comparison of the implicit times of at threshold for these ON and OFF responses, and allowed to determine whether these two pathways differed in their implicit time. At 540 nm and under a 7 log unit relative intensity background, the OFF response implicit time was consistently longer than that of the ON response, although the difference varied from fish to fish. The average implicit time difference in absolute values was 13.5 ± 5 ms (ranging from 7-19 ms, n=4) and the ON response implicit time was 71±13% (n=4) that of the OFF response for a stimulation of equal intensity.

Discussion

In addition to the biochemical changes associated with light adaptation (Chapter 1), changes in retinal connectivity also occur to remove the inputs from the photoreceptor type that is ineffective under the prevailing light conditions (Wagner, 1990). Thus, it is generally accepted that cone inputs to bipolar and horizontal cells are reduced in the dark-adapted state, and that the same is true for the rods in bright light conditions (Wagner, 1990). Changes in the organization of the receptive field of most retinal neurons are also influenced by dopamine during dark adaptation (Mangel and Dowling, 1987; Djamgoz and Yamada, 1990; Lasater, 1990). In addition, in fish, light adaptation involves photomechanical movements that expose the active photoreceptors to the light stimuli and hide the inactive ones (Douglas, 1982a, b; Ali and Klyne, 1985; Wagner, 1990). These

changes are under the influence of both neuronal and chemical (dopamine) cues (Wagner, 1990). These changes, which affect primarily the outer retina, also have repercussions at higher levels of processing (see Guenther and Zrenner, 1993, for example). The results of this study revealed several characteristics of the process of light adaptation in the inner retina of rainbow trout, which I discuss below.

General differences in ONR between light and dark adaptation

The main differences in the ONR between light and dark adaptation were that, on average, maximum amplitude of the waveform was higher for the light adapted than for the completely dark-adapted state, and that the OFF response was absent, or had a much higher threshold in the dark-adapted state. The ONR amplitude probably depends on several factors, among which the number of RGC fibers that fire in response to a given light stimulus (recruitment), and the average firing rate of these fibers. This last factor probably depends on the strength of photoreceptor inputs to the fibers, itself a function of photoreceptor sensitivity, response pooling and synaptic "gain" in the inner and outer plexiform layers. In addition, the time course of the response should also influence the amplitude of the response, as coordinated firing, i.e. the temporal coincidence of a given number of spikes, is likely to generate a higher local change in potential in the extracellular milieu and thus generate a larger mass response. Hence, several hypotheses for the higher amplitude of the cone response could explain the results I obtained. These, however should be regarded as highly speculative in light of the paucity of data on this particular subject.

First, the number of optic nerve fibers carrying the rod input may be lower than

that carrying cone inputs. This may be due to the relatively low number of rod photoreceptors in the juvenile trout retina, compared to older individuals in which rods tend to be the dominant photoreceptor type (see Lyall, 1957a). This relatively low number of rods may have contributed to the smaller ONR response in the dark-adapted state by influencing RGC recruitment, maximum firing rate, or both. Second, longer implicit time and larger temporal spread of the rod response may also have contributed to the lower amplitude observed. This is supported by the fact that the lower waveform amplitude in the dark-adapted state was also associated with a relative spread of the rod response compared to the cone response, as suggested by the half-bandwidth of the waveform. Thus, even with equal numbers of fibers firing in response to a light stimulus, and similar firing frequencies, lack of temporal coincidence in the firing of the "rod fibers" would have led to a flattened response, with larger width and smaller amplitude, which agrees with my findings.

Similar differences in the relative amplitude of rod- and cone-driven responses have also been observed in an amphibian. Intracellular recordings from *Xenopus* horizontal cells have revealed that maximal response amplitude in the dark-adapted state is about half of that in the light adapted state (Hassin and Witkovsky, 1983; Witkovsky and Stone, 1983). These authors, however, do not provide any explanation for this difference in maximal response amplitude. The results by Hassin and Witkovsky (1983) and Witkovsky and Stone (1983) suggest that the discrepancy in amplitude between rod and cone responses is present early in the visual process and that the differences I observed in the ONR may be a reflection of these discrepancies.

Also of interest was the absence of an OFF response in the dark-adapted state, which is similar to results obtained by Novales Flamarique and Hawryshyn (1996) in sockeye salmon. In goldfish, OFF responses recorded from dark-adapted RGCs appear to originate mostly from the L cone mechanism, and show a peak sensitivity that is about 1.5 Log unit lower than that for the rod-dominated ON response (Wheeler, 1979). My results suggest that in trout the rod system may also contribute little to the OFF response. Contribution to the OFF response mostly from cones would explain the inferred difference in the relative sensitivity of the ON and OFF responses in the dark-adapted state.

TVI curves: Scotopic and photopic systems

The TVI curves that I obtained generally conformed to the typical TVI curve shape (Enoch, 1972; Marriot, 1976; Frumkes, 1990; Hawryshyn, 1991). In such curves, each part normally represents the activity of the system or mechanism that is the most sensitive over that range of background intensities. As the TVI curves obtained in this study were comprised of two parts, this suggests the presence of two distinct systems, active at low and high relative background intensities, respectively. Furthermore, as the lower range of background intensities examined in this study encompassed conditions of complete darkness and dim illumination, the first part of the TVI curves likely represented the activity of the scotopic system. Indeed, it is acknowledged that under such conditions, rod photoreceptors are predominantly active (Wheeler, 1979; Hawryshyn, 1991). The second part of the TVI curves probably represented the activity of the photopic system. In the reminder of the discussion, I will refer to the range of relative background intensities corresponding to the first part of the TVI curves as scotopic conditions.

Likewise, photopic conditions will refer to those intensities corresponding to the second part.

Discrepancies between the shape of the second part of the TVI curve at 380 and 540 nm suggest that different cone mechanisms were active at these wavelengths. Given the spectral distribution of the adapting background, sensitivity of the L cone mechanism at 540 nm was likely minimal and therefore, at this wavelength, the ONR was probably dominated by input from the M cone mechanism. At 380 nm, identification of the active cone mechanism is more difficult to make due to the relative close proximity in λ_{max} of the UV and S cone mechanisms.

The slope for the linear part of the scotopic portion of the TVI curves was about 0.8. This value, which approaches 1, is consistent with a mechanism that obeys Weber's law (Granda and Sisson, 1989; Buser and Imbert, 1992; Frumkes, 1990; Hawryshyn, 1991). This means that brightness contrast sensitivity should remain fairly constant for most of the activity range of the scotopic systems. This value is much lower than that found psychophysically in goldfish (1.3: Hawryshyn, 1991). Some of the difference may be explained by the presence of saturation at higher background intensities in the rod TVI curve in Hawryshyn (1991). Different experimental conditions and techniques used may also account for some of the differences between trout and goldfish.

For the M cone mechanism, the slope of the linear portion of the TVI curve was estimated at between 0.8 and 1.0, which is in better accordance with Hawryshyn (1991) for the goldfish M mechanism. However, because of the small number of data points on which the slope estimate was based, conclusions beyond these would be speculative.

Rod-cone interaction in the trout retina?

The duplicity theory of vision, which stipulates that vision in vertebrates is subserved by two independent systems that are responsible for vision in low and high irradiance environments, respectively, was first proposed by Schultze in 1886 (Frumkes, 1990). Recent findings, however, have suggested that the independence of these two systems may not be complete. Interactions between the scotopic and photopic visual systems have been shown in mammals and amphibians (Dong et al. (1988); Frumkes, 1990; Frumkes and Eysteinsson, 1987, 1988; Hassin and Witkovsky, 1983), and I suggest they may also be present in fish.

In this study, the first indication of rod-cone interaction was a "dip" in the S-R curve obtained over 7 log units of stimulus intensities (Fig. 25). Absence of an interaction should have resulted in a monotonic increase in ONR amplitude, as reported by Olsen et al. (1986) and Schneider et al. (1986). These authors have reported such a dip in the S-R curve in cat (Olsen et al., 1986; Schneider et al., 1986; Schneider and Zrenner, 1987). Schneider et al. (1986) found that the S-R curve of the dark-adapted cat ERG b-wave was characterized by two maxima separated by a "dip" in waveform amplitude, which they attributed to inhibitory interactions between rods and cones with similar spectral sensitivities. Interestingly, these authors did not find this dip in the S-R curve from the ONR, which instead increased monotonically. These authors explain the discrepancy between the ERG and the ONR as reflecting the fact that in cat, the ONR is more cone-dominated than the ERG b-wave, which probably resulted in a masking of the rod-cone interaction. Schneider and Zrenner 's (1986) explanation would suggest the rod input to

the ONR is better represented juvenile trout than in cat.

A comparison of the TVI curves obtained at 540 and 620 nm revealed that, between about 2 and 5 log relative background intensity, threshold was lower then predicted by the theoretical TVI curves (arrowhead on Fig. 27B). This lower threshold was also characterized by implicit times that deviated from the trend established at the other wavelengths (compare Fig. 34A, B with 34 C). These results suggest the mixing of inputs from mechanisms that differed in their threshold and implicit times, leading to the generation of the intermediate values.

Interactions between rod and cone mechanisms have been documented in other species as well. In *Xenopus*, enhancement, as this rod cone interaction has been called, occurs when a weak green background adapting the rod is system is used, and leads to an increase in sensitivity of horizontal cells to red flashes (mediated by the cone system) (Hassin and Witkovsky, 1983; Witkovsky and Stone, 1983, 1987). The effect is seen only under mesopic conditions, when the horizontal cell responses reflect inputs from both the rod and cone photoreceptors. A background that adapts the red cones only is not effective at generating the effect, and neither is direct electrical stimulation of the horizontal cells themselves. Furthermore, the action spectrum of the effect is matched by the rod photopigment absorption curve. Finally, this type of rod cone interaction does not appear to be present in cells that are connected to the "blue rod" pathway, further indicating that this phenomenon is restricted to the longer wavelength part of the spectrum. In humans, a similar type of interaction has been shown to involve solely the L mechanism, as this phenomenon is absent in subjects that lack the long wavelength-

sensitive photopigment (protanopes) but is present in those lacking the middle wavelength-sensitive photopigment (deuteranopes) (Frumkes, 1990).

Mechanisms underlying the implicit time-stimulus relationship

The effects of stimulus intensity on the time course of visual responses have been qualitatively described on several occasions, but have rarely been quantified (McNaughton, 1990; Robson and Frishman, 1995). An important step in comparing physiological mechanisms between species, however, is the quantification of these effects. It is generally understood that increasing stimulus intensity leads to a decrease in the time course of responses recorded from the various neuronal elements of the retina (Cone, 1964; Schneider and Zrenner, 1987; Perry and McNaughton, 1991; Donner et al., 1995). Some exceptions exist, however (see Peachey et al., 1989; Baylor and Hodgkin, 1974). The data in this study provide quantitative information on the effects of adaptation and stimulus intensity on the response kinetics of the scotopic and photopic visual systems in trout. I have shown that ONR implicit time decreases with stimulus intensity according to a logarithmic function with a slope of -0.11, for the scotopic system.

The equation used in this study is empirical, and as such its various components may not represent directly any particular physiological mechanism. A slightly more complex equation was used recently by Robson and Frishman (1995) to analyze the cat dark-adapted ERG PII wave latency (bipolar cell activity). Robson and Frishman's (1995) equation (which I called the Robson-Frishman equation in the reminder of this discussion),

$$t_{crit} = t_d + (V_{crit} / kI)^{1/p}$$

where t_{crit} is the latency of the PII wave, t_d is a small fixed delay, V_{crit} an arbitrary criterion voltage, **k** a scaling factor and **I** the stimulus intensity, is a modified but generally equivalent form of equation (1). Exponent **1/p** of the Robson-Frishman equation is equivalent to slope **b** of equation (1). The Robson-Frishman equation describes the change in latency of a response with stimulus intensity in terms of a low-pass filter that transforms the information originating from the photoreceptors as it travels through the various layers of the retina. The number of stages that this low-pass filter possesses is equal to **p+1**, where **p** is the denominator of the exponent (**1/p**). In dark-adapted cat bipolar cells, Robson and Frishman found that an exponent of 0.2 (in absolute values) best fitted their results and thus argued that the low-pass filter possess 6 stages at the level of the ERG PII wave in dark-adapted cat:

$$1\backslash p = 0.2, \text{ and therefore}$$

$$p = 5 \text{ and the number of filters is}$$

$$p + 1 = 6 \text{ filters.}$$

When comparing equation (1) to that of Robson and Frishman (1995) for their data, fit was accurate (R^2=1.00), and the value of the slope **b** I obtained matched quite well that the exponent found by their equation (0.18 for equation (1) from this study, compared to 0.2 for their equation). It seems reasonable to assume that the slope **b** determined from equation (1) of the present study represents an acceptable approximation of the exponent **1/p** determined by the equation proposed by Robson and Frishman

Table 5: Compilation of rate of time course decrease with increasing irradiance for various photoreceptor types and using various techniques. The data were fitted with equation (1) to allow comparison with the results from this study. Goodness of fit is provided in the form of an R^2.

b	R^2	type of response	parameter	T (°C)	Reference	Figure
-0.10	0.98	trout dark ONR	implicit time	15	this study	--
-0.10	0.97	cat dark ONR[1]	implicit time	37	Schneider and Zrenner (1987)	2
-0.11	0.98	rat dark ERG b-wave	latency	37	Cone (1964)	3
-0.12	0.97	trout pineal[2]	implicit time	19	Kusmic et al., (1992)	4
-0.13	0.95	turtle cones[2]	crit. duration	--	Daly and Normann (1985)	5
-0.14	0.61	toad rods[2]	implicit time	18-25	Baylor et al., (1979)	Table 1
-0.14	0.88	salamander cones[3]	implicit time	20	Perry and McNaughton(1991)	3-4
-0.17	0.99	cat dark ERG b-wave[1]	implicit time	37	Schneider and Zrenner (1987)	4
-0.17	0.99	mudpuppy bipolar[2]	latency	--	Frumkes and Miller (1979)	5
-0.18	1.00	cat ERG PII wave	latency	37	Robson and Frishman (1995)	11
-0.19	0.98	human ERG b-wave[4]	latency	37	Hood and Birch (1992)	12[5]
-0.21	0.97	minnow pineal[2]	latency	--	Nakamura et al (1986)	4
-0.23	0.95	rat ERG a-wave[2]	latency	37	Arden and Ikeda (1968)	9
-0.25	1.00	salamander cones[5]	implicit time	20	Perry and McNaughton(1991)	3-4

[1] Implicit time measured from dark adapted b-wave.
[2] From intracellular recordings
[3] Logarithmic function fitted to all data for a single L cone (8 data points).
[4] Measured from dark adapted b-wave, as reported by Robson and Frishman (1995; Fig 12)
[5] Logarithmic function fitted to the steepest part of the curve only (first 4 data points).

(1995). Therefore, as the dark-adapted trout S-IT curve has a slope of 0.10 (see Table 5), the trout rod response has likely been transformed by an 11-stage low-pass filter by the time ONRs are recorded:

$b = 0.10$ and by approximation,

$0.10 \approx 1/p$, $p \approx 10$, and therefore the number of filters is

$p + 1 \approx 11$ filters.

According to Robson and Frishman (1995), the six-stage low-pass filter that they found in dark-adapted cat bipolar cells reflects the number of time-limiting biochemical steps that are involved in the transduction of light stimuli in rods and the transmission of the signal to the bipolar cell. According to these authors, 3 of the stages represent the isomerization of rhodopsin in rods, the activation of the G-protein transducin and the hydrolysis of cGMP by phosphodiesterase (see Fig. 6), whereas the other 3 stages represent a similar G-protein mediated biochemical cascade that is initiated in the bipolar cell postsynaptic membrane. The higher number of stages for the low-pass filter that can be inferred from the trout S-IT slope suggests additional time-limiting events in the transmission of visual information. The presence of 5 stages in addition to those found by Robson and Frishman (1995) in cat bipolar cells seems plausible, as in the present study neuronal signals from the rods had to travel to an additional retinal layer (RGC layer) before being recorded in the ONR. This explanation is consistent with results by Schneider and Zrenner (1987) in cat, which show a higher S-IT curve slope (and hence a lower number of stages) for the ERG b-wave (bipolar cell activity) than for the ONR

(Table 5: see below for description of slope determination of data from Schneider and Zrenner, 1987, and other sources). Even though scotopic trout data are consistent with the multi-stage low-pass filter hypothesis, I do not know how the change in the slope **b** observed with adaptation of the photopic system can be interpreted in these terms. Clearly, for the photopic system, the slope of the S-IT curve is not related to a fixed number of such stages.

Comparative aspects of the S-IT relationship

Having determined that implicit time varied logarithmically with stimulus intensity in rainbow trout, I wanted to know if this relationship also held in other species, from various vertebrate classes. A search through the literature reveals that this aspect of visual physiology has seldom been examined quantitatively. However, several studies provide graphical representations of the relationship between stimulus irradiance and response time course. I was therefore able to extract some quantitative information from various studies (by directly measuring values from graphs) and analyze it with equation (1). Some error is probably associated with the values measured, but this should not have led to any significant effect on the general shape of the curves obtained, nor should it affect the analysis I describe below.

The salient features of the data gathered from the literature are listed in Table 5, along with the various sources from which they were obtained. It can be seen that even though these data were collected from various species, from various retinal mechanisms, with several different techniques and under a range of ambient conditions, they still conform quite well to the simple logarithmic equation (1) that was fitted to the trout data.

Indeed, the average R^2 for the data presented in Table 5 is 0.95±0.05[9].

Although there is a good agreement between the data gathered from the literature and equation (1), there exists some variability regarding the value of the slope **b** among species. The value of this slope ranged from -0.09 to -0.24, with an average of -0.16±0.05 (mean±SD) for the values listed on Table 5. No overall relationship between the value of the slope and parameters such as the type of mechanism (rod or cone) responding, the level of recordings (photoreceptor, bipolar cell or RGC), animal group (classified as fish, amphibians, reptiles or mammals) or temperature was readily identifiable. The small amount of data precluded a detailed statistical analysis of possible relationships, however. It would seem, nonetheless, that interspecific differences exist that may mask possible effects of the various parameters mentioned above. In light of the previous discussion of the mechanisms underlying the value of the slope **b**, one may hypothesize that the variation observed among species reflects differences in the number of time-limiting steps involved in the transduction and transmission of visual information. More research is needed to elucidate the origin of these differences.

Interestingly, results from the trout scotopic S-IT slope compare well with data from Kusmic et al. (1992), who recorded intracellularly from rainbow trout pineal photoreceptors. Figure 36 depicts the log implicit time for our rod data and data from Kusmic et al. (1992; data taken from their Fig. 4). The only difference in the shape of the

---

[9] Data from Baylor et al. (1979) were excluded from the calculation as these data did not represent the direct change in implicit time with stimulus irradiance as measured from single photoreceptors, but pooled results for various intensities taken from different rod photoreceptors: inter photoreceptor variability was thus not taken into consideration, as is the case in the other data. The data nevertheless conform to the general trend.

Figure 36: Implicit time of rod responses from this study compared to data from Kusmic et al. (1992) for rainbow trout pineal photoreceptor intracellular responses. Data from this study are represented by empty diamonds, those from Kusmic et al. (1992) by full squares. Units for the horizontal axis are in log relative photons $cm^{-2} s^{-1}$.

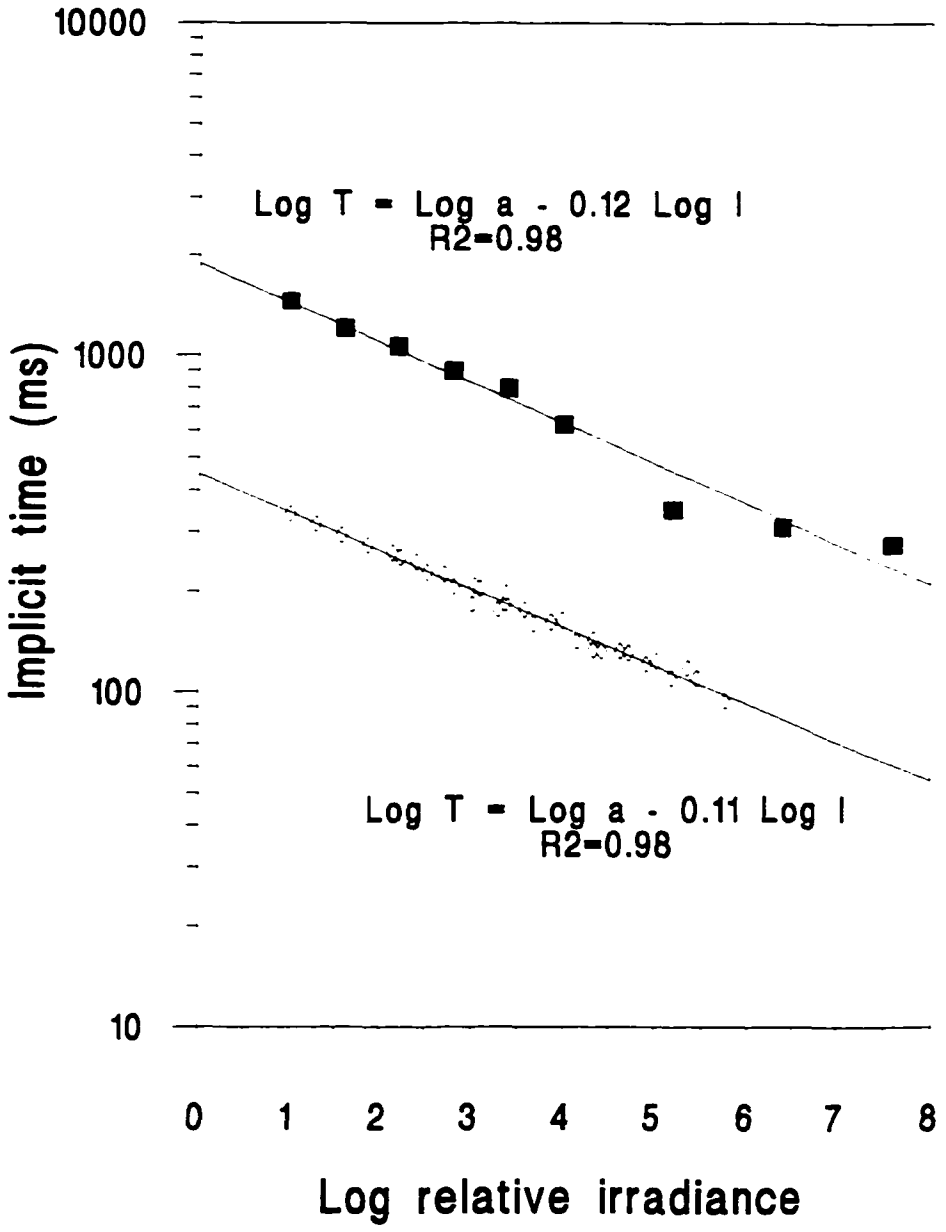
10000
1000
100
10
Implicit time (ms)
Log T = Log a - 0.12 Log I
R2=0.98
Log T = Log a - 0.11 Log I
R2=0.98
0
1
2
3
4
5
6
7
8
Log relative irradiance

S-IT curve between trout rods and pineal photoreceptors occurs at higher relative irradiances, and is probably due to saturation of the pineal photoreceptor response. Nevertheless, the comparison with the data from Kusmic et al. (1992) is warranted and suggestive, as proposed by these authors, of a correspondence between the physiology of rod and pineal photoreceptors in trout. These authors conclude that pineal photoreceptors behave like retinal photoreceptors because they show an intensity-related decrease in time-to-peak (implicit time) of their response, and because their S-R curve follows the Michaelis-Menton (Naka and Rushton, 1968) relationship. My results, obtained in the same species, confirm this proposition as far as the value of the S-IT slope is concerned (-0.11 for rods, -0.12 for pineal photoreceptors). It is noteworthy that although the S-IT slope is practically identical in trout rods and pineal photoreceptors, responses from the pineal encompass a range of implicit time values that is nearly 5 times that of rods (see Fig. 4 of Kusmic et al., 1992).

Similarities were also found between the trout and mammalian scotopic systems. Slope value for rat (Cone 1964) and cat (Schneider and Zrenner, 1987) S-IT curves was similar to trout (Table 5 and Fig. 37). The overall S-IT curves for rat and cat, however, were displaced toward shorter implicit times compared to the trout's (Fig. 37). This may be due to the higher temperature at which the mammalian body operates.

Figure 37:Figure 37: Comparison of trout scotopic S-IT data with ONR results from the literature. Scotopic ONR data from this study (Full diamonds) are compared with those from Cone (1964) (empty squares) and Schneider and Zrenner (1987) (full squares) which also used scotopic ONR recordings. Data have adjusted along the horizontal axis. Units for the horizontal axis are in log photons cm^{-2} s^{-1}.

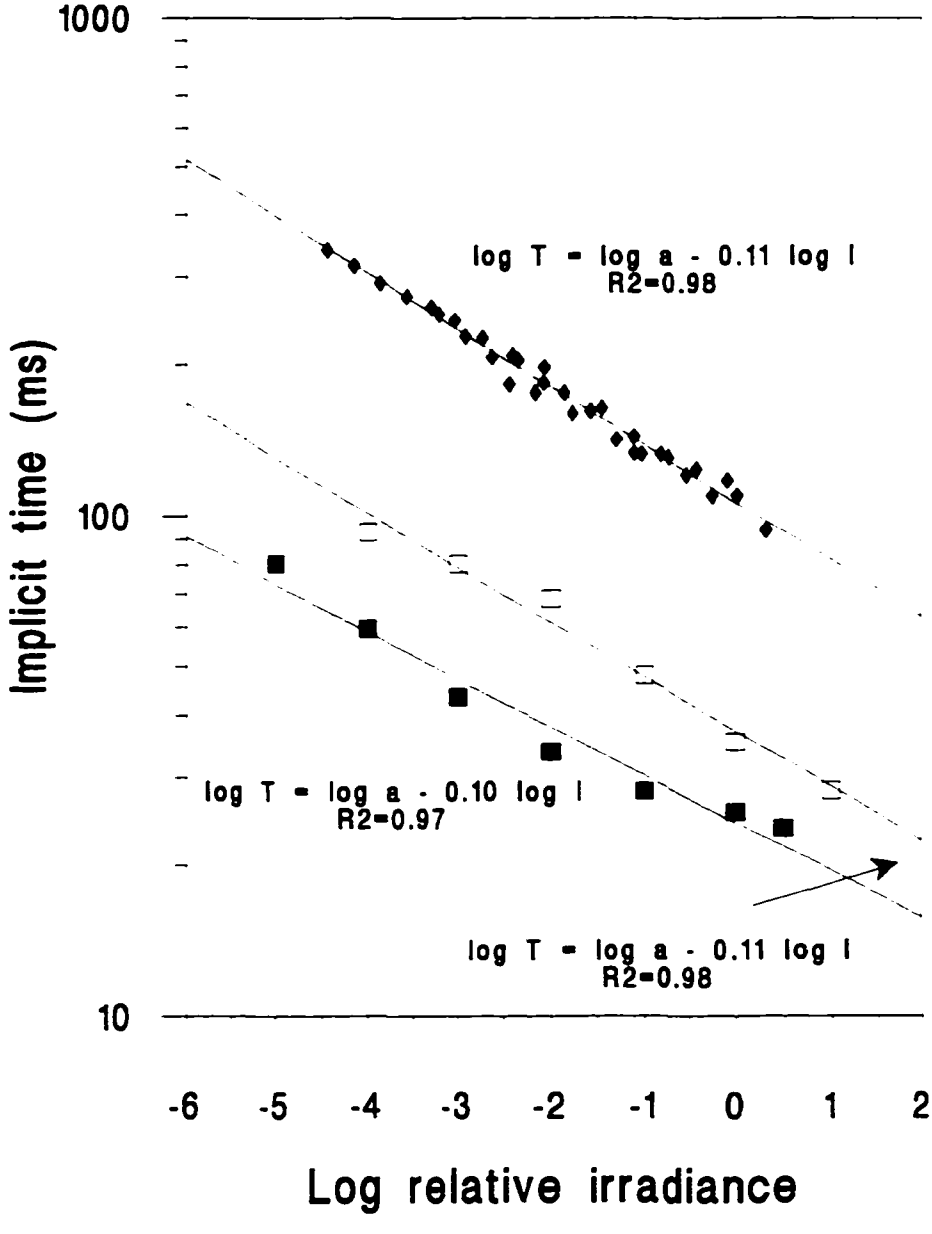
1000
100
10
Implicit time (ms)
log T = log a - 0.11 log I
R2=0.98
log T = log a - 0.10 log I
R2=0.97
log T = log a - 0.11 log I
R2=0.98
-6
-5
-4
-3
-2
-1
0
1
2
Log relative irradiance

Implicit time and light adaptation

The results from this study show that adaptation affects the time course of rod and cone pathways differently. The main difference I found was in the effect of adaptation on the slope **b** of the S-IT curve. Slope remained constant during light adaptation under scotopic conditions even though threshold, over the same range of intensities, increased by more than 3 log units. Conversely, under photopic conditions, slope **b** decreased with light adaptation, even though only slight changes in threshold were observed. Furthermore, these results suggest, as do those of Cone (1964) and Schneider and Zrenner (1987), that the mechanisms responsible for changes in threshold during adaptation are distinct from those that govern changes in implicit time. More specifically, this suggests that in trout, response implicit time does not show signs of adaptation under scotopic conditions; implicit time depends solely on stimulus irradiance, regardless of adaptation. This is in contrast to response amplitude, which varies with adaptation, as indicated by the horizontal shift of the S-R curve. In the photopic system, however, adaptation caused shifts along the intensity axis for the S-R curve, but also caused changes in slope and changes in the position of the S-IT curve along the intensity axis. This suggests that contrary to the scotopic system, both the sensitivity and implicit time of responses are influenced by adaptation in the photopic system.

For the scotopic system, implicit time at threshold decreased according to equation (2), with a slope of about -0.09 (Fig. 33). According to Donner et al. (1995), reported values for this slope vary from -0.09 to -0.28 among vertebrate species. Surprisingly, however, the value in trout approaches that found in mammals, but not that found in other

non-mammalian species such as the frog or the toad (Donner et al., 1995). In the common frog (*Rana temporaria*) scotopic system, for example, the slope under dark conditions was measured at -0.19 (Donner et al., 1995). In contrast, in rabbit and human rods, photocurrent measurements have yielded values of -0.09 (Donner, et al., 1995). As there are no data other mine for the teleost visual system, I cannot determine whether the value for trout is typical of teleosts in general. Nonetheless, the correspondence between the values in trout, rabbit, and human does suggest similarities in the physiology of the scotopic systems of teleosts and mammals.

Implicit time at threshold and chromatic adaptation

Under bright adapting conditions, near threshold, consistent disparities in the implicit time of responses near threshold existed between the various cone mechanisms. These were likely related to differences in the relative level of adaptation of the various cone mechanisms. Generally, implicit time at threshold was longest for the least adapted cone mechanisms, i.e. the UV and S cone mechanisms, whose absorption spectra overlapped little with the irradiance spectrum of the background. The L mechanism, however, did not seem to follow this rule, as suggested by the high variance associated with the results at 620 nm (Fig. 32). The high variance in the long wavelength part of the spectrum agrees with Palacios et al. (1996), Miller and Korenbrot (1991) and this work (chapter 6) and suggests that more than one class of L cone may be present in some fish species, each type characterized by its own kinetics. The biological significance of the various classes of L cones is unknown at present. Effects of backgrounds with varying spectral characteristics are investigated in more detail in the next chapter.

ON-OFF differences in implicit time

My finding of a systematic difference in implicit time between ON and OFF responses suggests additional delays in the transmission of visual information through the OFF channel may be introduced at the post-receptoral level. My results agree with those of Frumkes and Miller (1979), who found that the onset of depolarization in depolarizing bipolar cells occurred faster than the onset of repolarization in hyperpolarizing bipolar cells of the mudpuppy retina. As the ON and OFF responses originate partly from the activity of the depolarizing and hyperpolarizing types of bipolar cells, respectively, these results could probably be extended to the ONR response. The exact reason for this time course difference is not known.

The intimate relationship between implicit time and threshold that I described in the present study has potential implications for the determination of the inherent temporal properties of cone mechanisms, especially when adaptation is used as a mean of isolating cone mechanisms from one another. For example, Schuurmans and Zrenner (1981) report that the S cone mechanism has a longer latency than the L mechanism in the cat. This longer latency of the blue cone mechanism, however, was also accompanied by a lower threshold, suggesting that the difference observed by Schuurmans and Zrenner may be due in part to adaptation, and not necessarily to intrinsic differences in the properties of the two cone mechanisms. To determine whether the different cone photoreceptors in trout differ in their inherent temporal properties will require taking into consideration the relative state of adaptation of the various cone mechanisms.

Conclusions

In this chapter, I have revealed several properties of the light adaptation process in the trout visual system. First, the amplitude of the saturated ONR in fully dark-adapted conditions is about half that of the light-adapted state, and I suggest that this may be attributed to differences in the time course of the responses. Second, interactions between the scotopic and photopic systems may occur in the trout retina, as suggested by threshold values lower than predicted at intermediate background intensities. The mechanism that underlies this interaction remains unknown. Finally, I provided quantitative data on the effects of stimulus and background intensity on ONR implicit time for rainbow trout. These relationships were shown to fit a simple logarithmic function. Comparison of these data in trout with data from the literature indicated interspecific variation in the slope of the S-IT function. The absence of a correlation between the slope of the S-IT function and several parameters suggested that the variation present in vertebrates is likely species related.

Chapter 6: Chromatic adaptation, spectral sensitivity and implicit time of optic nerve responses in rainbow trout

Introduction

The visual system adjusts to ambient illumination levels through the process of light adaptation (Laughlin, 1989). Light adaptation affects various aspects of the retina's response to visual stimuli. At the photoreceptor level, light adaptation increases the threshold and shortens the response time or response latency (Arden and Ikeda, 1968; Baylor and Hodgkin, 1974; Norman and Werblin, 1974; Norman and Perlman, 1979; Copenhagen and Green, 1987; Schnapf et al., 1990; Koch, 1992; Moeller and Case, 1995). In addition, light adaptation shifts the response versus stimulus intensity (S-R) curve of cone photoreceptors along the intensity axis, thereby allowing them to function over their full dynamic range for a wide variety of background intensities (Malchow and Yazulla, 1988; Laughlin, 1989). Light adaptation also modifies the response characteristics of higher order such as bipolar and RGCs (Werblin, 1974; Werblin and Copenhagen, 1974).

In retinae that contain more than one cone mechanism, the spectral characteristics of ambient light can be adjusted to selectively adapt particular cone mechanisms (Enoch, 1972). This selective, or chromatic adaptation, has been shown to change the relative threshold of the different cone mechanisms (Enoch, 1972). In nature, especially in underwater environments, the spectral content of ambient light is normally biased toward a particular part of the spectrum (Loew and McFarland, 1990; Novales Flamarique et al.,

1992) and thus likely acts as a chromatically adapting background. As the underwater spectral distribution of ambient light changes throughout the day and varies with depth and location (Loew and McFarland, 1990; Novales Flamarique et al., 1992), chromatic adaptation of the different cone mechanisms is probably variable under natural conditions in aquatic animals. This likely influences the relative sensitivity and temporal properties of the cone mechanisms, especially at dusk and dawn, when the relative differences in the spectral distribution of ambient light are exacerbated (Novales Flamarique et al., 1992). Nonetheless, no attempt has been made to determine how the relative temporal properties of the different cone mechanisms would compare under differing chromatic backgrounds.

Whereas the previous chapter dealt with the effects of various background intensities on the sensitivity and time course of the optic nerve response, this chapter focuses on the effects of changes in the relative state of adaptation of the various cone mechanisms and their possible implications for neuronal coding in the light adapted trout retina. In this chapter, I therefore focused my attention on the effects of chromatic adaptation on: i) the relative sensitivity of the different cone mechanisms present in rainbow trout and ii) the temporal properties of optic nerve responses across the spectrum. I used backgrounds of varied spectral composition to determine the spectral sensitivity and the temporal characteristics of the ONR (Beaudet et al., 1993). Determination of the spectral sensitivity under the various adapting backgrounds was necessary to help identify the cone mechanisms that underlie the ONR at any particular wavelength, and provide an indication of the relative sensitivity of these various cone mechanisms. I predicted that under a given adapting background, both implicit time at

threshold and the rate of implicit time change with stimulus intensity would be highest for isolated mechanisms.

Material and methods

Study animals

I obtained the animals (rainbow trout, *Oncorhynchus mykiss*) from the Fraser Valley Trout Hatchery (Abbotsford, British Columbia). I kept the fish at 15°C under a constant photoperiod (12:12, light:dark) with an illumination level of 33.54 ± 14.39 mW cm^{-2} at the surface of the holding tank (white fluorescent illumination). The fish (18.1 ± 3.2g body weight, 12.6 ± 0.8cm total length) had been acclimatized to these holding conditions for a minimum of three months prior to their use. The protocol described herein has been approved by the University of Victoria Animal Care Committee.

Electrophysiological recordings

The surgical and recording procedures have been described previously (Beaudet et al., 1993) and will only be summarized briefly. I recorded multiunit responses from the optic nerve or the main optic tract of anesthetized animals (MS222, 1:10 000, Crescent Research Chemicals, Phoenix AZ) using a Teflon-coated silver wire (0.45 mm, A-M Systems) inserted through the surgically exposed optic tectum. Signals were differentially amplified 20 000-50 000 times with a pre-amplifier (Grass, P-50 Series), digitized and analyzed with a computer. Responses were typically multiphasic, composed of an initial negative potential followed by a positive deflection, and sometimes by another negative deflection (see Fig. 23). These were generated at the onset and offset of the stimulus (ON

and OFF responses respectively), and analyzed separately. At each test wavelength, response amplitude versus stimulus intensity (S-R) curves were generated for the ON and OFF responses and fitted with a third order polynomial function from which a threshold irradiance was determined. Sensitivity was determined from the reciprocal of this threshold irradiance A third order polynomial function was preferred to the Naka-Rushton function (Naka and Rushton, 1967) because it provided a better fit overall, especially at higher stimulus intensities. The threshold irradiance was that which elicited a criterion response of 30μV. The implicit time of the response at a given intensity-wavelength combination was given by the time between the onset (or the offset) of the light stimulus and the absolute maximum of the first deflection of the response (ON or OFF) (see Fig. 23). Thus, for each test wavelength, one S-R curve and one response S-IT curve were generated.

Determination of spectral sensitivity under the various adapting backgrounds served two major functions in addition to providing general information on the action spectra of the cone mechanisms present in the trout retina: i) it helped identify the cone mechanism underlying the optic nerve response at any particular wavelength and ii) it provided a means of assessing the relative sensitivity of the various cone mechanisms under these same backgrounds.

Background conditions and recording protocol

I used broad field stimulation of the intact, *in situ* eye. Stimuli were generated by a 450 W Xenon source whose spectral output was adjusted by a monochromator (ISA) and intensity by a 4.0 log unit Inconel coated neutral density wedge. Backgrounds were

generated by two 250 W halogen sources whose outputs were modified by the addition of interference and Inconel coated neutral density filters (Corion, Holliston, MA) in the optical paths. To determine the spectral and temporal characteristics of the four cone mechanisms (UV, S, M and L[10]) under various ambient light conditions, Stiles' technique of chromatic adaptation was used (see review by Enoch, 1972). Figure 38 depicts the spectral characteristics of the light backgrounds used to chromatically adapt the different cone mechanisms (as measured with a LI1800UW spectroradiometer, LiCor Instruments, Lincoln, NB). These backgrounds were chosen to selectively isolate the various cone mechanisms: **UV+S**, **M-**, **L-** and **M+L** cone mechanisms. As the UV and S mechanisms were not easily isolated from one another, they were isolated as a pair.

I subjected the animals to a given adapting background for a minimum of one hour before the beginning of each recording session. The recording protocol consisted in threshold determination at 15 test wavelengths ranging from 360 nm to 660 nm (16 wavelengths under the L mechanism isolating background condition). The test wavelengths were presented in a sequence that minimized selective adaptation of any particular cone mechanism by the stimulus. In addition, to determine the effect of chromatic adaptation on the kinetics of the response across the spectrum, implicit time was measured for each stimulus intensity-wavelength combination.

[10] The UV cone mechanism is most sensitive to UV light, the S, M and L mechanisms to what would be perceived by the human eye as blue, green and red light respectively.

Figure 38: Visual pigment absorption for the cones present in the juvenile rainbow trout, and spectral characteristics of the backgrounds used in the experiments. UV+S mechanisms isolating background was used to adapt the M and L cones. M mechanism isolating background adapted predominantly the UV, S and L cones. M+L mechanisms isolating background adapted the UV and S cones. L mechanism isolating background adapted the UV, S and M cones. Pigment absorption curves plotted according to Hawryshyn and Hárosi (1994).

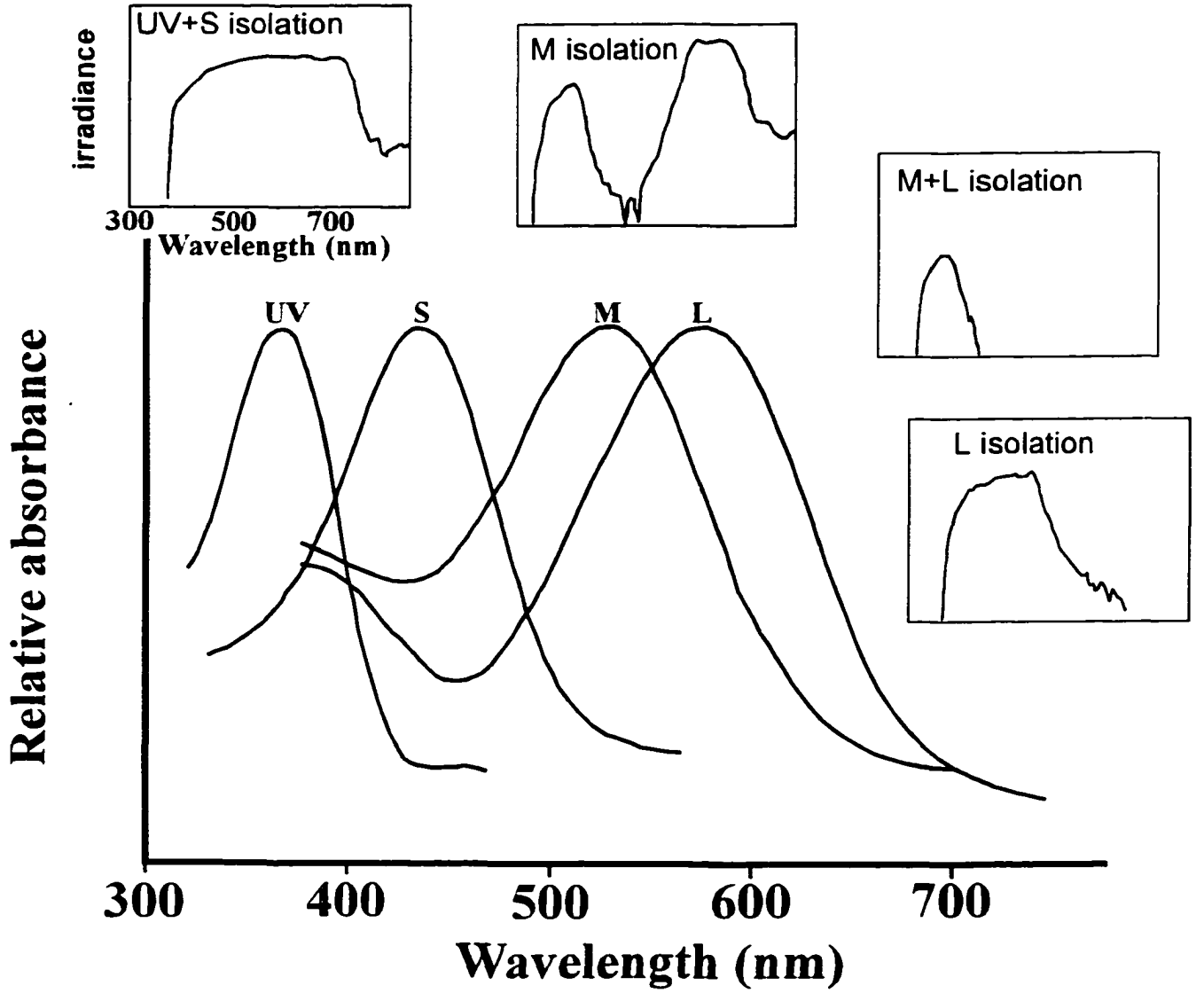
UV+S isolation
irradiance
300
500
700
Wavelength (nm)
M isolation
M+L isolation
L isolation
UV
S
M
L
Relative absorbance
300
400
500
600
700
Wavelength (nm)

Analysis

Under each adapting background, spectral sensitivity for both the ON and OFF responses were determined. Individual spectral sensitivity curves were normalized, then adjusted along the vertical axis to minimize inter-individual variation. The averages ± standard deviations (SD) for all fish were obtained from these normalized, vertically adjusted individual curves. Slopes of the S-IT curves for each test wavelength were determined using equation (1) (chapter 5). S-IT curves slopes obtained under a given adapting background were normalized to the absolute highest value and averages ± SD were computed for each test wavelength and plotted against wavelength. Therefore, in the remainder of the paper, higher slope values correspond to higher rates of implicit time decrease with stimulus intensity. Normalized S-IT curve slopes were compared within each background condition using Scheffé's multiple comparisons test at 0.05 level of significance (SPSS for Windows, SPSS Inc., Chicago, IL)[11]. I applied this test to a selected subsample comprised of four wavelengths approximating the wavelengths of maximal absorption of the cone types present in juvenile trout: 380, 420, 520 and 620 nm for the UV, S, M and L cones respectively (Fig. 38, adapted from Hawryshyn and Hárosi, 1994). The value of 380 nm was chosen for the UV mechanism because results were less consistent below this wavelength as the output of our stimulus decreased substantially. Response implicit time at threshold across the spectrum was determined for each

[11] Prior to testing, homogeneity of variance was tested using Levene's test of homogeneity (SPSS for Windows). Also, because Scheffé's multiple comparisons test adjusts the level of significance to take into account the increased probability of type I error associated with multiple comparisons, differences that appear to be present graphically may in fact not be statistically significant (Huck et al., 1974).

individual animal using the S-IT curves by choosing the implicit time that corresponded to the threshold irradiance determined from the corresponding S-R curve. Response implicit time values across the spectrum were normalized and averages ± SD calculated for all adapting background conditions. In addition, implicit time at each wavelength was determined for a stimulus of fixed intensity. The value of the fixed intensity was determined as the minimal intensity that triggered a response at all test wavelengths. Differences in implicit time observed across the spectrum were tested statistically using Scheffé's multiple comparison test (0.05 level of significance).

Results

Based on the results obtained in chapter 5, responses were assumed to originate from a fully light-adapted retina and, therefore, to reflect the activity of the photopic visual system, i.e. the cone photoreceptors. Furthermore, under conditions of full field stimulation, responses were presumed to originate from the center of RGCs' receptive field (Daw, 1968; Spekreijse et al., 1972; Werblin, 1974).

Spectral sensitivity: four cone mechanisms contribute to the ON response

Spectral sensitivity under the various adapting backgrounds revealed the presence of inputs to the ON response from the four cone mechanisms, namely the UV, S, M and L cone mechanisms (Fig. 39). Under UV+S mechanisms isolation, a predominant sensitivity peak, around 390 nm, was accompanied by secondary peaks indicative of S (λ_{max} 420 nm), M (λ_{max} 520 nm) and L (λ_{max} 620 nm) mechanisms inputs to the ON response (Fig. 39A, upper trace).

Figure 39: Relative spectral sensitivity of ON (filled squares) and OFF (empty squares) responses under UV+S (**A**), M (**B**), M+L (**C**) and L (**D**) isolation.

A Main sensitivity peak in the UV part of the spectrum for the ON response. For the OFF response, two peaks were present, in the UV+S mechanisms and M mechanism parts of the spectrum, respectively. **B** Under M mechanism isolation, single sensitivity peaks were found around 520 nm for both ON and OFF responses. **C** Maximum sensitivity for the ON response was found around 630 nm, and in the M mechanisms for the OFF response. **D** Under L mechanism isolation, highest sensitivity is found at L mechanisms for the ON response. The OFF spectral sensitivity was characterized by two peaks, one in the short, the other in the M mechanisms. In this and the following Figures, curves represent means±SD and n=5 under UV+short and L mechanism isolation and n=3 under middle and M+L mechanisms isolation. Error bars smaller than symbol when not visible.

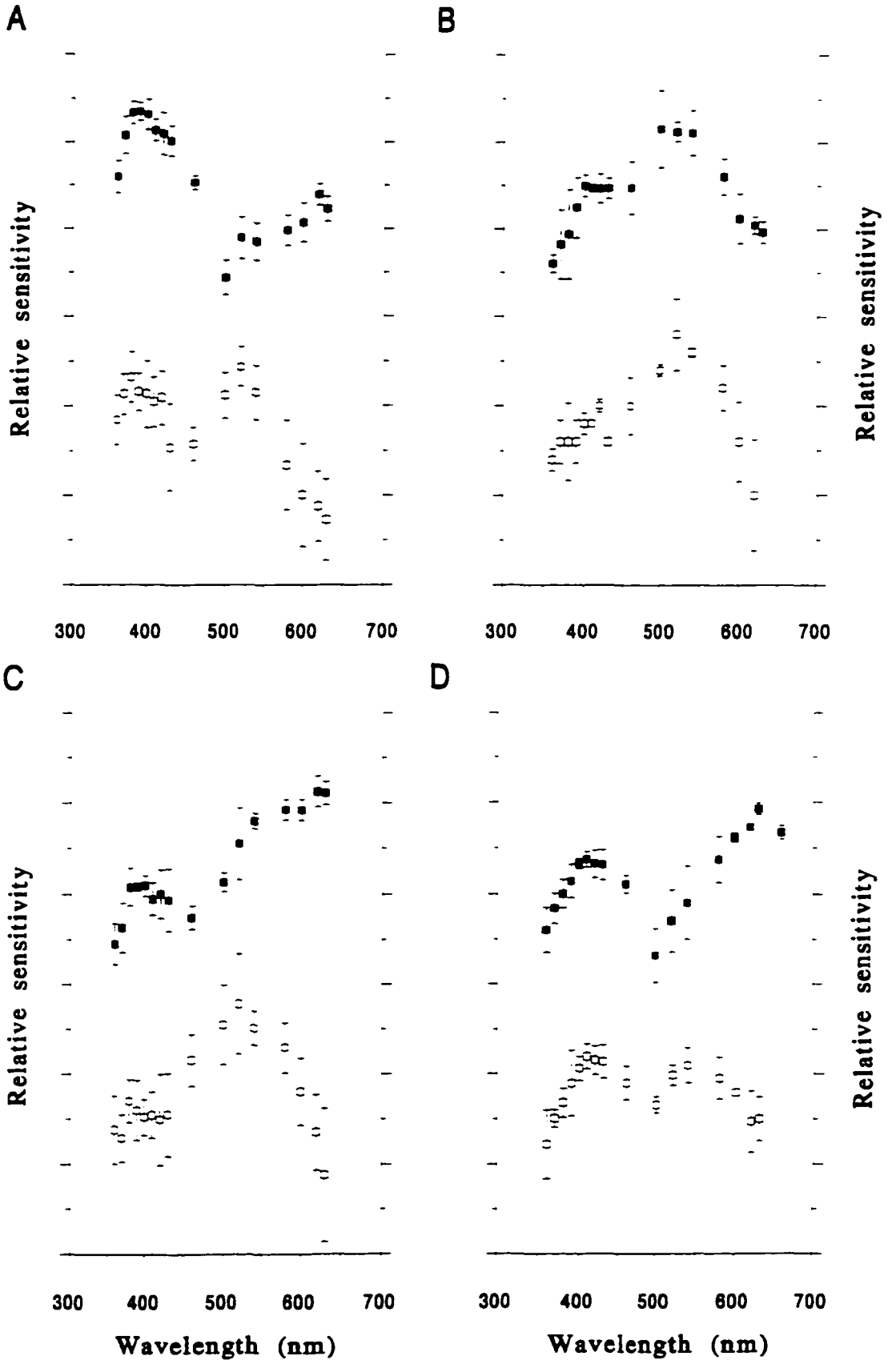
A
B
C
D
Relative sensitivity
Relative sensitivity
Relative sensitivity
Relative sensitivity
300
400
500
600
700
300
400
500
600
700
300
400
500
600
700
300
400
500
600
700
Wavelength (nm)
Wavelength (nm)

Under M mechanism isolation (Fig. 39B, upper trace), a single, prominent sensitivity peak was present at 520 nm. Under these background conditions, S mechanism input resulted in a slight increase in sensitivity around 400-430 nm. No input from the UV or L cone mechanisms could be discerned in this case.

Under M+L mechanisms isolation (Fig. 39C, upper trace), the spectral sensitivity curve was composed of three peaks. In addition to the prominent L mechanism sensitivity (λ_{max} ca. 620 nm), M mechanism input was also present (ca. 540 nm). In the short wavelength part of the spectrum (i.e. below ca. 500 nm), a single peak was present (ca. 400 nm).

Under L mechanism isolation (Fig. 39D, upper trace), two distinct sensitivity peaks were found: a prominent L mechanism sensitivity peak centered at 630 nm, and a secondary sensitivity peak, centered around 400-430 nm. There was no apparent contribution from the M cone mechanism.

Spectral sensitivity: two cone mechanisms contribute to the OFF response

The OFF response spectral sensitivity showed contributions from at least two cone mechanisms (Fig. 39, lower traces). It is important to note the shift in spectral sensitivity of the M-dominated OFF response depending on background conditions. The M cone mechanism sensitivity peaked at 520 nm under UV+S-, M- and M+L-mechanisms isolation, but at 540 nm under L mechanism isolation. Under all background conditions, input from the M mechanism was consistently present, around 520-540 nm (Fig. 39A-D, lower traces). The other input originated from the shorter wavelengths part of the

spectrum, likely from the S mechanism, but was present only under UV+S and L mechanism isolation (Fig. 39A, D, lower traces). Maximum sensitivity peaked around 410-430 nm under L-mechanism isolation; under UV+S mechanisms isolation, the wavelength of peak sensitivity could not be determined accurately due to the high variance in the results in this part of the spectrum.

Expression of sensitivity at shorter wavelengths in the OFF response appeared to be dependent upon the selective adaptation of the M mechanism. Expression of short wavelengths input to the OFF response was present only when the sensitivity of the M mechanism OFF input was depressed through chromatic adaptation. Thus, the short wavelength sensitivity peak was present under UV+S- and L-mechanisms isolation, both background conditions that selectively depressed the sensitivity of the M mechanism, but was absent otherwise (Fig. 39A, D, lower traces). In addition, displacement of the M sensitivity peak from 520 to 540 nm under conditions favoring the maximal expression of the OFF sensitivity peak at short wavelengths, may suggest an interaction between the M mechanism and a mechanism located at these shorter wavelengths (see Discussion). When the adaptation was released from the M mechanism, such as under M- and M+L-mechanisms isolation, M input dominated the OFF response (Fig. 39B, C, lower traces). The presence of a UV input to the OFF response could not be ascertained.

Chromatic adaptation and S-IT curves slope

As most of the variation observed occured in the ON response, this will be the focus of the present section. Generally, over the range of stimulus intensities used and for any particular background conditions, implicit time decreased with increasing stimulus

intensity according to equation (1), described in the preceding chapter, with stimulus intensity (Fig. 40). The relative **rate** of decrease of the ONR implicit time (i.e. the slope **b** of equation 1), however, varied across the spectrum for the ON, and depended on the background conditions, as exemplified in Figure 40. In this example, taken under L mechanism isolation, the slope of the S-IT curve at 630 nm was higher than for the other, more adapted wavelengths (360-540 nm). Slope **b** was thus highest for the isolated, and lowest for the adapted cone mechanisms. This rule, however, did not apply to the L mechanism under UV+S mechanisms isolation (Fig. 41A, lower trace). Under these conditions, S-IT curve slope for the L mechanism (630 nm) was significantly higher than that at 420 and 520 nm, although its sensitivity was lower than that of the isolated cone mechanisms (UV and S mechanisms: Fig. 41A, lower trace). Given the relative sensitivity of these mechanisms, the above mentioned rule would have dictated the slope **b** for the L mechanism be lower than that for the S mechanism. The S-IT curve slopes for the UV and S mechanisms, however, were significantly higher than that for the less sensitive M mechanism (520 nm).

Under M mechanism isolation, differences in slope **b** across the spectrum were not statistically significant, suggesting that the M mechanism dominated the ONR (Fig. 41B, lower trace). This is supported by the single, prominent sensitivity peak around 520 nm (Fig. 41B, upper trace).

As expected, under M+L mechanisms isolation, slope **b** for the less sensitive UV (380 nm) and S (420 nm) mechanisms, less sensitive, were significantly lower than that for the least adapted and therefore most sensitive L mechanism (Fig. 41C, lower trace).

Figure 40: S-IT of the trout ONR at selected test wavelengths under L mechanism isolation.

Slope on this graph is highest in absolute values for the L mechanism (630 nm). Average R^2 for the linear fits was for the curves shown 0.97 ± 0.01 SD. Units for the horizontal axis are in photons cm^{-2} s^{-1}.

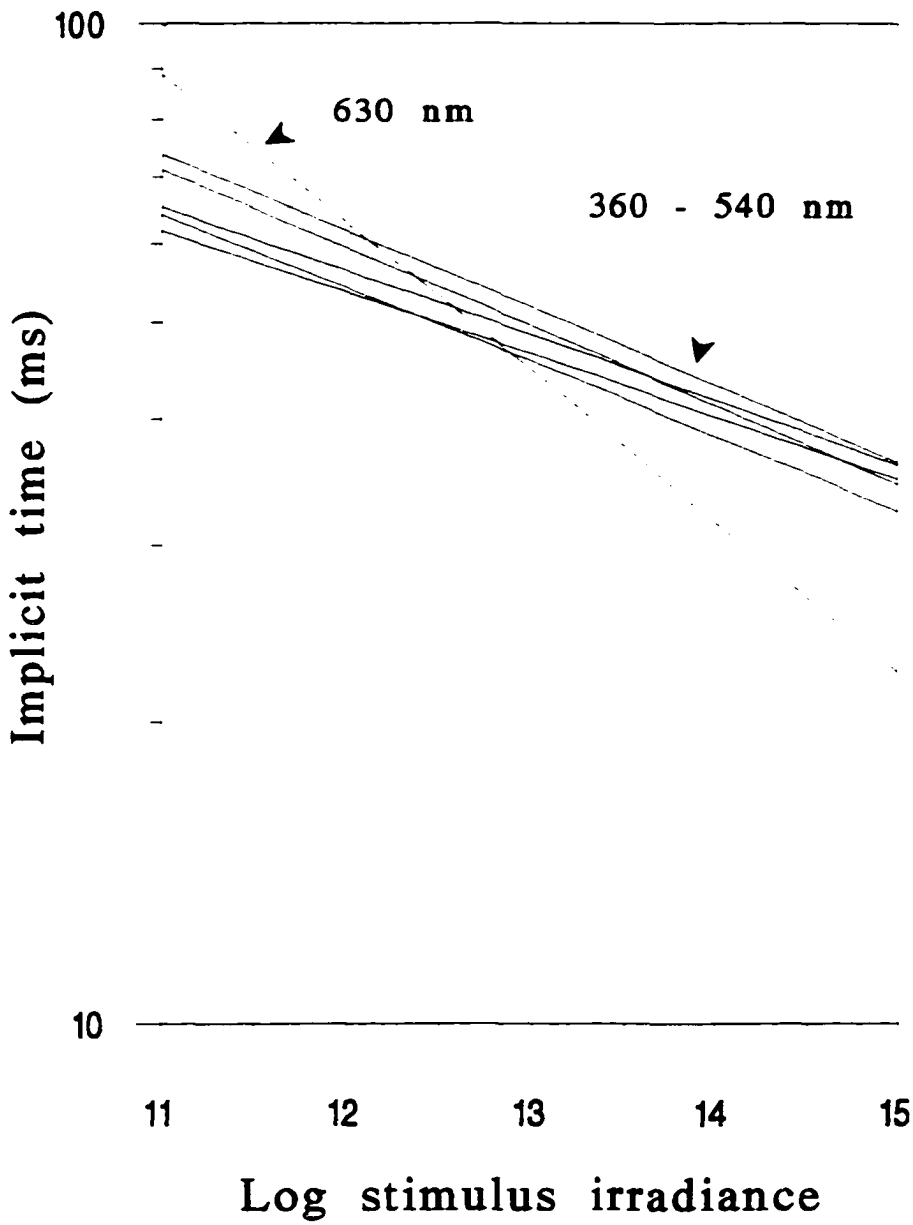
100
630 nm
360 - 540 nm
Implicit time (ms)
10
11
12
13
14
15
Log stimulus irradiance

Figure 41: Spectral sensitivity (upper trace) and S-IT curve slopes (lower trace) for the ON response under the various adapting backgrounds.

A The S-IT slopes are higher in the isolated part of the spectrum. Note, however, the unexpectedly high relative slope for the L mechanism (see text for discussion). **B** The S-IT slopes are not different from one another, indicating a domination of M inputs across the spectrum. **C** The S-IT curve slope is maximal for the L mechanism and unexpectedly low for the M mechanism despite its high sensitivity under M+L mechanisms isolation. **D** Values for the S-IT curves slope reflect the distribution of sensitivities, with the highest slopes for the L mechanism, and the lowest for the M mechanism. Backgrounds as in Fig. 39. Error bars smaller than symbol when not visible.

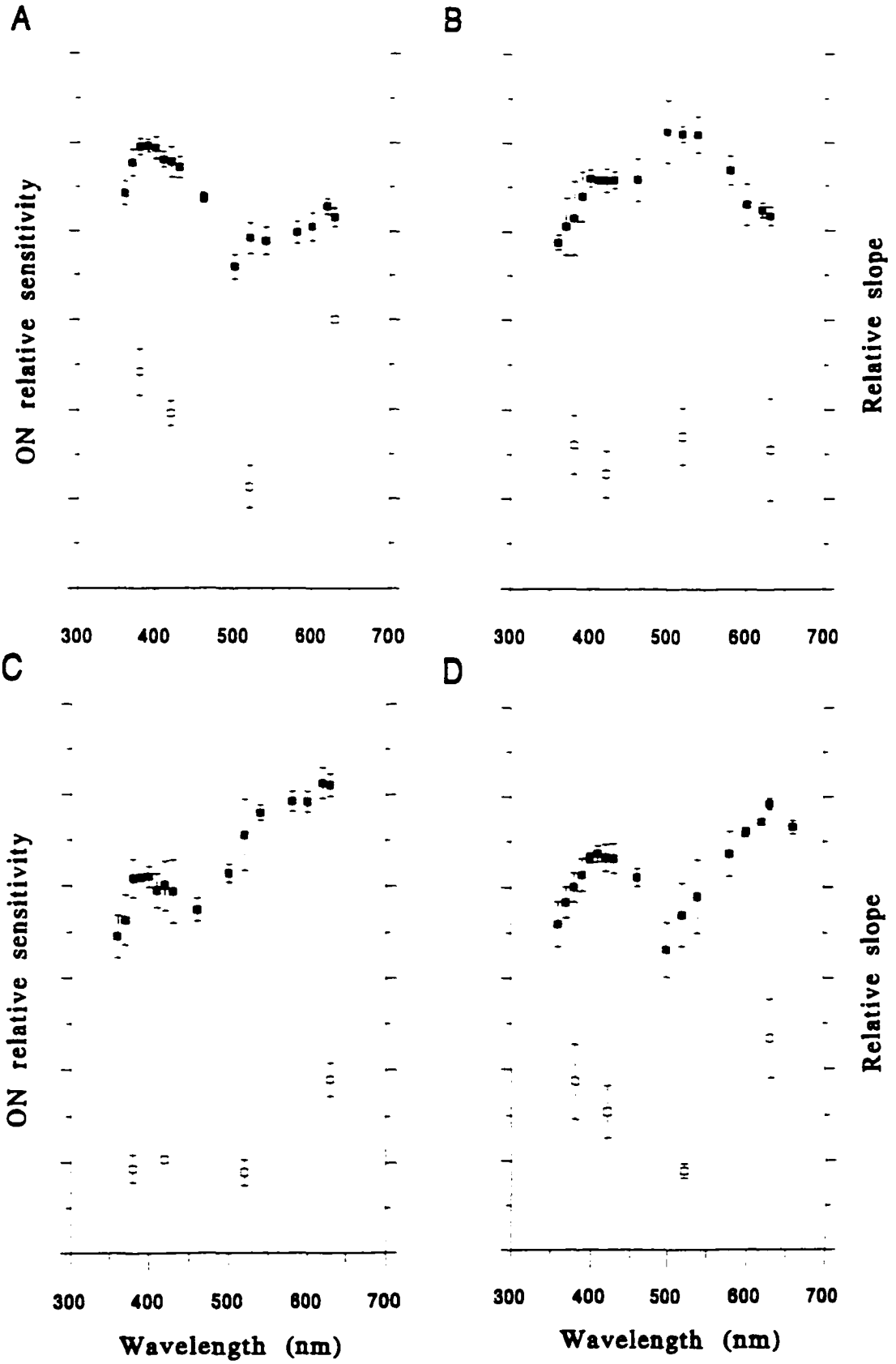
A
B
C
D
ON relative sensitivity
Relative slope
300
400
500
600
700
Wavelength (nm)

Stimulus-implicit time curve slope for the M mechanism (520 nm) was significantly lower than for the L mechanism (630 nm), but not different from those of the UV and S mechanisms (380 and 420 nm respectively). This was despite the higher sensitivity of the M mechanism relative to that of the UV and S mechanisms (Fig. 41C, lower trace). Again, this may have reflected a domination of the M mechanism at shorter wavelengths.

Under L mechanism isolation, slope **b** at 380 and 420 nm were intermediate between and not significantly different from those at 630 and 520 nm, which is in accordance with their intermediate sensitivity (Fig. 41D, lower trace). Finally, although there was some variation in the value of the S-IT slopes for the OFF response under the various backgrounds and for various wavelengths, the differences I observed were not consistent.

These data show that the state of adaptation generally influenced the rate at which implicit time decreased with stimulus intensity. As indicated by the lower **b** slopes for the most adapted cone mechanisms under each background condition, adaptation decreases the rate of implicit time change. This rule did not apply directly to the L mechanism. The higher slope of the S-IT curve at 630 nm under most background conditions was associated with a relatively high sensitivity of the L mechanism, although it was not as high as that of the isolated mechanisms, as seen under UV+S mechanisms isolation (Fig. 41A, lower traces).

Chromatic adaptation and ON response implicit time

Chromatic adaptation produced important differences in the response implicit time at threshold across the spectrum. Table 6 lists the average maximum and minimum implicit times at threshold for the various adapting backgrounds and the wavelengths at which they were found, and Table 7 the results from the statistical analyses. The largest difference in implicit time for the ON response (28 ms) was found between 630 nm and 500 nm, under L mechanism isolation. For the OFF response, the largest difference was 30 ms, between 360 nm and 600 nm, under UV+S mechanisms isolation, and between 500 nm and 630 nm, under M+L mechanisms isolation.

Parallels can be established between the effects of chromatic adaptation on the slope **b** and those on implicit time for the ON response. In both cases, implicit time at threshold and slope **b** tended to be less for the adapted cone mechanisms (compare Fig. 41, lower traces with Fig. 42, upper traces). Under UV+S mechanisms isolation, there were two statistically different groups of implicit time values: group 1 comprised values in the shorter and longer wavelengths part of the spectrum, and group 2 values in the middle part of the spectrum (Fig. 42A, lower trace). Group 1, which comprised the longest implicit times, probably represented inputs from the UV, S and L mechanisms (Fig. 42A, compare upper and lower traces). Implicit times for these mechanisms was significantly longer than that of the M mechanism (middle wavelengths part of the spectrum), whose sensitivity was also the lowest of all (Fig 42A, compare upper and lower traces).

Table 6: Relative difference in implicit time at threshold and for a fixed stimulus intensity (min-max) under the various background conditions

	UV+short		middle		middle+long		long	
	wavelength (nm)	latency (ms±SD)	wavelength (nm)	latency (ms±SD)	wavelength (nm)	latency (ms±SD)	wavelength (nm)	latency (ms±SD)
ON threshold								
max	400	61±7	500	57±8	630	56±4	630	65±11
min	540	34±5	600	34±3	360	47±4	500	37±9
difference		27		23		9		28
ON fixed intensity								
max	460	60±3	400	50±4	430	43±1	370	52±5
min	520	47±4	600	39±4	600	38±0	500	36±4
difference		13		11		5		16
OFF threshold								
max	360	63±3	430	72±7	500	79±10	460	67±7
min	600	33±4	600	48±7	630	49±14	500	43±8
difference		30		24		30		24

Table 7: Summary of the statistical significance of differences in implicit time between the various cone mechanisms

	Mechanisms	
Background	ON response	OFF response
UV+short	(UV, S, L) (M)*	(UV, S, M) (L)
Middle	(UV, S, M) (L)	(S) UV, M (L)
Middle+long	(UV, M) S (L)	(UV, S, M, L)
Long	(UV, S, L) (M)	(UV, S) (L, M)

*UV=380 nm, S=420 nm, M=520 nm and L=630 nm. Statistical difference at 0.05 significance with Scheffé's test for multiple comparisons. Significant difference present only between mechanisms enclosed in different sets of parentheses. No significant difference within sets of parentheses or between groups in parentheses and mechanism not enclosed in parentheses.

Figure 42: ON spectral sensitivity (upper trace) and implicit times (lower trace) under the various isolating backgrounds.

A Under UV+S mechanisms isolation, longest implicit times were found in the UV and short wavelengths parts of the spectrum, except for a group of unusually long implicit times for the L mechanism. **B** Implicit times were not statistically different across the spectrum under M mechanism isolation, except for the presence of significantly shorter implicit times for the L mechanism. **C** Longest implicit times were found for L mechanism under M+L mechanisms isolation. **D** Similar to UV+S mechanisms isolation, shortest implicit times were found for the M mechanism under L mechanism isolation. Backgrounds as in Figure 39. Error bars smaller than symbol when not visible. Groups with different numbers are statistically different from one another.

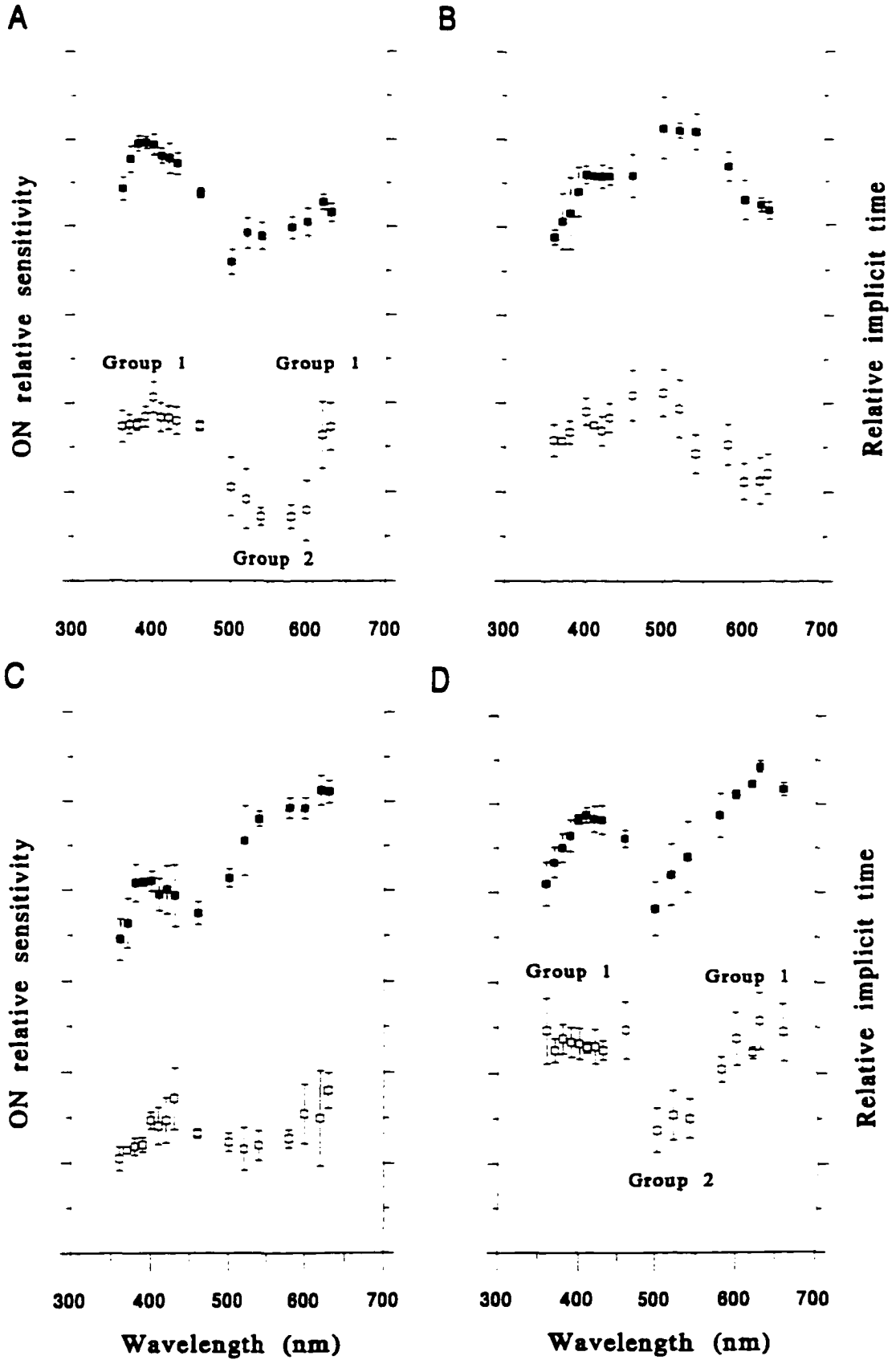
A
B
C
D
ON relative sensitivity
Relative implicit time
Group 1
Group 1
Group 2
Group 1
Group 1
Group 2
300
400
500
600
700
Wavelength (nm)

Under M mechanism isolation, implicit time for the M mechanism was amongst the longest (Fig. 42B, lower trace), but was only significantly longer than that at 630 nm. Despite the absence of a statistical difference in the mid to short wavelength part of the spectrum, there was a trend toward longer implicit times for the middle part of the spectrum (Fig. 42B, lower trace). This suggests response from the UV, short and middle wavelengths parts of the spectrum were probably dominated by M inputs, possibly in part through β-band absorption, but also influenced by input from the shorter wavelengths cone mechanisms (see Discussion).

Under M+L mechanisms isolation, implicit time for the L mechanism (630 nm) was significantly higher than that for the M and UV mechanisms but not different from that for the S mechanism, at 420 nm (Fig. 42C, lower trace). As with the S-IT curves slope, the difference in implicit time at threshold was therefore not different for the UV, S and M mechanisms. Implicit times under L mechanism isolation matched the spectral sensitivity, with the most sensitive cone mechanisms (L, then S and UV mechanisms) having longer implicit times than the most adapted, M mechanism (Fig. 42D, compare upper and lower traces). Together, these data argue for a longer implicit time of the L mechanism (see discussion).

Chromatic adaptation and implicit time for fixed stimulus intensity

Because chromatic adaptation leads to differences in the slope **b** across the spectrum, one would expect the differences in implicit time between the various cone mechanisms to diminish with increasing stimulus intensity. To test this hypothesis, I determined the

implicit time values across the spectrum for equal quantal stimuli (i.e. at a fixed intensity across the spectrum). In such a situation, stimulus intensity was near threshold for the less sensitive cone mechanisms, and suprathreshold for the most sensitive ones. Figure 43 represents the variation in ON response implicit times thus obtained (lower traces) and contrasts this with the values obtained at threshold under these same conditions (upper traces). Under UV+S mechanisms isolation, implicit time for a constant irradiance (13.5 Log photons) exhibited significant but smaller differences across the spectrum than what was found at threshold (Fig. 43A, compare upper and lower traces). Under M mechanism isolation, the distribution of implicit times at constant stimulus irradiance differed from that obtained at threshold (Fig. 43B, compare upper and lower traces). Implicit times tended to be longer in the shorter part of the spectrum at constant stimulus irradiance, as opposed to being longer the middle part of the spectrum at threshold. Although this trend toward longer implicit times at shorter wavelengths was clearly visible, differences were not statistically significant. Under M+L mechanisms isolation, differences were no longer statistically significant. Finally, under L mechanism isolation, implicit times at shorter wavelengths were the longest, and those for L mechanism merged with those of the M mechanisms leading to the presence of two groups of implicit times. Again, although the trend was clear, differences between these two groups were not statistically significant.

Chromatic adaptation and OFF response implicit time

Implicit time at threshold for the OFF response varied significantly across the spectrum under various adapting conditions (Fig. 44, lower traces, and Table 7). Under UV+S mechanisms isolation, two statistically different groups of implicit times were

Figure 43: ON implicit times at threshold (upper trace) and for a fixed stimulus irradiance (lower trace) across the spectrum under the various adapting backgrounds. Note lower relative implicit times for the M mechanism under M mechanism isolation for a fixed intensity, and for the L mechanism under L mechanism isolation. Backgrounds as in Figure 39. Error bars smaller than symbol when not visible.

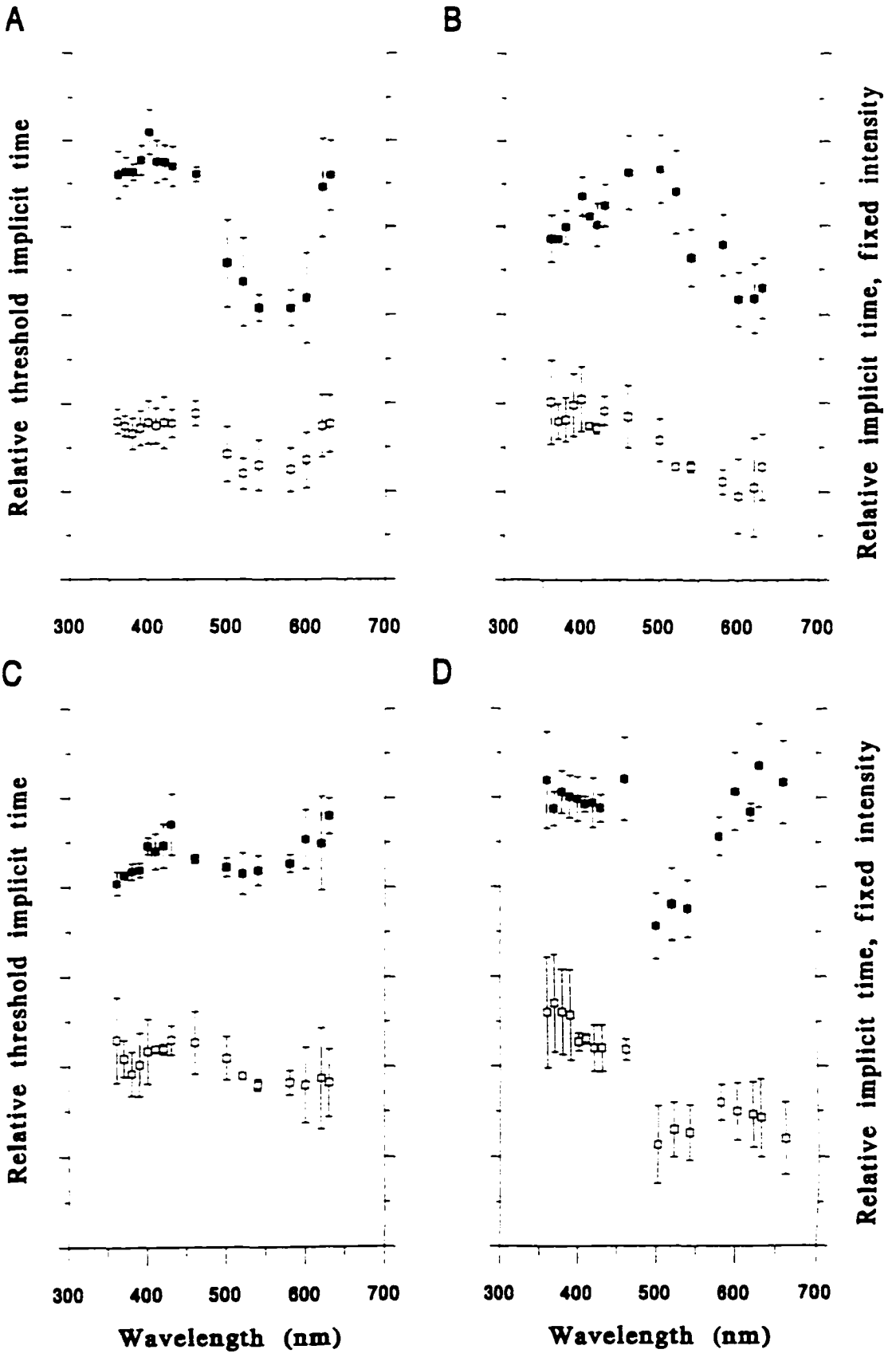
A
B
C
D
Relative threshold implicit time
Relative implicit time, fixed intensity
300
400
500
600
700
Wavelength (nm)

Figure 44: OFF spectral sensitivity (upper trace) and implicit time across the spectrum (lower trace) under the various isolating backgrounds.

Two groups of implicit times were present under UV+S and L mechanisms isolation (**A, D**),. In addition, under M mechanism isolation (**B**) lower trace suggests input from the S mechanism, which is not apparent from the spectral sensitivity curve alone. **C** No implicit time differences were present under M+L mechanisms isolation. **D** Note the shift in peak sensitivity of the M mechanism from 520nm to 540nm. Backgrounds as in Figure 39. Error bars smaller than symbol when not visible. Groups with different numbers are statistically different.

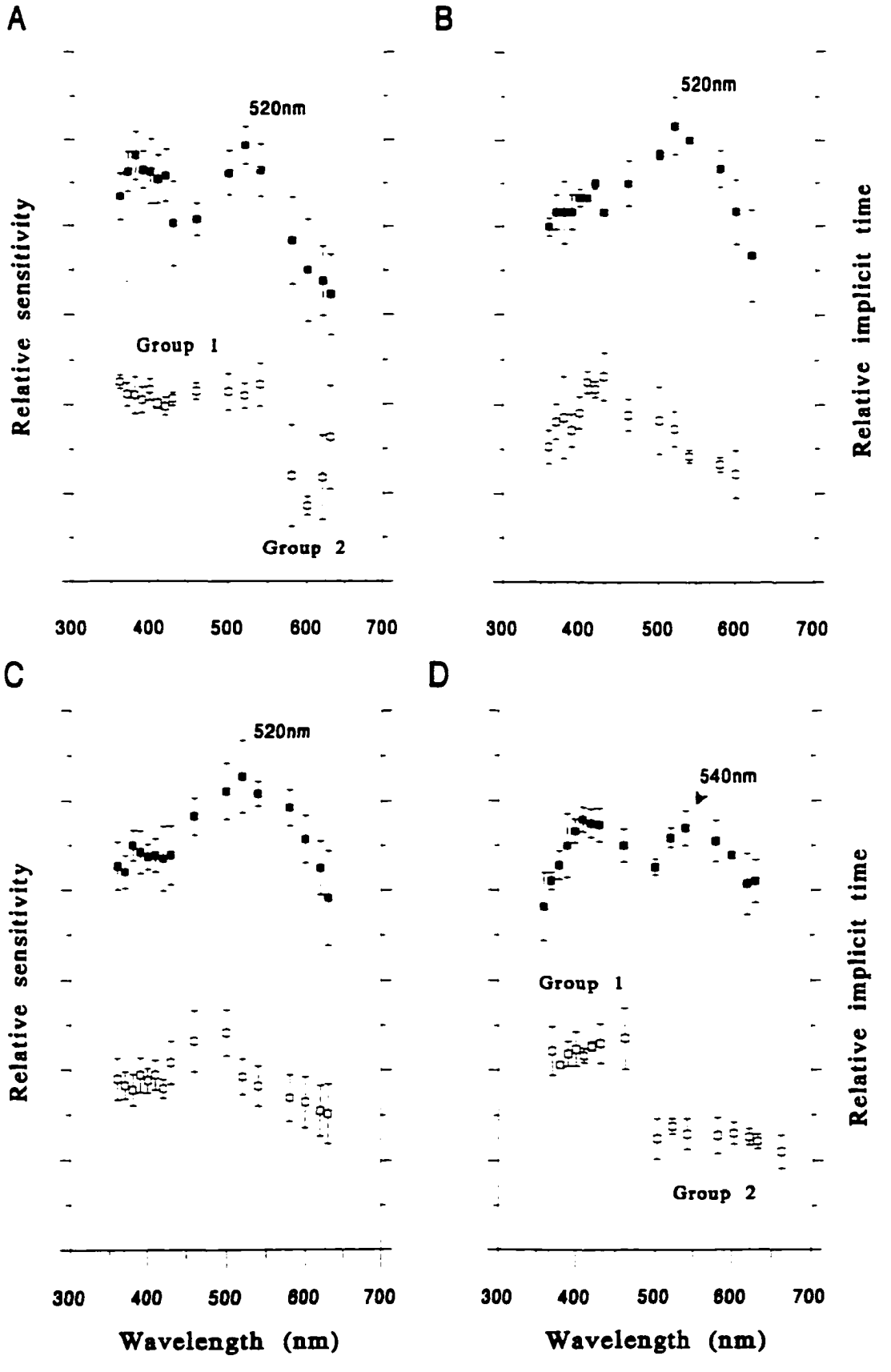
A
B
C
D
520nm
520nm
520nm
540nm
Group 1
Group 2
Group 1
Group 2
Relative sensitivity
Relative implicit time
Relative sensitivity
Relative implicit time
300
400
500
600
700
Wavelength (nm)
Wavelength (nm)

present (Fig. 44A, lower trace and Table 7). Group 1, which exhibited the longest implicit times, encompassed wavelengths in the UV to middle wavelengths part of the spectrum. The homogeneity in implicit times in this part of the spectrum (Fig. 44A, lower trace), coupled with the high variance in the short wavelengths part of the spectrum for the OFF spectral sensitivity (Fig. 44A, upper trace), suggests that the short wavelengths OFF sensitivity peak might actually be the expression of the M mechanism β-band absorption. Group 2, characterized by shorter implicit times, probably represented input from the L mechanism, although such input was not readily apparent in the spectral sensitivity curve (Fig. 44A, compare upper and lower trace). In this group, only implicit time at 600 nm was significantly different from the values from group 1. Implicit times at 580, 620 and 630 nm may have represented mixtures of inputs.

Under M mechanism isolation, longer implicit times at short wavelengths (ca. 420 nm) suggests the presence of an S mechanism input, although this is not apparent from the spectral sensitivity curve alone (Fig. 44B, compare upper and lower traces). Differences in implicit times between the short and long wavelengths were statistically significant (Table 7). Under M+L mechanisms isolation, where only one OFF sensitivity peak was found, implicit times across the spectrum were not statistically different (Fig. 44C, lower trace and Table 7).

Under L mechanism isolation, two significantly different groups of implicit times were also found (Fig. 44D, lower trace). Again, the longest implicit times, group 1, were found in the UV and short wavelengths part of the spectrum. The shorter implicit times, group 2, were found in the middle to long wavelengths parts of the spectrum. It is

noteworthy that although sensitivity was similar for the two OFF peaks under L mechanism isolation, implicit time was nevertheless longer at the shorter wavelengths. This suggests inherent implicit time differences between the S and M cone mechanisms (see Discussion).

Discussion

Spectral sensitivity: ON response

The spectral sensitivity results for the ON response support what has been previously found in juvenile rainbow trout using various techniques (psychophysics: Hawryshyn et al., 1989; electrophysiology: Beaudet et al., 1993; Coughlin and Hawryshyn, 1994a, b; microspectrophotometry: Hawryshyn and Hárosi, 1994). Using chromatic adaptation, it was possible to isolate the UV, M, and L cone mechanisms. The S cone mechanism could not be clearly isolated, but input from this mechanism were nevertheless visible. The location of the peak sensitivity for the UV cone mechanism (λ_{max} 390 nm) is consistent with what I found earlier with the same technique (chapter 2). It does not agree with the microspectrophotometry data for the absorption spectrum of the trout UV photopigment (Hawryshyn and Hárosi, 1994), probably because of interactions with the S mechanism. Hawryshyn and Hárosi (1991) found similar discrepancies between the absorption spectrum of the UV cone in carp and the location of the psychophysically determined UV spectral sensitivity peak, which they too attributed to interactions with the S mechanism. Sensitivity maximum for the M cone mechanism generally agreed with microspectrophotometry data in rainbow trout (Hawryshyn and Hárosi, 1994). Sensitivity

peak for the L mechanism (ca. 620 nm), however, also differed from MSP results (576 nm: Hawryshyn and Hárosi, 1994), probably due to interactions between the M and L mechanisms. The L sensitivity peak found in this study matches that found in sockeye salmon smolts by Novales Flamarique and Hawryshyn (1996), which suggests these animals probably also possess an L cone with λ_{max} in the 570-590 nm range.

Spectral sensitivity: OFF response

The present results for the OFF response spectral sensitivity, however, differ substantially from previous reports in some fish and mammals. Previous studies found the S cone mechanism contributes very little to the OFF response in single units in trout (Coughlin and Hawryshyn, 1994a, b), and not at all or very little to multiunit recordings from the goldfish optic nerve (Wheeler, 1979; DeMarco and Powers, 1991, 1993). Similarly, Daw (1968) and Beauchamp and Daw (1972) did not find any RGCs with S OFF input to the receptive field center in goldfish. In the monkey retina, neither Malpeli and Schiller (1978) nor Zrenner and Gouras (1981) report the presence of S OFF RGCs. Nonetheless, the present data show that under appropriate conditions, a prominent S peak is present in the optic nerve OFF response of trout. The finding of a noticeable contribution of the S mechanism to the OFF response is in better accordance with those of Beauchamp and Lovasik (1973) and Novales Flamarique and Hawryshyn (1996) in goldfish and juvenile sockeye salmon RGCs respectively, those of De Monasterio and Gouras (1975) and De Monasterio et al. (1975) in rhesus monkey RGCs and those of Valberg et al. (1986) in the macaque lateral geniculate nucleus. Thus, the S cone mechanism is probably an important contributor of inhibitory inputs to RGCs in trout and

in other vertebrates, albeit less so than the M mechanism. However, a more thorough investigation of the trout retina, using single unit recording techniques, would be necessary to determine the exact contribution of the S mechanism to the receptive field of RGCs.

The high sensitivity of the OFF curve in the short wavelength part of the spectrum under L mechanism isolation is not likely to have originated from β-band absorption of the M mechanism as the sensitivity of the two OFF peaks was very similar. It is known that the sensitivity of the β-band absorption is always at least 0.5-1.0 log unit lower than that of the α-band and, therefore, one would have expected the S OFF sensitivity to be that much lower than that of the M mechanism (Daw, 1968; Spekreijse et al., 1972; Werblin, 1974). Furthermore, our finding of two distinct groups of implicit times, matching the two OFF sensitivity peaks under L mechanism isolation, is further indication that the short wavelengths OFF sensitivity did not originate from the M inputs but from a different cone mechanism. Under UV+S mechanisms isolation, the presence of UV and S inputs to the OFF response could not be established with confidence due to the high variance in the results.

Interestingly, the input from the S cone mechanism to the OFF response appeared to be present only under certain circumstances (see also Novales Flamarique and Hawryshyn, 1996). The S cone mechanism input was expressed in the OFF response only when the sensitivity of the M cone mechanism was sufficiently depressed: S input to the OFF response was present under L mechanism isolation (and possibly also under UV+S mechanisms isolation), but not when the relative sensitivity of the M cone mechanism was

increased, such as under M and M+L mechanisms isolation. Contrary to the findings of Novales Flamarique and Hawryshyn (1996), however, I was able to generate spectral sensitivity curves for the OFF response that contained both the M and S maxima: in their study, Novales Flamarique and Hawryshyn (1996) could only isolate one of the two sensitivity peaks under a given adapting condition. The reason for their inability to detect the two peaks in a single curve is not clear.

Several reasons may explain the apparent domination of the M mechanism over the S mechanism in the OFF response. First, there could be a relatively higher number of M OFF fibers which, when not selectively adapted, could mask the S input and dominate the OFF response. This would be consistent with Guenther and Zrenner (1993) in cat who found the S mechanism to contribute very little to the response of single RGCs and with Valberg et al. (1986) who found that cells receiving inhibitory S inputs constitute a small portion (3.5%) of the entire population in the macaque LGN parvocellular layer.

The possible numerical domination of the M OFF fibers has been suggested previously in rainbow trout. Beaudet et al. (1993), for example, found that under UV isolation, the sensitivity of the M OFF fibers was always higher than that of the M ON fibers suggesting that they might be present in very high numbers. Similarly, Coughlin and Hawryshyn (1994a, b) found a predominance of single units with M OFF inputs in the optic nerve and brain of juvenile rainbow trout. Of the 38 units from which Coughlin and Hawryshyn (1994b) recorded, 29 received M mechanism OFF inputs, compared to 9 with L and 1 with S mechanisms input. Therefore, if the OFF S fibers are present in a small number relative to those with M inputs, as results of Coughlin and Hawryshyn (1994a, b)

suggest, then the S OFF response is more likely to be recorded when the sensitivity of the M cone mechanism is depressed. This numerical superiority of the M inputs at the RGC level may partly be explained by the fact that twice as many M cones as S cones are present per unit area in the photoreceptor layer of juvenile rainbow trout, assuming that one of the member of the double cones is always an M cone (see Hawryshyn and Hárosi, 1994).

In addition, the dependence of the S OFF response on the level of adaptation of the M cone mechanism could be the result of a negative or opponent interaction between these two cone mechanisms. There have been some reports of small numbers of units in which S-M opponency was present. Coughlin and Hawryshyn (1994a, b) found a few such units, with a S OFF in opposition to the M and L mechanisms in the optic nerve and torus semicircularis of juvenile trout. In macaques, Valberg et al. (1986) also found the S inhibitory inputs to the LGN parvocellular layer to be in opponency with the M inputs. Similarly, De Monasterio et al. (1975) described opponency between the S mechanism and the M and L mechanisms in 18% of the trichromatic ganglion cells sampled from the rhesus monkey retina. My finding of a displacement of the M OFF sensitivity peak from 520nm to 540nm under L mechanism isolation also concurs with Neumeyer's (1984) results which show psychophysically the inhibitory action of the S mechanism on the M mechanism in goldfish. Other reports in which both M and S inputs were present, however, always found them to act synergistically (goldfish: Beauchamp and Lovasik, 1973; rhesus monkey: Zrenner and Gouras, 1981). Finally, Mollon and Polden (1979) indicate that the sensitivity of the S cone mechanism might be controlled by the M and L

cone mechanisms, through a type of interaction that they qualify as being "not merely inhibitory". Thus, the results I obtained in this study suggest that inhibitory interactions, similar to those reported by various authors in rainbow trout and other species, may be responsible for the M mechanism-dependent expression of the S OFF response.

Finally, sampling bias against cells or fibers of small size, normally associated with single unit recording (Towe and Harding, 1970; Stone, 1973), may have contributed to the paucity of recordings from OFF S inputs in trout RGCs. If fibers receiving OFF S inputs were of small diameter but numerous, one would indeed have expected fewer single unit recordings with such input. Their smaller diameter, however, should not have prevented them from being a major part of the ONR, as this latter technique is less prone to sample bias resulting from size differences. This was not the case in this study: S OFF inputs did not represent a major part of the ONR response, and thus reflected the paucity of S OFF single units reported by other authors (Coughlin and Hawryshyn, 1994a,b).

Spectral sensitivity and implicit time: complementary measurements

An important outcome of this study is the discovery that spectral sensitivity data are well supplemented by also considering the temporal characteristics of the responses. The study of implicit times uncovered a complexity that is not always readily apparent from spectral sensitivity curves alone. This was best illustrated by our results for the OFF response under UV+S and M mechanisms isolation. In the first case, L inputs to the OFF response were not apparent in the spectral sensitivity curve, but they were revealed in the implicit time data. Similarly, S inputs to the OFF response, absent from the spectral sensitivity curve under M mechanism isolation, were apparent in the spectral implicit time

curve. Conversely, implicit times indicated that the presence of an OFF sensitivity peak in the shorter wavelength part of the spectrum under UV+S mechanisms isolation was probably not the result of input from the UV or S cone mechanisms. I therefore suggest the inclusion of temporal analyses in future examinations of spectral coding in the visual system, especially when the presence of input from multiple cone mechanisms is suspected.

Intrinsic implicit time differences between cone mechanisms?

The intrinsic latency of the various cone mechanisms, that is their response latency to flashes of light of equal quantal efficiency, when the level of adaptation is controlled for, have been shown to differ substantially. Brindley et al. (1966) were the first to demonstrate the distinctly lower temporal sensitivity of the human S mechanism as compared to that of the M and L mechanisms. This lower temporal sensitivity of the S mechanism has since been confirmed in human (Marks and Bornstein, 1973; Kelly, 1974;Wisowaty and Boynton, 1980) and shown in some animals, by a range of techniques (cat and macaque monkey: Schuurmans and Zrenner, 1981; rhesus monkey: Zrenner and Gouras, 1981; ground squirrel: Crognale and Jacobs, 1988). Some results of intracellular recording from cone photoreceptors have indicated that these differences in the S mechanism's temporal properties probably arise at the post-receptoral level as differences were not present in the photoreceptors themselves (macaque: Schnapf et al., 1990; giant danio: Palacios et al., 1996). Similarly, Crognale and Jacobs (1988), using electroretinogram recordings, came to the conclusion that the lower temporal sensitivity of the S mechanism originates at the post-receptoral level. Others, however, indicate that

temporal differences in the response of cones of different spectral type do exist, with S cones having the longest response latency at threshold (salamander: Perry and McNaughton, 1991). These contradictory results suggest more work is needed to determine whether the various classes of cones differ intrinsically in their temporal properties, or whether differences arise at the post-receptoral level, or both.

In this study, I did not find any indication that the intrinsic implicit time of the S mechanism at threshold was longer than that of the other cone mechanisms in trout. I found, however, that the L mechanism presented an unusually long implicit time. This was most obvious for the ON response under UV+S mechanisms adaptation where, although the L mechanism's sensitivity was less than that of either the UV or the S mechanism, implicit times were not statistically different. Furthermore, the slope of the L mechanism's S-IT curve was larger than that of either of the two isolated mechanisms under the same conditions. Had the implicit time at threshold and adaptation properties of the L mechanism been the same as that of the other cone mechanisms, one would have expected it to be shorter under these background conditions. Under these conditions, the slope of the S-IT curve for the L mechanism would also be expected to resemble that of the other adapted mechanism, the M mechanism. Shigematsu et al. (1978) and Yamada et al. (1985) found that in carp horizontal cells inputs from the L mechanism always had a longer latency than that of the M mechanism, especially in L-M opponent cells. Yamada et al. (1985) argue that the longer latency of the L mechanism results from the fact that the L input to these cells is not a direct one; the L would pass through a luminosity horizontal cell then the M cone, prior to reaching the L-M opponent cell. It is difficult, however, to

determine whether or not the latency comparisons reported by Yamada et al. (1985) were made for stimuli of comparable quantal efficiency under similar levels of light adaptation, and hence, truly represent intrinsic differences.

Differences between the temporal properties of the L mechanism and those of the other cone mechanisms have also been reported in other species. Miller and Korenbrot (1993), for example, found that twin cones (λ_{max} 560 nm) in the striped bass responded faster than the single cones (λ_{max} 542 nm). Palacios et al. (1996), while finding no difference between the short wave sensitive cones and the other cone types in zebrafish, found a subset of L cones that presented shorter latencies at threshold. In both cases, these faster cones also presented higher thresholds, which suggests that cones that are intrinsically less sensitive may present shorter latencies at threshold, probably because more light is required to stimulate them. The present results do not allow us to draw such conclusions concerning the sensitivity of the L cones in rainbow trout. The possibility, however, that a subset of L cones may be more sensitive than the other cones types probably deserves attention. In humans, Whitmore and Bowmaker (1995) found little and Wisowaty (1981) found no difference in the temporal characteristics of the M and L mechanisms. These authors did not comment, however, on the absence of differences in the absolute sensitivity of the various cone mechanisms.

Chromatic adaptation and implicit time

The present results showed that implicit time differences between the responses of various cone mechanisms depend on retinal adaptation state. This was shown to be especially true when the adapting backgrounds are spectrally biased, as is found in the

natural underwater environment; i.e. when they chromatically adapt the retina. It is known that increases in background intensity and, hence, in the level of light adaptation of photoreceptors lead to decreases in the time course of their response at threshold (chapter 5; Baylor and Hodgkin, 1974; Tauchi et al., 1984; Daly and Normann, 1985; Copenhagen and Green, 1987; Peachey et al., 1989, 1992; Koch, 1992). Adaptation in cone photoreceptors also results in the shifting of the S-R curve along the stimulus intensity axis and in its compression (Cone, 1964; Normann and Werblin, 1974), i.e. if one were to express the S-R curve mathematically as

$$V/V_{max} = I^n/(I^n+\sigma^n)$$

where **V** is the response amplitude at the irradiance **I**, $\mathbf{V_{max}}$ is the maximal response amplitude, σ the irradiance at which $V = 0.5\ V_{max}$ and **n** is an exponent normally between 0.7 and 1.0, light adaptation increases the value of σ and decreases V_{max} (Adelson, 1982). This behavior exhibited by the cone S-R curve is also recognizable in the retinal neurons that constitute the pathway from the photoreceptor layer to the brain: horizontal, bipolar amacrine and RGCs all exhibit these horizontal shift and compression of their S-R curves with an increase in background intensity (Werblin, 1974; Werblin and Copenhagen, 1974). My results indicate that the slope of the S-IT curve, as recorded from RGCs, is also influenced by light adaptation under photopic conditions. Light adaptation reduced the rate at which implicit time decreases with stimulus intensity, as demonstrated by the variation in S-IT curve slopes across the spectrum under various adapting conditions. A similar effect of light adaptation on RGC responses has been reported in frog, although the

effects of chromatic adaptation across the spectrum were not investigated (Donner, 1981; Donner et al., 1995).

The functional implication of this adaptation-dependent change in the S-IT slope is that increases in stimulus intensity beyond threshold levels should lead to decreases in the implicit time discrepancies across the spectrum. This was indicated by the study of the effects of a suprathreshold stimulus on implicit times across the spectrum (Fig. 43, compare upper and lower traces). These results suggest that temporally-sensitive interactions between the various cone mechanisms depend not only on the relative state of adaptation of these mechanisms, but also on stimulus intensity.

As indicated in this and other studies, decreases in response latency or response implicit time have been shown to occur with an increase in stimulus intensity (intracellular recordings from pineal photoreceptors: Nakamura et al., 1986; Kusmic et al., 1992; from horizontal cells: Shigematsu et al., 1978; Yamada et al., 1985), although the opposite has also been reported (human electroretinogram: Peachey et al., 1989; intracellular recordings from photoreceptors: Schnapf et al., 1989; Palacios et al., 1996). In my experiments, implicit time was found to decrease with stimulus intensity almost exclusively: a slight increase or no change in implicit time was noted only in the most adapted mechanisms. These slight increases, however, were in the order of a few milliseconds, and could probably have been attributed to the variability inherent to the recording procedures. Although unlikely, however, it is possible that significant increases in implicit time could have been found at stimulus intensities higher than those I was able to generate. Our optical system did not allow us to investigate this possibility.

Adaptation and implicit time: Implications for neuronal coding

Overall, these results show that chromatic adaptation results not only in shifts in the relative sensitivity of the various cone mechanisms but also in their temporal properties. This was best illustrated by the difference in implicit time at threshold between the M and L cone mechanisms under two different background conditions. Under L mechanism isolation, I found the implicit time of the L mechanism to be longer than that of the M mechanism by 28 ms. Under M mechanism isolation, the difference was of comparable size (23 ms) but in this case, however, the M mechanism exhibited the longest implicit time. The size of the difference in implicit time was in accordance with what I found previously (Chapter 5). Furthermore, differences in the slope of the S-IT curves indicate that the temporal relationships between the inputs originating from different cone mechanisms should change with stimulus intensity, suggesting that these temporal relationships are dynamic and highly dependent on the animal's visual context.

The effects of chromatic adaptation on the temporal properties of visual responses have potentially important consequences for neuronal integration within the visual system. The differences in implicit times observed across the spectrum suggest that differential adaptation could determine whether or not different chromatic inputs to higher levels of processing might temporally coincide, thereby influencing the efficacy of opponent interactions and the organization of visual neuron receptive fields (See Donner, 1981a, b). Differences in latencies between signals have also been invoked to explain the phenomenon called backward masking in which the threshold of a response to a stimulus is increased by the **subsequent** flashing of an adapting background (Frumkes, 1990).

Gouras and Zrenner (1979) showed that the presence of a delay between the response of receptive field center and surround leads to different behaviors of RGC depending on the frequency of flickering of light: at high flicker frequency, chromatic flicker triggers responses characteristic of the achromatic pathway. Gouras and Zrenner (1979) attribute this effect to a resonance phenomenon created by these differences in implicit time. The simple model proposed by Gouras and Zrenner is one example that underlines the importance of the temporal aspect of visual responses in processing of visual information by the visual system. I suggest that chromatic adaptation, because of its selective effects on the temporal properties of the various cone mechanisms may also play an important role in shaping neuronal interactions within the visual system, beyond the simple shifts in relative sensitivity.

As my results indicate, however, the temporal properties of the visual system are dynamic and their behavior is dependent on the ambient lighting conditions. The natural underwater environment behaves as a dynamic chromatic adapting background: not only does the spectral distribution of light vary with depth and time of day, but it also changes according to the direction of sight (Loew and McFarland, 1990; McFarland and Munz, 1975; see also Fig.4 in Novales Flamarique et al., 1992). I therefore conclude that temporal neuronal interactions in the visual system of fish are likely to be affected by chromatic adaptation in the underwater light environment.

Chapter 7: General discussion and conclusions

At the outset of this dissertation, our understanding of the ontogeny, anatomy and physiology of the salmonid visual system was fragmentary. The purpose of this study was to further our understanding of ontogenetic changes occur in the visual system in association with shifts to a new environment, and more frequent changes that occur in response to alterations in the level and spectral characteristics of ambient light. This work addressed the following gaps in our knowledge:

1) Although UV sensitivity and accessory corner cones had independently been shown to disappear during ontogeny, there had been made neither a direct correlation made between UV sensitivity and the presence of corner cones in the salmonid retina, nor had there been any recordings made from UV-sensitive RGCs.

2) The retinal structure of salmonids returning to spawn had received no attention, and consequently, it was not known whether corner cones were present at this later stage. Information on the retinal structure of wild returning salmonids was of particular importance given the recent finding that thyroxine could induce reintroduction of corner cones in the retina of rainbow trout that had previously lost them.

3) Although UV sensitivity was known to be present in the optic nerve and torus semicircularis of juvenile rainbow trout, it was not clear what neural pathways existed between these structures.

4) Studies had addressed the psychophysical aspects of light adaptation in fish, however little was known of its effects on the sensitivity and temporal properties of electrophysiological responses in RGCs.

5) Finally, the effects of chromatic adaptation on the relative temporal properties of RGC responses had not been examined systematically in vertebrates.

The following sections briefly review my findings and discuss their significance for the visual ecology of salmonids.

UV sensitivity and the coding of visual information

This work indicates that the UV cone mechanism primarily contributes to the ON component of RGC responses. These results represent an important advance in our understanding of the role that UV light may play in visually-guided behaviors, as they relate spectral sensitivity to the coding of visual information in the fish retina. Because UV sensitivity contributes primarily to the ON response, it is concerned mainly with the detection of increments in UV light intensity. It can thus be inferred that the salmonid visual system is designed to detect UV-reflecting targets. According to the contrast hypothesis (Lythgoe, 1968; McFarland and Munz, 1975), detection of bright objects is a property of photopigments (and hence the photoreceptors that contain them) whose spectral absorption is offset with respect to the prevailing spectrum of ambient light. In natural environments, offset photopigments are generally found in the retina of fish that inhabit the top few meters of the water column (McFarland and Munz, 1975; Munz and McFarland, 1975; McFarland, 1991b). Furthermore, offset photopigments are designed to

detect bright visual targets viewed against a background of spacelight in the horizontal or downward directions of sight (McFarland, 1991b). In the freshwater environment, UV-reflecting targets would therefore be viewed against a background dominated by mid-spectrum wavelengths (Novales Flamarique et al., 1992).

Although inputs to the OFF response from other cone mechanisms were found, inputs from the M cone mechanism were clearly dominant. Combination of the M cone mechanism-dominated OFF response with the UV ON response, may provide optimal abilities for the detection of UV-reflecting targets in the horizontal and downward directions of sight. This is because a UV-reflecting target seen against a mid-spectrum-dominated background would optimally stimulate RGCs in which UV and M inputs are in opponency, as in those reported by Coughlin and Hawryshyn (1994a, b) in rainbow trout. The concentration of corner cones in the dorso-temporal retina in sexually mature salmonids, lends support to the contention that UV sensitivity may be concerned with the detection of targets in the horizontal and downward directions of sight in these animals.

Ontogenetic changes in photoreceptor mosaics: a reversible process?

This dissertation identified a direct correspondence between ultraviolet light sensitivity and the presence of corner cones in the ventral retina of rainbow trout. This was done through examination of spectral sensitivity and retinal structure in the same individuals, using a technique that showed a minimum of sampling bias. My results suggest that the loss of UV sensitivity is linked to the disappearance of the accessory corner cones from most of the retina in rainbow trout. This and similar evidence was

believed to indicate that UV sensitivity in salmonid fishes was linked to the early stages of life history (Bowmaker and Kunz, 1987; Hawryshyn et al., 1989; Browman and Hawryshyn, 1992; Kusmic et al., 1993). The detection of substantial areas containing corner cones in sexually mature Pacific salmonid fishes, however, suggests that UV sensitivity is recovered later in life, at the time when the animals return to their natal stream to reproduce. One of the most interesting aspects of UV sensitivity described in this dissertation is thus its apparent ontogenetic plasticity, which may extend to the latest stages of the salmonid life history.

Most reports of adaptive ontogenetic changes in the vertebrate visual system have pointed to a one-way process of anatomical and physiological transformations[12] (see chapter 1). In most cases, these ontogenetic adaptations appeared to result from the delaying of certain developmental events to match the changes in environmental conditions. The delay in the addition of rods and double cones until metamorphosis in flatfishes represents but one of these types of processes. In other animals, including salmonid fishes, photoreceptor types are removed from the retina at some time during development. No other study, however, has directly examined the possibility that in the wild, these processes observed during one stage of an animal's life history are reversed at a later one.

---

[12] The changes in the chromophoric content of visual pigments represent one exception to this statement (see chapter 1). However, this type of change is not comparable to the changes that are believed to take place in the salmonid retina and that are being postulated here. The A1/A2 system of fish has been known to be highly labile; this was not the case for neuronal structures themselves like photoreceptors.

The possible return of UV sensitivity in salmonid fishes carries important implications regarding the ability of the nervous system to modify itself, reversibly, in response to changes in environmental conditions. These implications are as follows: i) plasticity, in the form of latent multipotent precursor cells has to be present within the retina, ii) because of the possible relationship between these "plastic events" and environmental changes, there is a need for a communication system between the relevant environmental factors and the UV cone disappearance or reappearance, and iii) local elements also have to regulate the proliferation of the UV cones. Experiments in a laboratory setting suggest a link between the levels of circulating thyroxine hormone and the "plastic events" that affect the UV cone population (Browman and Hawryshyn, 1992, 1994). Thus, the results from this study and those of Browman and Hawryshyn are consistent with a scenario in which thyroxine levels play a role the early disappearance of UV cones from the salmonid retina, and their reappearance later in life (Fig. 45).

The late reappearance of UV cones suggests that the role UV sensitivity plays in visually-guided behaviors in salmonid fishes may not be restricted to the earlier stages. It is still not known, however, if UV sensitivity plays the same role in small and sexually mature animals. There is some indication that UV sensitivity may play a role in feeding in juvenile salmonids and other species (Browman et al., 1995; Loew et al., 1993). It is unlikely, however, that UV sensitivity is involved in feeding in larger animals as salmon normally cease to feed during the upstream migration (Burgner, 1991; Healy, 1991; Salo, 1991). Some authors have suggested that UV sensitivity in fish may play a role in the

Figure 45: Proposed developmental trajectory of UV cones in the salmonid retina. Under the postulated control of the hormone thyroxine, accessory corner cones (A) are lost from the retina at the time of smoltification. At a later stage of their life history, salmonids experience the reappearance of their accessory corner cones, possibly also under the control of thyroxine. A, accessory corner cone; DC, double cone; SC, central single cone. The asterisks indicate the location from which corner cones in the smolt-adult individuals are missing.

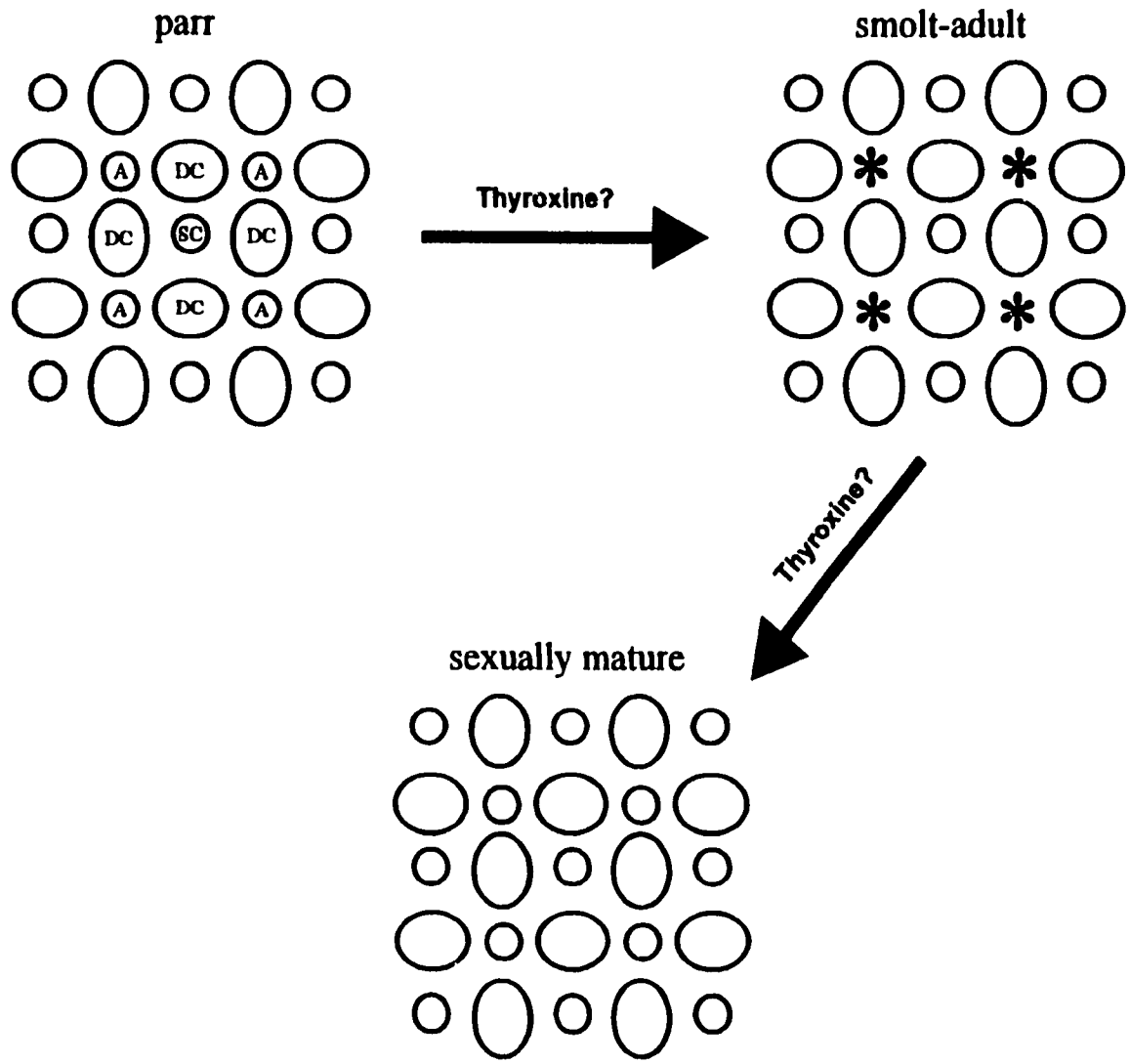
parr
smolt-adult
Thyroxine?
Thyroxine?
sexually mature
A
DC
SC

detection of and orientation to plane-polarized light, and hence facilitate homing behavior (Hawryshyn et al., 1991; Parkyn and Hawryshyn, 1994). This hypothesis requires further study, as does the suggestion that UV sensitivity may play a role in mating and intraspecific recognition, as postulated for birds (Goldsmith, 1994; Bennett et al., 1996).

Several questions regarding the fate of the UV cones in the salmonid retina remain, and could form a basis for future investigations. First, although there exists some indication that the UV cones are lost from the retina through the process of apoptosis or programmed cell death, there is no clear evidence that this is actually the case. Kunz et al. (1994) suggest, based on their finding of pyknotic bodies in the germinal zone of the Atlantic salmon retina, that UV cones are lost via apoptosis at the time of smoltification. Labelling of apoptotic cells, ideally coupled with *in situ* hybridization with phenotypic markers is needed to clearly determine the fate of the UV cones in the juvenile salmonid retina. In addition, controlled thyroxine manipulation experiments performed by Browman and Hawryshyn (1992, 1994) should be repeated on pre-reproductive salmonids and should include a topographic examination of the retina and the marking of cellular proliferation, with BrdU for example (Cameron, 1995). This would provide direct evidence that the UV cones Browman and Hawryshyn (1994) found in larger, thyroxine-treated individuals resulted from late cellular addition. An attempt should also be made to use these same techniques to examine the retina of salmonids at varying stages of their return migration to determine the timing of the corner cone reappearance in the wild.

Substrate for developmental adaptation[13]

The transformations of the visual system described in this dissertation suggest that the visual system of some vertebrates must retain plasticity during ontogeny. Similarly, the documented addition of RGCs in the frog, or double cones in winter flounder at the time of metamorphosis suggests that the retina of these animals contains undifferentiated precursors during their larval development, within portions of the retina that are otherwise functional and differentiated. Potential for plasticity late in life has also been revealed in regeneration experiments. In fish and amphibians, partially destroyed retina (or any part of the CNS for that matter) can regenerate. In goldfish, the potential for retinal regeneration has been demonstrated using ouabain injections (Maier and Wolburg, 1979)and laser ablation (Braisted et al., 1994; Raymond, 1991b). Although it was initially believed that stem cells named "rod precursors" were responsible for the generation of all cell types within the regenerated retina (Raymond et al., 1988), recent evidence indicates that rod precursors may actually be giving rise only to rods and that the other cell types originate from as yet unidentified precursors (Braisted et al., 1994). Local interactions are probably responsible for the induction of cellular differentiation leading to retinal regeneration (Raymond, 1991a).

The pathways of cellular differentiation involved in retinal regeneration may be the same ones involved in the ontogenetic changes in the visual system described in this dissertation. In this case, however, local cell interactions may be replaced or supplemented by hormonal actions. Hormones have been shown to affect the survival of

[13] This will appear in part as Beaudet and Hawryshyn (accepted).

cells, both within the visual system and in the rest of the body (Browman and Hawryshyn, 1992, 1994; Kaltenbach, 1953; Hoskins, 1990). Thyroxine, as mentioned above, has been implicated in the disappearance and the reappearance of the UV cones in rainbow trout (Browman and Hawryshyn, 1992). Kelley et al. (1995) suggests thyroxine and retinoic acid induce the differentiation of embryonic retinal precursors into photoreceptors, *in vitro*.

This raises the interesting question of whether or how the plasticity associated with ontogenetic changes in the visual system may be related to the ability of the visual system to regenerate. In other words, is the evolution of regeneration in some way linked to the plasticity that is required by visual systems to adapt to changing environmental conditions? Results by Kurz-Isler and Wolburg (1982) at least question the possible dependence of "ontogenetic plasticity" on the presence of regenerative abilities. These authors found that the rainbow trout retina, despite the "ontogenetic plasticity" identified in this study, possesses limited regenerative abilities. More research is obviously needed to clarify any potential relationship between these two factors.

From the retina to the torus semicircularis

Understanding the biology of UV sensitivity and UV vision requires an understanding of the anatomy and physiology of the various visual pathways to the brain. Chapter 4 of this dissertation added some building blocks to our knowledge of the anatomy of various visual pathways in the brain of rainbow trout. It is now clear that ipsilateral projections are present in juvenile rainbow trout although previous studies

(Pinganaud and Clairambault, 1979; Mansour-Robaey and Pinganaud, 1991) suggested that they were absent. These ipsilateral projections did not occur at the optic chiasm but decussated more caudally, through the posterior commissure, and appeared to terminate in the ipsilateral pretectal area. These fibers were in small number compared to the massive contingent of contralateral retinal projections. One of the reasons why Pinganaud and Clairambault (1979) did not find these ipsilateral projections in rainbow trout may be that the animals used by these authors were more ontogenetically advanced than the ones I studied. The visual system of trout undergoes dramatic modifications at the time of smoltification, and these may affect the ipsilateral projections. Whether there is a link between the loss of UV sensitivity and the possible disappearance of the ipsilateral projections in trout remains a highly speculative matter, but one that deserves more investigation.

In chapter 4, I used a sensitive double-labelling technique (Fritzsch and Wilm, 1990) to identify possible pathways between the retina and the torus semicircularis that did not involve the optic tectum in juvenile rainbow trout. This investigation was prompted by the discovery of numerous single units receiving UV inputs in the torus semicircularis and the optic nerve but not in the optic tectum of trout (Coughlin and Hawryshyn, 1994a), as well as an earlier report of direct retinal projections to the torus semicircularis in sockeye salmon smolts (Ebbesson et al., 1988). The absence of UV inputs to the optic tectum suggested that the UV information was reaching the torus semicircularis via an alternate pathway. The only alternate pathway I identified involved the accessory optic center (the *centrum opticum basale thalami* of Pinganaud and Clairambault, 1979) as the

intermediary between the retina and the torus semicircularis. The next step in the investigation of the UV sensitive central pathways should involve a combination of single unit recordings and neuronal tract tracing, following a two-fold approach: First, single unit recording should be carried from those areas of the brain that I have identified as possible "relay stations" for the UV information. Second, more detailed anatomical studies should be carried out, using techniques that generate electron-dense precipitates, to allow ultrastructural examinations.

Light adaptation in the trout retina

Chapters 5 and 6 qualitatively and quantitatively described the process of light adaptation in trout RGCs. In contrast to most studies carried out on non-mammalian vertebrates to date, particular attention was directed toward the effect of differences in the intensity and spectral content of the background on the sensitivity and temporal properties of ONRs. The relationship between stimulus intensity and response implicit time for the scotopic system conformed to a logarithmic function with a slope of -0.10. This value suggests that the visual information in the dark-adapted trout retina is submitted to a low-pass filter with 11 time-limiting stages, from the triggering of the phototransduction cascade to the generation of the ONR. Aside from the 6 stages accounted for by the phototransduction cascade and the G-protein-mediated bipolar response, this means that at least 5 additional stages filter the visual information before the ONR is recorded. The identity of the physiological mechanisms that underlie the activity of these postulated stages is not known at this point, but similarity in the value of slope **b** between trout, cat and rat suggests an organization that may be shared to a certain extent among vertebrates.

The slope **b** value found in trout fell within the range of values calculated from data reported in the literature (i.e. from -0.10 to -0.24). Interspecific differences in the value of **b** could not be explained by any single factor. Within a species such as the cat (Schneider and Zrenner, 1987), however, differences in the value of **b** could be related to the level of recording and thus, to the postulated number of time-limiting steps in the transmission of visual information. It is probably too soon to venture into attempting to explain these interspecific differences. More comparative data are obviously needed.

Similar to the S-IT curve, there are interspecific differences the slope of the implicit time at threshold curve for the scotopic system, among vertebrates. In trout, implicit time at threshold varied logarithmically with relative background intensity, with a slope of -0.09. This differed from values obtained in amphibians, but was very similar to those from mammalian species (see Donner et al., 1995 for a review). The fact the trout data were closer to those found in guinea pig, cat and rabbit than in the frog or the toad (Donner et al., 1995) may be an indication that the scotopic system of amphibians is not typical of that of vertebrates in general.

Selective adaptation of the various cone mechanisms led to differences in the sensitivity and temporal properties of ONRs across the spectrum. The results I obtained reflected changes that took place in receptive fields centers of RGCs, and did not allow direct examination of possible center-surround differences in temporal properties with chromatic adaptation. However, as mentioned by Donner (1995), changes in the temporal characteristics recorded from the RGC level generally reflect those that occur in the photoreceptors themselves. This suggests that the implicit time differences generated by

chromatic adaptation of the various cone mechanisms should equally affect receptive field center and surround, as both receive their inputs from the same general pool of photoreceptors. Thus, it is likely that chromatic adaptation creates temporal differences between the responses of receptive field centers and surrounds that differ in their spectral sensitivity. Under varying ambient light conditions, center-surround interactions, and possibly also the visual perceptions of animals, are likely to be variable due to differences in response sensitivity and implicit time.

A qualitative model of light adaptation in the trout retina

The data from chapters 5 and 6 provide the basis for a qualitative model of the effects of adaptation on the temporal properties of RGC responses in the salmonid retina (Fig. 46). As seen in chapter 5, implicit time changed logarithmically with stimulus intensity following the same function for the scotopic system, regardless of adaptation level (within a certain ranges of relative background intensities). This is represented in Figure 46A, where the S-IT curves for three backgrounds of increasing relative intensity (adaptation increasing in the following order: dotted line<solid line<dashed line) fall on a single line. From the behavior of these S-IT curves, one would be tempted to infer that the response intensity curve would show a similar behavior with increasing background intensity, namely that it could be described by a single function, as in Figure 46B. This is not the case, however. Rather, light adaptation leads mostly to a shift of the S-R curve towards higher intensities, along the abscissa (Fig. 46D; Werblin and Copenhagen, 1974). Thus, there appears to be a decoupling between the processes responsible for response amplitude and response implicit time adaptation in the scotopic system, similar to that

Figure 46: Qualitative model of light adaptation in the trout retina.

On these graphs, log intensity increases to the right, and response implicit time and amplitude increase upward. **A** Influence of light adaptation on the S-IT curve in the dark-adapted trout retina. 1, 2 and 3 represent increasing levels of light adaptation. Slope b remains unchanged with light adaptation, and S-IT curve is displaced along the function described by a single equation. **B** Effects of light adaptation on the S-R curve, as inferred from the model shown in A. **C** Effects of light adaptation on the S-IT curve in the light adapted rainbow trout retina. 1, 2 and 3 represent increasing levels of light adaptation. With adaptation, slope b decreases in value, and the S-IT curve is displaced along the log implicit time and intensity axes. A single equation is thus no longer sufficient to describe the various S-IT curves. **D** Behavior of the S-R curve with light adaptation, as reported in chapter 5. Light adaptation, in this case, causes a shift of the S-R curve toward higher intensities, along the abscissa.

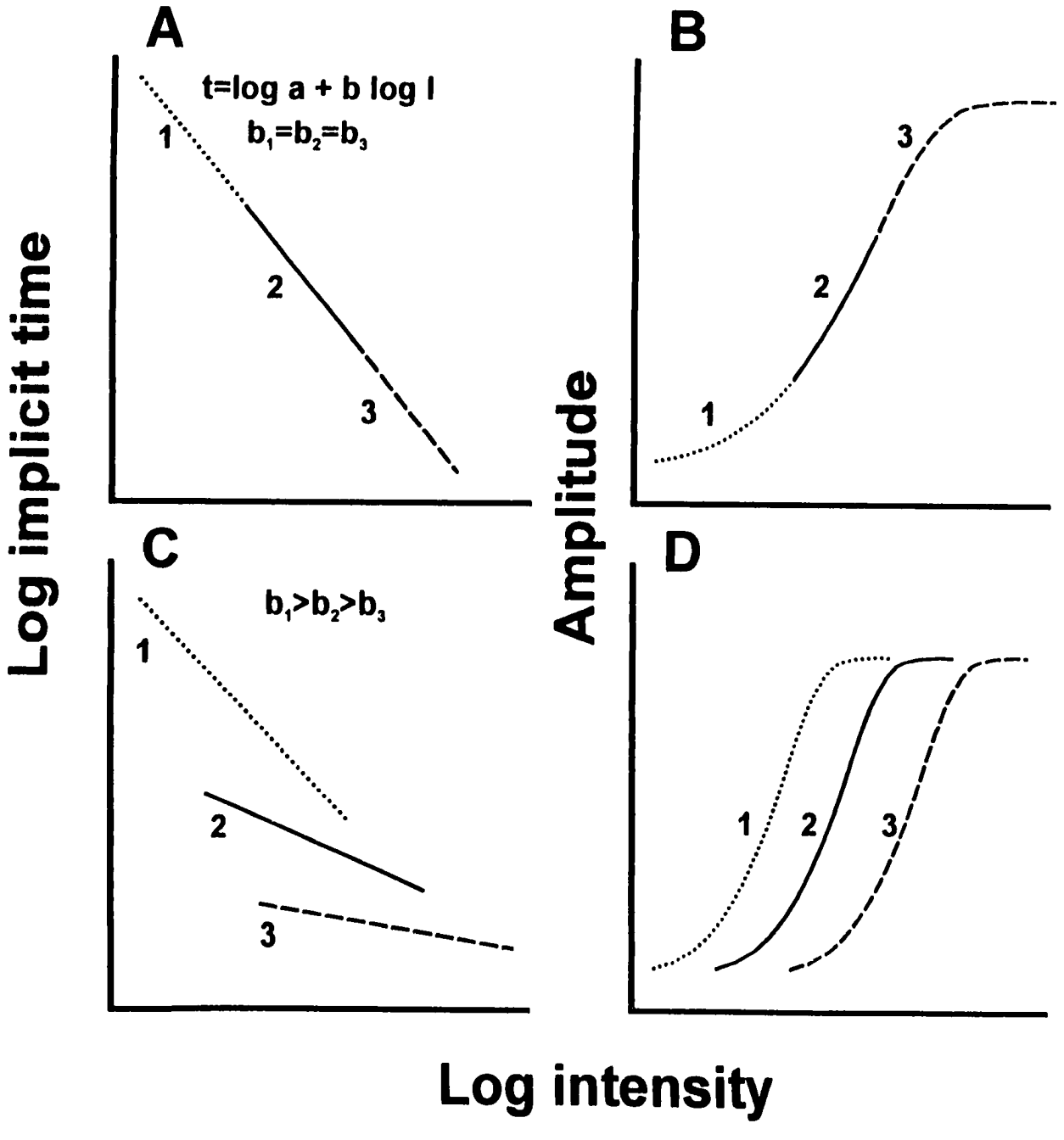
A
t=log a + b log I
$b_1=b_2=b_3$
1
2
3
B
1
2
3
C
$b_1>b_2>b_3$
1
2
3
D
1
2
3
Log implicit time
Amplitude
Log intensity

suggested by the results of Cone (1964) in rat and those of Schneider and Zrenner (1987) in cat.

In the photopic system, the response of the S-R and S-IT curves to light adaptation seemed to be more congruent (Fig. 46C). Displacements along the log implicit time and intensity axes, and changes in the slope of the S-IT curves were accompanied with displacements along the log intensity axis for the S-R curves. The model proposed in Figure 46 argues for a difference in the adaptational properties of rods and cones, at least in the trout retina. Since similar results were found in rat (Cone, 1964) and cat (Schneider and Zrenner, 1987), this difference between rods and cones may be widespread among vertebrates. The fact that the results obtained by Donner et al. (1995) in frogs differ from those in trout and some mammals, may indicate that the amphibian visual system represents a unique case, in which the rods possess more cone-like features than rods from other animals. This is supported by the fact that amphibians possess various spectral types of rods, a characteristic typical of the cone system in other vertebrae classes. Thus, results from this study cast some doubt on the widespread utility of the amphibian visual system as a model for the study of adaptation of the scotopic system and suggests that the teleost eye may be a more appropriate model for the study of adaptation of the vertebrate visual system.

Literature cited

Adelson, E.H. (1982). Saturation and adaptation in the rod system. Vision Research, 22:1299-1312.

Ahlbert, I.-B. (1969). The organization of the cone cells in the retinae of four teleosts with different feeding habits (*Perca fluvialis* L., *Lucioperca lucioperca* L., *Acerina cernua* L., *Coregonus albula* L.). Arkives fur Zoologie 22:445-481.

Ahlbert, I.-B. (1976). Organization of the cone cells in the retinae of salmon (*Salmo salar*) and trout (*Salmo trutta trutta*) in relation to their feeding habits. Acta Zoologica (Stockh), 57:13-35.

Ali, M.A. and Anctil, M. (1976). The Retinas of Fishes: An atlas. Berlin: Springer.

Ali, M.A. and Klyne, M.A. (1985). Vision in Vertebrates. New York: Plenum Press, 272p.

Allen, D.M., McFarland, W.N., Munz, F.W. and Poston, H.A. (1973). Changes in the visual pigments of trout. Canadian Journal of Zoology, 51:901-914.

Archer, S. and Lythgoe, J.N. (1990). The visual pigment basis for cone polymorphisms in the guppy, *Poecilia reticulata*. Vision Research, 30:225-233.

Archer, S., Hope, A. and Partridge, J.C. (1995). The molecular basis for the green-blue sensitivity shift in the rod visual pigments of the European eel. Proceedings of the Royal Society of London Series B-Biological Sciences, 262:289-295.

Arden, G.B. and Ikeda, H. (1968). The minimum latency of the a-wave. Journal of Physiology, 197:529-549.

Arnold, K. and Neumeyer, C. (1987). Wavelength discrimination in the turtle *Pseudemys scripta elegans*. Vision Research, 27:1501-1511.

Avery, J.A., Bowmaker, J.K., Djamgoz, M.B.A. and Downing, J.E.G. (1982). Ultra-violet sensitive receptors in a freshwater fish. Journal of Physiology, 334:23.

Barlow, H.B., Fitzhugh, R. and Kuffler, S.W. (1957). Changes of organization in the receptive fields of the cat's retina during dark adaptation. Journal of Physiology, 137:338-354.

Barthel, L.K. and Raymond, P.A. (1990). Improved method for obtaining 3-μm cryosections for immunocytochemistry. Journal of Histochemistry and Cytochemistry, 38:1383-1388.

Bathelt, V.D. (1970). Experimentelle und vergleichend morphologische untersuchungen am visuellen system von teleostiern. Zoologische Jahrber Abt Anatomische Ontogenie Tiere 87:402-470.

Baylor, D.A. and Hodgkin, A.L (1973). Detection and resolution of visual stimuli by turtle photoreceptors. Journal of Physiology, 234:163-198.

Baylor, D.A. and Hodgkin, A.L. (1974). Changes in time scale and sensitivity in turtle photoreceptors. Journal of Physiology, 242:729-758.

Baylor, D.A. and Nunn, B.J. (1986). Electrical properties of the light-sensitive conductance of rods of the salamander *Ambystoma tigrinum*. Journal of Physiology, 371:115-145.

Baylor, D.A., Lamb, T.D. and Yau, K.-W. (1979). The membrane current of single rod outer segments. Journal of Physiology, 288:589-611.

Beatty, D.D. (1975). Visual pigments of the American eel *Anguilla rostrata*. Vision Research, 15:771-776.

Beatty, D.D. (1984). Visual pigments and the labile scotopic visual system of fish. Vision Research, 24:1563-1573.

Beauchamp, R.D. and Daw, N.W. (1972). Rod and cone input to single goldfish optic nerve fibers. Vision Research, 12:1201-1212.

Beauchamp, R.D. and Lovasik, J.V. (1973). Blue mechanism response of single goldfish optic fibers. Journal of Neurophysiology, 36:925-939.

Beaudet, L. (1995). Labelling of the neuronal tracts associated with the torus semicircularis of the midbrain in rainbow trout. Society for Neuroscience Abstracts, 21:690.

Beaudet, L. and Hawryshyn, C.W. (accepted). Ecological aspects of vertebrate visual ontogeny. In S.N. Archer, M.B.A. Djamgoz, E. Loew, J.C. Partridge and S. Vallerga (eds.): Adaptive Mechanisms in the Ecology of Vision, London: Chapman and Hall.

Beaudet, L., Novales Flamarique, I. and Hawryshyn, C.W. (in press). Cone photoreceptor topography in the retina of sexually mature Pacific salmonid fishes. Journal of Comparative Neurology.

Beaudet, L., Browman, H.I and Hawryshyn, C.W. (1993). Optic nerve response and retinal structure in rainbow trout of different sizes. Vision Research, 33:1739-1746.

Bennett, A.T.D. and Cuthill, I.C. (1994). Ultraviolet vision in birds: What is its function. Vision Research, 34:1471-1478.

Bennett, A.T.D., Cuthill, I.C., Partridge, J.C. and Maier, E.J. (1996). Ultraviolet vision and mate choice in zebra finches. Nature, 380:433-435.

Bernard, G.D. (1987). Spectral characterization of butterfly L-receptors using extended Dartnall/MacNichol template functions. Journal of the Optical Society of America A, Series 2, 4:123.

Blaxter J.H.S. (1968). Light intensity, vision and feeding in young plaice. Journal of Experimental Marine Biology and Ecology, 2:293-307.

Boehlert, G.W. (1979). Retinal development in postlarval through juvenile *Sebastes diploproa* adaptions to a changing photic environment. Revue de Canadiene de Biologie, 38:265-280.

Bowmaker, J.K. and Kunz, Y.W. (1987). Ultraviolet receptors, tetrachromatic vision and retinal mosaics in the brown trout (Salmo trutta): age-dependent changes. Vision Research, 27:2101-2108.

Bowmaker, J.K. (1990) Visual pigments of fishes. In R.H. Douglas and M.B.A. Djamgoz (eds): The Visual System of Fish. London: Chapman and Hall, pp. 81-108.

Bowmaker, J.K., Thorpe, A. and Douglas, R.H. (1991). Ultraviolet-sensitive cones in the goldfish. Vision Research, 30:349-352.

Brainard, G.C., Barker, F.M., Hoffman, R.J., Stetson, M.H., Hanifin, J.P., Podolin, P.L. and Rollag, M.D. (1994). Ultraviolet regulation of neuroendocrine and circadian physiology in rodents. Vision Research, 34:1521-1522.

Braisted, J.E., Essman, T.F. and Raymond, P.A. (1994). Selective regeneration of photoreceptors in goldfish retina. Development, 120:2409-2419.

Brindley, G.S., du Croz, J.J. and Rushton, W.A.H. (1966). The flicker fusion frequency of the blue-sensitive mechanism of colour vision. Journal of Physiology, 183:497-500.

Browman H.I. and Hawryshyn, C.W. (1992). Thyroxine induces a precocial loss of ultraviolet photosensitivity in rainbow trout (*Oncorhynchus mykiss*, Teleostei). Vision Research, 32:2303-2312.

Browman, H.I., and Hawryshyn, C.W. (1994). The developmental trajectory of ultraviolet photosensitivity in rainbow trout is altered by thyroxine. Vision Research, 34:1397-1406.

Browman, H.I., Novales Flamarique, I. and Hawryshyn, C.W. (1994). Ultraviolet photoreception contributes to the foraging performance of two species of zooplanktivorous fishes. Journal of Experimental Biology, 186:187-198.

Browman, H.I., Gordon, W.C., Evans, B.I. and O'Brien, W.J. (1990). Correlation between histological and behavioral measures of visual acuity in a zooplanktivorous fish, the white crappie (*Pomoxis annularis*). Brain, Behavior and Evolution, 35:85-97.

Burgner, R.L. (1991). Life history of the sockeye salmon (*Oncorhynchus nerka*). In C Groot and L. Margolis (eds.): Pacific Salmon Life Histories, Vancouver: UBC Press, pp.1-117.

Butler, A.B. and Saidel, W.M. (1993). Retinal projections in teleost fishes: patterns, variations, and questions. Comparative Biochemistry and Physiology A, 104:431-442.

Butler, A.B., Wullimann, M.F. and Northcutt, R.G. (1991). Comparative cytoarchitectonic analysis of some visual pretectal nuclei in teleosts. Brain, Behavior and Evolution, 38:92-114.

Cameron, D.A. (1995). Asymmetric retinal growth in the adult teleost green sunfish (*Lepomis cyanellus*). Visual Neuroscience, 12:95-102.

Cameron, D.A., and Pugh, Jr., E.N. (1991). Double cones as a basis for a new type of polarization vision in vertebrates. Nature, 353:161-164.

Cameron, D.A., and Easter, Jr., S.S. (1993). The cone photoreceptor mosaic of the green sunfish, *Lepomis cyanellus*. Visual Neuroscience, 10:375-384.

Champalbert, G., Macquart-Moulin, C., Patriti, G. and Chiki, D. (1991). Ontogenic variations in the phototaxis of larval and juvenile sole *Solea solea* L. Journal of Experimental Marine Biology and Ecology, 149:207-225.

Chen, D.-M. and Goldsmith, T.H. (1986). Four spectral classes of cones in the retinas of birds. Journal of Comparative Physiology A, 159:473-479.

Cobbs, W.H. and Pugh, E.N. (1987). Kinetics and components of the flash photocurrent of isolated retinal rods of the larval salamander, *Ambystoma tigrinum*. Journal of Physiology, 394:529-572.

Collin, S.P. (1987). Retinal topography in reef teleosts. Ph.D. dissertation, University of Queensland, St. Lucia, Australia.

Collin, S.P., and Pettigrew, J.D. (1988a). Retinal topography in reef teleosts. I. Some species with well-developed areae but poorly-developed streaks. Brain, Behavior and Evolution, 30:269-282.

Collin, S.P., and Pettigrew, J.D. (1988b). Retinal topography in reef teleosts. II. Some species with prominent horizontal streaks and high-density areae. Brain, Behavior and Evolution, 30:283-295.

Collin, S.P., and Ali, M.A. (1994). Multiple areas of acute vision in two freshwater teleosts, the creek chub, *Semotilus atromaculatus* (Mitchill) and the cutlips minnow, *Exoglossum maxillingua* (Lesueur). Canadian Journal of Zoology, 72:721-730.

Cone, R.A. (1964). The rat electroretinogram. I. Contrasting effects of adaptation on the amplitude and latency of the b-wave. Journal of General Physiology, 47:1089-1105.

Cone, R.A. (1973). The internal transmitter model for visual excitation: some quantitative implications. In H. Langer (ed): Biochemistry and Physiology of Visual Pigments, New York: Springer-Verlag, pp. 275-282.

Copenhagen, D.R. and Green, D.G. (1987). Spatial spread of adaptation within the cone network of turtle retina. Journal of Physiology, 393:763-776.

Corujo, A. and Anadón, R. (1990). The development of the diencephalon of the rainbow trout (*Salmo gairdneri* Richardson). Thalamus and hypothalamus. Journal Hirnforschung, 30:669-680.

Coughlin, D.J. and Hawryshyn, C.W. (1994a). The contribution of ultraviolet and short-wavelength sensitive cone mechanisms to color vision in rainbow trout. Brain, Behavior and Evolution, 43:219-232.

Coughlin, D.J. and Hawryshyn, C.W. (1994b). Ultraviolet sensitivity in the torus semicircularis of juvenile trout (*Oncorhynchus mykiss*). Vision Research, 34:1407-1413.

Cresticelli, F. (1958). The natural history of photopigments,. In Newburgh (ed): Photobiology, Corvallis: Colloquium, Oregon State College, pp.30-51.

Cresticelli, F. (1972). The visual cells and visual pigments of the vertebrate eye. In H.J.A. Dartnall (ed): Textbook of Sensory Physiology, Berlin: Springer-Verlag, pp. 246-363.

Cresticelli, F. (1990). The natural history of visual pigments: 1990. Progress in Retinal Research, 11:2-30.

Crognale, M. and Jacobs, G.A. (1988). Temporal properties of the short-wavelength cone mechanism: a comparison of receptor and postreceptor signals in the ground squirrel. Vision Research, 28:1077-1082.

Cronin, T.W., Marshall, N.J., Quinn, C.A. and King, C.A. (1994). Ultraviolet photoreception in mantis shrimp. Vision Research, 34:1443-1452.

Daly, S.J. and Normann, R.A. (1985). Temporal information processing in cones: effects of light adaptation on temporal summation and modulation. Vision Research, 25:1197-1206.

Dartnall, H.J.A., Lander, M.R and Munz, F.W. (1961). Periodic changes in the visual pigment of a fish. In B Christiansen and B. Buchmann (eds): Progress in Photobiology, Amsterdam: Elsevier, pp.203-213.

Daw, N.W. (1968). Colour-coded ganglion cells in the goldfish retina: extension of their receptive fields by means of new stimuli. Journal of Physiology, 197:567-592.

De Marco, P.J. and Powers, M.K. (1991). Spectral sensitivity of ON and OFF responses from the optic nerve of goldfish. Visual Neuroscience, 6:207-217.

De Marco, P.J. and Powers, M.K. (1993). APB alters photopic spectral sensitivity of the goldfish retina. Vision Research, 34:1-9.

De Miguel, E., Rodicio, M.C. and Anadón, R. (1990). Organization of the visual system in larval lampreys: An HRP study. Journal of Comparative Neurology, 302:529-542.

De Monasterio, F.M. and Gouras, P. (1975). Functional properties of ganglion cells of the rhesus monkey retina. Journal of Physiology, 251:167-195.

De Monasterio, F.M., Gouras, P. and Tolhurst, D.J. (1975). Trichromatic colour opponency in ganglion cells of the rhesus monkey retina. Journal of Physiology, 251:197-216.

de Wolf, F.A., Schellart, N.A.M. and Hoogland, P.V. (1983). Octavolateral projections to the torus semicircularis in the trout, Salmo gairdneri. Neuroscience Letters, 38:209-213.

Deutschlander, M.E. and Phillips, J.B. (1995). Characterization of an ultraviolet photoreception mechanism in the retina of an amphibian, the axolotl (*Ambystoma mexicanum*). Neuroscience Letters, 197:93-96.

Donner, K. (1981a). Receptive fields of frog retinal ganglion cells: response formation and light-dark-adaptation. Journal of Physiology, 319:131-142.

Donner, K. (1981b). How the latencies of excitation and inhibition determine ganglion cell thresholds and discharge patterns in the frog. Vision Research, 21:1689-1692.

Donner, K., Koskelainen, A., Djupsund, K. and Hemilä, S. (1995). Changes in retinal time scale under background light: observations on rods and ganglion cells in the frog retina. Vision Research, 35:2255-2266.

Douglas, R.H. (1982a). An endogenous crepuscular rhythm of rainbow trout (*Salmo gairdneri*) photomechanical movements. Journal of Experimental Biology, 96:377-388.

Douglas, R.H. (1982b). The function of photomechanical movements in the retina of the rainbow trout (*Salmo gairdneri*). Journal of Experimental Biology, 96:389-403.

Douglas, R.H. (1986). Photopic spectral sensitivity of a teleost fish, the roach (Rutilus rutilus), with special reference to its ultraviolet sensitivity. Journal of Comparative Physiology A, 159:415-421.

Douglas, R.H., Partridge, J.C. and Hope, A.J. (1995). Visual and lenticular pigments in the eyes of demersal deep-sea fishes. Journal of Comparative Physiology A, 177:111-122.

Downing, J.E.G., Djamgoz, M.B.A. and Bowmaker, J.K. (1986). Photoreceptors of a cyprinid fish, the roach: morphological and spectral characteristics. Journal of Comparative Physiology A, 159:859-868.

Dunlop, S.A. and Beazley, L.D. (1987). Cell death in the developing retinal ganglion cell layer of the wallaby *Serotonix brachyurus*. Journal of Comparative Neurology, 264:14-23.

Dunlop, S.A. and Beazley, L.D. (1981). Changing retinal ganglion cell distribution in the frog *Heleiloporus eyrei*. Journal of Comparative Neurology, 202:221-236.

Dunlop, S.A. and Beazley, L.D. (1984). A morphometric study of the retinal ganglion cell layer and optic nerve from metamorphosis in *Xenopus laevis*. Vision Research, 24:417-427.

Ebbesson, S.O.E., Bazer, G.T., Reynolds, J.B. and Bailey, R.P. (1988). Retinal projections in sockeye salmon smolts (*Oncorhynchus nerka*). Cell and Tissue Research, 252:215-218.

Echteler, S.M. (1984). Connections of the auditory midbrain in a teleost fish, *Cyprinus carpio*. Journal of Comparative Neurology, 230:536-551.

Echteler, S.M. (1985a). Tonotopic organization in the midbrain of a teleost fish. Brain Research, 338:387-391.

Echteler, S.M. (1985b). Organization of the central auditory pathways in a teleost fish, *Cyprinius carpio*. Journal of Comparative Physiology A, 156:267-280.

Emmerton, J., and Delius, J.D. (1980). Wavelength discrimination in the "visible" and ultraviolet spectrum by pigeons. Journal of Comparative Physiology A, 141:47-52.

Engström, K. (1960). Cone types and cone arrangement in the retinae of some cyprinids. Acta Zoologica (Stockh), 41:277-295.

Engström, K. (1963a). Cone types and cone arrangements in teleost retinae. Acta Zoologica (Stockh), 44:179-243.

Engström, K. (1963b) Structure, organization and ultrastructure of the visual cells in the teleost family *Labridae*. Acta Zoologica (Stockh), 44:1-41.

Enoch, J.M. (1972). The two-color threshold technique of Stiles and derived color mechanisms. In D. Jameson and M. Hurvich (eds): Handbook of Sensory Physiology, VII, 4,Berlin: Springer-Verlag, pp. 537-567.

Evans B.I., and Fernald, R.D. (1990). Metamorphosis and fish vision. Journal of Neurobiology, 21:1037-1052.

Evans, B.I. and Fernald, R.D. (1993). Retinal transformation at metamorphosis in the winter flounder (*Pseudopleuronectes americanus*). Visual Neuroscience, 10:1055-64.

Evans, B.I., Hárosi, F.I. and Fernald, R.D. (1993). Photoreceptor spectral absorbance in larval and adult winter flounder (*Pseudopleuronectes americanus*). Visual Neuroscience, 10:1065-1071.

Fain, G.L. (1976). Sensitivity of toad rods: dependence on wave-length and background illumination. Journal of Physiology, 261:71-101.

Fain, G.L., Matthews, H.R. and Cornwall, M.C. (1996). Dark adaptation in vertebrate photoreceptors. Trends in Neurosciences, 19:502-507.

Fein, A. and Szuts, E.Z. (1982). Photoreceptors: Their Role in Vision. IUPAB Biophysics series, Cambridge: Cambridge University Press, pp. 212.

Fernald, R.D. (1990). The optical system of fishes. In R.H. Douglas and M.B.A. Djamgoz (eds): The Visual System of Fish, London: Chapman and Hall, pp.81-107.

Fernald, R.D., and Hirata, (1977). Field study of *Haplochromis burtoni*: habitats and co-habitants. Environmental Biology of Fishes, 2:299-308.

Fesenko, E.E., Kolesnikov, S.S. and Lyubarski, A.L. (1985). Induction by cyclic GMP of cationic conductance in plasma membrane of retinal rod outer segment. Nature, 313:310-313.

Fleishman, L.J., Loew, EL and Leal, M. (1993). UV vision in lizards. Nature, 365:397.

Frank, B.D. and Hollyfield, J.G. (1987). Retina of the tadpole and frog: Delayed dendritic development in a subpopulation of ganglion cells coincident with metamorphosis. Journal of Comparative Neurology, 266:435-444.

Fritzsch, B. and Wilm, C. (1990). Dextran amines in neuronal tracing. Trends in Neurosciences, 13:14.

Frumkes, T.E. (1990). Classical and modern psychophysical studies of dark and light adaptation and their relationship to underlying retinal function. In K.N. Leibovic (ed): Science of Vision, New York: Springer-Verlag, 487p.

Frumkes, T.E. and Eysteinsson, T. (1987). Suppressive rod-cone interaction in distal vertebrate retina: intracellular records from *Xenopus* and *Necturus*. Journal of Neurophysiology, 57:1361-1382.

Frumkes, T.E. and Miller, R.F. (1979). Pathways and polarities of synaptic interactions in the inner retina of the mud puppy: II. Insight revealed by an analysis of latency and threshold. Brain Research, 161:13-24.

Goldsmith, T. H. (1994). Ultraviolet receptors and color vision: Evolutionary implications and a dissonance of paradigms. Vision Research, 34:1479-1487.

Goldsmith, T.H. (1980). Hummingbirds can see near ultraviolet light. Science, 207:786-788.

Gouras, P. and Zrenner, E. (1979). Enchancement of luminance flicker by color-opponent mechanisms. Science, 205:587-589.

Gouras, P. and Zrenner, E. (1981). Color coding in primate retina. Vision Research, 21:1591-1598.

Govardovskii, V.I. and Lychakov, D.V. (1984). Visual cells and visual pigments of the lamprey, *Lampetra fluvialis*. Journal of Comparative Physiology A, 154:279-286.

Granda, A.M. and Sisson, D.F. (1989). Psychophysically derived visual mechanisms in turtle. I--Spectral properties. Vision Research, 29:93-105.

Gruberg, E.R., Hughes, T.E. and Karten, H.J. (1994). Synaptic interrelationships between the optic tectum and the ipsilateral nucleus isthmi in *Rana pipiens*. Journal of Comparative Neurology, 339:353-364.

Guenther, E. and Zrenner, E. (1993). The spectral sensitivity of dark- and light-adapted cat retinal ganglion cells. Journal of Neurophysiology, 13:1543-1550.

Hárosi ,F.I. and Hashimoto, Y. (1983). Ultraviolet visual pigment in a Vertebrate: a tetrachromatic cone system in the Dace. Science, 222:1021-1023.

Hárosi, F.I. and Fukurotani, K. (1986). Correlation between cone absorbance and horizontal cell response from 300 to 700 nm in fish. Investigative Ophthalmology and Visual Science (Suppl.), 27:192.

Hárosi, F.I. (1994). An analysis of two spectral properties of vertebrate visual pigments. Vision Research, 34:1359-1367.

Harosi, F.I. and Kleinschmidt, J. (1993). Visual pigments in the sea lamprey, *Petromizon marinus*. Visual Neuroscience, 10:711-715.

Hashimoto, Y., Harosi, F.I., Ueki, K. and Fukurotani, K.-K. (1988). Ultra-violet-sensitive cone in the color-coding systems of cyprinid retinas. Neuroscience Research (Suppl.), 8:S81-S95.

Hassin, G. and Witkovsky, P. (1983). Intracellular recording from identified photoreceptors and horizontal cells of the *Xenopus* retina. Vision Research, 23:921-931.

Hawryshyn, C.W. and Beauchamp, R.D. (1985). Ultraviolet photosensitivity in goldfish: an independent UV retinal mechanism. Vision Research, 25:11-20.

Hawryshyn, C.W. and Harosi, F.I. (1991). Ultraviolet photoreception in carp: Microspectrophotometry and behaviorally determined action spectra. Vision Research, 30:567-576.

Hawryshyn, C.W. (1991). Light-adaptation properties of the ultraviolet-sensitive cone mechanism in comparison to the other receptor mechanisms in goldfish. Visual Neuroscience, 6:293-301.

Hawryshyn, C.W. (1991). Spatial summation of cone mechanisms in goldfish. Vision Research, 30:563-566.

Hawryshyn, C.W. and Hárosi, F.I. (1994). Spectral characteristics of visual pigments in rainbow trout (*Oncorhynchus mykiss*). Vision Research, 34:1393-1396.

Hawryshyn, C.W., Arnold, M.G., Bowering, E. and Cole, R.L. (1990). Spatial orientation of rainbow trout to plane-polarized light: the ontogeny of E-vector discrimination and spectral sensitivity characteristics. Journal of Comparative Physiology A, 166:565-574.

Hawryshyn, C.W., Arnold, M.G., Chiasson, D.J. and Martin, P.C. (1989). The ontogeny of ultraviolet photosensitivity in rainbow trout. (*Salmo gairdneri*). Visual Neuroscience, 2,:247-254.

Hawryshyn, C.W., Beaudet, L. and Browman, H.I. (1991). Spectral sensitivity of optic nerve ON and OFF responses in two teleost fishes. Society for Neuroscience Abstracts, 17:1376.

Healey, M.C. (1991). Life history of chinook salmon (*Oncorhynchus tshawytscha*). In C Groot and L. Margolis (eds): Pacific Salmon Life Histories, Vancouver: UBC Press, pp.311-394.

Henderson, M.A. and Northcote, T.G. (1988). Retinal structure of sympatric and allopatric populations of cutthroat trout (*Salmo clarki clarki*) and Dolly Varden char (*Salvelinus malma*) in relation to their spatial distribution. Canadian Journal of Fisheries and Aquatic Sciences, 45:1321-1326.

Hoar, W.S. (1988). The physiology of smolting salmonids. Fish Physiology XIB:275-3443.

Holmqvist, B.I, Östholm, T. and Ekström P. (1992). DiI tracing in combination with immunocytochemistry for analysis of connectivities and chemoarchitectonics of specific neural systems in a teleost, the Atlantic salmon. Journal of Neuroscience Methods, 42:45-63.

Hood, D.C. and Birch, D.G. (1993). Light adaptation of human rod photoreceptors: the leading edge of the human a-wave and models for rod receptor activity. Vision Research, 33:1605-1618.

Hoskins, S.G. (1990). Metamorphosis of the amphibian eye. Journal of Neurobiology, 21:970-989.

Huck, S.W., Cormier, W.H. and Bounds, W.G., Jr. (1974). Reading Statistics and Research. New York: Harper Collins, 387p.

Ito, H., Sakamoto, N. and Takatsuji, K. (1982). Cytoarchitecture, fiber connections, and ultrastructure of nucleus isthmi in a teleost (*Navodon modestus*) with a special reference to degenerating isthmic afferents from the optic tectum and nucleus pretectalis. Journal of Comparative Neurology, 205:299-311.

Jacobs, G.H. and Deegan, J.F. II (1994). Sensitivity to ultraviolet light in the gerbil (*Meriones unguiculatus*): characteristics and mechanisms. Vision Research, 34:1433-1441.

Jacobs, G.H., Neitz, J. and Deegan, J.F. II (1991). Retinal receptors in rodents maximally sensitive to ultraviolet light. Nature, 353:655-666.

Just, J.J., Kraus-Just, J. and Check, D.A. (1981). Survey of chordate metamorphosis. In L.I. Gilbert and E. Frieden (eds): Metamorphosis, New York: Plenum Press, pp.265-326.

Kaltenbach, J.C. (1953). Local action of thyroxin on amphibian metamorphosis. II. Development of the eyelids, nictitating membrane, cornea, and extrinsic ocular muscles in *Rana pipiens* larvae effected by thyroxin-cholesterol implants. Journal of Experimental Zoology, 122:41-50.

Kelley, M.W., Turner, J.K. and Reh, T.A. (1995). Ligands of steroid/thyroid receptors induce cone photoreceptors in vertebrate retina. Development, 121:3777-3785.

Kelly, D.H. (1974). Spatio-temporal frequency characteristics of color-vision mechanisms. Journal of the Optical Society of America, 64:983-990.

Kennedy, M C. and Rubinson, K. (1977). Retinal projections in larval, transforming and adult sea lamprey, *Petromyzon marinus*. Journal of Comparative Neurology, 171:465-480.

Koch, K.-W. (1992). Biochemical mechanism of light adaptation in vertebrate photoreceptors. Trends in Biochemical Sciences, 17:307-311.

Koutalos, Y. and Yau, K.-W. (1996). Regulation of sensitivity in vertebrate rod photoreceptors by calcium. Trends in Neurosciences, 19:73-81.

Kunz, Y.W. (1987). Tracts of putative ultraviolet receptors in the retina of the two-year-old brown trout (*Salmo trutta*) and the Atlantic salmon (*Salmo salar*). Experientia, 43:2102-1204.

Kunz, Y.W., Wildenburg, G., Goodrich, L. and Callaghan, E. (1994). The fate of the ultraviolet receptors in the retina of the Atlantic salmon (*Salmo salar*). Vision Research, 34:1375-1383.

Kurz-Isler, G. and Wolburg, H. (1982). Morphological study on the regeneration of the retina in the rainbow trout after ouabain-induced damage: evidence of dedifferentiation of photoreceptor cells. Cell and Tissue Research, 225:165-178.

Kusmic, C., Barsanti, L., Passarelli, V. and Gualtieri, P. (1993). Photoreceptor morphology and visual pigment content in the pineal organ and in the retina of juvenile and adult trout, *Salmo irideus*. Micron, 24:279-286.

Kusmic, C., Marchiafava, P.L. and Strettoi, E. (1992). Photoresponses and light adaptation of pineal photoreceptors in the trout. Proceedings of the Royal Society of London Series B, 248:149-157.

Lamb, T.D. (1981). The involvement of rod photoreceptors in dark adaptation. Vision Research, 21:1773-1782.

Lamb, T.D. and Matthews, H.R. (1988). External and internal actions in the response of salamander rods to altered external calcium concentrations. Journal of Physiology, 403:473-494.

Lasater, E.M. (1990). Neurotransmitters and neuromodulators of the fish retina. . In R. H. Douglas and M.B.A. Djamgoz (eds): The Visual System of Fish, London: Chapman and Hall, pp.211-238.

Laughlin, S.B. (1989). The role of sensory adaptation in the retina. Journal of Experimental Biology, 146:39-62.

Loew, E.R. (1994). A third, ultraviolet-sensitive, visual pigment in the tokay gecko (*Gekko gekko*). Vision Research, 34:1427-1431.

Loew, E.R. and McFarland, W.N. (1990). The underwater visual environment. In R. H. Douglas and M.B.A. Djamgoz (eds): The Visual System of Fish, London: Chapman and Hall, pp.1-43.

Loew, E.R. and Wahl, C.M. (1991). A short-wavelength sensitive cone mechanism in juvenile yellow perch, *Perca flavescens*. Vision Research, 30:353-360.

Loew, E.R., Govardovskii, V.I., Rohlich, P. and Szél, A. (1996). Microspectrophotometric and immunocytochemical identification of ultraviolet photoreceptors in geckos. Visual Neuroscience, 13:247-256.

Loew, E.R., McFarland, W.N., Mills, E.L. and Hunter D. (1993). A chromatic action spectrum for planktonic predation by juvenile yellow perch, *Perca flavescens*. Canadian Journal of Zoology, 71:384-386.

Logiudice, F.T., and Laird, R.J. (1994). Morphology and density distribution of cone photoreceptor in the retina of the Atlantic stingray, *Dasyatis sabina*. Journal of Morphology, 221:277-289.

Lolley, R.N. and Lee, R.H. (1990). Cyclic GMP and photoreceptor function. FASEB Journal, 4:3001-3008.

Lu, Z. and Fay, R.R. (1993). Acoustic response properties of single units in the torus semicircularis of the goldfish, *Carassius auratus*. Journal of Comparative Physiology A, 173:33-48.

Lyall, A.H. (1957a). The growth of the trout retina. Quarterly Journal of Microscopical Science, 98:101-110.

Lyall, A.H. (1957b). Cone arrangements in teleost retinae. Quarterly Journal of Microscopical Science, 98:189-201.

Lythgoe, J.N. (1968). Visual pigments and visual range underwater. Vision Research, 8:997-1012.

Lythgoe, J.N. (1979). The Ecology of Vision. Oxford: Clarendon Press.

Maier, E.J. (1994). Ultraviolet vision in a passeriform bird: from receptor spectral sensitivity to overall spectral sensitivity in *Leiothrix lutea*. Vision Research, 34:1415-1418.

Maier, E.J. and Bowmaker, J.K. (1993). Colour vision in the passeriform bird, *Leiothrix lutea*: correlation of visual pigment absorbance and oil droplet transmission with spectral sensitivity. Journal of Comparative Physiology A, 172:295-301.

Maier, W. and Wolburg, H. (1979). Regeneration of the goldfish retina after exposure to different doses of ouabain. Cell Tissue Research, 202:99-118.

Malchow, R.P. and Yazulla, S. (1988). Light adaptation of rod and cone luminosity horizontal cells of the retina of the goldfish. Brain Research, 443:222-230.

Malpeli, J.G. and Schiller, P.H. (1978). Lack of blue OFF-center cells in the visual system of the monkey. Brain Research, 141:385-386.

Mangel, S.C. and Dowling, J.E. (1987). The interplexiform-horizontal cell system in the fish retina: effects of dopamine, light stimulation and time in the dark. Proceedings of the Royal Society of London B, 231:91-121.

Mansour-Robaey, S. and Pinganaud, G. (1991). Développement du tractus optic chez la truite Salmo gairdneri Rich. Comptes Rendus de l'Académie des Sciences de Paris, tome 312, Série III:107-112.

Manteuffel, G. and Naujoks-Manteuffel, C. (1990). Anatomical connections and electrophysiological properties of toral dorsal tegmental neurons in the terrestrial urodele *Salamandra salamandra*. Journal of Himforschung, 30:65-76.

Marc, R.E., and Sperling, H.G. (1976). The chromatic organization of the goldfish retina. Vision Research, 16:1211-1224.

Markle, D.F., Harris, P.M. and Toole, C.L. (1992). Metamorphosis and an overview of early-life-history stages in Dover sole *Microstomus pacificus*. Fish Bulletin, 90:285-301.

Marks, L.E. and Bornstein, M.H. (1973). Spectral sensitivity by constant ccf: effect of chromatic adaptation. Journal of the Optical Society of America, 63:220-226.

Mathis, U., Schaeffel, F. and Howland, H.C. (1988). Visual optics in toads (*Bufo americanus*). Journal of Comparative Physiology A, 163:201-213.

Matthews, H.R. (1991). Incorporation of chelator into guinea-pig rods shows that calcium mediates mammalian photoreceptor light adaptation. Journal of Physiology, 436:93-105.

McDonald C.G. and Hawryshyn, C.W. (1995). Intraspecific variation of spectral sensitivity in threespine stickleback (*Gasterosteus aculeatus*) from different photic regimes. Journal of Comparative Physiology A, 176:255-260.

McDonald, C.G., Reimchen, T.E. and Hawryshyn, C.W. (1995). Nuptial color loss and signal masking: an analysis using video imaging. Behavior, 132:963-977.

McFarland, W.N. (1991). The visual world of coral reef fishes. In P.F. Sale (ed): The Ecology of Fishes on Coral Reefs, San Diego: Academic Press, pp.16-38.

McFarland, W.N. (1991). Light in the sea: the optical world of elasmobranchs. Journal of Experimental Zoology, Supplement 5:3-12.

McFarland, W.N. and Allen, D.M. (1977). The effect of extrinsic factors on two distinctive rhodopsin-porphyropsin systems. Canadian Journal of Zoology, 55:1000-1009.

McFarland, W.N. and Loew, E.R. (1994). Ultraviolet visual pigments in marine fishes of the family Pomacentridae. Vision Research, 34:1393-1396.

McFarland, W.N., and Muntz, F.W. (1975). Part III: the evolution of photopic visual pigments in fishes. Vision Research, 15:1071-1080.

McNaughton, P.A (1990). Light response of vertebrate photoreceptors. Physiological Reviews, 70:847-883.

Meek, H.J. (1990). Tectal morphology: connections, neurones and synapses. In R. H. Douglas and M.B.A. Djamgoz (eds): The Visual System of Fish, London. Chapman and Hall, pp.239-277.

Miller, J.L. and Korenbrot, J.I. (1993). Phototransduction and adaptation in rods, single cones, and twin cones of the striped bass retina: a comparative study. Visual Neuroscience, 10:653-667.

Moeller, J.F. and Case, J.F. (1995). Temporal adaptations in visual systems of deep-sea crustaceans. Marine Biology, 123:47-54.

Mollon, J.D. and Polden, P.G. (1979). Post-receptoral adaptation. Vision Research, 19:435-440.

Munk, O. (1990). Changes in the visual cell layer of the duplex retina during growth of the eye of a deep-sea teleost, *Gempylus serpens* Cuvier, 1829. Acta Zoologica, 71:89-95.

Muntz, W.A and Reuter, T. (1966). Visual pigments and spectral sensitivity in *Rana temporaria* and other European tadpoles. Vision Research, 6:601-618.

Muntz, W.A. and Mouat, G.S.V. (1984). Annual variations in the visual pigments of brown trout inhabiting lochs providing different light environments. Vision Research, 24:1575-1580.

Munz, F.W. and McFarland, W.N. (1975). Part I: Presumptive cone pigments extracted from tropical marine fishes. Vision Research, 15:1045-1062.

Naka, K.-I. and Rushton, W.A.H. (1967). The generation and spread of S-potentials in fish (*Cyprinidae*). Journal of Physiology, 192:437-461.

Nakamura, T., Thiele, G. and Meissl, H. (1986). Intracellular responses from the photosensitive pineal organ of the teleost, *Phoxinus phoxinus*. Journal of Comparative Physiology A, 159:325-330.

Nakatani, K. and Yau, K.-W. (1988). Calcium and light adaptation in retinal rods and cones. Nature, 334:69-71.

Nakatani, K., Tamura, T. and Yau, K.-W. (1991). Light adaptation in retinal rods of the rabbit and two other nonprimate mammals. Journal of General Physiology, 97:413-435.

Narayanan, K. and Khan, A.A. (1995). The visual cells of the corsula mullet. Journal of Fish Biology, 47:367-376.

Neave, D.A. (1984). The development of visual acuity in larval plaice (*Pleuronectes platessa* L.) and turbot (*Scophthalmus maximus* L.). Journal of Experimental Marine Biology and Ecology, 78:167-175.

Nederstigt, L.J.A. and Schellart, N.A.M. (1986). Acousticolateral processing in the torus semicircularis of the trout *Salmo gairdneri*. Pflugers Archives, 406:151-157.

Neumeyer, C. and Arnold, K. (1989). Tetrachromatic color vision in the becomes trichromatic under white adaptation light of moderate intensity. Vision Research, 29:1719-1727.

Neumeyer, C. (1984). On spectral sensitivity in the goldfish. Evidence for neural interactions between different "cone mechanisms". Vision Research, 24:1223-1231.

Neumeyer, C. (1985). An ultraviolet receptor as a fourth receptor type in goldfish color vision. Naturwissenschaften, 72:162-163.

Nguyen, V.S. and Straznicky, C. (1989). The development and the topographic organization of the retinal ganglion cell layer in *Bufo marinus*. Experimental Brain Research, 75:345-353.

Nicol, G.D. and Bownds, M.D. (1989). Calcium regulates some, but not all, aspects of light adaptation in rod photoreceptors. Journal of General Physiology, 94:233-259.

Nieuwenhuys, R. and Pouwels, E. (1983). The brain stem of actinopterygian fishes. In G.G. Northcutt and R.E. Davis (eds): Fish Neurobiology, Ann Arbor: University of Michigan Press, pp. 25-87.

Normann, R.A. and Perlman, I. (1979). The effects of background illumination on photoresponses of red and green cones. Journal of Physiology, 286:491-507.

Normann, R.A. and Werblin, F.S. (1974). Control of retinal sensitivity. I. Light and dark adaptation of vertebrate rods and cones. Journal of General Physiology, 63:37-61.

Northcote, T.G. (1969). Patterns and mechanisms in the lakeward migratory behaviour of juvenile trout. In T.G. Northcote (ed): Symposium on Salmon and Trout in Streams, Vancouver: University of British Columbia, pp.183-203.

Northcutt, R.G. and Wullimann, M.F. (1988). The visual system in teleost fishes: morphological patterns and trends. In J. Atema, R.R. Fay, A.N. Popper and W.N. Tavolga (eds): Sensory Biology of Aquatic Animals, New York: Springer-Verlag, pp.515-552.

Northmore, D.P.M. (1973). Spectral sensitivity of the rudd (*Scardinius erythrophthalmus*). Unpublished Ph.D. Thesis, University of Sussex.

Northmore, D.P.M. (1977). Spatial summation and light adaptation in the goldfish visual system. Nature, 268:450-451.

Novales Flamarique, I. (1997). Vertebrate detection of polarized light. Ph.D. Dissertation, Victoria: University of Victoria.

Novales Flamarique, I. and Hawryshyn, C.W. (1996). Retinal development and visual sensitivity of young Pacific sockeye salmon (*Oncorhynchus nerka*). Journal of Experimental Biology, 199:869-882.

Novales Flamarique, I. and Hawryshyn, C.W. (in press). Is the use of underwater polarized light by fish restricted to crepuscular time periods? Vision Research.

Novales Flamarique, I., Hendry, A. and Hawryshyn, C.W. (1992). The photic environment of a salmonid nursery lake. Journal of Experimental Biology, 169:121-141.

Novales Flamarique, I., Oldenbourg, R. and Hárosi, F.I. (1995). Transmission of polarized light through sunfish double cones reveals minute optical anisotropies. Biology Bulletin, 189:220-222.

Oakley, B. and Schafer, R. (1985). Experimental neurobiology: a laboratory manual. Ann Arbor: University of Michigan Press, p.367.

Ohman, P. (1976). Fine structure of photoreceptors and associated neurons in the retina of *Lampetra fluviatilis* (Cyclostomi). Vision Research, 16:659-662.

Olsen, B.T., Schneider, T. and Zrenner, E. (1986). Characteristics of rod driven OFF-responses in cat ganglion cells. Vision Research, 26:835-845.

Oppenheim, R.W. (1991). Cell death during development of the nervous system. Annual Review of Neuroscience, 14:453-501.

Palacios, A.G. and Varela, F.J. (1992). Color mixing in the pigeon (*Columba livia*) II: A psychophysical determination in the middle, short and near-UV wavelength range. Vision Research, 32:1947-1953.

Palacios, A.G., Goldsmith, T.H. and Bernard, G.D. (1996). Sensitivity of cones from a cyprinid fish (*Danio aequipinnatus*) to ultraviolet and visible light. Visual Neuroscience, 13:411-421.

Pankhurst, N.W. (1984). Retinal development in larval and juvenile European eel, *Anguilla anguilla* (L.). Canadian Journal of Zoology, 62:335-343.

Pankhurst, P.M., Pankhurst, N.W. and Montgomery, J.C. (1993). Comparison of behavioural and morphological measures of visual acuity during ontogeny in the teleost fish *Forsterygion varium*, Tripterygiidae (Forster, 1801). Brain, Behavior and Evolution, 42:178-188.

Parkyn, D.C., and Hawryshyn, C.W. (1994). Polarized light sensitivity in rainbow trout (Oncorhynchus mykiss): characterization from multiunit ganglion cell responses in the optic nerve fibres. Journal of Comparative Physiology A, 172: 493-500.

Parrish, J.W., Ptacek, J.A. and Will, K.L. (1984). The detection of near-ultraviolet light by nonmigratory and migratory birds. Auk, 101:53-58.

Peachey, N.S., Alexander, K.R., Derlacki, D.J. and Fishman, G.A. (1992). Light adaptation, rods and the human flicker ERG. Visual Neuroscience, 8:145-150.

Peachey, N.S., Alexander, K.R., Fishman, G.A. and Derlacki, D.J. (1989). Properties of the human cone system electroretinogram during light adaptation. Applied Optics, 28:1145-1150.

Perry, R.J. and McNaughton, P.A. (1991). Response properties of cones from the retina of the tiger salamander. Journal of Physiology, 433:561-587.

Pinganaud, G. and Clairambault, P. (1975). Sur l'architecture des voies optiques primaires de la truite (*Salmo irideus* Gibb.). Comptes Rendus de l'Académie des Sciences de Paris, Série D, tome 281:411-414.

Pinganaud, G. and Clairambault, P. (1979). The visual system of the trout *Salmo irideus* Gibb. A degeneration and radioautographic study. Journal Hirnforschung, 20:413-431.

Polansky, J.R. and Bennett, T.P. (1973). Alterations in physical parameters and proteins of lens from *Rana catesbeiana* during development. Developmental Biology, 33:380-408.

Pomeranz, B. (1972). Metamorphosis of frog vision: changes in ganglion cell physiology and anatomy. Experimental Neurology, 82:187-199.

Potter, I.C. (1980). Ecology of larval and metamorphosing lampreys. Canadian Journal of Fisheries and Aquatic Sciences, 37:1641-1657.

Powers, M.K. and Easter, S.S. Jr (1978). Absolute visual sensitivity of goldfish. Vision Research, 18:1137-1147.

Prasada Rao, P.D. and Sharma, S.C. (1982). Retinofugal pathways in juvenile and adult catfish, *Ictalurus (Ameiurus) punctatus*: an HRP and autoradiographic study. Journal of Comparative Neurology, 210:37-48.

Pugh, E.N. Jr. and Lamb, T.D. (1990). Cyclic GMP and calcium: the internal messengers of excitation and adaptation in vertebrate photoreceptors. Vision Research, 30:1923-1942.

Raymond, P.A. (1991a). Cell determination and positional cues in the teleost retina: development of photoreceptors and horizontal cells. In C. Shatz and D.M.K. Lam (eds): Development of the Visual System, Boston: M.I.T. Press, (Retina Research Foundation Symposium) vol. 3, pp.59-78.

Raymond, P.A. (1991b). Retinal regeneration in teleost fish. In E Rubel (ed): Regeneration of Vertebrate Sensory Cells, Chichester: Ciba Foundation Symposium, Vol. 160, pp.171-191.

Raymond, P.A., Reifler, M.J. and Rivlin, P.K. (1988). Regeneration of goldfish retina: Rod precursors are a likely source of regenerated cells. Journal of Neurobiology, 19(5):431-463.

Reuter, T. (1969). Visual pigments and ganglion cell activity in the retinae of tadpoles and adult frogs (*Rana Temporaria* L.). Acta Zoologica, 122:1-64.

Robson, J.G. and Frishman, L.J. (1995). Response linearity and kinetics of the cat retina: the bipolar cell component of the dark-adapted electroretinogram. Visual Neuroscience, 12:837-850.

Rowe, M.P., Engheta, N., Easter, Jr., S.S. and Pugh, Jr., E.N. (1994). Graded-index model of a fish double cone exhibits differential polarization sensitivity. Journal of the Optical Society of America A, 11:55-70.

Salo, E.O. (1991). Life history of chum salmon (*Oncorhynchus keta*). In C Groot and L. Margolis (eds): Pacific Salmon Life Histories, Vancouver: UBC Press, pp.231-310.

Schellart, N.A.M. (1990). The visual pathways and central non-tectal processing. . In R. H. Douglas and M.B.A. Djamgoz (eds): The Visual System of Fish,. London: Chapman and Hall, pp.345-372.

Schnapf, J.L., Nunn, B.J., Meister, M. and Baylor, D.A. (1990). Visual transduction in cones of the monkey *Macaca fascicularis*. Journal of Physiology, 427:681-713.

Schneider, T. and Zrenner, E. (1987). The variable interdependence of amplitude and implicit-time in PIII, b-wave and optic nerve responses of the cat. Experimental Eye Research, 45:655-664.

Schneider, T., Olsen, B.T. and Zrenner, E. (1986). Characteristics of the rod-cone transition in electroretinogram and optic nerve response. Clinical Vision Science, 1:81-91.

Schuurmans, R.P. and Zrenner, E. (1981). Responses of the blue sensitive cone system from the visual cortex and the arterially perfused eye in cat and monkey. Vision Research, 21:1611-1615.

Shand, J. (1993). Changes in the spectral absorption of cone visual pigments during the settlement of the goatfish *Upeneus tragula*: the loss of red sensitivity as a benthic existence begins. Journal of Comparative Physiology A, 173:115-121.

Shand, J. (1997). Ontogenetic changes in retinal structure and visual acuity: a comparative study of coral-reef teleosts with differing post-settlement lifestyles. Environmental Biology of Fishes,

Shand, J. (1993). Changes in the spectral absorption of cone visual pigments during the settlement of the goatfish *Upeneus tragula*: the loss of red sensitivity as a benthic existence begins. Journal of Comparative Physiology A, 173:115-121.

Shand, J. (1994). Changes in retinal structure during development and settlement of the goatfish *Upeneus tragula*. Brain, Behavior and Evolution, 43:51-60.

Shand, J., Partridge, J.C., Archer, S.N., Potts, G.W. and Lythgoe, J.N. (1988). Spectral absorbance changes in the violet/blue sensitive cones of the juvenile pollack, *Pollachius pollachius*. Journal of Comparative Physiology A, 163:699-703.

Shigematsu, Y., Yamada, M. and Fuwa, M. (1978). Latency measurement of the color coded S-potentials in the carp retina. Vision Research, 18:1435-1437.

Sivak, J.G. and Warburg, M.R. (1980). Optical metamorphosis of the eye of *Salamandra salamandra*. Canadian Journal of Zoology, 58:2059-2064.

Sivak, J.G. and Warburg, M.R. (1983). Changes in optical properties of the eye during metamorphosis of an anuran, *Pelobates syriacus*. Journal of Comparative Physiology A, 150:329-332.

Spekreijse, H. and Norton, A.L. (1970). The dynamic characteristics of color-coded S-potentials. Journal of General Physiology, 56:1-15.

Spekreijse, H., Wagner, H.G. and Wolbarsht, M.L. (1972). Spectral and spatial coding of ganglion cell responses in goldfish retina. Journal of Neurophysiology, 35:73-86.

Stell, W.K., and Hárosi, F.I. (1976). Cone structure and visual pigment content in the retina of the goldfish. Vision Research, 16:647-657.

Stenkamp, D.L., Hisatomi, O., Barthel, L.K., Tokunaga, F. and Raymond, P.A. (1996). Temporal expression of rod and cone opsins in embryonic goldfish retina predicts the spatial organization of the cone mosaic. Investigative Ophthalmology in Visual Science, 37:363-376.

Stone, J. (1973). Sampling properties of microelectrodes assessed in the cat's retina. Journal of Neurophysiology, 36:1071-1079.

Straznicky, K. and Gaze, R.M. (1971). The growth of the retina in *Xenopus laevis*: an autoradiographic study. Journal of Embryology and Experimental Morphology, 26:67-79.

Studnicka, F.K. (1912). Ueber die Entwicklung und die Bedeutung der Seitenaugen von Ammocoetes. Anatomischer Anzeiger, 41:561-578.

Szél, A., and Röhlich. P. (1992). Two cone types of rat retina detected by anti-visual pigment antibodies. Experimental Eye Research, 55:47-52.

Tauchi, M., Yang, X.-L. and Kaneko, A. (1984). Depolarizing responses of L-type external horizontal cells in the goldfish retina under intense chromatic background. Vision Research, 24:867-870.

Tovée, M.J., Bowmaker, J.K. and Mollon, J.D. (1992). The relationship between cone pigments and behavioural sensitivity in a new world monkey (*Callithrix jacchus jacchus*). Vision Research, 32:867-878.

Towe, A.L. and Harding, G.W. (1970). Extracellular microelectrode sampling bias. Experimental Neurology, 29:366-381.

Uchida, K. and Morita, Y. (1990). Intracellular responses from UV-sensitive cells in the photosensory pineal organ. Brain Research, 534:237-242.

Valberg, A., Lee, B.B. and Tigwell, D.A. (1986). Neurones with strong inhibitory S-cone inputs in the macaque lateral geniculate nucleus. Vision Research, 26:1061-1064.

van der Meer, H.J. (1992). Constructional morphology of photoreceptor patterns in percomorph fish. Acta Biotheoretica, 40:51-85.

van der Meer, H.J., and Anker, G.Ch. (1984). Retinal resolving power and sensitivity of the photopic system in seven haplochromine species (Teleostei, Cichlidae). Netherlands Journal of Zoology, 34:197-209.

van der Meer, H.J., and Bowmaker, J.K. (1995). Interspecific variation of photoreceptors in four co-existing haplochromine cichlid fishes. Brain, Behavior and Evolution, 45:232-240.

Vanegas, H. (1974). Basic relationships for visual information processing in optic tectum of fish. Acta Cientifica Venezolana, 25:98-106.

Villa, P., Bedmar, M.D. and Baron, M. (1991). Studies on rod horizontal cell S-potential in dependence of the dark/light adapted state: a comparative study in *Cyprinus carpio* and *Scyliorhinus canicula* retinas. Vision Research, 30:425-435.

Vlitala, J., Korpimaki, E., Palokangas, P. and Kolvula, M. (1995). . Nature, 373:425-427.

Vos Hzn, J.J., Coemans, M.A.J.M. and Nuboer, J.F.W. (1994). The photopic sensitivity of the yellow field of the pigeon's retina to ultraviolet light. Vision Research, 34:1419-1425.

Wagner, H.J (1990). Retinal structure of fishes. In R.H. Douglas and M.B.A. Djamgoz (eds): The Visual System of Fish, London: Chapman and Hall, pp.109-157.

Wald, G. (1945). The chemical evolution of vision. Harvey Lectures, 41:117-160.

Werblin, F.S. (1974). Control of retinal sensitivity. II. Lateral interactions at the outer plexiform layer. Journal of General Physiology, 63:62-87.

Werblin, F.S. and Copenhagen, D.R. (1974). Control of retinal sensitivity. III. Lateral interactions at the inner plexiform layer. Journal of Physiology, 63:88-110.

Wheeler, T.G. (1979). Retinal ON and OFF responses convey different chromatic information to the CNS. Brain Research, 160:145-149.

Wheeler, T.G. (1979). Retinal red sensitivity under dark adapted conditions. Brain Research, 175:140-144.

Whitmore, A.V. and Bowmaker, J.K. (1995). Differences in the temporal properties of human longwave- and middlewave-sensitive cones. European Journal of Neuroscience, 7:1420-1423.

Wikler, K.C., Williams, R.W., and Rakic, P. (1990). Photoreceptor mosaic: number and distribution of rods and cones in the rhesus monkey retina. Journal of Comparative Neurology, 297:499-508.

Wild, J.M. (1995). Convergence of somatosensory and auditory projections in the avian torus semicircularis, including the central auditory nucleus. Journal of Comparative Neurology, 358:465-486.

Williamson, M., and Keast, A. (1988). Retinal structure relative to feeding in the rock bass (*Ambloplites rupestris*) and bluegill (*Lepomis macrochirus*). Canadian Journal of Zoology, 66:2840-2846.

Wilt, F.H. (1959). The differentiation of visual pigments in metamorphosing larvae of *Rana catesbeiana*. Developmental Biology, 1:199-233.

Wisowaty, J.J. (1981). Estimates for the temporal response characteristics of chromatic pathways. Journal of the Optical Society of America, 71:970-977.

Wisowaty, J.J. and Boynton, R.M. (1980). Temporal modulation sensitivity of the blue mechanism: measurement made without chromatic adaptation. Vision Research, 20:895-909.

Wong, R.O.L. and Hughes, A. (1987). Role of cell death in the topogenesis of neuronal distributions in the developing cat retinal ganglion cell layer. Journal of Comparative Neurology, 262:496-511.

Wortel, J.F., Rugenbrink, H. and Nuboer, J.F.W. (1987). The photopic spectral sensitivity of the dorsal and ventral retinae of the chicken. Journal of Comparative Physiology A, 160:151-154.

Yamada, M., Shigematsu, Y. and Fuwa, M. (1985). Latency of horizontal cell response in the carp retina. Vision Research, 25:767-774.

Yoshikami, S. and Hagins, W. A. (1971). Light, calcium and the photocurrent of rods and cones. Biophysical Journal, 11:47.

Young, R.W. (1984). Cell death during differentiation of the retina in the mouse. Journal of Comparative Neurology, 229:362-373.

Zaunreiter, M., Junger, H. and Kotrschal, K. (1991). Retinal morphology of cyprinid fishes: a quantitative histological study of ontogenetic and interspecific variation. Vision Research, 30:383-394.

Zrenner, E and Gouras, P. (1981). Characteristics of the blue sensitive cone mechanism in primate retinal ganglion cells. Vision Research, 21:1605-1609.

APPENDIX A: UV sensitivity in juvenile cutthroat trout (*Salmo clarki*)

The cutthroat trout retina contains a retinal mosaic typical of that of the other salmonids that have been investigated to date (Henderson and Northcote, 1988). More specifically, the adult cutthroat trout retinal mosaic is composed of four double cones surrounding a central single cone. From Fig. 1 of Henderson and Northcote (1988), however, it is obvious that the mosaic also contains a few accessory corner cones, or putative UV cones. Unfortunately, these authors do not comment on the presence of these cones, nor do they give precise information regarding the retinal location of the histological section they present. The presence of sparsely distributed accessory corner cones suggests, however, that the retina of the juvenile may contain a full complement of UV putative cones, as in rainbow trout (Beaudet et al., 1993) and brown trout (Bowmaker and Kunz, 1987) This possibility prompted this small investigation of the spectral sensitivity of juvenile cutthroat trout.

Spectral sensitivity was determined according to the technique described in chapter 2, and will not be described here. The Figure on the next page illustrates the spectral sensitivity of 3 (mean±SD) cutthroat trout obtained under chromatic adaptation. High sensitivity was found in both the UV and short parts of the spectrum for the ON response, suggesting that the animals possessed both UV and S cone mechanisms. In addition, M and L sensitivity peaks were also present. This was in accordance with what I found in rainbow trout (see chapters 2 and 6). In addition, the OFF response was dominated by inputs from the middle part of the spectrum, in accordance with the contention that it represents a shadow detecting mechanism tuned to the mid-spectrum of ambient light.

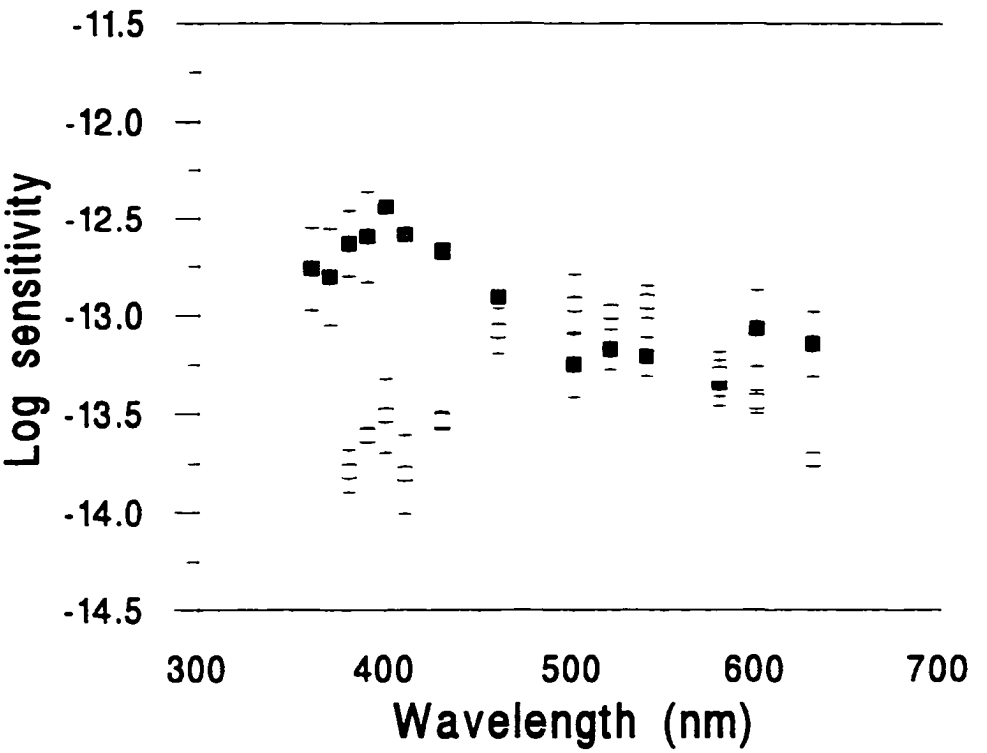
-11.5
-12.0
-12.5
-13.0
-13.5
-14.0
-14.5
Log sensitivity
300
400
500
600
700
Wavelength (nm)

APPENDIX B: Spectral sensitivity in the cichlid *Haplochromis burtoni*

Spectral sensitivity of one individual *H. burtoni* as determined from ONR recordings under an UV+S isolating background similar to that used in the experiments described in chapter 2 (next page). ON response is dominated by a sensitivity peak with λ_{max} around 460 nm. OFF response λ_{max} was found around 480-500 nm.

H. BURTONI "ON" AND "OFF" RESPONSES

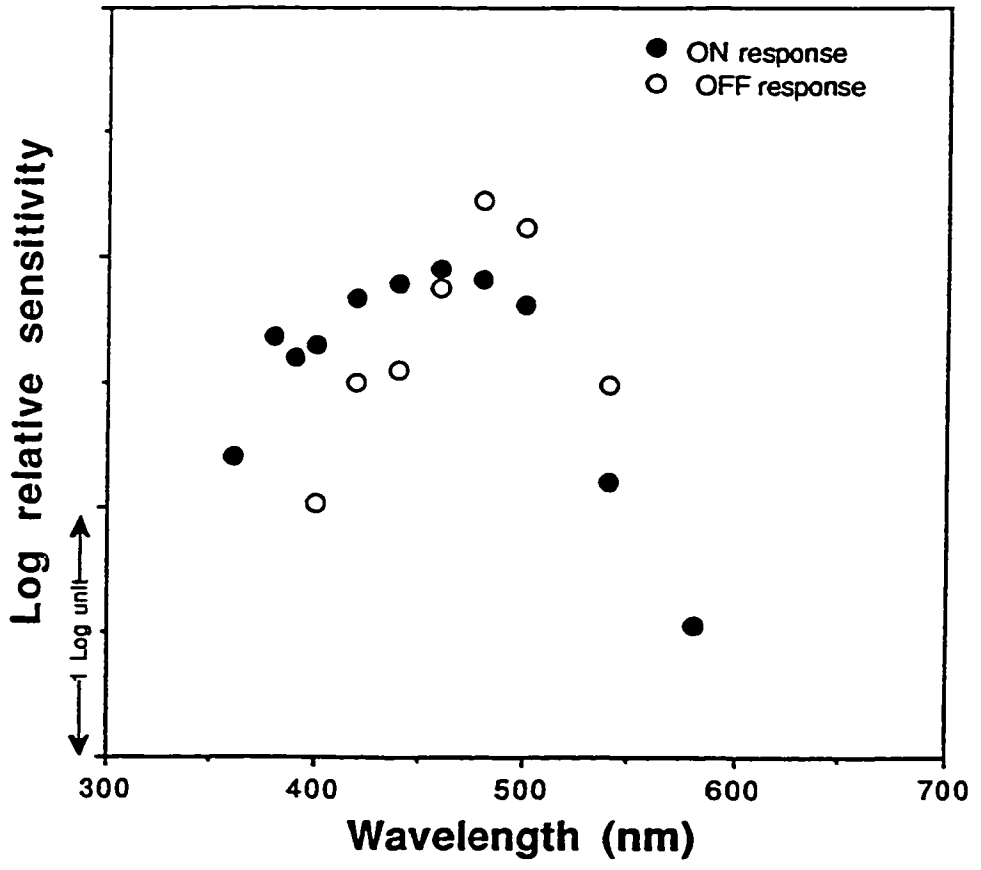

APPENDIX C: Irradiances for background intensities used in chapter 5.

Neutral density filters	relative log value	irradiance (μW)
0.0	9	$2X10^{3}$
1.0	8	$2.75X10^{2}$
2.0	7	2.0X10
3.0	6	2.8
4.0	5	$2X10^{-1}$
5.0	4	$2.5X10^{-2}$
6.0	3	$2.5X10^{-3}$
7.0	2	$2.5X10^{-4}$
8.0	1	$2X10^{-5}$
Dark	-1	--